Universidad de Concepción
Dirección de Postgrado
Facultad de Ciencias Físicas y Matemáticas
Programa de Doctorado en Ciencias Aplicadas
con Mención en Ingeniería Matemática

ANÁLISIS NUMÉRICO DE PROBLEMAS DIRECTOS E INVERSOS EN DINÁMICA DE FLUIDOS

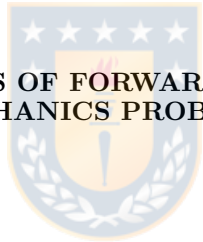

NUMERICAL ANALYSIS OF FORWARD AND INVERSE FLUID MECHANICS PROBLEMS

Tesis para optar al grado de Doctor en Ciencias
Aplicadas con mención en Ingeniería Matemática

Cristian Esteban Cárcamo Sánchez
Concepción-chile
2021

Profesor Guía: Rodolfo Araya
CI^{2}MA y Departamento de Ingeniería Matemática
Universidad de Concepción, Chile

Cotutor: Cristóbal Bertoglio
Bernoulli Institute
University of Groningen, The Netherlands

Numerical Analysis for forward and inverse fluid mechanics problems

Cristian Esteban Cárcamo Sánchez

Directores de Tesis: Rodolfo Araya, Universidad de Concepción, Chile.
Cristóbal Bertoglio, University of Groningen, The Netherlands.
Director de Programa: Raimung Bürger, Universidad de Concepción, Chile.

Comisión evaluadora

Prof. Malte Braack, University of Kiel, Germany.

Prof. Santiago Badia, Monash University, Australia.

Prof. Arjan van der Schaft, University of Groningen, The Netherlands.

Prof. Rodolfo Rodriguez, Universidad de Concepción, Chile.

Comisión examinadora

Firma: _____
Prof. Malte Braack, University of Kiel, Germany.

Firma: _____
Prof. Gabriel Barrenechea, University of Strathclyde, United Kingdom.

Firma: _____
Prof. Arjan van der Schaft, University of Groningen, The Netherlands.

Firma: _____
Prof. Rodolfo Rodriguez, Universidad de Concepción, Chile.

Calificación: _____

Concepción, 2 de Septiembre de 2021

Summary

This dissertation deal with numerical approximation methods of incompressible fluid problems, such as Oseen, nonlinear Darcy and Navier-Stokes equations. As our main contribution, we proposed and analyzed two new finite element schemes for the calculation of fluid problem solution, and we compared the performance of two other traditional methods commonly used to recover the pressure of the blood circulating in arteries.

In the Introduction we provided the context of the thesis, starting with the motivation and objectives of this project. A theoretical framework and the state-of-the-art is presented as well as a brief overview on the thesis.

In Chapter 1 we have addressed the Oseen equation from a viewpoint of a linearized Navier-Stokes equation. We have employed the novel Multiscale Hybrid Mixed (MHM) Method to solve the Oseen equation, proving that its weak formulation is well-posed, both a discrete and continuous problem. The main contribution here was the proposal of the first MHM method for advection-dominate flows with a mass-preserving local velocity field. We presented the first a posteriori error analysis of the MHM method applied to a non-symmetric operator, introducing and analyzing a new residual a posterior estimator, with the respective efficiency and reliability test. Furthermore, the adaptive method has been assessed by numerical experiments.

In Chapter 2, using a change of variable, we dealt with a nonlinear Darcy equation with pressure-depending viscosity, turning it into a linear problem. We have proposed a stabilized scheme for the linear problem, where we have performed an a priori error analysis and also proposed a residual a posteriori estimator, testing its efficiency and reliability to compute solutions. It has been checked that the problem is well-posed using the classical fixed point strategy. The solutions of the nonlinear Darcy problem are recovered by post-processing. The numerical examples indicated the existence of superconvergence when the proposed method is assessed, thus confirming the theory. The utility of the stabilized method for a 3D problem was also tested.

In Chapter 3 we have selected some methods used to recover the pressure, the Pressure Poisson equation (PPE) and the Stokes equation (STE) being the most used ones. For the PPE we have analyzed the cases considering the viscous term of the Navier-Stokes equation and also the opposite case. In both cases the error analysis was performed , obtaining convergence only in the first case, being this of order $\mathcal{O}(h^{1/2})$. For the STE the analysis was conducted using the traditional Taylor-Hood spaces and PSPG method. Although both methods of numerical computation allows us to obtain the same order of convergence, that is $\mathcal{O}(h)$, the numerical examples indicated that there are some differences between them, leading to the conclusion that the most cost-effective one is the STE solved with PSPG method, even over the PPE with the viscous term.

Resumen

Este trabajo de tesis aborda métodos de aproximación numérica para problemas de fluido incompresible, tales como las ecuaciones de Oseen, Darcy no lineal y Navier-Stokes. Nuestra principal contribución corresponde a la proposición y análisis de dos nuevos esquemas de elementos finitos para el cálculo de soluciones de problemas de fluidos, y la comparación del funcionamiento de otros dos métodos tradicionales usados para recuperar la presión de la sangre en movimiento en las arterias.

En la Introducción damos a conocer el contexto de la tesis, comenzando con la motivación y objetivos de esta. También se describen el marco teórico, la relación del trabajo tesis con métodos actuales, y un breve resumen sobre esta.

En el Capítulo 1 hemos abordado la ecuación de Oseen, desde el punto de vista de una ecuación de Navier-Stokes linealizada. Hemos aplicado el nuevo Método Mixto Multiescala Híbrido a la ecuación de Oseen, probando que su formulación débil corresponde a un problema bien puesto, tanto continua como discreta. En este capítulo la principal contribución corresponde a la aplicación método MHM a un operador no simétrico, introduciendo y analizando un nuevo estimador residual a posteriori, con la demostración que prueba su eficiencia y confiabilidad. Además, el método adaptativo ha sido evaluado por medio de experimentos numéricos.

En el capítulo 2, mediante un cambio de variable, abordamos una ecuación de Darcy no lineal, cuya viscosidad depende de la presión, convirtiéndola en un problema lineal. Hemos propuesto un esquema estabilizado para el problema lineal, donde hemos realizado el análisis de error a priori y también propuesto un estimador residual a posteriori, probando su eficiencia y confiabilidad para el cálculo de soluciones. Se ha verificado que el problema esté bien puesto usando la clásica estrategia del punto fijo. Las soluciones del problema de Darcy no lineal para la presión original son recuperadas mediante postproceso. Los ejemplos numéricos muestran la existencia de superconvergencia cuando el método propuesto es implementado, satisfaciendo los órdenes de convergencia que indica la teoría. Por último, se probó la utilidad del método estabilizado para un problema 3D.

En el capítulo 3 hemos seleccionado algunos métodos usados para recuperar la presión, donde los más usados son el Pressure Poisson Equation (PPE) y el Stokes Equation (STE). Para el PPE hemos analizado los casos considerando el término viscoso y también en caso contrario. En ambos casos se realizó análisis de error a priori, obteniendo solo convergencia si se considera el término viscoso, siendo este de orden $\mathcal{O}(h^{1/2})$. Para el STE, el análisis fue realizado usando los tradicionales espacios de Taylor-Hood y el método PSPG. A pesar de que ambos métodos de cálculo numérico nos permiten obtener el mismo orden de convergencia, es decir $\mathcal{O}(h)$, los ejemplos numéricos indican que existe diferencia entre ellos, permitiendo concluir que el método más costo-efectivo es el STE implementado con PSPG, incluso por sobre el PPE con término viscoso.

Acknowledgments

Firstly, my gratitude goes to God, who put everything in its place so that I could reach this objective, for bein my helper and my strength in every moment of this long process. Secondly, to my wife, thanks for being my faithful partner and the best mom; Thanks for understanding me and encouraging me to do everything. To my daughter Matilde (someday she will read this phrase), I am sorry for not being always available for you to play and share. To my parents whose gave me the best legacy: education. Special mention to my father who passed away during my PhD studies. To my sisters and my parents-in-law for the special support in these years.

My sincere gratitude to my tutors Rodolfo Araya and Cristóbal Bertóglio for trusting me to work on this thesis, for the patience and the willingness, motivation, intensity and initiative.

To Abner Poza for being my brother, colleague, friend and motivating me to learn and to have my feet on the ground.

To my dear friends and generation classmates, Bryan, Paul, Rafa, and Willian, for helping me and supporting me, as well as for teaching me that in life you should be happy on the good and bad days.

To my colleagues of the CI^{2}MA, mainly to Ramiro, Paulo, and Victor. To the administrative team members Lorena, Jorge and Paola and, especially, to Professor Gabriel Gatica for his management and concern for the center's needs while he was its director. Also, to Professors Raimund Burger and Rodolfo Rodríguez for every action to help us while they were directors of the doctoral program.

To the Bernoulli Institute family in Groningen, to Jigar, Jeremías, Ronald, Erik and Sven, dank u wel.

Finally, I would like to thank to the Dirección de Postgrados of the University of Concepción, to the Agencia Nacional de Investigación y Desarrollo (ANID) of the Chilean government, to the CI^{2}MA-CMM, and to the University of Groningen for the financial support during my PhD.

Cristian Cárcamo

Agradecimientos

Primeramente, mi gratitud es a Dios por poner todo en su lugar para que yo pueda alcanzar este objetivo, por ser mi ayuda y mi fuerza en cada momento de este largo proceso. En segundo lugar, a mi esposa, gracias por ser mi fiel compañera y la mejor mamá; gracias por entenderme y animarme a hacer las cosas. A mi hija Matilde (algún día ella leerá esta frase), perdón por no estar siempre disponible para ti, para jugar y compartir. A mis padres, quienes me dieron esta buena herencia: la educación. Especial mención a mi padre quien partió de esta vida durante mis estudios de doctorado. A mis hermanas y mis suegros por el especial apoyo en todos estos años.
Mi sincera gratitud a mis tutores Rodolfo Araya y Cristóbal Bertoglio por confiar en mí para trabajar esta tesis, por la paciencia y buena disposición, motivación, intensidad e iniciativa. A Abner Poza por ser mi hermano, colega, amigo y motivarme a aprender y a tener los pies en la tierra.
A mis amigos y compañeros de generación, Bryan, Paul, Rafa and Willian, por ayudarme y apoyarme, y por enseñarme que se debe ser feliz en días buenos y malos.
A mis compañeros del CI^{2}MA, principalmente a Ramira, Paulo y Víctor. Al equipo administrativo Lorena, Jorge y Paola, y espacialmente, al profesor Gabriel Gatica por la gestión y preocupación por las necesidades del centro mientras fue su director. También, a los profesores Raimund Burger y Rodolfo Rodríguez por cada acción para ayudarnos mientras fueron directores del programa de doctorado.
A la familia del Bernoulli Institute in Groningen, a Jigar, Jeremías, Ronald, Erik y Sven, dank u wel.
Finalmente, me gustaría agradecer a la dirección de postgrados de la Universidad de Concepción, a la Agencia Nacional de Investigación y Desarrollo (ANID) del Gobierno de Chile, al Basal CI^{2}MA-CMM y a la Universidad de Groningen por el apoyo financiero durante mi doctorado.

Cristian Carcamo

Contents

List of Figures

List of Tables

Introduction

Motivation

The fluid mechanics plays an important role in the modeling and study of the behaviour of gases and liquids in motion, and it also a fundamental tool in diverse areas such as oceanography, biomedicine, geology, among others. The tsunamis after earthquakes, the blood flowing in arteries and veins, the oil extraction, are some of the many examples where it is possible to model through fluid mechanics. Most of the time, the modeling of these problems is represented by a partial differential equation (PDE), such as the well-known Navier-Stokes equations (NSE) introduced by Claude-Louis Navier (1785-1836) and George Stokes (1819-1903) and the Darcy equations introduced by Henry Darcy (1803-1858). These equations are obtained by applying the laws of conservation and mass for NSE (see [2, 59]) and Darcy's Law ([66]).

The limitations of analytical methods to find solutions for these equations have led scientists and engineers to develop numerical methods. An outstanding method is the so-called continuous Galerkin finite element method (FEM), which arose from the need to solve complex elasticity and structural analysis problems. Later on, some FEM-based methods, such as stabilized FEM, hybrid FEM, among others, were introduced (see [15, 75, 105, 110, 135]).

Also within the framework of hybrid methods, in [67] the design and analysis of the Hybrid High-Order (HHO) methods are reported. This method was introduced for diffusive problems characterized by allowing polytopal meshes, non-star shaped elements and hanging nodes.

In [15] the authors present the Multiscale Hybrid Mixed (MHM) method for an elliptic model, which consists of the relaxation of the continuity of the primal variable by using of Lagrange multipliers, while assuring the strong continuity of the normal component of the flux. On the other hand, there are the stabilized methods which are efficient schemes to solve numerically PDE because they allow us the usage of high polynomial orders to compute the solutions with a low computational cost. Here, we are interested in contributing to the design, analysis and implementation of high order methods, such as hybrid and stabilized methods, to compute approximated solutions of equations. Besides, we want to contribute to answering questions about the cost-efficiency of methods used to reconstruct the pressure of a fluid. Some of these methods are the Pressure Poisson Equation (PPE) [92, 130] and the Stokes Equation (STE) [146], among others tath can be found in [37].

Objectives of the thesis

1. Multiscale hybrid mixed (MHM) method to solve numerically the Oseen equations. This method is deducted, presented, analyzed and implemented in Chapter 1.
2. Stabilized finite element method for a nonlinear Darcy equation, with the viscosity depending exponentially on the pressure. This new stabilized scheme is presented, analyzed and assessed in Chapter 2.
3. A strategy for the convergence analysis of current methods used for the pressure reconstruction is introduced in Chapter 3.

The multiscale hybrid mixed (MHM) method

Multiscale phenomena problems are present in many applications and their numerical approximations represents a great challenge. There are several examples, including lung modeling, neural modeling, flow in porous medium, among others. The main physical characteristic of these problems is the presence of different important physical scales. Mathematically, this means that the derivatives of the solution might blow up when any parameter goes to zero [105]. When these problems are approached in the context of partial differential equations (PDE) the phenomena can be characterized by a small parameter or by the domain itself [119]. A powerful technique to deal with multiscale problems is using hybrid schemes, consisting in a decomposition of a coupled problem into a set of independent (or local) problems that are, subsequently, assembled. These schemes are introduced in [135], where it is also possible to find the analysis of the method. From this idea emerge other schemes such as mixed finite element [21], [42], [87], hybrid discontinuous Galerkin (HDG) [61], and more recently, the hybrid high order method [67] and multiscale hybrid mixed (MHM) method [15], [16], [14].

The MHM method consists in a decoupling of the global problem into local problems by introducing a Lagrange multiplier.

To this end, let us consider the hybrid scheme of (7) of a mixed problem: *Find* $(\boldsymbol{u},p,\boldsymbol{\lambda},\rho)\in \mathbf{V}\times Q\times\boldsymbol{\Lambda}\times\mathbb{R}$ *such that*

$$\begin{cases} a(\boldsymbol{u},\boldsymbol{v})+b(\boldsymbol{v},p)+(\boldsymbol{\lambda},\boldsymbol{v})_{\partial\mathcal{T}_H}=(\boldsymbol{f},\boldsymbol{v})_{\mathcal{T}_H} & \text{for all } \boldsymbol{v}\in\mathbf{V},\\ b(\boldsymbol{u},q)+(\rho,q)_\Omega=0 & \text{for all } q\in Q,\\ (\boldsymbol{\mu},\boldsymbol{u})_{\partial\mathcal{T}_H}=\langle\boldsymbol{\mu},\boldsymbol{g}\rangle_{\partial\Omega} & \text{for all } \boldsymbol{\mu}\in\boldsymbol{\Lambda},\\ (\xi,p)_\Omega=0 & \text{for all } \xi\in\mathbb{R}. \end{cases} \tag{1}$$

where $\{\mathcal{T}_h\}_{h>0}$ is a family of regular triangulations of $\overline{\Omega}$ composed of the elements K, $(\cdot,\cdot)_{\partial\mathcal{T}_H}:=\sum_{K\in\mathcal{T}_H}\langle\cdot,\cdot\rangle_{\partial K}$, $(\cdot,\cdot)_X$ is the L^2-inner product and $(\cdot,\cdot)_{\mathcal{T}_H}:=\sum_{K\in\mathcal{T}_H}(\cdot,\cdot)_K$.

Equivalently, we can write the problem (1) as follows: *Find* $(\boldsymbol{u},p,\boldsymbol{\lambda},\rho)\in\mathbf{V}\times Q\times\boldsymbol{\Lambda}\times\mathbb{R}$ *such that*

$$\mathcal{A}((\boldsymbol{u},p),(\boldsymbol{v},q))+\mathcal{B}((\boldsymbol{\lambda},\rho),(\boldsymbol{v},q))=\mathcal{F}(\boldsymbol{v},q)\qquad\forall\,(\boldsymbol{v},q)\in\mathbf{V}\times Q \tag{2}$$

$$\mathcal{B}((\boldsymbol{\mu},\xi),(\boldsymbol{u},p))=\mathcal{G}(\boldsymbol{\mu},\xi)\qquad\forall\,(\boldsymbol{\mu},\xi)\in\boldsymbol{\Lambda}\times\mathbb{R}, \tag{3}$$

with

$$\begin{aligned}\mathcal{A}((\boldsymbol{u},p),(\boldsymbol{v},q)) &:= a(\boldsymbol{u},\boldsymbol{v})+b(\boldsymbol{v},p)-b(\boldsymbol{u},q),\\ \mathcal{B}((\boldsymbol{\mu},\xi),(\boldsymbol{v},q)) &:= (\boldsymbol{\mu},\boldsymbol{v})_{\partial\mathcal{T}_H}+(\xi,q)_\Omega,\\ \mathcal{F}(\boldsymbol{v},q) &:= (f,\boldsymbol{v})_{\mathcal{T}_H},\\ \mathcal{G}(\boldsymbol{\mu},\xi) &:= (\boldsymbol{\mu},\boldsymbol{g})_{\partial\Omega}\end{aligned}$$

We pursue to characterize the solution of (2)-(2) as a collection of solutions of local problems which are assembled using solutions to a global problem. In what follows, we will assume for a given space that $X|_K := X(K)$ and $\mathcal{A}_K, \mathcal{B}_K, \mathcal{F}_K$ and $\mathcal{G}_K$ meaning that $\mathcal{A}, \mathcal{B}, \mathcal{F}$ and $\mathcal{G}$ are being applied locally. If we test the (2) locally on each K for $(\boldsymbol{v},q,\boldsymbol{\mu},xi) = (\boldsymbol{v}|_K, q|_K, \boldsymbol{0}, 0)$ we get

$$\mathcal{A}_K((\boldsymbol{u},p),(\boldsymbol{v},q)) = -\mathcal{B}_K((\boldsymbol{\lambda},\rho),(\boldsymbol{v},q)) + \mathcal{F}_K(\boldsymbol{v},q) \qquad \forall\,(\boldsymbol{v},q)\ \in\ \mathbf{V}(K)\times Q(K). \tag{4}$$

Owing to the linearity of problem (4), we formally write

$$\boldsymbol{u} = \boldsymbol{u}^{\boldsymbol{\lambda}} + \boldsymbol{u}^{\boldsymbol{f}} + \boldsymbol{u}^{\rho} \qquad \text{and} \qquad p = p^{\boldsymbol{\lambda}} + p^{\boldsymbol{f}} + p^{\rho}. \tag{5}$$

Now, testing $(\boldsymbol{v},q,\boldsymbol{\mu},\xi) = (\boldsymbol{0},0,\boldsymbol{\mu},\xi)$ in (3) and using (5), the global problem (3) reads: *Find* $(\boldsymbol{\lambda},\rho) \in \boldsymbol{\Lambda}\times\mathbb{R}$ *such that*

$$\mathcal{B}((\boldsymbol{u}^{\boldsymbol{\lambda}},p^{\boldsymbol{\lambda}}),(\boldsymbol{\mu},\xi)) + \mathcal{B}((\boldsymbol{u}^{\rho},p^{\rho}),(\boldsymbol{\mu},\xi)) = \mathcal{G}(\boldsymbol{\mu},\xi) - \mathcal{B}((\boldsymbol{u}^{\boldsymbol{f}},p^{\boldsymbol{f}}),(\boldsymbol{\mu},\xi)) \qquad \forall\,(\boldsymbol{\mu},\xi)\ \in\ (\boldsymbol{\Lambda},\mathbb{R}). \tag{6}$$

The functions used in (5) and (6) are given as follows: *Find* $(\boldsymbol{u}^x,p^x) \in \mathbf{V}\times Q$ *such that*

$$\mathcal{A}_K((\boldsymbol{u}^x,p^x),(\boldsymbol{v},q)) = \mathcal{F}^x(\boldsymbol{v},q) \quad \forall\,(\boldsymbol{v},q)\ \in\ \mathbf{V}(K)\times Q(K),$$

where $x \in \{\boldsymbol{\lambda},\boldsymbol{f},\rho\}$, $F^{\boldsymbol{\lambda}}(\boldsymbol{v},q) := -\langle\boldsymbol{\lambda},\boldsymbol{v}\rangle_K$, $F^{\boldsymbol{f}}(\boldsymbol{v},q) := (\boldsymbol{f},\boldsymbol{v})_K$ and $F^{\rho}(\boldsymbol{v},q) := -(\rho,q)_K$

We want to apply this scheme to the Oseen Equations which consists of seeking the velocity $\boldsymbol{u}$ and pressure p solving the linear equation.

$$\begin{aligned}-\nu\Delta\boldsymbol{u} + (\nabla\boldsymbol{u})\boldsymbol{\alpha} + \gamma\boldsymbol{u} + \nabla p &= \boldsymbol{f}\\ \nabla\cdot\boldsymbol{u} &= 0\\ \boldsymbol{u} &= \boldsymbol{g},\end{aligned} \tag{7}$$

with ν as the diffusion coefficient, $\boldsymbol{\alpha}$ as the convective velocity and γ corresponding to a positive constant.

Stabilized finite element methods

The stabilized finite element methods arose in the 1970s in order to amend certain deficiencies that the traditional Galerkin schemes presented. Mainly, the pursued aim is to achieve the inf-sup stability or ellipticity of the bilinear form containing the unknown(s), maintaining the properties of the classical finite element methods. The first proposal was was driven by the need of overcoming the instability of advection-diffusion equations [52, 104, 50]. If we

consider the bilinear form $\mathcal{A} : X \times X \to \mathbb{R}$, $\mathcal{F} : X_2 \to \mathbb{R}$ and the problem: Find $u \in X$ such that

$$\mathcal{A}(u,v) = \mathcal{F}(v) \quad \text{for all } v \in X, \tag{8}$$

where (8) corresponds to the variational formulation of the problem

$$L(u) = f, \tag{9}$$

with L as an elliptic differential operator. It is also clear that

$$\begin{aligned} \mathcal{A}(u,v) &:= (L(u),v) = (u,L^*v) \quad \text{for all } u,v \in X, \\ \mathcal{F}(v) &:= (f,v) \quad \text{for all } v \in X, \end{aligned}$$

where $(\cdot,\cdot)_X$ corresponds to the scalar product in X.

The basic idea of the stabilization techniques is the addition of a term $S(\cdot,\cdot,\cdot)$ which depends on the residual of the differential form of the equation (9), turning (8) into: Find $u \in X$ such that

$$\mathcal{A}(u,v) + S(f,u,v) = \mathcal{F}(v) \quad \text{for all } v \in X. \tag{10}$$

A choice for the stabilization term is:

$$S(f,u,v) = \tau \cdot (L(u) - f, \tilde{L}(v)), \tag{11}$$

and also, we can to contextualize (11) in each element of a $\mathcal{T}_h$ partition as follows:

$$S(f,u,v) = \sum_{K \in \mathcal{T}_H} \tau_h \cdot (L(u) - f, \tilde{L}(v))_K, \tag{12}$$

where τ and τ_h are the stabilizing parameters, which will be defined according to the problem and the mesh [107], [108], [69], [81]. On the other hand, each choice of the $\tilde{L}(\cdot)$ operator will rise to a different stabilized method, being some popular methods the Streamline-Upwind Petrov-Galerkin (SUPG) method [52] which adds up an additional diffusion term to the Galerkin problem (10) in the direction of the streamlines. Consequently, a generalization of the SUPG method is the Galerkin/Least-Squares (GLS) method whose essential feature is to expand the Galerkin problem (10) with a least-squares form of the residuals that are based on the corresponding differential equations.

In this part of the thesis, the interest will be centered on applying a residual stabilization of the form of (11) to the nonlinear Darcy equation with pressure-dependent viscosity. That is,

$$\begin{cases} \alpha(\tilde{p})\,\tilde{\boldsymbol{u}} + \nabla \tilde{p} &= \boldsymbol{f} \quad \text{in } \Omega, \\ \nabla \cdot \tilde{\boldsymbol{u}} &= 0 \quad \text{in } \Omega, \\ \tilde{p} &= \tilde{\varphi} \quad \text{on } \Gamma_D, \\ \tilde{\boldsymbol{u}} \cdot \boldsymbol{n} &= 0 \quad \text{on } \Gamma_N, \end{cases} \tag{13}$$

where all the details will be given in chapter 2.

The reason to analyze this problem is due to its importance to realize that the flow characteristics of a fluid with pressure-dependent viscosity can be significantly different from the flow characteristics of a fluid with constant viscosity.

Pressure estimation methods from velocity measurements

These methods are based on directly inserting the measured velocity field into the Navier-Stokes Equations and therefore solving for the pressure field. There aret three families of techniques, which have as their main advantage their low computational cost due to the low order of the interpolated velocity.

Let us consider an incompressible Newtonian fluid in a bounded domain Ω, modeled by the steady Navier-Stokes equations:

$$\begin{aligned} -\nu\Delta\boldsymbol{u} + (\boldsymbol{u}\cdot\nabla)\boldsymbol{u} + \nabla p &= \boldsymbol{0} \quad \text{in } \Omega \\ \nabla\cdot\boldsymbol{u} &= 0 \quad \text{in } \Omega, \end{aligned} \tag{14}$$

where $\boldsymbol{u}, p$ are the fluid velocity and pressure, respectively, and ν represents the viscosity of the fluid. The main idea starts with the assumption that $\boldsymbol{u}$ is known and then (14) turns into

$$\nabla p = \nu\Delta\boldsymbol{u} - (\boldsymbol{u}\cdot\nabla)\boldsymbol{u}, \tag{15}$$

where the only one unknown is the pressure, while the velocity corresponds to the measured data.

The first and most popular technique capable of estimating RPD from full-field data is the so-called Pressure Poisson Estimator (PPE), which consists of applying the $\nabla\cdot$ operator in the equation (15), with appropriate Neumann boundary conditions for the pressure [92]. This problem consists of: Find $p \in P$ such that

$$(\nabla p, \nabla q)_\Omega = \nu(\Delta\boldsymbol{u}, \nabla q)_\Omega - ((\boldsymbol{u}\cdot\nabla)\boldsymbol{u}, \nabla q)_\Omega \qquad \forall\, q \in P,$$

being $P = H^1(\Omega) \cap L^2_0(\Omega)$. According to [37], the diffusive term is not considered because the viscous part of the pressure gradient in large vessels is negligible anyway. Besides, in the same article, they use finite element spaces of order 1 to interpolate the velocity and, in consequence, the laplacian of $\boldsymbol{u}$ is canceled. Later on, it was reported in [130] an alternative formulation that considers the diffusive term, allowing to get a better performance in the discrete context where the convergence of order $\mathcal{O}(h^{1/2})$ is observed.

An alternative formulation of estimating of the pressure was reported in [146] where the left-hand side of (15) is perturbed with the Laplacian of an auxiliary divergence-free velocity field $\boldsymbol{w}$, which will be considered as an unknown. In this chapter the equation (15) is converted into the problem: Find $(\boldsymbol{w}, p) \in \mathbf{V} \times P$ such that

$$(\nabla\boldsymbol{w}, \nabla\boldsymbol{v})_\Omega - (p, \nabla\cdot\boldsymbol{v})_\Omega + (q, \nabla\cdot\boldsymbol{w})_\Omega = -\nu(\nabla\boldsymbol{u}, \nabla\boldsymbol{v})_\Omega - ((\boldsymbol{u}\cdot\nabla)\boldsymbol{u}, \boldsymbol{v})_\Omega \quad \forall (\boldsymbol{w}, q) \in \mathbf{V} \times P,$$

where $\mathbf{V} \times P = [H^1_0(\Omega)]^d \times L^2_0(\Omega)$.

Other methods are reported in [37]. Some of them are the WERP which uses the classical energy relation of an incompressible Newtonian fluid; the integrated STE, which considers a modification of the original STE, by taking advantage of the regularity of the auxiliary velocity field and integrating the convective and viscous terms by parts; The Darcy estimator (DAE) where a divergence-free function is added directly, and instead of STE we get a Darcy equation; the Integral momentum relative pressure estimator (IMRP), which involves a modification of the WERP. We do not provide an analysis of these methods given that only the PPE and STE methods allow to retrieve the full pressure maps and the DAE has shown a similar performance to the PPE but with a higher computational cost.

Thesis Overview

- **An adaptive multiscale hybrid-mixed method for the Oseen equations**: A novel residual a posteriori error estimator for the Oseen equations achieves efficiency and reliability by including multi-level contributions in its construction. Originates from the Multiscale Hybrid Mixed (MHM) method, the estimator combines residuals from the skeleton of the first-level partition of the domain, along with the contributions from element-wise approximations. The second-level estimator is local and infers the accuracy of multiscale basis computations as part of the MHM framework. Also, the face-degrees of freedom of the MHM method shape the estimator and induce a new face-adaptive procedure on the mesh's skeleton only. As a result, the approach avoids re-meshing the first-level partition, which makes the adaptive process affordable and straightforward on complex geometries. Several numerical tests confirm theoretical results.
- **An adaptive stabilized finite element method for the Darcy's equations with pressure-dependent viscosities:** This chapter aims to introduce and analyze an adaptive stabilized finite element method to solve a nonlinear Darcy equation with a pressure-dependent viscosity and mixed boundary conditions. We stated the discrete problem's well-posedness and optimal error estimates, in natural norms, under standard assumptions. Next, we introduce and analyze a residual-based a posteriori error estimator for the stabilized scheme. Finally, we present some two- and three-dimensional numerical examples which confirm our theoretical results.
- **Error analysis of pressure reconstruction from discrete velocities:** Magnetic Resonance Imaging allows to measure the three-dimensional velocity field of blood flows. Therefore, several methods have been proposed to reconstruct the pressure field from such measurements using the incompressible Navier-Stokes equations. However, those measurements are obtained at limited spatial resolution given by the voxel dimensions in the image. Therefore, the velocity entering to the right-hand-side corresponds to a piecewise linear interpolation of the exact velocity. In this chapter we propose a strategy for convergence analysis of state-of-the-art pressure reconstruction methods. We show that many terms of different convergence order appear. However, numerical results show that linear order terms dominate, even when increasing the polynomial degree of the pressure.

Introducción

Motivación

La mecánica de fluidos juega un importante rol en el modelamiento y estudio del comportamiento de gases y líquidos en movimientos, siendo también una herramienta fundamental en diversas áreas tales como la oceanografía, biomedicina, geología, entre otras. Los tsunamis posteriores a los terremotos, el flujo sanguíneo en las arterias y venas, la extracción de petróleo, son algunos de los ejemplos donde es posible modelar por medio de mecánica de fluidos. El modelamiento de estos problemas, la mayoría de las veces, es representado por una ecuación diferencial parcial, siendo algunas de estas las conocidas ecuaciones de Navier Stokes (NSE introducidas por Claude-Louis Navier (1785-1836) y George Stokes (1819-1903), y las ecuaciones de Darcy introducidas por Henry Darcy (1803-1858). Estas ecuaciones son obtenidas aplicando las leyes de conservación (ver [2, 59]) y masa para la primera y la ley de Darcy para la segunda ([66]).

Las limitaciones de los métodos analíticos para encontrar soluciones para estas ecuaciones han llevado a científicos e ingenieros a desarrollar los métodos numéricos. Un destacado método es el llamado Método de Elementos Finitos de Galerkin continuo, originado a partir de la necesidad de resolver problemas complejos en elasticidad y análisis estructural. Más tarde, fueron introducidos algunos métodos basados en FEM tales como stabilized FEM, hybrid FEM, entre otros, (ver [15, 75, 105, 110, 135]).

También en el marco de los métodos híbridos en [67] se reporta el análisis y diseño del método Hybrid High-Order (HHO). Este método fue introducido para problemas difusivos caracterizados por permitir el uso de mallas politopales, elementos non-star shaped y nodos colgantes.

En [15] los autores presentan el método Multiscale Hybrid Mixed (MHM) para un problema elíptico, el cual consiste en la relajación de la continuidad de la variable primal por medio del uso de multiplicadores de Lagrange, mientras se asegura la continuidad fuerte de la componente normal del flujo. Por otro lado, existen los llamados métodos estabilizados los cuales son esquemas eficientes para resolver numéricamente EDPs gracias a que permite el uso de altos órdenes polinomiales para calcular las soluciones con un bajo costo computacional. Aquí, estamos interesados en contribuir al diseño, análisis e implementación de métodos de alto orden, tales como los métodos híbridos y estabilizados, para calcular las soluciones aproximadas de ecuaciones. Además, queremos contribuir a responder preguntas sobre el costo-eficiencia de métodos usados para reconstruir la presión de un fluido. Algunos de estos métodos son el Poisson Equation (PPE) [92, 130] y el Stokes Equation (STE) [146], entre otros que se pueden encontrar en [37].

Objetivos de la tesis

1. Método Multiscale hybrid mixed (MHM) para resolver numéricamente las ecuaciones de Oseen. Este método es deducido, presentado, analizado e implementado en el Capítulo 1.
2. Método de elementos finitos para una ecuación de Darcy no lineal, con la viscosidad dependiendo exponencialmente de la presión. Este nuevo esquema es presentado, analizado y evaluado e el Capítulo 2.
3. Se introduce una estrategia para el análisis de convergencia de métodos actuales usados para la reconstrucción de la presión en el Capítulo 3.

El método multiscale hybrid mixed (MHM)

Problemas de fenómenos multiescala están presentes en muchas aplicaciones y sus aproximaciones numéricas representan un gran desafío. Existen variados ejemplos, incluyendo modelamiento pulmonar, modelamiento neuronal, flujo en medio poroso, entre otros. La principal característica física de estos problemas es la presencia de diferentes e importantes escalas físicas. Matemáticamente, esto significa que las derivadas de la solución pueden explotar cuando algún parámetro se hace cero [105]. Cuando estos problemas son aproximados en el contexto de ecuaciones diferenciales parciales (EDPs) los fenómenos pueden ser caracterizados por un pequeño parámetro o por el dominio en sí mismo [119]. Una técnica poderosa para tratar problemas multiescala es por medio de esquemas híbridos, los cuales consistes en una descomposición de un problema acoplado en un conjunto de problemas independientes (o locales) que son, en consecuencia, ensamblados. Estos esquemas son introducidos en [135], donde es también posible encontrar el análisis del método. A partir de esta idea aparecen otros métodos las como mixed finite element [21], [21, 42, 87], hybrid discontinuous Galerkin (HDG) [61] y más recientemente el método hybrid high order method (HHO) [67] y el método multiscale hybrid mixed (MHM) [15, 16, 14].

El método MHM consiste en un desacoplamiento del problema global en problemas locales por medio de la introducción de un multiplicador de Lagrange.

Deseamos aplicar este esquema a la ecuación de Oseen la cual consiste en buscar la velocidad $\boldsymbol{u}$ y la presión p resolviendo la ecuación lineal

$$\begin{aligned} -\nu\Delta\boldsymbol{u} + (\nabla\boldsymbol{u})\boldsymbol{\alpha} + \gamma\boldsymbol{u} + \nabla p &= \boldsymbol{f} \\ \nabla\cdot\boldsymbol{u} &= 0 \\ \boldsymbol{u} &= \boldsymbol{g}, \end{aligned} \tag{16}$$

con ν el coeficiente de difusión, $\boldsymbol{\alpha}$ la velocidad convectiva y γ una constante positiva.

Para este fin, consideremos el esquema híbrido de (16) de un problema mixto: *Hallar* $(\boldsymbol{u}, p, \boldsymbol{\lambda}, \rho) \in \mathbf{V}\times Q\times\boldsymbol{\Lambda}\times\mathbb{R}$ *tal que*

$$\begin{cases} a(\boldsymbol{u},\boldsymbol{v}) + b(\boldsymbol{v},p) + (\boldsymbol{\lambda},\boldsymbol{v})_{\partial\mathcal{T}_H} = (\boldsymbol{f},\boldsymbol{v})_{\mathcal{T}_H} & \text{for all } \boldsymbol{v}\in\mathbf{V}, \\ b(\boldsymbol{u},q) + (\rho,q)_\Omega = 0 & \text{for all } q\in Q, \\ (\boldsymbol{\mu},\boldsymbol{u})_{\partial\mathcal{T}_H} = \langle\boldsymbol{\mu},\boldsymbol{g}\rangle_{\partial\Omega} & \text{for all } \boldsymbol{\mu}\in\boldsymbol{\Lambda}, \\ (\xi,p)_\Omega = 0 & \text{for all } \xi\in\mathbb{R}. \end{cases} \tag{17}$$

donde $\{\mathcal{T}_h\}_{h>0}$ es una familia de triangulaciones regulares de $\overline{\Omega}$ compuesta por elementos de K, $(\cdot,\cdot)_{\partial\mathcal{T}_H} := \sum_{K\in\mathcal{T}_H}\langle\cdot,\cdot\rangle_{\partial K}$, $(\cdot,\cdot)_X$ es el producto internoL^2- y $(\cdot,\cdot)_{\mathcal{T}_H} := \sum_{K\in\mathcal{T}_H}(\cdot,\cdot)_K$.

Equivalentemente, podemos escribir el problema (17) como sigue: *Hallar* $(\boldsymbol{u},p,\boldsymbol{\lambda},\rho)\in \mathbf{V}\times Q\times\boldsymbol{\Lambda}\times\mathbb{R}$ *tal que*

$$\mathcal{A}((\boldsymbol{u},p),(\boldsymbol{v},q))+\mathcal{B}((\boldsymbol{\lambda},\rho),(\boldsymbol{v},q)) = \mathcal{F}(\boldsymbol{v},q) \qquad \forall\,(\boldsymbol{v},q)\in\mathbf{V}\times Q \tag{18}$$

$$\mathcal{B}((\boldsymbol{\mu},\xi),(\boldsymbol{u},p)) = \mathcal{G}(\boldsymbol{\mu},\xi) \qquad \forall\,(\boldsymbol{\mu},\xi)\in\boldsymbol{\Lambda}\times\mathbb{R}, \tag{19}$$

con

$$\begin{aligned}\mathcal{A}((\boldsymbol{u},p),(\boldsymbol{v},q)) &:= a(\boldsymbol{u},\boldsymbol{v})+b(\boldsymbol{v},p)-b(\boldsymbol{u},q),\\ \mathcal{B}((\boldsymbol{\mu},\xi),(\boldsymbol{v},q)) &:= (\boldsymbol{\mu},\boldsymbol{v})_{\partial\mathcal{T}_H}+(\xi,q)_\Omega,\\ \mathcal{F}(\boldsymbol{v},q) &:= (f,\boldsymbol{v})_{\mathcal{T}_H},\\ \mathcal{G}(\boldsymbol{\mu},\xi) &:= (\boldsymbol{\mu},\boldsymbol{g})_{\partial\Omega}\end{aligned}$$

Perseguimos caracterizar la solución de (18)-(19) como una colección de soluciones de problemas locales los cuales son ensamblados usando soluciones para un problema global. En lo que sigue, asumiremos para un espacio dado que $X|_K := X(K)$ y $\mathcal{A}_K,\mathcal{B}_K,\mathcal{F}_K$ y $\mathcal{G}_K$ siendo las aplicaciones locales de $\mathcal{A},\mathcal{B},\mathcal{F}$ y $\mathcal{G}$.

Si testeamos (18) localmente en cada K por $(\boldsymbol{v},q,\boldsymbol{\mu},xi) = (\boldsymbol{v}|_K,q|_K,\mathbf{0},0)$ obtenemos

$$\mathcal{A}_K((\boldsymbol{u},p),(\boldsymbol{v},q)) = -\mathcal{B}_K((\boldsymbol{\lambda},\rho),(\boldsymbol{v},q))+\mathcal{F}_K(\boldsymbol{v},q) \qquad \forall\,(\boldsymbol{v},q)\in\mathbf{V}(K)\times Q(K). \tag{20}$$

Debido a la linealidad del problema (20), formalmente escribimos

$$\boldsymbol{u} = \boldsymbol{u}^{\boldsymbol{\lambda}}+\boldsymbol{u}^{\boldsymbol{f}}+\boldsymbol{u}^{\rho} \qquad \text{and} \qquad p = p^{\boldsymbol{\lambda}}+p^{\boldsymbol{f}}+p^{\rho}. \tag{21}$$

Ahora, testiando $(\boldsymbol{v},q,\boldsymbol{\mu},\xi) = (\mathbf{0},0,\boldsymbol{\mu},\xi)$ en (19) y usando (21), el problema global (19) se lee: *Hallar* $(\boldsymbol{\lambda},\rho)\in\boldsymbol{\Lambda}\times\mathbb{R}$ *tal que*

$$\mathcal{B}((\boldsymbol{u}^{\boldsymbol{\lambda}},p^{\boldsymbol{\lambda}}),(\boldsymbol{\mu},\xi))+\mathcal{B}((\boldsymbol{u}^{\rho},p^{\rho}),(\boldsymbol{\mu},\xi)) = \mathcal{G}(\boldsymbol{\mu},\xi)-\mathcal{B}((\boldsymbol{u}^{\boldsymbol{f}},p^{\boldsymbol{f}}),(\boldsymbol{\mu},\xi)) \qquad \forall\,(\boldsymbol{\mu},\xi)\in(\boldsymbol{\Lambda},\mathbb{R}). \tag{22}$$

Las funciones usadas en (21) y (22) son dadas como sigue: *Hallar* $(\boldsymbol{u}^x,p^x)\in\mathbf{V}\times Q$ *tal que*

$$\mathcal{A}_K((\boldsymbol{u}^x,p^x),(\boldsymbol{v},q)) = \mathcal{F}^x(\boldsymbol{v},q) \quad \forall\,(\boldsymbol{v},q)\in\mathbf{V}(K)\times Q(K),$$

where $x\in\{\boldsymbol{\lambda},\boldsymbol{f},\rho\}$, $F^{\boldsymbol{\lambda}}(\boldsymbol{v},q) := -\langle\boldsymbol{\lambda},\boldsymbol{v}\rangle_K$, $F^{\boldsymbol{f}}(\boldsymbol{v},q) := (\boldsymbol{f},\boldsymbol{v})_K$ and $F^{\rho}(\boldsymbol{v},q) := -(\rho,q)_K$

Método de elementos finitos estabilizados

Los métodos de elementos finitos estabilizados nacieron en los años 70 con el fin de corregir ciertas deficiencias que los esquemas de Galerkin tradicional presentaron. Principalmente, el fin que persiguen es lograr la inf-sup estabilidad o elipticidad de la forma bilineal que contiene las incógnitas, manteniendo las buenas propiedades de los métodos de elementos finitos

clásicos. La primera propuesta fue motivada para superar la inestabilidad las ecuaciones de advección-difusión [52, 104, 50].

Si consideramos la forma bilineal $\mathcal{A}: X \times X \to \mathbb{R}$, $\mathcal{F}: X_2 \to \mathbb{R}$ y el problema: *Hallar* $u \in X$ *tal que*

$$\mathcal{A}(u,v) = \mathcal{F}(v) \quad \text{para todo} \, v \in X, \tag{23}$$

donde (23) corresponde a la formulación variacional del problema

$$L(u) = f, \tag{24}$$

con L un operador diferencial elíptico, es claro que

$$\begin{aligned} \mathcal{A}(u,v) &:= (L(u),v) = (u, L^* v) \quad \text{for all } u, v \in X, \\ \mathcal{F}(v) &:= (f,v) \quad \text{para todol } v \in X, \end{aligned}$$

donde $(\cdot,\cdot)_X$ corresponde al producto escalar en X.

La idea básica de las técnicas de estabilización es la adición de un término $S(\cdot,\cdot,\cdot)$ dependiente del residual de la forma diferencial de la ecuación (24), convirtiendo (23) en: *Hallar* $u \in X$ *tal que*

$$\mathcal{A}(u,v) + S(f,u,v) = \mathcal{F}(v) \quad \text{para todo} \, v \in X. \tag{25}$$

Una elección para el término de estabilizacion es:

$$S(f,u,v) = \tau \cdot (L(u) - f, \tilde{L}(v)), \tag{26}$$

y también podemos contextualizar (26) en cada el elemento de una partición $\mathcal{T}_h$ como sigue:

$$S(f,u,v) = \sum_{K \in \mathcal{T}_H} \tau_h \cdot (L(u) - f, \tilde{L}(v))_K, \tag{27}$$

donde τ y τ_h son parámetros de estabilización, los cuales serán definidos de acuerdo al problema y a la malla [107, 108, 69, 81].

Por otro lado, cada elección del operador $\tilde{L}(\cdot)$ dará origen a un método estabilizado diferente, siendo algunos de los más populares el Streamline-Upwind Petrov-Galerkin (SUPG) [52] el cual agrega un término de difusión adicional al problema de Galerkin (25) en la dirección de las streamlines. En consecuencia, una generalización del método SUPG es el Galerkin/Least-Squares (GLS), método cuyo principal característica es expandir el problema de (25) en una forma de mínimos cuadrados de los residuales que están basados en la correspondiente ecuación diferencial.

En esta parte de la tesis, nuestro interés estará centrado en aplicar una estabilización residual de la forma (26) a la ecuación de Darcy no lineal con viscosidad dependiente de la presión. Es decir,

$$\begin{cases} \alpha(\tilde{p})\,\tilde{\boldsymbol{u}} + \nabla \tilde{p} &= \boldsymbol{f} \quad \text{in } \Omega, \\ \nabla \cdot \tilde{\boldsymbol{u}} &= 0 \quad \text{in } \Omega, \\ \tilde{p} &= \tilde{\varphi} \quad \text{on } \Gamma_D, \\ \tilde{\boldsymbol{u}} \cdot \boldsymbol{n} &= 0 \quad \text{on } \Gamma_N, \end{cases} \tag{28}$$

donde todos los detalles serán dados en el capítulo 2.

La razón para analizar este problema se debe a que es importante darse cuenta de que las características del flujo de un fluido con viscosidad presión-dependiente puede ser significativamente diferente a un las características de un flujo de un fluido con viscosidad constante.

Métodos de estimación de presión a partir de mediciones de velocidad.

Estos métodos están basados en insertar directamente el campo de velocidad medido en las ecuaciones de Navier-Stokes y, por lo tanto, resolver para el campo de presión. Existen tres familias de técnicas, las cuales tienen como principal ventaja su bajo costo computacional debido al bajo orden de la velocidad interpolad.

Consideremos un fluido Newtoniano e incompresible en un dominio acotado Ω, modelado por las ecuaciones de Navier-Stokes estacionarias:

$$\begin{aligned} -\nu\Delta\boldsymbol{u}+(\boldsymbol{u}\cdot\nabla)\boldsymbol{u}+\nabla p &= \mathbf{0} \qquad \text{in } \Omega \\ \nabla\cdot\boldsymbol{u} &= 0 \qquad \text{in } \Omega, \end{aligned} \tag{29}$$

donde $\boldsymbol{u}, p$ son la velocidad y la presión del fluido, respectivamente, y ν es la viscosidad del fluido. La idea principal comienza asumiendo que $\boldsymbol{u}$ es conocida y entonces (29) se transforma en

$$\nabla p = \nu\Delta\boldsymbol{u} - (\boldsymbol{u}\cdot\nabla)\boldsymbol{u}, \tag{30}$$

donde la única incógnita es la presión, mientras que la velocidad corresponde a la fuente medida.

La primera y más popular técnica capaz de estimar RPD a partir de datos de campo-completos es el llamado Pressure Poisson Estimator (PPE), el cual consiste en aplicar el operador $\nabla\cdot$ en la ecuación (30), con condiciones de frontera Neumann apropiadas para la presión [92]. Este problema consiste de: *Hallar* $p \in P$ *tal que*

$$(\nabla p, \nabla q)_\Omega = \nu(\Delta\boldsymbol{u}, \nabla q)_\Omega - ((\boldsymbol{u}\cdot\nabla)\boldsymbol{u}, \nabla q)_\Omega \qquad \forall\, q \in P,$$

siendo $P = H^1(\Omega)\cap L^2_0(\Omega)$. De acuerdo a [37], el término difusivo no es considerado, ya que la parte viscosa del gradiente de presión en grandes vasos es de cualquier modo insignificante. Además, en el mismo artículo, ellos usan espacios de elementos finitos de orden 1 para interpolar la velocidad y, en consecuencia, el laplaciano de $\boldsymbol{u}$ es cancelado. Más tarde, fue reportado en [130] una formulación alternativa que considera el término difusivo, permitiendo obtener a partir de este método un mejor desempeño en el contexto discreto donde se observa convergencia de orden $\mathcal{O}(h^{1/2})$.

Una formulación alternativa de estimación de la presión fue reportada en [146] donde el lado izquierdo de (30) es perturbado con el laplaciano de un campo de velocidad auxiliar de divergencia libre y con condición Dirichlet nula, el cual es considerado como una incógnita. En este trabajo, la ecuación, (30) se convierte en el problema: *Hallar* $(\boldsymbol{w}, p) \in \mathbf{V}\times P$ *tal que*

$$(\nabla\boldsymbol{w}, \nabla\boldsymbol{v})_\Omega - (p, \nabla\cdot\boldsymbol{v})_\Omega + (q, \nabla\cdot\boldsymbol{w})_\Omega = -\nu(\nabla\boldsymbol{u}, \nabla\boldsymbol{v})_\Omega - ((\boldsymbol{u}\cdot\nabla)\boldsymbol{u}, \boldsymbol{v})_\Omega \quad \forall (\boldsymbol{w}, q) \in \mathbf{V}\times P,$$

donde $\mathbf{V}\times P = [H^1_0(\Omega)]^d \times L^2_0(\Omega)$.

Otros métodos están reportados en [37]. Algunos de ellos son el WERP, el cual utiliza la clásica relajación de energía de un fluido Newtoniano incompresible; el STE integrado, el cual considera una modificación del STE original, tomando ventajas de la regularidad del campo de velocidad auxiliar e integrando por partes el término convectivo y viscoso; El DAE donde una función de divergencia libre es agregado directamente, y en vez de STE obtenemos una ecuación de Darcy; el IMRP el cual consiste en una modificación del WERP. No mostramos análisis de estos métodos dado que solo el PPE y el STE permiten recuperar los mapas de presión completos y el DAE tiene un funcionamiento similar al PPE pero con un costo computacional más alto.

Resumen de Tesis

- **An adaptative multiscale hybrid-mixed method for the Oseen equations**: Un nuevo estimador de error residual a posteriori para las ecuaciones de Oseen logra eficiencia y confiabilidad, incluyendo contribuciones de niveles múltiples en su construcción. Originado del método Multiscale Hybrid Mixed (MHM), el estimador combina residuales a partir del esqueleto de la partición de primer nivel del dominio, junto con las contribuciones de aproximaciones por elementos. El estimador de segundo nivel es local e infiere la exactitud de los cálculos de base multiescala como parte del marco de referencia de MHM. También, los grados de libertad de las caras del método MHM da forma al estimador e induce un nuevo procedimiento adaptativo sólo sobre las caras del esqueleto. Como un resultado, la aproximación evita re-mallar la partición del primer nivel, el cual hace al proceso adaptativo asequible y sencillo sobre geometrías complejas. Varios tests numéricos confirman los resultados teóricos.

- **An adaptive stabilized finite element method for the Darcy's equations with pressure dependent viscosities:** Este capítulo tiene como objetivo introducir y analizar un método de elementos finitos estabilizados adaptativos para resolver una ecuación de Darcy no lineal con viscosidad presión-dependiente y condiciones de frontera mixta. Establecemos que el problema está bien puesto y estimamos errores optimales, en normas naturales, bajo supuestos estándar. Luego, introducimos y analizamos un estimador de error a posteriori residual para el esquema estabilizado. Finalmente, presentamos algunos ejemplos numéricos en dos y tres dimensiones los cuales confirman nuestros resultados teóricos.

- **Error analysis of pressure reconstruction from discrete velocities:** Imágenes de resonancia magnética permiten medir los campos de velocidad de forma tridimensional de fluido sanguíneo. Por lo tanto, varios métodos han sido propuestos para reconstruir los campos de presión a partir de tales mediciones usando ecuaciones de Navier-Stokes incompresible. Sin embargo, estas mediciones son obtenidas en una resolución espacial dada por las dimensiones de los voxel en las imágenes. Por lo tanto, la velocidad entrante al lado derecho corresponde a una interpolación lineal a trozos de la velocidad exacta. En este capítulo proponemos una estrategia para el análisis de convergencia de métodos actuales de reconstrucción de presión. Mostramos que aparecen términos de distinto orden de convergencia. Sin embargo, los resultados numéricos muestra que dominan los términos de orden lineal, incluso cuando se incrementa el grado polinomial de la presión.

CHAPTER 1

An adaptative multiscale hybrid-mixed method for the Oseen equations

The content of this chapter was published in R. Araya, C. Cárcamo, A. Poza, F. Valentin. "An adaptive multiscale hybrid-mixed method for the Oseen equations". In: *Advances in Computational Mathematics* (2021) 47(15). [14].

1.1 Introduction

Fluid flow simulations rely on efficient numerical schemes shaped to account for large and small scale structures of the velocity and pressure fields. Typical problems are fluid flows in porous media and turbulent flows, for instance. For those problems, the computational cost involving in numerical schemes that cope with small scales of the approximate solution is costly, especially when one considers time-dependent problems in three-dimensional geometries. For this reason, multiscale numerical methods have been attracted attention in the last decades by their "embarrassingly" parallel nature, which turn out to be an excellent option to leverage the new generation of massive high-performance computers.

The Multiscale Hybrid-Mixed (MHM) method is a member of the family of multiscale finite element methods. Multiscale methods have its origin in [23] for the one-dimensional Poisson problem, and they were further extended to higher dimensional cases in [102, 103]. Overall, the multiscale methods rely on incorporating fine scales of the solutions through basis functions, with an impact on the accuracy of coarse-scale solutions, which can be computed on a coarse partition with precision. Other members of this family are the Heterogeneous Multiscale method (HMM) [72], the Variational Multiscale method (VMS) [6], the Generalized Multiscale finite element method [74], the Localized Orthogonal Decomposition method (LOD) [100], the Petrov-Galerkin Enriched method (PGEM) [13, 26, 82], the Residual Local Projection method (RELP) [80, 27, 11], to mention a few. A posteriori error estimator for some of these schemes can be reviewed in [1, 24, 57, 101, 109, 127, 132, 147, 17], and the references therein.

Regarding the MHM method, it relies on the characterization of the exact solution as a byproduct of the hybridization of the continuous problem on a coarse mesh (first-level mesh). As a result, the exact fields decompose as the solutions of a series of local problems coupled through a global problem defined on the skeleton of the first-level partition. In such an infinite-dimensional setting, the local problems are entirely independent of one another and account for the multiscale nature of the problem. Discretization uncouples global and

local problems, and the latter responds for the multiscale basis computation. Thereby, the expensive part of the algorithm can be naturally solved in parallel computers. The MHM method was initially introduced for the Darcy equation in [97] and analyzed in [15, 131], and extented to models based on the Stokes operator in [16] and [13].

In this chapter, we extend the MHM method for the Oseen equations and proposes and analyses a new multiscale residual, a posteriori error estimator. It relies strongly on the MHM's structure, and as a result, the estimator splits into two-levels: First η_1 accounts for the jump of the discrete velocity on the skeleton of the first-level mesh, and then, a second-level estimator η_2 estimates the error associated to the approximation of the local problems (multiscale basis, mostly). We prove local efficiency and reliability for the multiscale estimator following the ideas of [15, 19, 96] for η_1 and [19] for η_2. Also, it leads to a new adaptive strategy on the mesh's skeleton only. As a result, the algorithm of adaption avoids re-meshing the first-level partition, which makes the adaptive process affordable and straightforward to be used on complex geometries. Other numerical schemes share similarities with the MHM method but are also essentially different in their constructions and properties. For instance, we mention the Multiscale Mortar Method [20], the DEM [77], and the HDG method [62], for the Oseen equations [56], among others. For a small list of a posteriori error estimators for two-level method, see, for example, [156, 76, 112, 136, 158, 39] and the references therein.

The chapter outlines as follows. In Section 1.2, we introduce the model problem, notations, and some preliminary results. Section 1.3 revisits the main aspects of the MHM methodology to propose new first- and second-level MHM methods for the Oseen equations. The main results of this chapter are in Section 1.4, wherein one proposes and analyses a new and multi-level a posteriori error estimator based on the MHM method. Numerical validations asses theoretical results lie in Section 1.5.

1.2 Model problem and preliminaries

1.2.1 The model

Let $\Omega \subset \mathbb{R}^d$, $d \in \{2,3\}$, be a bounded open set with polygonal boundary $\partial\Omega$. Given $\boldsymbol{f} \in L^2(\Omega)^d$ and $\boldsymbol{g} \in H^{1/2}(\partial\Omega)^d$ with $\int_{\partial\Omega} \boldsymbol{g}\cdot\boldsymbol{n}\,ds = 0$, where $\boldsymbol{n}$ represents the outer normal vector to $\partial\Omega$, the Oseen problem consists of finding a velocity field $\boldsymbol{u}$ and scalar pressure p, such that

$$\begin{aligned} -\nu\Delta\boldsymbol{u} + (\nabla\boldsymbol{u})\boldsymbol{\alpha} + \gamma\boldsymbol{u} + \nabla p &= \boldsymbol{f} \quad \text{in } \Omega, \\ \nabla\cdot\boldsymbol{u} &= 0 \quad \text{in } \Omega, \\ \boldsymbol{u} &= \boldsymbol{g} \quad \text{on } \partial\Omega, \end{aligned} \tag{1.1}$$

where the diffusion coefficient ν is a positive constant, $\boldsymbol{\alpha} \in W^{1,\infty}(\Omega)^d$ is a convective velocity field and γ a given scalar function. We assume in this chapter that γ is a positive constant and that there exists a positive constant γ_m such that, for all $x \in \Omega$, it holds

$$\gamma_0 := \gamma - \frac{1}{2}\nabla\cdot\boldsymbol{\alpha}(\boldsymbol{x}) \geq \gamma_m. \tag{1.2}$$

Remark 1.1. *Observe that model (1.1) may represent a step in the time discretization of the unsteady Navier–Stokes equations, where $\gamma = 1/\Delta t$, with Δt the time interval length, and $\boldsymbol{\alpha}$ the velocity field evaluated in the previous time step.*

The standard variational mixed formulation associated to (1.1) reads: *Find* $\boldsymbol{u} \in H^1(\Omega)^d$, *with* $\boldsymbol{u} = \boldsymbol{g}$ *on* $\partial\Omega$, *and* $p \in L^2_0(\Omega)$, *such that*

$$\begin{aligned} a(\boldsymbol{u},\boldsymbol{v}) + b(\boldsymbol{v},p) &= (\boldsymbol{f},\boldsymbol{v})_\Omega \qquad \text{for all } \boldsymbol{v} \in H^1_0(\Omega)^d, \\ b(\boldsymbol{u},q) &= 0 \qquad\qquad\quad \text{for all } q \in L^2_0(\Omega). \end{aligned} \tag{1.3}$$

The bilinear forms $a(\cdot,\cdot)$ and $b(\cdot,\cdot)$ are defined by

$$a(\boldsymbol{w},\boldsymbol{v}) := (\nu\nabla\boldsymbol{w},\nabla\boldsymbol{v})_\Omega + ((\nabla\boldsymbol{w})\boldsymbol{\alpha},\boldsymbol{v})_\Omega + (\gamma\,\boldsymbol{w},\boldsymbol{v})_\Omega,$$

for all $\boldsymbol{w} \in H^1(\Omega)^d$, $\boldsymbol{v} \in H^1_0(\Omega)^d$ and

$$b(\boldsymbol{v},q) := -(\nabla\cdot\boldsymbol{v},q)_\Omega,$$

for all $\boldsymbol{v} \in H^1(\Omega)^d$ and $q \in L^2_0(\Omega)$, where the spaces have their usual meaning. Using that

$$((\nabla\boldsymbol{u})\boldsymbol{\alpha},\boldsymbol{v})_\Omega = -(\boldsymbol{u},(\nabla\boldsymbol{v})\boldsymbol{\alpha})_\Omega - ((\nabla\cdot\boldsymbol{\alpha})\boldsymbol{u},\boldsymbol{v})_\Omega + ((\boldsymbol{\alpha}\cdot\boldsymbol{n})\boldsymbol{u},\boldsymbol{v})_{\partial\Omega}, \tag{1.4}$$

for all $\boldsymbol{u},\boldsymbol{v} \in H^1(\Omega)^d$, follows that the bilinear form $a(\cdot,\cdot)$ can be rewritten in a skew-symmetry form as

$$a(\boldsymbol{u},\boldsymbol{v}) := (\nu\nabla\boldsymbol{u},\nabla\boldsymbol{v})_\Omega + \frac{1}{2}((\nabla\boldsymbol{u})\boldsymbol{\alpha},\boldsymbol{v})_\Omega - \frac{1}{2}(\boldsymbol{u},(\nabla\boldsymbol{v})\boldsymbol{\alpha})_\Omega + (\gamma_0\,\boldsymbol{u},\boldsymbol{v})_\Omega,$$

for all $\boldsymbol{u} \in H^1(\Omega)^d$ and $\boldsymbol{v} \in H^1_0(\Omega)^d$.

Remark 1.2. *Assumption* (1.2) *implies the coercivity of* $a(\cdot,\cdot)$ *in* $H^1_0(\Omega)^d$, *which combined with the classical inf–sup condition in* $b(\cdot,\cdot)$, *leads to the existence and unique solution for* (1.3).

1.2.2 Hybridization

Now we head to the definition of an equivalent hybrid form of (1.3). To this end, we introduce a regular family $\{\mathcal{T}_H\}_{H>0}$ of triangulations of $\overline{\Omega}$, composed of elements K, with diameter H_K, and we set $H := \max\{H_K : K \in \mathcal{T}_H\}$. Hereafter, we shall use the terminology usually employed for three-dimensional domains, with the restriction to two-dimensional problems being straightforward. We denote by $\mathcal{E}_H$ the set of all faces (edges) F of elements $K \in \mathcal{T}_H$ and by $\mathcal{E}_0$ the set of inner faces. To each face F of $\mathcal{E}_H$, we associate a normal $\boldsymbol{n}$ taking care to ensure this is directed outward on $\partial\Omega$. For each $K \in \mathcal{T}_H$ we further denote by $\boldsymbol{n}^K$ the outward normal on ∂K, and let $\boldsymbol{n}^K_F := \boldsymbol{n}^K|_F$ for each $F \subset \partial K$. We denote by $\mathcal{T}_{\tilde{H}}(F)$ a partition of $F \in \mathcal{E}_H$, by $H_{\tilde{F}}$ the size of $\tilde{F} \in \mathcal{T}_{\tilde{H}}(F)$ and $\tilde{H} = \max\left\{H_{\tilde{F}} : \tilde{F} \in \mathcal{T}_{\tilde{H}}(F)\right\}$.

The following spaces will be used in the sequel

$$\begin{aligned} \mathbf{V} &:= H^1(\mathcal{T}_H)^d := \{\boldsymbol{v} \in L^2(\Omega)^d \,:\, \boldsymbol{v}|_K \in H^1(K)^d \quad \text{for all } K \in \mathcal{T}_H\}, \\ H(\mathrm{div};\Omega) &:= \{\boldsymbol{\tau} \in L^2(\Omega)^{d\times d} \,:\, \mathrm{div}\boldsymbol{\tau} \in L^2(\Omega)^d\}, \\ \boldsymbol{\Lambda} &:= \left\{\boldsymbol{\sigma}\,\boldsymbol{n}^K|_{\partial K} \in H^{-1/2}(\partial K)^d \quad \text{for all } K \in \mathcal{T}_H : \boldsymbol{\sigma} \in H(\mathrm{div};\Omega)\right\}, \\ Q &:= L^2(\Omega). \end{aligned}$$

We define an inner product on $\mathbf{V}$ by

$$(\boldsymbol{u},\boldsymbol{v})_{\mathbf{V}} := \frac{1}{d_\Omega^2}(\boldsymbol{u},\boldsymbol{v})_\Omega + \sum_{K\in\mathcal{T}_H}(\nabla\boldsymbol{u},\nabla\boldsymbol{v})_K \quad \text{for all } \boldsymbol{u},\boldsymbol{v}\in\mathbf{V},$$

where d_Ω is the diameter of Ω, $(\cdot,\cdot)_D$ the L^2 inner product in $L^2(D)$, $D\subset\Omega$. We equip the spaces $H(\mathrm{div};\Omega)$ and $\mathbf{V}$ with the following norms,

$$\|\boldsymbol{\sigma}\|_{\mathrm{div}} := \left\{\sum_{K\in\mathcal{T}_H}\left[\|\boldsymbol{\sigma}\|_{0,K}^2 + d_\Omega^2\|\nabla\cdot\boldsymbol{\sigma}\|_{0,K}^2\right]\right\}^{1/2} \quad \text{and} \quad \|\boldsymbol{v}\|_{\mathbf{V}} := (\boldsymbol{v},\boldsymbol{v})_{\mathbf{V}}{}^{1/2},$$

respectively. For the space $\boldsymbol{\Lambda}$, we use the quotient norm, i.e.,

$$\|\boldsymbol{\mu}\|_{\boldsymbol{\Lambda}} := \inf_{\substack{\boldsymbol{\sigma}\in H(\mathrm{div};\Omega)\\ \boldsymbol{\sigma}\boldsymbol{n}^K=\boldsymbol{\mu}\text{ on }\partial K, K\in\mathcal{T}_H}} \|\boldsymbol{\sigma}\|_{\mathrm{div}}. \tag{1.5}$$

We denote by $(\cdot,\cdot)_{\mathcal{T}_H}$ and $(\cdot,\cdot)_{\partial\mathcal{T}_H}$ the following

$$(\boldsymbol{w},\boldsymbol{v})_{\mathcal{T}_H} := \sum_{K\in\mathcal{T}_H}(\boldsymbol{w},\boldsymbol{v})_K \qquad \text{and} \qquad (\boldsymbol{\mu},\boldsymbol{v})_{\partial\mathcal{T}_H} := \sum_{K\in\mathcal{T}_H}\langle\boldsymbol{\mu},\boldsymbol{v}\rangle_{\partial K},$$

where $\boldsymbol{w},\boldsymbol{v}\in\mathbf{V}$ and $\boldsymbol{\mu}\in\boldsymbol{\Lambda}$, and $\langle\cdot,\cdot\rangle_{\partial K}$ is the duality pair between $H^{-1/2}(\partial K)^d$ and $H^{1/2}(\partial K)^d$.

We recall from Lemma 8.3 in [15] that the norm (1.5) is equivalent to a dual norm, namely,

$$\frac{\sqrt{2}}{2}\|\boldsymbol{\mu}\|_\Lambda \le \sup_{\boldsymbol{v}\in\mathbf{V}}\frac{(\boldsymbol{\mu},\boldsymbol{v})_{\partial\mathcal{T}_H}}{\|\boldsymbol{v}\|_{\mathbf{V}}} \le \|\boldsymbol{\mu}\|_{\boldsymbol{\Lambda}} \quad \text{for all } \boldsymbol{\mu}\in\boldsymbol{\Lambda}. \tag{1.6}$$

Above and hereafter, we lighten the notation and understand the supremum to be taken over sets excluding the zero function, even though this is not specifically indicated.

We introduce the norm $\|(\cdot,\cdot)\|_{\mathbf{V}\times Q}$ for the product space $\mathbf{V}\times Q$, by

$$\|(\boldsymbol{v},q)\|_{\mathbf{V}\times Q} := \left\{\|\boldsymbol{v}\|_{\mathbf{V}}^2 + \|q\|_Q^2\right\}^{1/2},$$

with $\|q\|_Q := \|q\|_{0,\Omega}$. Finally, for each $K\in\mathcal{T}_H$, we define the local spaces $\mathbf{V}(K) := H^1(K)^d$ and $Q(K) := L^2(K)$, with the follows norms

$$\begin{aligned}
\|\boldsymbol{v}\|_{\mathbf{V}(K)} &:= \left\{d_\Omega^{-2}\|\boldsymbol{v}\|_{0,K}^2 + \|\nabla\boldsymbol{v}\|_{0,K}^2\right\}^{1/2},\\
\|q\|_{Q(K)} &:= \|q\|_{0,K},\\
\|(\boldsymbol{v},q)\|_{\mathbf{V}(K)\times Q(K)} &:= \left\{\|\boldsymbol{v}\|_{\mathbf{V}(K)}^2 + \|q\|_{Q(K)}^2\right\}^{1/2},
\end{aligned}$$

for all $\boldsymbol{v}\in\mathbf{V}(K)$ and $q\in Q(K)$.

Now, we consider the definition for the jump over a face $F=\partial K^+\cap\partial K^-\in\mathcal{E}_0$ of a function $\boldsymbol{v}\in\mathbf{V}$ as follows:

$$[\![\boldsymbol{v}]\!] := (\boldsymbol{v}|_{K^+})|_F - (\boldsymbol{v}|_{K^-})|_F,$$

and the average by

$$\{\{\boldsymbol{v}\}\} := \frac{1}{2}\Big(\boldsymbol{v}|_{K^+} + \boldsymbol{v}|_{K^-}\Big).$$

We update the notation $a(\cdot,\cdot)$ and $b(\cdot,\cdot)$ by extending them to the space $\mathbf{V}$ as follows

$$a(\boldsymbol{w},\boldsymbol{v}) := \sum_{K\in\mathcal{T}_H} a_K(\boldsymbol{w},\boldsymbol{v}),$$

with

$$a_K(\boldsymbol{w},\boldsymbol{v}) := (\nu\nabla\boldsymbol{u},\nabla\boldsymbol{v})_K + \frac{1}{2}\left((\nabla\boldsymbol{u})\boldsymbol{\alpha},\boldsymbol{v}\right)_K - \frac{1}{2}\left(\boldsymbol{u},(\nabla\boldsymbol{v})\boldsymbol{\alpha}\right)_K + (\gamma_0\boldsymbol{u},\boldsymbol{v})_K, \tag{1.7}$$

and

$$b(\boldsymbol{v},q) := \sum_{K\in\mathcal{T}_H} b_K(\boldsymbol{v},q) \quad \text{with} \quad b_K(\boldsymbol{v},q) := -(\nabla\cdot\boldsymbol{v},q)_K,$$

for all $\boldsymbol{w},\boldsymbol{v}\in\mathbf{V}$, $q\in Q$.

We consider the following hybrid formulation of problem (1.3): *Find* $(\boldsymbol{u},p,\boldsymbol{\lambda},\rho)\in\mathbf{V}\times Q\times\boldsymbol{\Lambda}\times\mathbb{R}$ *such that*

$$\begin{cases} a(\boldsymbol{u},\boldsymbol{v}) + b(\boldsymbol{v},p) + (\boldsymbol{\lambda},\boldsymbol{v})_{\partial\mathcal{T}_H} = (\boldsymbol{f},\boldsymbol{v})_{\mathcal{T}_H} & \text{for all } \boldsymbol{v}\in\mathbf{V},\\ b(\boldsymbol{u},q) + (\rho,q)_\Omega = 0 & \text{for all } q\in Q,\\ (\boldsymbol{\mu},\boldsymbol{u})_{\partial\mathcal{T}_H} = \langle\boldsymbol{\mu},\boldsymbol{g}\rangle_{\partial\Omega} & \text{for all } \boldsymbol{\mu}\in\boldsymbol{\Lambda},\\ (\xi,p)_\Omega = 0 & \text{for all } \xi\in\mathbb{R}. \end{cases} \tag{1.8}$$

In formulation (1.8), the velocity and pressure belong a priori to a larger space than the solutions of the original problem (1.3). Note that the third equation in (1.8) imposes $H^1(\Omega)$–conformity on the velocity, and the fourth the mean value of the pressure equal zero. Concerning the solvability of problem (1.8) we have the following result

Theorem 1.1. *The function* $(\boldsymbol{u},p)\in H^1(\Omega)^d\times L^2_0(\Omega)$, *with* $\boldsymbol{u}=\boldsymbol{g}$ *on* $\partial\Omega$, *is the unique solution of* (1.3) *if and only if* $(\boldsymbol{u},p,\boldsymbol{\lambda},\rho)\in\mathbf{V}\times Q\times\boldsymbol{\Lambda}\times\mathbb{R}$ *is the unique solution of* (1.8). *Moreover, it holds* $\rho=0$ *and*

$$\boldsymbol{\lambda} = \left((-\nu\nabla\boldsymbol{u}+p\boldsymbol{I})\boldsymbol{n}^K + \frac{1}{2}(\boldsymbol{u}\otimes\boldsymbol{\alpha})\boldsymbol{n}^K\right)\Big|_{\partial K} \quad \text{for all } K\in\mathcal{T}_H, \tag{1.9}$$

where $\boldsymbol{I}$ *is the* $d\times d$ *identity tensor.*

Proof. Let $(\boldsymbol{u},p)$ be the solution of (1.3), and define the functional $\mathcal{F}:\mathbf{V}\longrightarrow\mathbb{R}$ by

$$\mathcal{F}(\boldsymbol{v}) := (\boldsymbol{f},\boldsymbol{v})_{\mathcal{T}_H} - (\nu\nabla\boldsymbol{u},\nabla\boldsymbol{v})_{\mathcal{T}_H} - \frac{1}{2}((\nabla\boldsymbol{u})\boldsymbol{\alpha},\boldsymbol{v})_{\mathcal{T}_H} + \frac{1}{2}(\boldsymbol{u},(\nabla\boldsymbol{v})\boldsymbol{\alpha})_{\mathcal{T}_H} - (\gamma_0\boldsymbol{u},\boldsymbol{v})_{\mathcal{T}_H} + (\nabla\cdot\boldsymbol{v},p)_{\mathcal{T}_H},$$

for all $\boldsymbol{v}\in\mathbf{V}$. It is clear that $\mathcal{F}$ is continuous and vanishes on $H^1_0(\Omega)^d$. From Lemma 1 in [135], there exists a unique $\boldsymbol{\lambda}\in\boldsymbol{\Lambda}$ such that $\mathcal{F}(\boldsymbol{v}) = (\boldsymbol{\lambda},\boldsymbol{v})_{\partial\mathcal{T}_H}$ for all $\boldsymbol{v}\in\mathbf{V}$, thus the first equation in (1.8) holds. Now integrating by parts we get

$$\sum_{K\in\mathcal{T}_H}(\boldsymbol{\lambda},\boldsymbol{v})_{\partial K} = \sum_{K\in\mathcal{T}_H}\Big[(\boldsymbol{f},\boldsymbol{v})_K - (\nu\nabla\boldsymbol{u},\nabla\boldsymbol{v})_K - \frac{1}{2}((\nabla\boldsymbol{u})\boldsymbol{\alpha},\boldsymbol{v})_K + \frac{1}{2}(\boldsymbol{u},(\nabla\boldsymbol{v})\boldsymbol{\alpha})_K$$

$$
\begin{aligned}
&\quad - (\gamma_0 \boldsymbol{u}, \boldsymbol{v})_K + (\nabla \cdot \boldsymbol{v}, p)_K \Big] \\
&= \sum_{K \in \mathcal{T}_H} ((-\nu \nabla \boldsymbol{u} + p\boldsymbol{I})\boldsymbol{n}^K + \frac{1}{2}(\boldsymbol{u} \otimes \boldsymbol{\alpha})\boldsymbol{n}^K, \boldsymbol{v})_{\partial K},
\end{aligned}
$$

for all $\boldsymbol{v} \in \mathbf{V}$, and then (1.9) holds.

On the other hand, since that $(\nabla \cdot \boldsymbol{u}, q)_{\mathcal{T}_H} = (\nabla \cdot \boldsymbol{u}, q)_\Omega = 0$ for all $q \in L^2_0(\Omega)$, Lemma 5 in [16] guarantees that there exists a unique $\rho \in \mathbb{R}$ such that $(\nabla \cdot \boldsymbol{u}, q)_{\mathcal{T}_H} = (\rho, q)_\Omega$ for all $q \in Q$ and so the second equation of (1.8) holds. Now, using Gauss's Theorem, we get,

$$
\|\rho\|^2_{0,\Omega} = \sum_{K \in \mathcal{T}_H} (\boldsymbol{u} \cdot \boldsymbol{n}^K, \rho)_{\partial K} = (\boldsymbol{u} \cdot \boldsymbol{n}, \rho)_{\partial\Omega} = (\boldsymbol{g} \cdot \boldsymbol{n}, \rho)_{\partial\Omega}.
$$

By the compatibility condition, we have that $(\boldsymbol{g} \cdot \boldsymbol{n}, \rho)_{\partial\Omega} = 0$ and then $\rho = 0$. Next, take $\boldsymbol{q} \in H(\mathrm{div};\Omega)$, and define $\boldsymbol{\mu} = \boldsymbol{q}\boldsymbol{n}^K$ on ∂K for all $K \in \mathcal{T}_H$. Using integration by parts we have

$$
(\boldsymbol{\mu}, \boldsymbol{u})_{\partial \mathcal{T}_H} = \sum_{K \in \mathcal{T}_H} \langle \boldsymbol{q}\boldsymbol{n}^K, \boldsymbol{u} \rangle_{\partial K} = \sum_{F \in \mathcal{E}_H} (\llbracket \boldsymbol{q} \rrbracket, \{\!\{\boldsymbol{u}\}\!\})_F + (\{\!\{\boldsymbol{q}\}\!\}, \llbracket \boldsymbol{u} \rrbracket)_F = (\boldsymbol{\mu}, \boldsymbol{g})_{\partial\Omega},
$$

this prove the third equation of (1.8). The fourth equation is true since $p \in L^2_0(\Omega)$ and $\xi \in \mathbb{R}$. This way we conclude that $(\boldsymbol{u}, p, \boldsymbol{\lambda}, \rho) \in \mathbf{V} \times Q \times \boldsymbol{\Lambda} \times \mathbb{R}$ satisfies (1.8) with $\rho = 0$, and

$$
\boldsymbol{\lambda} = \left[(-\nu \nabla \boldsymbol{u} + p\,\boldsymbol{I})\,\boldsymbol{n}^K + \frac{1}{2}\,(\boldsymbol{u} \otimes \boldsymbol{\alpha})\,\boldsymbol{n}^K \right] \Big|_{\partial K} \qquad \text{for all } K \in \mathcal{T}_H.
$$

Reciprocally, let $(\boldsymbol{u}, p, \boldsymbol{\lambda}, 0) \in \mathbf{V} \times Q \times \boldsymbol{\Lambda} \times \mathbb{R}$ the unique solution of (1.8). From the fourth equation of (1.8) we have that $p \in L^2_0(\Omega)$. Let $\boldsymbol{u_g} \in H^1(\Omega)^d$ such that $\boldsymbol{u_g} = \boldsymbol{g}$ on $\partial\Omega$. Then, $\boldsymbol{u} - \boldsymbol{u_g} \in \mathbf{V}$ and using the third equation of (1.8) we have that $(\boldsymbol{\mu}, \boldsymbol{u} - \boldsymbol{u_g})_{\partial \mathcal{T}_H} = 0$ for all $\boldsymbol{\mu} \in \boldsymbol{\Lambda}$. This way, from Lemma 1 in [135], $\boldsymbol{u} - \boldsymbol{u_g} \in H^1_0(\Omega)^d$ and then $\boldsymbol{u} \in H^1(\Omega)^d$ with $\boldsymbol{u} = \boldsymbol{g}$ on $\partial\Omega$. From the second equation of (1.8) and considering $q \in L^2_0(\Omega)$ we get $b(\boldsymbol{u}, q) = 0$. Finally, using Lemma 1 of [135] and the first equation of (1.8) we have that

$$
a(\boldsymbol{u}, \boldsymbol{v}) + b(\boldsymbol{v}, q) = (\boldsymbol{f}, \boldsymbol{v})_{\mathcal{T}_H},
$$

for all $\boldsymbol{v} \in H^1_0(\Omega)^d$, where we used $(\boldsymbol{\lambda}, \boldsymbol{v})_{\partial \mathcal{T}_H} = 0$. Therefore, $(\boldsymbol{u}, p)$ solves (1.3). Uniqueness of (1.8) follows from the uniqueness of (1.3). □

1.2.3 Standard results at local level

For the discrete analysis, we select two local finite dimensional spaces $\mathbf{V}_h(K) \subset \mathbf{V}(K)$ and $Q_h(K) \subset Q(K)$, whose functions are defined over a shape–regular partition of K, denoted by $\{\mathcal{T}_h^K\}_{h>0}$, where h is the characteristic length of $\mathcal{T}_h^K$. Particularly, hereafter we adopt the following polynomial spaces

$$
\mathbf{V}_h(K) := \left\{ \boldsymbol{v}_h \in \mathbf{V}(K) \cap C^0(K)^d : \boldsymbol{v}_h|_\tau \in \mathbb{P}_k(\tau)^d \ \text{ for all } \tau \in \mathcal{T}_h^K \right\}, \tag{1.10}
$$

and

$$Q_h(K) := \left\{ q_h \in Q(K) \cap C^0(K) : q_h|_\tau \in \mathbb{P}_n(\tau) \text{ for all } \tau \in \mathcal{T}_h^K \right\}, \tag{1.11}$$

where $\mathbb{P}_s(\tau)$ is the space of polynomial functions in $\tau \in \mathcal{T}_h^K$, with total degree less than or equal to s, $s \geq 1$. Thus we define the global finite dimensional spaces as

$$\mathbf{V}_h := \bigoplus_{K \in \mathcal{T}_H} \mathbf{V}_h(K) \quad \text{and} \quad Q_h := \bigoplus_{K \in \mathcal{T}_H} Q_h(K).$$

The set of faces ζ of $\mathcal{T}_h^K$ is denoted by

$$\mathcal{E}_h^K := \mathcal{E}_0^K \cup \mathcal{E}_b^K,$$

where $\mathcal{E}_0^K$ is the set of internal faces and $\mathcal{E}_b^K = \mathcal{E}_h^K \setminus \mathcal{E}_0^K$, i.e., $\mathcal{E}_b^K$ are the faces of $\tau \in \mathcal{T}_h^K$ which belong to ∂K. Also, for each $\tau \in \mathcal{T}_h^K$ and $\zeta \in \mathcal{E}_h^K$, we denote by $\mathcal{N}(\tau)$ the set of nodes of τ, $\mathcal{N}(\zeta)$ the set of nodes of ζ, $\mathcal{E}(\tau)$ the set of edges of τ and then we define

$$\omega_\zeta := \bigcup_{\zeta \in \mathcal{E}(\tau')} \tau', \qquad \tilde{\omega}_\tau := \bigcup_{\mathcal{N}(\tau) \cap \mathcal{N}(\tau') \neq \phi} \tau', \qquad \tilde{\omega}_\zeta := \bigcup_{\mathcal{N}(\zeta) \cap \mathcal{N}(\tau') \neq \phi} \tau'.$$

In the rest of this chapter, we will use the following notation

$$\begin{aligned} a \preceq b &\Longleftrightarrow a \leq C\, b, \\ a \succeq b &\Longleftrightarrow a \geq C\, b, \\ a \simeq b &\Longleftrightarrow a \preceq b \text{ and } a \succeq b, \end{aligned}$$

where the positive constant C is independent of any mesh size.

Also, we will use standard bubble functions and some of the results associated with them. For simplicity, we consider the case with $d = 2$, but the same kind of results are valid with $d = 3$.

For all $\tau \in \mathcal{T}_h^K$, we define the element bubble function b_τ^K by

$$b_\tau^K := 27 \prod_{x \in \mathcal{N}(\tau)} \lambda_x,$$

where λ_x corresponds to the barycentric coordinates associated to node x. Let $\hat{\tau}$ be the standard reference element with vertices $\tilde{n}_1 = (1,0)$, $\tilde{n}_2 = (0,1)$ and $\tilde{n}_3 = (0,0)$ and define the edge bubble function by

$$b_{\hat{\zeta}}^{\hat{K}} = 4\hat{\lambda}_3\hat{\lambda}_1,$$

where $\hat{\zeta} := \{(v,0) : v \in [0,1]\}$. For $\zeta \in \mathcal{E}_H$ assume that $\omega_\zeta = \tau_1 \cup \tau_2$ and $G_{\zeta,i}$ be the (orientation preserving) affine transformation defined in Figure 1.1 such that $G_{\zeta,i}(\hat{\tau}) = \tau_i$ and $G_{\zeta,i}(\hat{\zeta}) = \zeta$, with $i = 1,2$. We define the bubble function associated with ζ by

$$b_\zeta^K := \begin{cases} b_{\hat{\zeta}}^{\hat{K}} \circ G_{\zeta,i}^{-1}, & \text{on } \tau_i, \quad i = 1,2, \\ 0 & \text{on } \quad \Omega \setminus \omega_\zeta. \end{cases}$$

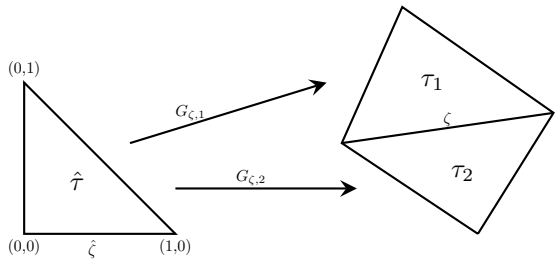

Figure 1.1: Affine transformation $G_{\zeta,i}, i = 1,2$ with $d = 2$.

Let $\hat{\Pi} := \{(x,0) : x \in \mathbb{R}\}$ and let $\hat{Q} : \mathbb{R}^2 \to \hat{\Pi}$ be the orthogonal projection from $\mathbb{R}^2$ to $\hat{\Pi}$. We introduce the lifting operator $\hat{P}_{\hat{\zeta}} : \mathbb{P}_k(\hat{\zeta}) \to \mathbb{P}_k(\hat{\tau})$ given by

$$\hat{s} \longmapsto \hat{P}_{\hat{\zeta}}(\hat{s}) = \hat{s} \circ \hat{Q}.$$

Let $\tau_i \subseteq \omega_\zeta$. We define the lifting operator $P_{\zeta,\tau_i} : \mathbb{P}_k(\zeta) \to \mathbb{P}_k(\tau_i)$ by

$$P_{\zeta,\tau_i}(s) = \hat{P}_{\hat{\zeta}}(s \circ G_{\zeta,i}) \circ G_{\zeta,i}^{-1}.$$

Using these notations, we can define a lifting operator $P_\zeta : \mathbb{P}_k(\zeta) \to \mathbb{P}_k(\omega_\zeta)$ by

$$s \in \mathbb{P}_k(\zeta) \longmapsto P_\zeta(s) := \begin{cases} P_{\zeta,\tau_1}(s) & \text{in } \tau_1, \\ P_{\zeta,\tau_2}(s) & \text{in } \tau_2, \end{cases}$$

for $\boldsymbol{s} = (s_1, s_2) \in \mathbb{P}_k(\zeta)^2$, we define $\boldsymbol{P}_\zeta^K(\boldsymbol{s})$ by

$$\boldsymbol{P}_\zeta^K(\boldsymbol{s}) = (P_\zeta(s_1), P_\zeta(s_2)).$$

The next result can be prove using scaling argument.

Theorem 1.2. *Let $K \in \mathcal{T}_H$ and b_τ^K and b_ζ^K be the bubbles functions corresponding to $\tau \in \mathcal{T}_h^K$ and $\zeta \in \mathcal{E}_h^K$, respectively . Then*

$$\begin{aligned}
&\|\boldsymbol{v}_h\|_{0,\tau}^2 \preceq (b_\tau^K \boldsymbol{v}_h, \boldsymbol{v}_h)_\tau \preceq \|\boldsymbol{v}_h\|_{0,\tau}^2, \\
&\|\boldsymbol{v}_h\|_{0,\tau}^2 \preceq \|b_\tau^K \boldsymbol{v}_h\|_{0,\tau} + h_\tau |b_\tau^K \boldsymbol{v}_h|_{1,\tau} \preceq \|\boldsymbol{v}_h\|_{0,\tau}, \\
&\|\boldsymbol{v}_h\|_{0,\zeta}^2 \preceq (b_\zeta^K \boldsymbol{v}_h, \boldsymbol{v}_h)_\zeta \preceq \|\boldsymbol{v}_h\|_{0,\zeta}^2, \\
&h_\tau^{-1/2} \|b_\zeta^K \boldsymbol{v}_h\|_{0,\tau} + h_\tau^{1/2} |b_\zeta^K \boldsymbol{v}_h|_{1,\tau} \preceq \|\boldsymbol{v}_h\|_{0,\zeta},
\end{aligned}$$

for all $\boldsymbol{v}_h \in \mathbb{P}_n(\mathcal{T}_h^K)$, $n \geq 0$.

Proof. See Theorem 2.2 and Theorem 2.4 in [9]. □

Lemma 1.1. *We have that*

$$\|\boldsymbol{v}\|_{0,F}^2 \preceq H_F \left\{ H_K^{-2} \|\boldsymbol{v}\|_{0,K}^2 + |\boldsymbol{v}|_{1,K}^2 \right\},$$

for all $K \in \mathcal{T}_H$, $F \subset \partial K$ and $\boldsymbol{v} \in \mathbf{V}(K)$.

Proof. See Theorem 3.10 in [4] or (10.3.8) in [43]. □

Theorem 1.3. *For all $q \in Q(K)$, we have that*

$$\sup_{\boldsymbol{v}\in\mathbf{V}(K)} \frac{b_K(\boldsymbol{v},q)}{\|\boldsymbol{v}\|_{\mathbf{V}(K)}} \succeq \|q\|_{Q(K)}.$$

Proof. See Theorem 2.1 in [19]. □

For each $K \in \mathcal{T}_H$, we denote by $\mathcal{C}_h^K : \mathbf{V}(K) \to \mathbf{V}_1^K$, the Clément interpolation operator, where

$$\mathbf{V}_1^K := \left\{ \boldsymbol{v}_h \in C(K)^d : \boldsymbol{v}_h \in \mathbb{P}_1(\tau)^d,\ \forall\, \tau \in \mathcal{T}_h^K \right\}.$$

For all $\tau \in \mathcal{T}_h^K$ and all $\zeta \in \mathcal{E}_h^K$, this operator satisfies the following estimates (see [60], [75])

$$\begin{aligned} \|\mathcal{C}_h^K(\boldsymbol{v})\|_{0,\tau} &\preceq \|\boldsymbol{v}\|_{0,\tilde{\omega}_\tau}, \\ \|\boldsymbol{v} - \mathcal{C}_h^K(\boldsymbol{v})\|_{0,\tau} &\preceq h_\tau |\boldsymbol{v}|_{1,\tilde{\omega}_\tau}, \\ \|\boldsymbol{v} - \mathcal{C}_h^K(\boldsymbol{v})\|_{0,\zeta} &\preceq h_\zeta^{1/2} |\boldsymbol{v}|_{1,\tilde{\omega}_\zeta}, \end{aligned} \tag{1.12}$$

for all $\boldsymbol{v} \in \mathbf{V}(K)$.

1.3 The MHM method

In this section, we present the MHM method as a consequence of a characterization of the exact solution in terms of a local–global system equivalent to (1.8).

1.3.1 Characterizing the exact solution

The goal of the Multiscale Hybrid-Mixed approach is to take advantage of the local nature of problem (1.8), by decomposing it into independent local problems coupled with a face-based global problem. Using these ideas, the hybrid formulation (1.8) is equivalently to: *Find* $(\boldsymbol{u}, p, \boldsymbol{\lambda}, \rho) \in \mathbf{V} \times Q \times \boldsymbol{\Lambda} \times \mathbb{R}$ *such that*

$$\begin{cases} (\boldsymbol{\mu}, \boldsymbol{u})_{\partial\mathcal{T}_H} = \langle \boldsymbol{\mu}, \boldsymbol{g} \rangle_{\partial\Omega} & \text{for all } \boldsymbol{\mu} \in \boldsymbol{\Lambda}, \\ (\xi, p)_\Omega = 0 & \text{for all } \xi \in \mathbb{R}, \end{cases} \tag{1.13}$$

$$\begin{cases} a(\boldsymbol{u}, \boldsymbol{v}) + b(\boldsymbol{v}, p) + (\boldsymbol{\lambda}, \boldsymbol{v})_{\partial\mathcal{T}_H} = (\boldsymbol{f}, \boldsymbol{v})_{\mathcal{T}_H} & \text{for all } \boldsymbol{v} \in \mathbf{V}, \\ b(\boldsymbol{u}, q) + (\rho, q)_\Omega = 0 & \text{for all } q \in Q. \end{cases} \tag{1.14}$$

Note that system (1.14) can be localized in each $K \in \mathcal{T}_H$ by testing (1.13)-(1.14) with $(\boldsymbol{v}, q, \boldsymbol{\mu}, \xi) = (\boldsymbol{v}|_K, q|_K, \mathbf{0}, 0)$. This gives us

$$\begin{cases} a_K(\boldsymbol{u}, \boldsymbol{v}) + b_K(\boldsymbol{v}, p) = -\langle \boldsymbol{\lambda}, \boldsymbol{v} \rangle_{\partial K} + (\boldsymbol{f}, \boldsymbol{v})_K & \text{for all } \boldsymbol{v} \in \mathbf{V}(K), \\ b_K(\boldsymbol{u}, q) = -(\rho, q)_K & \text{for all } q \in Q(K). \end{cases} \tag{1.15}$$

Also from (1.15), $(\boldsymbol{u}, p)$ can be computed in terms of $\boldsymbol{\lambda}$ and ρ . Specifically, owing to the linearity of problem (1.15), the exact solution decompose as follows

$$\boldsymbol{u} = \boldsymbol{u}^{\boldsymbol{\lambda}} + \boldsymbol{u}^{\boldsymbol{f}} + \boldsymbol{u}^{\rho} \quad \text{and} \quad p = p^{\boldsymbol{\lambda}} + p^{\boldsymbol{f}} + p^{\rho}, \tag{1.16}$$

where the functions used in (1.16) are given by:

- $(\boldsymbol{u}^{\boldsymbol{\lambda}},p^{\boldsymbol{\lambda}})\in\mathbf{V}\times Q$ such that $\boldsymbol{u}^{\boldsymbol{\lambda}}|_K$ and $p^{\boldsymbol{\lambda}}|_K$ satisfy

$$\begin{cases} a_K(\boldsymbol{u}^{\boldsymbol{\lambda}},\boldsymbol{w})+b_K(\boldsymbol{w},p^{\boldsymbol{\lambda}})=-\langle\boldsymbol{\lambda},\boldsymbol{w}\rangle_{\partial K} & \text{for all } \boldsymbol{w}\in\mathbf{V}(K),\\ b_K(\boldsymbol{u}^{\boldsymbol{\lambda}},q)=0 & \text{for all } q\in Q(K); \end{cases} \tag{1.17}$$

- $(\boldsymbol{u}^{\boldsymbol{f}},p^{\boldsymbol{f}})\in\mathbf{V}\times Q$ such that $\boldsymbol{u}^{\boldsymbol{f}}|_K$ and $p^{\boldsymbol{f}}|_K$ satisfy

$$\begin{cases} a_K(\boldsymbol{u}^{\boldsymbol{f}},\boldsymbol{w})+b_K(\boldsymbol{w},p^{\boldsymbol{f}})=(\boldsymbol{f},\boldsymbol{w})_K & \text{for all } \boldsymbol{w}\in\mathbf{V}(K),\\ b_K(\boldsymbol{u}^{\boldsymbol{f}},q)=0 & \text{for all } q\in Q(K); \end{cases} \tag{1.18}$$

- $(\boldsymbol{u}^{\rho},p^{\rho})\in\mathbf{V}\times Q$ such that $\boldsymbol{u}^{\rho}|_K$ and $p^{\rho}|_K$ satisfy

$$\begin{cases} a_K(\boldsymbol{u}^{\rho},\boldsymbol{w})+b_K(\boldsymbol{w},p^{\rho})=0 & \text{for all } \boldsymbol{w}\in\mathbf{V}(K),\\ b_K(\boldsymbol{u}^{\rho},q)=-(\rho,q)_K & \text{for all } q\in Q(K). \end{cases} \tag{1.19}$$

Next, testing (1.13) with $(\boldsymbol{v},q,\boldsymbol{\mu},\xi)=(\mathbf{0},0,\boldsymbol{\mu},\xi)$ and using (1.16), we obtain the following global problem: *Find* $(\boldsymbol{\lambda},\rho)\in\boldsymbol{\Lambda}\times\mathbb{R}$ *such that*

$$\begin{cases} (\boldsymbol{\mu},\boldsymbol{u}^{\boldsymbol{\lambda}}+\boldsymbol{u}^{\rho})_{\partial\mathcal{T}_H}=(\boldsymbol{\mu},\boldsymbol{g})_{\partial\Omega}-(\boldsymbol{\mu},\boldsymbol{u}^{\boldsymbol{f}})_{\partial\mathcal{T}_H}, & \forall\boldsymbol{\mu}\in\boldsymbol{\Lambda}\\ (\xi,p^{\boldsymbol{\lambda}}+p^{\rho})_{\Omega}=-(\xi,p^{\boldsymbol{f}})_{\Omega}, & \forall\xi\in\mathbb{R}, \end{cases} \tag{1.20}$$

for all $\boldsymbol{\mu}\in\boldsymbol{\Lambda}$ and $\xi\in\mathbb{R}$.

Remark 1.3. *Following [16], it is possible to prove that* $\rho=0$*, and therefore* (1.16) *reduces to*

$$\boldsymbol{u}=\boldsymbol{u}^{\boldsymbol{\lambda}}+\boldsymbol{u}^{\boldsymbol{f}} \quad \textit{and} \quad p=p^{\boldsymbol{\lambda}}+p^{\boldsymbol{f}}. \tag{1.21}$$

We define a local bilinear form B_K given by

$$B_K((\boldsymbol{w},r),(\boldsymbol{v},q)):=a_K(\boldsymbol{w},\boldsymbol{v})+b_K(\boldsymbol{v},r)-b_K(\boldsymbol{w},q), \tag{1.22}$$

with $(\boldsymbol{w},r),(\boldsymbol{v},q)\in\mathbf{V}(K)\times Q(K)$, and naturally we denote

$$B((\boldsymbol{w},r),(\boldsymbol{v},q)):=\sum_{K\in\mathcal{T}_H}B_K((\boldsymbol{w},r),(\boldsymbol{v},q)).$$

Theorem 1.4. *We have that local problems* (1.17)–(1.19) *are well–posed, and it holds*

$$\|(\boldsymbol{w},r)\|_{\mathbf{V}(K)\times Q(K)}\preceq\sup_{(\boldsymbol{v},q)\in\mathbf{V}(K)\times Q(K)}\frac{B_K((\boldsymbol{w},r),(\boldsymbol{v},q))}{\|(\boldsymbol{v},q)\|_{\mathbf{V}(K)\times Q(K)}}.$$

Proof. Thanks to Theorem 1.3 we have an inf–sup condition for $b_K(\cdot,\cdot)$, and using the ellipticity of $a_K(\cdot,\cdot)$, give in (1.7), the result follows. □

Remark 1.4. *From* (1.7) *the coercivity of* $a_K(\cdot,\cdot)$ *over* $\mathbf{V}(K)$ *holds. Then, using Theorem 1.3, and the inf–sup condition the well-posedness of* (1.17)–(1.20) *follows. Next, using Theorem 1.4 and the Riesz Representation Theorem, the bilinear form* B *satisfies a global inf–sup condition with a constant independent of* H *and* h*, and only depending on* d_Ω*, and* d*, respectively.*

1.3.2 The method

The characterization of the exact solution $(\boldsymbol{u},p)$ in terms of the global–local system (1.17)–(1.20) yield the MHM method. Consider a finite dimensional space $\boldsymbol{\Lambda}_H$ of $\boldsymbol{\Lambda}$ such that

$$\boldsymbol{\Lambda}_0 \subseteq \boldsymbol{\Lambda}_H \subset \boldsymbol{\Lambda} \cap L^2(\mathcal{E}_H)^d,$$

with

$$\boldsymbol{\Lambda}_0 := \left\{ \boldsymbol{\sigma}\boldsymbol{n}^K|_F \in \mathbb{P}_0(F)^d \text{ for all } F \subset \partial K,\ K \in \mathcal{T}_H : \boldsymbol{\sigma} \in H(\mathrm{div};\Omega) \right\},$$

where $\mathbb{P}_0(F)$ is the space of constant polynomial defined on F. In this chapter, we search for approximating Lagrange multipliers in the space spanned by piecewise polynomial functions, i.e.,

$$\boldsymbol{\Lambda}_H = \boldsymbol{\Lambda}_l := \left\{ \boldsymbol{\mu} \in \boldsymbol{\Lambda} \,:\, \boldsymbol{\mu}|_{\tilde{F}} \in \mathbb{P}_l(\tilde{F})^d,\ \tilde{F} \in \mathcal{T}_{\tilde{H}}(F),\ \text{ for all } F \subset \partial K,\ K \in \mathcal{T}_H \right\},$$

where $\mathbb{P}_l(F)$ is the space of piecewise polynomial functions on F of degree less than or equal $l \geq 0$.

Unlike the usual interpolation choice [135], the functions in $\boldsymbol{\Lambda}_H$ may be discontinuous on faces $F \in \mathcal{E}_H$. Such a choice preserves the conformity of the MHM method and turns out to be central to maintaining the quality of the approximation when coefficients jump across faces. This will be explored in the numerical section.

Specifically, the solution of (1.20) is approximated by $(\boldsymbol{\lambda}_H,\rho_H) \in \boldsymbol{\Lambda}_H \times \mathbb{R}$, which is the solution to the *one-level MHM method*

$$\begin{cases} (\boldsymbol{\mu}_H, \boldsymbol{u}^{\boldsymbol{\lambda}_H} + \boldsymbol{u}^{\rho_H})_{\partial\mathcal{T}_H} = (\boldsymbol{\mu}_H, \boldsymbol{g})_{\partial\Omega} - (\boldsymbol{\mu}_H, \boldsymbol{u}^{\boldsymbol{f}})_{\partial\mathcal{T}_H}, \\ (\xi_H, p^{\boldsymbol{\lambda}_H} + p^{\rho_H})_\Omega = -(\xi_H, p^{\boldsymbol{f}})_\Omega, \end{cases} \tag{1.23}$$

for all $\boldsymbol{\mu}_H \in \boldsymbol{\Lambda}_H$ and $\xi_H \in \mathbb{R}$, where $\boldsymbol{u}^{\boldsymbol{\lambda}_H}, \boldsymbol{u}^{\boldsymbol{f}}, \boldsymbol{u}^{\rho_H}$ and pressures $p^{\boldsymbol{\lambda}_H}, p^{\boldsymbol{f}}, p^{\rho_H}$ solve (1.17)–(1.19). Thus, the *one level* solution $(\boldsymbol{u}_H,p_H)$ is given through the expressions

$$\boldsymbol{u}_H := \boldsymbol{u}^{\boldsymbol{\lambda}_H} + \boldsymbol{u}^{\boldsymbol{f}} + \boldsymbol{u}^{\rho_H} \quad \text{and} \quad p_H := p^{\boldsymbol{\lambda}_H} + p^{\boldsymbol{f}} + p^{\rho_H}.$$

Note that to make the one level MHM method effective, we need to solve local problems (1.17)–(1.19), exactly, which is, en general, not possible. To overcome this, we introduce the *two-level MHM method* which consists of: *Find* $(\boldsymbol{\lambda}_H,\rho_H) \in \boldsymbol{\Lambda}_H \times \mathbb{R}$ *such that*

$$\begin{cases} (\boldsymbol{\mu}_H, \boldsymbol{u}_h^{\boldsymbol{\lambda}_H} + \boldsymbol{u}_h^{\rho_H})_{\partial\mathcal{T}_H} = (\boldsymbol{\mu}_H, \boldsymbol{g})_{\partial\Omega} - (\boldsymbol{\mu}_H, \boldsymbol{u}_h^{\boldsymbol{f}})_{\partial\mathcal{T}_H}, \\ (\xi_H, p_h^{\boldsymbol{\lambda}_H} + p_h^{\rho_H})_\Omega = -(\xi_H, p_h^{\boldsymbol{f}})_\Omega, \end{cases} \tag{1.24}$$

for all $(\boldsymbol{\mu}_H,\xi_H) \in \boldsymbol{\Lambda}_H \times \mathbb{R}$. In this chapter, we adopt a stabilized finite element method [25] to approximate the solution of the local problems (1.17)–(1.19) computing the approximated velocities $\boldsymbol{u}_h^{\boldsymbol{\lambda}_H}, \boldsymbol{u}_h^{\boldsymbol{f}}, \boldsymbol{u}_h^{\rho_H}$ and pressures $p_h^{\boldsymbol{\lambda}_H}, p_h^{\boldsymbol{f}}, p_h^{\rho_H}$.

As such, the two-level discrete solution $(\boldsymbol{u}_{H,h},p_{H,h})$ is given through the expressions

$$\boldsymbol{u}_{H,h} := \boldsymbol{u}_h^{\boldsymbol{\lambda}_H} + \boldsymbol{u}_h^{\boldsymbol{f}} + \boldsymbol{u}_h^{\rho_H} \quad \text{and} \quad p_{H,h} := p_h^{\boldsymbol{\lambda}_H} + p_h^{\boldsymbol{f}} + p_h^{\rho_H}.$$

Such a choice makes the appealing option of using equal-order nodal pairs of interpolation spaces for the velocity and the pressure variables (i.e. $k = n$ in (1.10) and (1.11)) as the

second–level solver. For completeness, we recall (see [25] for details) that this scheme consists of: *Find* $(\boldsymbol{u},p)\in \mathbf{V}_h(K)\times Q_h(K)$ *such that*

$$B_K^s((\boldsymbol{u},p),(\boldsymbol{v},q)) = F_K^s(\boldsymbol{v},q) \quad \text{for all } (\boldsymbol{v},q)\in \mathbf{V}_h(K)\times Q_h(K), \tag{1.25}$$

where

$$\begin{aligned} B_K^s((\boldsymbol{u},p),(\boldsymbol{v},q)) := B_K((\boldsymbol{u},p),(\boldsymbol{v},q)) + \sum_{\tau\in\mathcal{T}_h^K} \kappa_\tau(\nabla\cdot\boldsymbol{u},\nabla\cdot\boldsymbol{v})_\tau \\ - \sum_{\tau\in\mathcal{T}_h^K} \delta_\tau(-\nu\Delta\boldsymbol{u}+(\nabla\boldsymbol{u})\boldsymbol{\alpha}+\gamma\boldsymbol{u}+\nabla p,-\nu\Delta\boldsymbol{v}-(\nabla\boldsymbol{v})\boldsymbol{\alpha}+\gamma\boldsymbol{v}-\nabla q)_\tau, \end{aligned}$$

and

$$F_K^s(\boldsymbol{v},q) := F_K(\boldsymbol{v},q) - \sum_{\tau\in\mathcal{T}_h^K} \delta_\tau(\boldsymbol{f},-\nu\Delta\boldsymbol{v}-(\nabla\boldsymbol{v})\boldsymbol{\alpha}+\gamma\boldsymbol{v}-\nabla q)_\tau.$$

The stabilization parameters are given by

$$\kappa_\tau := \|\boldsymbol{\alpha}\|_{\infty,\tau}\, h_\tau \min\{1,Pe_\tau^2\}, \quad \text{and} \quad \delta_\tau := \frac{h_\tau^2}{\gamma h_\tau^2 \max\left\{1,Pe_\tau^1\right\} + \frac{4\nu}{m_\tau}\max\left\{1,Pe_\tau^2\right\}}, \tag{1.26}$$

where the local *Péclet* numbers are defined by

$$Pe_\tau^1 := \frac{4\nu}{\gamma h_\tau^2 m_\tau} \quad \text{and} \quad Pe_\tau^2 := \frac{m_\tau\|\boldsymbol{\alpha}\|_{\infty,\tau}h_\tau}{4\nu}.$$

and $m_\tau := \min\left\{\frac{1}{3},C_k\right\}$ with

$$C_k\, h_\tau^2\, \|\Delta\boldsymbol{v}\|_{0,\tau}^2 \le \|\nabla\boldsymbol{v}\|_{0,\tau}^2 \quad \text{for all } \boldsymbol{v}\in\mathbf{V}_h(K). \tag{1.27}$$

Here C_k is a constant that depends only on d and the polynomial degree chosen for the velocity (see [81]).

Owing to definitions (3.28)–(1.27), the local solutions in (1.17)–(1.19) are approximated, in each $K\in\mathcal{T}_H$, by the solutions of the following discrete problems:

- *Find* $(\boldsymbol{u}_h^{\boldsymbol{\lambda}_H},p_h^{\boldsymbol{\lambda}_H})\in\mathbf{V}_h(K)\times Q_h(K)$ *such that*

$$B_K^s((\boldsymbol{u}_h^{\boldsymbol{\lambda}_H},p_h^{\boldsymbol{\lambda}_H}),(\boldsymbol{v},q)) = -\langle\boldsymbol{\lambda}_H,\boldsymbol{v}\rangle_{\partial K} \quad \text{for all } (\boldsymbol{v},q)\in\mathbf{V}_h(K)\times Q_h(K); \tag{1.28}$$

- *Find* $(\boldsymbol{u}_h^{\boldsymbol{f}},p_h^{\boldsymbol{f}})\in\mathbf{V}_h(K)\times Q_h(K)$ *such that*

$$B_K^s((\boldsymbol{u}_h^{\boldsymbol{f}},p_h^{\boldsymbol{f}}),(\boldsymbol{v},q)) = F_K^s(\boldsymbol{v},q) \quad \text{for all } (\boldsymbol{v},q)\in\mathbf{V}_h(K)\times Q_h(K); \tag{1.29}$$

- *Find* $(\boldsymbol{u}_h^{\rho_H},p_h^{\rho_H})\in\mathbf{V}_h(K)\times Q_h(K)$ *such that*

$$B_K^s((\boldsymbol{u}_h^{\rho_H},p_h^{\rho_H}),(\boldsymbol{v},q)) = (\rho_H,q)_K \quad \text{for all } (\boldsymbol{v},q)\in\mathbf{V}_h(K)\times Q_h(K). \tag{1.30}$$

Remark 1.5. *As in the continuous case, in the discrete case we can prove that* $\rho_H = 0$*, following the same ideas from [16] and hence the solutions of the one-level and two-level MHM methods, can be characterized as follows*

$$\boldsymbol{u}_H := \boldsymbol{u}^{\boldsymbol{\lambda}_H} + \boldsymbol{u}^{\boldsymbol{f}} \quad \textit{and} \quad p_H := p^{\boldsymbol{\lambda}_H} + p^{\boldsymbol{f}}, \tag{1.31}$$

$$\boldsymbol{u}_{H,h} := \boldsymbol{u}_h^{\boldsymbol{\lambda}_H} + \boldsymbol{u}_h^{\boldsymbol{f}} \quad \textit{and} \quad p_{H,h} := p_h^{\boldsymbol{\lambda}_H} + p_h^{\boldsymbol{f}}. \tag{1.32}$$

1.4 A multiscale a posteriori error estimator

In this section, we define a two–level residual error estimator. Let η_1 be the *first–level a posteriori error estimator*, given by

$$\eta_1 := \left\{ \sum_{K\in\mathcal{T}_H} \sum_{F\subset\partial K} \eta_{1,F}^2 \right\}^{1/2},$$

where

$$\eta_{1,F} := \frac{\|\boldsymbol{R}_F\|_{0,F}}{H_F^{1/2}},$$

with

$$\boldsymbol{R}_F := \begin{cases} -\frac{1}{2}\left[\!\left[\boldsymbol{u}_{H,h}\right]\!\right], & F\in\mathcal{E}_0, \\ \\ \boldsymbol{g}-\boldsymbol{u}_{H,h}, & F\in\mathcal{E}_H\setminus\mathcal{E}_0. \end{cases}$$

Recalling that, $\left\{\mathcal{T}_h^K\right\}_{h>0}$ is a regular family of triangulations of $K\in\mathcal{T}_H$, we define residuals over each $\tau\in\mathcal{T}_h^K$ and $\zeta\in\mathcal{E}_h^K$, respectively, as follows:

$$\boldsymbol{R}_\tau^K := \left(\nu\Delta\boldsymbol{u}_{H,h} - (\nabla\boldsymbol{u}_{H,h})\boldsymbol{\alpha} - \gamma\boldsymbol{u}_{H,h} - \nabla p_{H,h} + \boldsymbol{f}\right)|_\tau,$$

and

$$\boldsymbol{R}_\zeta^K := \begin{cases} \left[\!\left[-\nu\dfrac{\partial\boldsymbol{u}_{H,h}}{\partial\boldsymbol{n}_\zeta^\tau} + p_{H,h}\boldsymbol{n}_\zeta^\tau + \dfrac{1}{2}(\boldsymbol{u}_{H,h}\otimes\boldsymbol{\alpha})\boldsymbol{n}_\zeta^\tau \right]\!\right] & \text{on } \zeta\in\mathcal{E}_0^K, \\ -\boldsymbol{\lambda}_H - \nu\dfrac{\partial\boldsymbol{u}_{H,h}}{\partial\boldsymbol{n}_\zeta^\tau} + p_{H,h}\boldsymbol{n}_\zeta^\tau + \dfrac{1}{2}(\boldsymbol{u}_{H,h}\otimes\boldsymbol{\alpha})\boldsymbol{n}_\zeta^\tau & \text{on } \zeta\in\mathcal{E}_b^K. \end{cases}$$

Its global version reads

$$\eta_{2,K} := \left\{ \sum_{\tau\in\mathcal{T}_h^K} \left(h_\tau^2\|\boldsymbol{R}_\tau^K\|_{0,\tau}^2 + \|\nabla\cdot\boldsymbol{u}_{H,h}\|_{0,\tau}^2 \right) + \sum_{\zeta\in\mathcal{E}_h^K} h_\zeta\|\boldsymbol{R}_\zeta^K\|_{0,\zeta}^2 \right\}^{1/2}, \tag{1.33}$$

and, thus, the *global second–level estimator* is defined by

$$\eta_2 := \frac{1}{2^{2l}}\left[\sum_{K\in\mathcal{T}_H} \eta_{2,K}^2 \right]^{1/2},$$

where l is the polynomial degree on faces. Summing up first and second level contributions, the global a posteriori error estimator η reads

$$\eta := \eta_1 + \eta_2. \tag{1.34}$$

1.4.1 Technical results

In this subsection, we introduce some technical results that will be useful to establish our main results. First, we present a residual functional which can be characterized in terms of local residuals on each $\tau\in\mathcal{T}_h^K$ and $\zeta\in\mathcal{E}_h^K$.

Lemma 1.2. *Let $(\boldsymbol{u}_{H,h}, p_{H,h})$ be the solution from two-level MHM method given by (1.32). Define the local residual functional $\boldsymbol{R}_h : \mathbf{V}(K) \to \mathbb{R}$, by*

$$\boldsymbol{R}_h(\boldsymbol{v}) := (\boldsymbol{f}, \boldsymbol{v})_K - \langle \boldsymbol{\lambda}_H, \boldsymbol{v} \rangle_{\partial K} - a_K(\boldsymbol{u}_{H,h}, \boldsymbol{v}) - b_K(p_{H,h}, \boldsymbol{v}),$$

for all $\boldsymbol{v} \in \mathbf{V}(K)$. Then,

$$\boldsymbol{R}_h(\boldsymbol{v}) = \sum_{\tau \in \mathcal{T}_h^K} (\boldsymbol{R}_\tau^K, \boldsymbol{v})_\tau + \sum_{\zeta \in \mathcal{E}_h^K} (\boldsymbol{R}_\zeta^K, \boldsymbol{v})_\zeta,$$

for all $\boldsymbol{v} \in \mathbf{V}(K)$.

Proof. Using the identity (1.4) on each $\tau \in \mathcal{T}_h^K$, equations (1.17) and (1.18), and integrating by parts, we have that

$$\begin{aligned}
\boldsymbol{R}_h(\boldsymbol{v}) &= -\langle \boldsymbol{\lambda}_H, \boldsymbol{v} \rangle_{\partial K} + (\boldsymbol{f}, \boldsymbol{v})_K - (\nu \nabla \boldsymbol{u}_{H,h}, \boldsymbol{v})_K - \frac{1}{2}((\nabla \boldsymbol{u}_{H,h})\boldsymbol{\alpha}, \boldsymbol{v})_K \\
&\quad + \frac{1}{2}(\boldsymbol{u}_{H,h}, (\nabla \boldsymbol{v})\boldsymbol{\alpha})_K - (\gamma_0 \boldsymbol{u}_{H,h}, \boldsymbol{v})_K + (\nabla \cdot \boldsymbol{v}, p_{H,h})_K \\
&= -\langle \boldsymbol{\lambda}_H, \boldsymbol{v} \rangle_{\partial K} + \sum_{\tau \in \mathcal{T}_h^K} \Bigg[(\boldsymbol{f}, \boldsymbol{v})_\tau - (\nu \nabla \boldsymbol{u}_{H,h}, \boldsymbol{v})_\tau - \frac{1}{2}((\nabla \boldsymbol{u}_{H,h})\boldsymbol{\alpha}, \boldsymbol{v})_\tau \\
&\quad + \frac{1}{2}(\boldsymbol{u}_{H,h}, (\nabla \boldsymbol{v})\boldsymbol{\alpha})_\tau - (\gamma_0 \boldsymbol{u}_{H,h}, \boldsymbol{v}) + (\nabla \cdot \boldsymbol{v}, p_{H,h})_\tau \Bigg] \\
&= -\langle \boldsymbol{\lambda}_H, \boldsymbol{v} \rangle_{\partial K} + \sum_{\tau \in \mathcal{T}_h^K} \Bigg[(\boldsymbol{f}, \boldsymbol{v})_\tau + (\nu \Delta \boldsymbol{u}_{H,h}, \boldsymbol{v})_\tau \\
&\quad - \left(\frac{\partial \boldsymbol{u}_{H,h}}{\partial \boldsymbol{n}^\tau}, \boldsymbol{v} \right)_{\partial \tau} - ((\nabla \boldsymbol{u}_{H,h})\boldsymbol{\alpha}, \boldsymbol{v})_\tau - \frac{1}{2}((\nabla \cdot \boldsymbol{\alpha})\boldsymbol{u}_{H,h}, \boldsymbol{v})_\tau + \frac{1}{2}((\boldsymbol{\alpha} \cdot \boldsymbol{n}^\tau)\boldsymbol{u}_{H,h}, \boldsymbol{v})_{\partial \tau} \\
&\quad - \left(\left(\gamma - \frac{1}{2}(\nabla \cdot \boldsymbol{\alpha}) \right) \boldsymbol{u}_{H,h}, \boldsymbol{v} \right)_\tau - (\nabla p_{H,h}, \boldsymbol{v})_\tau + (p_{H,h} \boldsymbol{n}^\tau, \boldsymbol{v})_{\partial \tau} \Bigg] \\
&= \sum_{\zeta \in \mathcal{E}_0^K} \left(\left[\left[-\nu \frac{\partial \boldsymbol{u}_{H,h}}{\partial \boldsymbol{n}_\zeta^\tau} + p_{H,h} \boldsymbol{n}_\zeta^\tau + \frac{1}{2}(\boldsymbol{\alpha} \cdot \boldsymbol{n}_\zeta^\tau)\boldsymbol{u}_{H,h} \right] \right], \boldsymbol{v} \right) \\
&\quad + \sum_{\zeta \in \mathcal{E}_b^K} \left(-\boldsymbol{\lambda}_H - \nu \frac{\partial \boldsymbol{u}_{H,h}}{\partial \boldsymbol{n}_\zeta^\tau} + p_{H,h} \boldsymbol{n}_\zeta^\tau + \frac{1}{2}(\boldsymbol{\alpha} \cdot \boldsymbol{n}_\zeta^\tau)\boldsymbol{u}_{H,h}, \boldsymbol{v} \right) + \sum_{\tau \in \mathcal{T}_h^K} (\boldsymbol{R}_\tau^K, \boldsymbol{v})_\tau \\
&= \sum_{\tau \in \mathcal{T}_h^K} (\boldsymbol{R}_\tau^K, \boldsymbol{v})_\tau + \sum_{\zeta \in \mathcal{E}_h^K} (\boldsymbol{R}_\zeta^K, \boldsymbol{v})_\zeta,
\end{aligned}$$

which conclude the proof. □

The following result gives us a bound for the norm of the difference between the one- and two-level MHM solutions $(\boldsymbol{u}_H, p_H)$ and $(\boldsymbol{u}_{H,h}, p_{H,h})$, respectively. As expected, such estimates depend on the approximation property of the second level solver.

Lemma 1.3. *Let* $(\boldsymbol{u}_H, p_H)$ *and* $(\boldsymbol{u}_{H,h}, p_{H,h})$*, be given in* (1.31) *and* (1.32)*, respectively. Then*

$$\|(\boldsymbol{u}_H - \boldsymbol{u}_{H,h}, p_H - p_{H,h})\|_{\mathbf{V}(K)\times Q(K)} \preceq \eta_{2,K},$$

for all $K \in \mathcal{T}_H$.

Proof. Let $(e_h^{\boldsymbol{u}}, e_h^p) := (\boldsymbol{u}_H - \boldsymbol{u}_{H,h}, p_H - p_{H,h})$. From (1.17), (1.18), (1.22), and Lemma 1.2, we have

$$\begin{aligned} B_K((e_h^{\boldsymbol{u}}, e_h^p), (\boldsymbol{v}, q)) &= B_K((\boldsymbol{u}_H, p_H), (\boldsymbol{v}, q)) - B_K((\boldsymbol{u}_{H,h}, p_{H,h}), (\boldsymbol{v}, q)) \\ &= -\langle \boldsymbol{\lambda}_H, \boldsymbol{v}\rangle_{\partial K} + (\boldsymbol{f}, \boldsymbol{v})_K - B_K((\boldsymbol{u}_{H,h}, p_{H,h}), (\boldsymbol{v}, q)) \\ &= \boldsymbol{R}_h(\boldsymbol{v}) + b_K(\boldsymbol{u}_{H,h}, q) \\ &= \sum_{\tau\in\mathcal{T}_h^K} \left[(\boldsymbol{R}_\tau^K, \boldsymbol{v})_\tau - (\nabla\cdot\boldsymbol{u}_{H,h}, q)_\tau \right] + \sum_{\zeta\in\mathcal{E}_h^K} (\boldsymbol{R}_\zeta^K, \boldsymbol{v})_\zeta, \end{aligned} \tag{1.35}$$

for all $\boldsymbol{v} \in \mathbf{V}(K)$ and $q \in Q(K)$. For $K \in \mathcal{T}_H$, let $\boldsymbol{v}_h := \mathcal{C}_h^K(\boldsymbol{v})$ with $\boldsymbol{v} \in \mathbf{V}(K)$. Then, replacing $\boldsymbol{v}$ by $\boldsymbol{v} - \boldsymbol{v}_h$ in (1.35) and using Cauchy–Schwarz inequality, we get

$$\begin{aligned} &B_K((e_h^{\boldsymbol{u}}, e_h^p), (\boldsymbol{v} - \boldsymbol{v}_h, q)) \\ &\le \sum_{\tau\in\mathcal{T}_h^K} \left[\|\boldsymbol{R}_\tau^K\|_{0,\tau}\|\boldsymbol{v} - \boldsymbol{v}_h\|_{0,\tau} + \|\nabla\cdot\boldsymbol{u}_{H,h}\|_{0,\tau}\|q\|_{0,\tau} \right] + \sum_{\zeta\in\mathcal{E}_h^K} \|\boldsymbol{R}_\zeta^K\|_{0,\zeta}\|\boldsymbol{v} - \boldsymbol{v}_h\|_{0,\zeta}. \end{aligned} \tag{1.36}$$

On other hand, using (1.22), (1.28) and (1.29), and taking $(\boldsymbol{v}, q) = (\boldsymbol{v}_h, 0)$, we get

$$\begin{aligned} &B_K((e_h^{\boldsymbol{u}}, e_h^p), (\boldsymbol{v}_h, 0)) \\ &= a_K(\boldsymbol{u}_H - \boldsymbol{u}_{H,h}, \boldsymbol{v}_h) + b_K(\boldsymbol{v}_h, p_H - p_{H,h}) \\ &= a_K(\boldsymbol{u}_H, \boldsymbol{v}_h) + b_K(\boldsymbol{v}_h, p_H) - \left[a_K(\boldsymbol{u}_{H,h}, \boldsymbol{v}_h) + b_K(\boldsymbol{v}_h, p_{H,h}) \right] \\ &= -\langle \boldsymbol{\lambda}_H, \boldsymbol{v}_h\rangle_{\partial K} + (\boldsymbol{f}, \boldsymbol{v}_h)_K - \left[a_K(\boldsymbol{u}_h^{\boldsymbol{\lambda}_H}, \boldsymbol{v}_h) + b_K(\boldsymbol{v}_h, p_h^{\boldsymbol{\lambda}_H}) \right. \\ &\quad \left. + a_K(\boldsymbol{u}_h^{\boldsymbol{f}}, \boldsymbol{v}_h) + b_K(\boldsymbol{v}_h, p_h^{\boldsymbol{f}}) \right] \\ &= \sum_{\tau\in\mathcal{T}_h^K} \delta_\tau(\nu\Delta\boldsymbol{u}_{H,h} - (\nabla\boldsymbol{u}_{H,h})\boldsymbol{\alpha} - \gamma\boldsymbol{u}_{H,h} - \nabla p_{H,h} + \boldsymbol{f}, -\nu\Delta\boldsymbol{v}_h - (\nabla\boldsymbol{v}_h)\boldsymbol{\alpha} + \gamma\boldsymbol{v}_h)_\tau \\ &\quad + \sum_{\tau\in\mathcal{T}_h^K} \kappa_\tau(\nabla\cdot\boldsymbol{u}_{H,h}, \nabla\cdot\boldsymbol{v}_h)_\tau \\ &= \sum_{\tau\in\mathcal{T}_h^K} \left[\delta_\tau(\boldsymbol{R}_\tau^K, -\nu\Delta\boldsymbol{v}_h - (\nabla\boldsymbol{v}_h)\boldsymbol{\alpha} + \gamma\boldsymbol{v}_h)_\tau + \kappa_\tau(\nabla\cdot\boldsymbol{u}_{H,h}, \nabla\cdot\boldsymbol{v}_h)_\tau \right]. \end{aligned} \tag{1.37}$$

From the definition of δ_τ in (1.26), it is possible to show that $\delta_\tau \le \min\left\{ \frac{h_\tau^2}{12\nu}, \frac{h_\tau}{\|\boldsymbol{\alpha}\|_\infty} \right\}$, thus using (1.27) we get

$$\begin{aligned} &\delta_\tau\| -\nu\Delta\boldsymbol{v}_h - (\nabla\boldsymbol{v}_h)\boldsymbol{\alpha} + \gamma\boldsymbol{v}_h\|_{0,\tau} \\ &\le \nu C_k^{-1}\delta_\tau h_\tau^{-1}\|\nabla\boldsymbol{v}_h\|_{0,\tau} + \delta_\tau\|\boldsymbol{\alpha}\|_\infty\|\nabla\boldsymbol{v}_h\|_{0,\tau} + \delta_\tau\gamma\|\boldsymbol{v}_h\|_{0,\tau} \end{aligned}$$

$$\leq C_k^{-1} h_\tau \|\nabla \boldsymbol{v}_h\|_{0,\tau} + h_\tau \|\nabla \boldsymbol{v}_h\|_{0,\tau} + \frac{\gamma}{\|\boldsymbol{\alpha}\|_\infty} h_\tau \|\boldsymbol{v}_h\|_{0,\tau}$$
$$\preceq h_\tau \|\boldsymbol{v}_h\|_{1,\tau}. \tag{1.38}$$

Now, using the fact that $\kappa_\tau \leq \|\boldsymbol{\alpha}\|_\infty h_\tau$, and an inverse inequality, we get

$$\kappa_\tau (\nabla \cdot \boldsymbol{u}_{H,h}, \nabla \cdot \boldsymbol{v}_h)_{0,\tau} \leq \kappa_\tau \|\nabla \cdot \boldsymbol{u}_{H,h}\|_{0,\tau} \|\nabla \cdot \boldsymbol{v}_h\|_{0,\tau} \leq \sqrt{d} \|\boldsymbol{\alpha}\|_\infty h_\tau \|\nabla \cdot \boldsymbol{u}_{H,h}\|_{0,\tau} \|\nabla \boldsymbol{v}_h\|_{0,\tau}$$
$$\preceq \|\nabla \cdot \boldsymbol{u}_{H,h}\|_{0,\tau} \|\boldsymbol{v}_h\|_{0,\tau}. \tag{1.39}$$

Finally, using (1.36)–(1.39), the properties (1.12), Cauchy-Schwarz inequality and mesh regularity, we arrive at

$$\begin{aligned}
&B_K((e_h^{\boldsymbol{u}}, e_h^p), (\boldsymbol{v}, q)) \\
&= B_K((e_h^{\boldsymbol{u}}, e_h^p), (\boldsymbol{v} - \boldsymbol{v}_h, q)) + B_K((e_h^{\boldsymbol{u}}, e_h^p), (\boldsymbol{v}_h, 0)) \\
&\preceq \sum_{\tau \in \mathcal{T}_h^K} \left[\|\boldsymbol{R}_\tau^K\|_{0,\tau} \|\boldsymbol{v} - \boldsymbol{v}_h\|_{0,\tau} + \|\nabla \cdot \boldsymbol{u}_{H,h}\|_{0,\tau} \|q\|_{0,\tau} \right] + \sum_{\zeta \in \mathcal{E}_h^K} \|\boldsymbol{R}_\zeta^K\|_{0,\zeta} \|\boldsymbol{v} - \boldsymbol{v}_h\|_{0,\zeta} \\
&\quad + \sum_{\tau \in \mathcal{T}_h^K} \|\nabla \cdot \boldsymbol{u}_{H,h}\|_{0,\tau} \|\boldsymbol{v}_h\|_{0,\tau} + \sum_{\tau \in \mathcal{T}_h^K} h_\tau \|\boldsymbol{R}_\tau^K\|_{0,\tau} \|\boldsymbol{v}_h\|_{1,\tau} \\
&\preceq \sum_{\tau \in \mathcal{T}_h^K} \left[h_\tau \|\boldsymbol{R}_\tau^K\|_{0,\tau} |\boldsymbol{v}|_{1,\tilde{\omega}_\tau} + \|\nabla \cdot \boldsymbol{u}_{H,h}\|_{0,\tau} \|q\|_{0,\tau} \right] + \sum_{\zeta \in \mathcal{E}_h^K} h_\zeta^{1/2} \|\boldsymbol{R}_\zeta^K\|_{0,\zeta} |\boldsymbol{v}|_{1,\tilde{\omega}_\zeta} \\
&\quad + \sum_{\tau \in \mathcal{T}_h^K} \|\nabla \cdot \boldsymbol{u}_{H,h}\|_{0,\tau} \|\boldsymbol{v}_h\|_{0,\tau} + \sum_{\tau \in \mathcal{T}_h^K} h_\tau \|\boldsymbol{R}_\tau^K\|_{0,\tau} \|\boldsymbol{v}_h\|_{1,\tau} \\
&\preceq \left\{ \sum_{\tau \in \mathcal{T}_h^K} \left[h_\tau^2 \|\boldsymbol{R}_\tau^K\|_{0,\tau}^2 + \|\nabla \cdot \boldsymbol{u}_{H,h}\|_{0,\tau}^2 + \sum_{\zeta \in \mathcal{E}_h^K} h_\zeta \|\boldsymbol{R}_\zeta^K\|_{0,\zeta}^2 \right] \right\}^{1/2} \times \\
&\quad \left\{ \sum_{\tau \in \mathcal{T}_h^K} \left[|\boldsymbol{v}|_{1,\tilde{\omega}_\tau}^2 + \|q\|_{0,\tau}^2 + \|\boldsymbol{v}\|_{1,\tau}^2 \right] + \sum_{\zeta \in \mathcal{E}_h^K} |\boldsymbol{v}|_{1,\tilde{\omega}_\tau}^2 \right\}^{1/2} \\
&\preceq \eta_{2,K} \|(\boldsymbol{v}, q)\|_{\mathbf{V}(K) \times Q(K)}.
\end{aligned}$$

Finally, applying Theorem 1.4 we get the desired result. □

Remark 1.6. *Note that testing (1.28) with $(\boldsymbol{v}, q) = (\boldsymbol{0}, 1|_K)$, we get*

$$\int_K \nabla \cdot \boldsymbol{u}_h^{\boldsymbol{\lambda}_H} = 0,$$

and using the analogous equation for the one-level MHM method we can prove that

$$\int_K \nabla \cdot \boldsymbol{u}^{\boldsymbol{\lambda}_H} = 0.$$

The next result establishes an estimate for the error on first–level pressure in terms of the first–level velocity error and the second–level estimator.

Lemma 1.4. *Let $\boldsymbol{\lambda} \in \boldsymbol{\Lambda}$ and $\boldsymbol{\lambda}_H \in \boldsymbol{\Lambda}_H$ be the solutions of problems (1.20) and (1.23) respectively. Then, we have*

$$\|p^{\boldsymbol{\lambda}} - p^{\boldsymbol{\lambda}_H}\|_Q \preceq \|\boldsymbol{u}^{\boldsymbol{\lambda}} - \boldsymbol{u}^{\boldsymbol{\lambda}_H}\|_{\mathbf{V}} + \eta_2.$$

Proof. Let $\boldsymbol{w} := \frac{1}{d}\boldsymbol{x} \in H^1(\Omega)^d$, then $\nabla \cdot \boldsymbol{w} = 1$ and $\nabla \boldsymbol{w} = \frac{1}{d}\boldsymbol{I}$. Then, using the first equation from (1.17), (1.28), and the Remark 1.6, we have

$$\begin{aligned}
&\int_K p^{\boldsymbol{\lambda}_H} dx = a_K(\boldsymbol{u}^{\boldsymbol{\lambda}_H}, \boldsymbol{w}) + \langle \boldsymbol{\lambda}_H, \boldsymbol{w} \rangle_{\partial K} \\
&= (\nu \nabla \boldsymbol{u}^{\boldsymbol{\lambda}_H}, \nabla \boldsymbol{w})_K + \frac{1}{2}((\nabla \boldsymbol{u}^{\boldsymbol{\lambda}_H})\boldsymbol{\alpha}, \boldsymbol{w})_K - \frac{1}{2}(\boldsymbol{u}^{\boldsymbol{\lambda}_H}, (\nabla \boldsymbol{w})\boldsymbol{\alpha})_K + (\gamma_0 \boldsymbol{u}^{\boldsymbol{\lambda}_H}, \boldsymbol{w})_K + \langle \boldsymbol{\lambda}_H, \boldsymbol{w} \rangle_{\partial K} \\
&= \frac{\nu}{d}\int_K \nabla \cdot \boldsymbol{u}^{\boldsymbol{\lambda}_H} dx + \frac{1}{2}((\nabla \boldsymbol{u}^{\boldsymbol{\lambda}_H})\boldsymbol{\alpha}, \boldsymbol{w})_K - \frac{1}{2}(\boldsymbol{u}^{\boldsymbol{\lambda}_H}, (\nabla \boldsymbol{w})\boldsymbol{\alpha})_K + (\gamma_0 \boldsymbol{u}^{\boldsymbol{\lambda}_H}, \boldsymbol{w})_K + \langle \boldsymbol{\lambda}_H, \boldsymbol{w} \rangle_{\partial K} \\
&= \frac{\nu}{d}\int_K \nabla \cdot \boldsymbol{u}_h^{\boldsymbol{\lambda}_H} dx + \frac{1}{2}((\nabla \boldsymbol{u}^{\boldsymbol{\lambda}_H})\boldsymbol{\alpha}, \boldsymbol{w})_K - \frac{1}{2}(\boldsymbol{u}^{\boldsymbol{\lambda}_H}, (\nabla \boldsymbol{w})\boldsymbol{\alpha})_K + (\gamma_0 \boldsymbol{u}^{\boldsymbol{\lambda}_H}, \boldsymbol{w})_K + \langle \boldsymbol{\lambda}_H, \boldsymbol{w} \rangle_{\partial K} \\
&= (\nu \nabla \boldsymbol{u}_h^{\boldsymbol{\lambda}_H}, \nabla \boldsymbol{w})_K + \frac{1}{2}((\nabla \boldsymbol{u}^{\boldsymbol{\lambda}_H})\boldsymbol{\alpha}, \boldsymbol{w})_K - \frac{1}{2}(\boldsymbol{u}^{\boldsymbol{\lambda}_H}, (\nabla \boldsymbol{w})\boldsymbol{\alpha})_K + (\gamma_0 \boldsymbol{u}^{\boldsymbol{\lambda}_H}, \boldsymbol{w})_K + \langle \boldsymbol{\lambda}_H, \boldsymbol{w} \rangle_{\partial K} \\
&= -\frac{1}{2}((\nabla \boldsymbol{u}_h^{\boldsymbol{\lambda}_H})\boldsymbol{\alpha}, \boldsymbol{w})_K + \frac{1}{2}(\boldsymbol{u}_h^{\boldsymbol{\lambda}_H}, (\nabla \boldsymbol{w})\boldsymbol{\alpha})_K - (\gamma_0 \boldsymbol{u}_h^{\boldsymbol{\lambda}_H}, \boldsymbol{w})_K + (\nabla \cdot \boldsymbol{w}, p_h^{\boldsymbol{\lambda}_H})_K \\
&\quad + \sum_{\tau \in \mathcal{T}_h^K} \delta_\tau(-\nu \Delta \boldsymbol{u}_h^{\boldsymbol{\lambda}_H} + (\nabla \boldsymbol{u}_h^{\boldsymbol{\lambda}_H})\boldsymbol{\alpha} + \gamma \boldsymbol{u}_h^{\boldsymbol{\lambda}_H} + \nabla p_h^{\boldsymbol{\lambda}_H}, -(\nabla \boldsymbol{w})\boldsymbol{\alpha} + \gamma \boldsymbol{w})_\tau \\
&\quad - \sum_{\tau \in \mathcal{T}_h^K} \kappa_\tau(\nabla \cdot \boldsymbol{u}_h^{\boldsymbol{\lambda}_H}, \nabla \cdot \boldsymbol{w})_\tau + \frac{1}{2}((\nabla \boldsymbol{u}^{\boldsymbol{\lambda}_H})\boldsymbol{\alpha}, \boldsymbol{w})_K - \frac{1}{2}(\boldsymbol{u}^{\boldsymbol{\lambda}_H}, (\nabla \boldsymbol{w})\boldsymbol{\alpha})_K + (\gamma_0 \boldsymbol{u}^{\boldsymbol{\lambda}_H}, \boldsymbol{w})_K \\
&= \int_K p_h^{\boldsymbol{\lambda}_H} dx + \frac{1}{2}\big(\nabla(\boldsymbol{u}^{\boldsymbol{\lambda}_H} - \boldsymbol{u}_h^{\boldsymbol{\lambda}_H})\boldsymbol{\alpha}, \boldsymbol{w}\big)_K - \frac{1}{2}(\boldsymbol{u}^{\boldsymbol{\lambda}_H} - \boldsymbol{u}_h^{\boldsymbol{\lambda}_H}, (\nabla \boldsymbol{w})\boldsymbol{\alpha})_K + (\gamma_0(\boldsymbol{u}^{\boldsymbol{\lambda}_H} - \boldsymbol{u}_h^{\boldsymbol{\lambda}_H}), \boldsymbol{w})_K \\
&\quad + \sum_{\tau \in \mathcal{T}_h^K} \delta_\tau(-\nu \Delta \boldsymbol{u}_h^{\boldsymbol{\lambda}_H} + (\nabla \boldsymbol{u}_h^{\boldsymbol{\lambda}_H})\boldsymbol{\alpha} + \gamma \boldsymbol{u}_h^{\boldsymbol{\lambda}_H} + \nabla p_h^{\boldsymbol{\lambda}_H}, -(\nabla \boldsymbol{w})\boldsymbol{\alpha} + \gamma \boldsymbol{w})_\tau \\
&\quad - \sum_{\tau \in \mathcal{T}_h^K} \kappa_\tau(\nabla \cdot \boldsymbol{u}_h^{\boldsymbol{\lambda}_H}, \nabla \cdot \boldsymbol{w})_\tau
\end{aligned} \tag{1.40}$$

Moreover, using similar arguments as above, we can prove that

$$\begin{aligned}
\int_K p^{\boldsymbol{f}} dx &= \int_K p_h^{\boldsymbol{f}} dx + \frac{1}{2}\big(\nabla(\boldsymbol{u}^{\boldsymbol{f}} - \boldsymbol{u}_h^{\boldsymbol{f}})\boldsymbol{\alpha}, \boldsymbol{w}\big)_K - \frac{1}{2}(\boldsymbol{u}^{\boldsymbol{f}} - \boldsymbol{u}_h^{\boldsymbol{f}}, (\nabla \boldsymbol{w})\boldsymbol{\alpha})_K + (\gamma_0(\boldsymbol{u}^{\boldsymbol{f}} - \boldsymbol{u}_h^{\boldsymbol{f}}), \boldsymbol{w})_K \\
&\quad + \sum_{\tau \in \mathcal{T}_h^K} \delta_\tau(-\nu \Delta \boldsymbol{u}_h^{\boldsymbol{f}} + (\nabla \boldsymbol{u}_h^{\boldsymbol{f}})\boldsymbol{\alpha} + \gamma \boldsymbol{u}_h^{\boldsymbol{f}} + \nabla p_h^{\boldsymbol{f}} - \boldsymbol{f}, -(\nabla \boldsymbol{w})\boldsymbol{\alpha} + \gamma \boldsymbol{w})_\tau - \sum_{\tau \in \mathcal{T}_h^K} \kappa_\tau(\nabla \cdot \boldsymbol{u}_h^{\boldsymbol{f}}, \nabla \cdot \boldsymbol{w})_\tau.
\end{aligned} \tag{1.41}$$

Note that from the definition of $\boldsymbol{w}$ we have that $\|\boldsymbol{w}\|_{1,\Omega}$ is a constant depending only on the domain Ω and the dimension d.

Now, from the second equation of (1.20), (1.40), (1.41) and Lemma 1.3, we get

$$\int_\Omega (p^{\boldsymbol{\lambda}} - p^{\boldsymbol{\lambda}_H}) dx = \sum_{K \in \mathcal{T}_H} \left(\int_K p^{\boldsymbol{\lambda}} dx - \int_K p^{\boldsymbol{\lambda}_H} dx \right) = \sum_{K \in \mathcal{T}_H} \left(- \int_K p^{\boldsymbol{f}} dx - \int_K p^{\boldsymbol{\lambda}_H} dx \right)$$

$$
\begin{aligned}
&= \sum_{K\in\mathcal{T}_H}\Bigg(-\int_K p_h^{\boldsymbol{f}}dx-\frac{1}{2}\big(\nabla(\boldsymbol{u}^{\boldsymbol{f}}-\boldsymbol{u}_h^{\boldsymbol{f}})\boldsymbol{\alpha},\boldsymbol{w}\big)_K+\frac{1}{2}(\boldsymbol{u}^{\boldsymbol{f}}-\boldsymbol{u}_h^{\boldsymbol{f}},(\nabla\boldsymbol{w})\boldsymbol{\alpha})_K-(\gamma_0(\boldsymbol{u}^{\boldsymbol{f}}-\boldsymbol{u}_h^{\boldsymbol{f}}),\boldsymbol{w})_K\\
&\quad-\sum_{\tau\in\mathcal{T}_h^K}\delta_\tau(-\nu\Delta\boldsymbol{u}_h^{\boldsymbol{f}}+(\nabla\boldsymbol{u}_h^{\boldsymbol{f}})\boldsymbol{\alpha}+\gamma\boldsymbol{u}_h^{\boldsymbol{f}}+\nabla p_h^{\boldsymbol{f}}-\boldsymbol{f},-(\nabla\boldsymbol{w})\boldsymbol{\alpha}+\gamma\boldsymbol{w})_\tau+\sum_{\tau\in\mathcal{T}_h^K}\kappa_\tau(\nabla\cdot\boldsymbol{u}_h^{\boldsymbol{f}},\nabla\cdot\boldsymbol{w})_\tau\\
&\quad-\int_K p_h^{\boldsymbol{\lambda}_H}dx-\frac{1}{2}\big(\nabla(\boldsymbol{u}^{\boldsymbol{\lambda}_H}-\boldsymbol{u}_h^{\boldsymbol{\lambda}_H})\boldsymbol{\alpha},\boldsymbol{w}\big)_K+\frac{1}{2}(\boldsymbol{u}^{\boldsymbol{\lambda}_H}-\boldsymbol{u}_h^{\boldsymbol{\lambda}_H},(\nabla\boldsymbol{w})\boldsymbol{\alpha})_K-(\gamma_0(\boldsymbol{u}^{\boldsymbol{\lambda}_H}-\boldsymbol{u}_h^{\boldsymbol{\lambda}_H}),\boldsymbol{w})_K\\
&\quad-\sum_{\tau\in\mathcal{T}_h^K}\delta_\tau(-\nu\Delta\boldsymbol{u}_h^{\boldsymbol{\lambda}_H}+(\nabla\boldsymbol{u}_h^{\boldsymbol{\lambda}_H})\boldsymbol{\alpha}+\gamma\boldsymbol{u}_h^{\boldsymbol{\lambda}_H}+\nabla p_h^{\boldsymbol{\lambda}_H},-(\nabla\boldsymbol{w})\boldsymbol{\alpha}+\gamma\boldsymbol{w})_\tau\\
&\quad+\sum_{\tau\in\mathcal{T}_h^K}\kappa_\tau(\nabla\cdot\boldsymbol{u}_h^{\boldsymbol{\lambda}_H},\nabla\cdot\boldsymbol{w})_\tau\Bigg)\\
&= \sum_{K\in\mathcal{T}_H}\Bigg(-\frac{1}{2}\nabla(\boldsymbol{u}_H-\boldsymbol{u}_{H,h})\boldsymbol{\alpha},\boldsymbol{w})_K+\frac{1}{2}(\boldsymbol{u}_H-\boldsymbol{u}_{H,h},(\nabla\boldsymbol{w})\boldsymbol{\alpha})_K-(\gamma_0(\boldsymbol{u}_H-\boldsymbol{u}_{H,h}),\boldsymbol{w})_K\\
&\quad+\sum_{\tau\in\mathcal{T}_h^K}\delta_\tau(\nu\Delta\boldsymbol{u}_{H,h}-(\nabla\boldsymbol{u}_{H,h})\alpha-\gamma\boldsymbol{u}_{H,h}-\nabla p_{H,h}-\boldsymbol{f},-(\nabla\boldsymbol{w})\boldsymbol{\alpha}+\gamma\boldsymbol{w})_\tau\\
&\quad+\sum_{\tau\in\mathcal{T}_h^K}\kappa_\tau(\nabla\cdot\boldsymbol{u}_{H,h},\nabla\cdot\boldsymbol{w})_\tau\Bigg)\\
&\preceq \sum_{K\in\mathcal{T}_H}\Bigg(|\boldsymbol{u}_H-\boldsymbol{u}_{H,h}|_{1,K}\|\boldsymbol{\alpha}\|_{\infty,K}\|\boldsymbol{w}\|_{0,K}+\|\boldsymbol{u}_H-\boldsymbol{u}_{H,h}\|_{0,K}|\boldsymbol{w}|_{1,K}\|\boldsymbol{\alpha}\|_{\infty,K}\\
&\quad+\|\gamma_0\|_{\infty,K}\|\boldsymbol{u}_H-\boldsymbol{u}_{H,h}\|_{0,K}\|\boldsymbol{w}\|_{0,K}+\|\boldsymbol{\alpha}\|_{\infty,K}\sum_{\tau\in\mathcal{T}_h^K}\delta_\tau\|\boldsymbol{R}_\tau^K\|_{0,\tau}|\boldsymbol{w}|_{1,\tau}\\
&\quad+\gamma\sum_{\tau\in\mathcal{T}_h^K}\delta_\tau\|\boldsymbol{R}_\tau^K\|_{0,\tau}\|\boldsymbol{w}\|_{1,\tau}+\sum_{\tau\in\mathcal{T}_h^K}\kappa_\tau\|\nabla\cdot\boldsymbol{u}_{H,h}\|_{0,\tau}|\boldsymbol{w}|_{1,\tau}\Bigg)\\
&\preceq \sum_{K\in\mathcal{T}_H}\Bigg(|\boldsymbol{u}_H-\boldsymbol{u}_{H,h}|_{1,K}\|\boldsymbol{\alpha}\|_{\infty,K}\|\boldsymbol{w}\|_{1,K}+\|\boldsymbol{u}_H-\boldsymbol{u}_{H,h}\|_{0,K}|\boldsymbol{w}|_{1,K}\|\boldsymbol{\alpha}\|_{\infty,K}\\
&\quad+\|\gamma_0\|_{\infty,K}\|\boldsymbol{u}_H-\boldsymbol{u}_{H,h}\|_{0,K}\|\boldsymbol{w}\|_{1,K}+\|\boldsymbol{\alpha}\|_{\infty,K}\Big(\sum_{\tau\in\mathcal{T}_h^K}\delta_\tau\|\boldsymbol{R}_\tau^K\|_{0,\tau}^2\Big)^{1/2}\Big(\sum_{\tau\in\mathcal{T}_h^K}\delta_\tau|\boldsymbol{w}|_{1,\tau}^2\Big)^{1/2}\\
&\quad+\gamma\Big(\sum_{\tau\in\mathcal{T}_h^K}\delta_\tau\|\boldsymbol{R}_\tau^K\|_{0,\tau}^2\Big)^{1/2}\Big(\sum_{\tau\in\mathcal{T}_h^K}\delta_\tau\|\boldsymbol{w}\|_{0,\tau}^2\Big)^{1/2}\\
&\quad+\Big(\sum_{\tau\in\mathcal{T}_h^K}\kappa_\tau\|\nabla\cdot\boldsymbol{u}_{H,h}\|_{0,\tau}^2\Big)^{1/2}\Big(\sum_{\tau\in\mathcal{T}_h^K}\kappa_\tau\|\boldsymbol{w}\|_{1,\tau}^2\Big)^{1/2}\Bigg)
\end{aligned}
$$

$$\preceq \sum_{K\in\mathcal{T}_H}\Bigg(|\boldsymbol{u}_H-\boldsymbol{u}_{H,h}|_{1,K}\|\boldsymbol{\alpha}\|_{\infty,K}\|\boldsymbol{w}\|_{1,K}+\|\boldsymbol{u}_H-\boldsymbol{u}_{H,h}\|_{0,K}|\boldsymbol{w}|_{1,K}\|\boldsymbol{\alpha}\|_{\infty,K}$$
$$+\|\gamma_0\|_{\infty,K}\|\boldsymbol{u}_H-\boldsymbol{u}_{H,h}\|_{0,K}\|\boldsymbol{w}\|_{1,K}+\Bigg(\sum_{\tau\in\mathcal{T}_h^K}\delta_\tau\|\boldsymbol{R}_\tau^K\|_{0,\tau}^2\Bigg)^{1/2}|\boldsymbol{w}|_{1,K}$$
$$+\Bigg(\sum_{\tau\in\mathcal{T}_h^K}\delta_\tau\|\boldsymbol{R}_\tau^K\|_{0,\tau}^2\Bigg)^{1/2}\|\boldsymbol{w}\|_{1,K}+\Bigg(\sum_{\tau\in\mathcal{T}_h^K}\kappa_\tau\|\nabla\cdot\boldsymbol{u}_{H,h}\|_{0,\tau}^2\Bigg)^{1/2}\|\boldsymbol{w}\|_{1,K}\Bigg)$$
$$\preceq \eta_2. \tag{1.42}$$

Now, define $\boldsymbol{\mu}:=\boldsymbol{\lambda}-\boldsymbol{\lambda}_H$ and $p^{\boldsymbol{\mu}}:=p^{\boldsymbol{\lambda}}-p^{\boldsymbol{\lambda}_H}$. Using the orthogonal decomposition $p^{\boldsymbol{\mu}}=\tilde{p}+p_0$, where $\tilde{p}\in L_0^2(\Omega)$ and $p_0:=\dfrac{1}{|\Omega|}\displaystyle\int_\Omega p^{\boldsymbol{\mu}}$, there exists $\tilde{\boldsymbol{w}}\in H_0^1(\Omega)^d$ (see [71]) with $\nabla\cdot\tilde{\boldsymbol{w}}=\tilde{p}$ in Ω and $|\tilde{\boldsymbol{w}}|_{1,\Omega}\leq C\|\tilde{p}\|_{0,\Omega}$, where $C>0$ is independent of H and h. From (1.17), it holds

$$a(\boldsymbol{u}^{\boldsymbol{\mu}},\tilde{\boldsymbol{w}})+b(\tilde{\boldsymbol{w}},p^{\boldsymbol{\mu}})=-(\mu,\tilde{\boldsymbol{w}})_{\mathcal{T}_H}=0. \tag{1.43}$$

Hence, using (1.42) and (1.43), we have that

$$\begin{aligned}\|p^{\boldsymbol{\mu}}\|_Q^2&=(p^{\boldsymbol{\mu}},p^{\boldsymbol{\mu}})_\Omega=(p^{\boldsymbol{\mu}},\tilde{p})_\Omega+(p^{\boldsymbol{\mu}},p_0)_\Omega=(p^{\boldsymbol{\mu}},\nabla\cdot\tilde{\boldsymbol{w}})_\Omega+(p^{\boldsymbol{\mu}},p_0)_\Omega\\&=-b(\tilde{\boldsymbol{w}},p^{\boldsymbol{\mu}})+(p^{\boldsymbol{\mu}},p_0)_\Omega=a(\boldsymbol{u}^{\boldsymbol{\mu}},\tilde{\boldsymbol{w}})+(p^{\boldsymbol{\mu}},p_0)_\Omega\\&=\nu(\nabla\boldsymbol{u}^{\boldsymbol{\mu}},\nabla\tilde{\boldsymbol{w}})_\Omega+\frac{1}{2}((\nabla\boldsymbol{u}^{\boldsymbol{\mu}})\boldsymbol{\alpha},\tilde{\boldsymbol{w}})_\Omega-\frac{1}{2}(\boldsymbol{u}^{\boldsymbol{\mu}},(\nabla\tilde{\boldsymbol{w}})\boldsymbol{\alpha})_\Omega+(\gamma\boldsymbol{u}^{\boldsymbol{\mu}},\tilde{\boldsymbol{w}})_\Omega+(p^{\boldsymbol{\mu}},p_0)_\Omega\\&\preceq|\boldsymbol{u}^{\boldsymbol{\mu}}|_{1,\Omega}|\tilde{\boldsymbol{w}}|_{1,\Omega}+|\boldsymbol{u}^{\boldsymbol{\mu}}|_{1,\Omega}\|\boldsymbol{\alpha}\|_{\infty,\Omega}\|\tilde{\boldsymbol{w}}\|_{0,\Omega}+\|\boldsymbol{u}^{\boldsymbol{\mu}}\|_{0,\Omega}\|\boldsymbol{\alpha}\|_{\infty,\Omega}|\tilde{\boldsymbol{w}}|_{1,\Omega}+\gamma\|\boldsymbol{u}^{\boldsymbol{\mu}}\|_{1,\Omega}\|\tilde{\boldsymbol{w}}\|_{1,\Omega}\\&\quad+\|p^{\boldsymbol{\mu}}\|_{0,\Omega}\|p_0\|_{0,\Omega}\\&\preceq(\|\boldsymbol{u}^{\boldsymbol{\mu}}\|_{\mathbf{V}}+\|p_0\|_{0,\Omega})\|p^{\boldsymbol{\mu}}\|_Q\\&\preceq(\|\boldsymbol{u}^{\boldsymbol{\mu}}\|_{\mathbf{V}}+\eta_2)\|p^{\boldsymbol{\mu}}\|_Q,\end{aligned}$$

we conclude that

$$\|p^{\boldsymbol{\mu}}\|_Q\preceq\|\boldsymbol{u}^{\boldsymbol{\mu}}\|_{\mathbf{V}}+\eta_2,$$

and the result follows. □

Lemma 1.5. *Let $\boldsymbol{u}^{\boldsymbol{\lambda}}$ and $\boldsymbol{u}^{\boldsymbol{\lambda}_H}$ be the solutions of (1.20) and (1.23), respectively. Then we have*

$$\|\boldsymbol{u}^{\boldsymbol{\lambda}}-\boldsymbol{u}^{\boldsymbol{\lambda}_H}\|_{\mathbf{V}}\preceq\eta.$$

Proof. Let $\boldsymbol{\mu}:=\boldsymbol{\lambda}-\boldsymbol{\lambda}_H$. We notice from (1.17) and (1.22), that

$$-(\boldsymbol{\mu},\boldsymbol{u}^{\boldsymbol{\mu}})_{\partial\mathcal{T}_H}=\sum_{K\in\mathcal{T}_H}B_K((\boldsymbol{u}^{\boldsymbol{\mu}},p^{\boldsymbol{\mu}}),(\boldsymbol{u}^{\boldsymbol{\mu}},p^{\boldsymbol{\mu}}))=\sum_{K\in\mathcal{T}_H}\nu(\nabla\boldsymbol{u}^{\boldsymbol{\mu}},\nabla\boldsymbol{u}^{\boldsymbol{\mu}})_K+\gamma_0(\boldsymbol{u}^{\boldsymbol{\mu}},\boldsymbol{u}^{\boldsymbol{\mu}})_K\geq C_1\|\boldsymbol{u}^{\boldsymbol{\mu}}\|_{\mathbf{V}}^2. \tag{1.44}$$

Now, combining (1.6) and (1.17), we find that

$$\frac{\sqrt{2}}{2}\|\boldsymbol{\mu}\|_{\boldsymbol{\Lambda}}\leq\sup_{\boldsymbol{v}\in\mathbf{V}}\frac{-\displaystyle\sum_{K\in\mathcal{T}_H}B_K((\boldsymbol{u}^{\boldsymbol{\mu}},p^{\boldsymbol{\mu}}),(\boldsymbol{v},0))}{\|\boldsymbol{v}\|_{\mathbf{V}}}$$

$$
\begin{aligned}
&\quad - \sum_{K\in\mathcal{T}_H} \left[a_K(\boldsymbol{u}^{\boldsymbol{\mu}},\boldsymbol{v}) + b_K(\boldsymbol{v},p^{\boldsymbol{\mu}})\right] \\
&= \sup_{\boldsymbol{v}\in\mathbf{V}} \frac{}{\|\boldsymbol{v}\|_{\mathbf{V}}} \\
&\preceq (\|\boldsymbol{u}^{\boldsymbol{\mu}}\|_{\mathbf{V}} + \|p^{\boldsymbol{\mu}}\|_Q),
\end{aligned}
$$

and using Lemma 1.4, we get

$$
\|\boldsymbol{\mu}\|_{\boldsymbol{\Lambda}} \preceq \|\boldsymbol{u}^{\boldsymbol{\mu}}\|_{\mathbf{V}} + \eta_2. \tag{1.45}
$$

According to Lemma 4.2 in [19], there exists $\boldsymbol{\chi}\in\mathbf{V}$ satisfying

$$
(\boldsymbol{\mu},\boldsymbol{\chi})_{\partial\mathcal{T}_H} = \langle\boldsymbol{\mu},\boldsymbol{g}\rangle_{\partial\Omega} - (\boldsymbol{\mu},\boldsymbol{u}_{H,h})_{\partial\mathcal{T}_H} \quad \text{for all } \boldsymbol{\mu}\in\boldsymbol{\Lambda},
$$

and

$$
\|\boldsymbol{\chi}\|_{\mathbf{V}} \preceq \eta_1.
$$

Then, using this result, (1.8), (1.32), (1.44), (1.45) and Lemma 1.3, we obtain

$$
\begin{aligned}
C_1\|\boldsymbol{u}^{\boldsymbol{\mu}}\|_{\mathbf{V}}^2 \le -(\boldsymbol{\mu},\boldsymbol{u}^{\boldsymbol{\mu}})_{\partial\mathcal{T}_H} &= -(\boldsymbol{\mu},\boldsymbol{u}^{\boldsymbol{\lambda}} - \boldsymbol{u}^{\boldsymbol{\lambda}_H})_{\partial\mathcal{T}_H} \\
&= -(\boldsymbol{\mu},\boldsymbol{u}^{\boldsymbol{\lambda}} + \boldsymbol{u}^{\boldsymbol{f}} - (\boldsymbol{u}^{\boldsymbol{\lambda}_H} + \boldsymbol{u}^{\boldsymbol{f}}))_{\partial\mathcal{T}_H} \\
&= -\langle\boldsymbol{\mu},\boldsymbol{g}\rangle_{\partial\Omega} + (\boldsymbol{\mu},\boldsymbol{u}^{\boldsymbol{\lambda}_H} + \boldsymbol{u}^{\boldsymbol{f}})_{\partial\mathcal{T}_H} \\
&= -\langle\boldsymbol{\mu},\boldsymbol{g}\rangle_{\partial\Omega} + (\boldsymbol{\mu},\boldsymbol{u}_{H,h})_{\partial\mathcal{T}_H} + (\boldsymbol{\mu},\boldsymbol{u}_H - \boldsymbol{u}_{H,h})_{\partial\mathcal{T}_H} \\
&= -(\boldsymbol{\mu},\boldsymbol{\chi})_{\partial\mathcal{T}_H} + (\boldsymbol{\mu},\boldsymbol{u}_H - \boldsymbol{u}_{H,h})_{\partial\mathcal{T}_H} \\
&\le \|\boldsymbol{\mu}\|_{\boldsymbol{\Lambda}}(\|\boldsymbol{\chi}\|_{\mathbf{V}} + \|\boldsymbol{u}_H - \boldsymbol{u}_{H,h}\|_{\mathbf{V}}) \\
&\le C_2\,\|\boldsymbol{\mu}\|_{\boldsymbol{\Lambda}}(\eta_1+\eta_2) \\
&\le C_2\,(\|\boldsymbol{u}^{\boldsymbol{\mu}}\|_{\mathbf{V}} + \eta_2)(\eta_1+\eta_2) \\
&\le C_2\,\eta\|\boldsymbol{u}^{\boldsymbol{\mu}}\|_{\mathbf{V}} + C_2\,\eta^2
\end{aligned}
$$

Now, using the inequality (1.44) and the inequality $ab \le \frac{\delta}{2}a^2 + \frac{1}{2\delta}b^2$ with $\delta > \frac{C_2}{2C_1}$, we arrive at

$$
\|\boldsymbol{u}^{\boldsymbol{\mu}}\|_{\mathbf{V}} \preceq \eta.
$$

□

Theorem 1.5.

$$
\|(\boldsymbol{u}-\boldsymbol{u}_H, p-p_H)\|_{\mathbf{V}\times Q} \preceq \eta. \tag{1.46}
$$

Proof. Using Lemmas 1.4 and 1.5, the result follows. □

1.4.2 Local efficiency and reliability analysis

Before to state the main result of this chapter, we need first an auxiliary result

Theorem 1.6. *Let $K\in\mathcal{T}_H$. For each $\tau\in\mathcal{T}_h^K$ there holds*

$$
h_\tau\|\boldsymbol{R}_\tau^K\|_{0,\tau} \preceq \left[h_\tau\|\boldsymbol{u}-\boldsymbol{u}_{H,h}\|_{0,\tau} + (1+h_\tau)|\boldsymbol{u}-\boldsymbol{u}_{H,h}|_{1,\tau} + \|p-p_{H,h}\|_{0,\tau}\right], \tag{1.47}
$$

and

$$\|\nabla\cdot\boldsymbol{u}_{H,h}\|_{0,\tau}\preceq|\boldsymbol{u}-\boldsymbol{u}_{H,h}|_{1,\tau}.$$

Furthermore, for each $\zeta\in\mathcal{E}_0^K$ *we have*

$$h_\zeta^{1/2}\|\boldsymbol{R}_\zeta^K\|_{0,\zeta}\preceq\sum_{\tau\in\omega_\zeta}\left[|\boldsymbol{u}-\boldsymbol{u}_{H,h}|_{1,\tau}+\|\boldsymbol{u}-\boldsymbol{u}_{H,h}\|_{0,\tau}+\|p-p_{H,h}\|_{0,\tau}\right],$$

and for all $\zeta\in\mathcal{E}_b^K$ *there holds*

$$h_\zeta^{1/2}\|\boldsymbol{R}_\zeta^K\|_{0,\zeta}\preceq\sum_{\tau\in\omega_\zeta}\left[|\boldsymbol{u}-\boldsymbol{u}_{H,h}|_{1,\tau}+\|\boldsymbol{u}-\boldsymbol{u}_{H,h}\|_{0,\tau}+\|p-p_{H,h}\|_{0,\tau}\right]+\|\boldsymbol{\lambda}-\boldsymbol{\lambda}_H\|_{-\frac{1}{2},\partial K}.\tag{1.48}$$

Proof. We define $\boldsymbol{b}_\tau^K:=b_\tau^K\boldsymbol{R}_\tau^K$ and $\boldsymbol{b}_\zeta^K:=b_\zeta^K\boldsymbol{P}_\zeta^K(\boldsymbol{R}_\zeta^K)$. Using integration by parts and Theorem 1.2, we arrive at

$$\begin{aligned}
(\boldsymbol{R}_\tau^K,\boldsymbol{b}_\tau^K)_\tau&=\left(\nu\Delta\boldsymbol{u}_{H,h}-(\nabla\boldsymbol{u}_{H,h})\boldsymbol{\alpha}-\gamma\boldsymbol{u}_{H,h}-\nabla p_{H,h}+\boldsymbol{f},\boldsymbol{b}_\tau^K\right)_\tau\\
&=\left(\nu\Delta(\boldsymbol{u}_{H,h}-\boldsymbol{u})-(\nabla(\boldsymbol{u}_{H,h}-\boldsymbol{u}))\boldsymbol{\alpha}-\gamma(\boldsymbol{u}_{H,h}-\boldsymbol{u})-\nabla(p_{H,h}-p),\boldsymbol{b}_\tau^K\right)_\tau\\
&\leq\nu|\boldsymbol{u}-\boldsymbol{u}_{H,h}|_{1,\tau}|\boldsymbol{b}_\tau^K|_{1,\tau}+|\boldsymbol{u}-\boldsymbol{u}_{H,h}|_{1,\tau}\|\boldsymbol{\alpha}\|_\infty\|\boldsymbol{b}_\tau^K\|_{0,\tau}+\gamma\|\boldsymbol{u}-\boldsymbol{u}_{H,h}\|_{0,\tau}\|\boldsymbol{b}_\tau^K\|_{0,\tau}\\
&\quad+\sqrt{d}\|p-p_{H,h}\|_{0,\tau}|\boldsymbol{b}_\tau^K|_{1,\tau}\\
&\preceq\left((1+h_\tau^{-1})|\boldsymbol{u}-\boldsymbol{u}_{H,h}|_{1,\tau}+\|\boldsymbol{u}-\boldsymbol{u}_{H,h}\|_{0,\tau}+h_\tau^{-1}\|p-p_{H,h}\|_{0,\tau}\right)\|\boldsymbol{R}_\tau^K\|_{0,\tau},
\end{aligned}$$

and then

$$h_\tau\|\boldsymbol{R}_\tau^K\|_{0,\tau}\preceq\left[h_\tau\|\boldsymbol{u}-\boldsymbol{u}_{H,h}\|_{0,\tau}+(1+h_\tau)|\boldsymbol{u}-\boldsymbol{u}_{H,h}|_{1,\tau}+\|p-p_{H,h}\|_{0,\tau}\right].$$

Again, by Theorem 1.2, we obtain that

$$\begin{aligned}
\|\nabla\cdot\boldsymbol{u}_{H,h}\|_{0,\tau}^2&\preceq(\nabla\cdot\boldsymbol{u}_{H,h},b_\tau^K\nabla\cdot\boldsymbol{u}_{H,h})_\tau\\
&\preceq(\nabla\cdot\boldsymbol{u}_{H,h},b_\tau^K\nabla\cdot\boldsymbol{u}_{H,h})_\Omega\\
&\preceq(\nabla\cdot(\boldsymbol{u}_{H,h}-\boldsymbol{u}),b_\tau^K\nabla\cdot\boldsymbol{u}_{H,h})_\Omega\\
&\preceq|\boldsymbol{u}_{H,h}-\boldsymbol{u}|_{1,\tau}\|\nabla\cdot\boldsymbol{u}_{H,h}\|_{0,\tau},
\end{aligned}$$

and therefore

$$\|\nabla\cdot\boldsymbol{u}_{H,h}\|_{0,\tau}\preceq|\boldsymbol{u}_{H,h}-\boldsymbol{u}|_{1,\tau}.$$

Let $\zeta\in\mathcal{E}_0^K$. From Lemma 1.2 and Theorem 1.2, we find that

$$\begin{aligned}
(\boldsymbol{R}_\zeta^K,\boldsymbol{b}_\zeta^K)_\zeta&=\boldsymbol{R}_h(\boldsymbol{b}_\zeta^K)-\sum_{\tau\in\omega_\zeta}(\boldsymbol{R}_\tau^K,\boldsymbol{b}_\zeta^K)_\tau\\
&\preceq\sum_{\tau\in\omega_\zeta}\Big[|\boldsymbol{u}-\boldsymbol{u}_{H,h}|_{1,\tau}|\boldsymbol{b}_\zeta^K|_{1,\tau}+\|\boldsymbol{u}-\boldsymbol{u}_{H,h}\|_{0,\tau}\|\boldsymbol{b}_\zeta^K\|_{0,\tau}+|\boldsymbol{u}-\boldsymbol{u}_{H,h}|_{1,\tau}\|\boldsymbol{b}_\zeta^K\|_{0,\tau}+
\end{aligned}$$

$$\|p-p_{H,h}\|_{0,\tau}|\boldsymbol{b}_\zeta^K|_{1,\tau}+\|\boldsymbol{R}_\tau^K\|_{0,\tau}\|\boldsymbol{b}_\zeta^K\|_{0,\tau}\Big]$$
$$\preceq \sum_{\tau\in\omega_\zeta}\Big[h_\tau^{-1/2}|\boldsymbol{u}-\boldsymbol{u}_{H,h}|_{1,\tau}+h_\tau^{1/2}\|\boldsymbol{u}-\boldsymbol{u}_{H,h}\|_{0,\tau}+h_\tau^{1/2}|\boldsymbol{u}-\boldsymbol{u}_{H,h}|_{1,\tau}+$$
$$h_\tau^{-1/2}\|p-p_{H,h}\|_{0,\tau}+h_\tau^{1/2}\|\boldsymbol{R}_\tau^K\|_{0,\tau}\Big]\|\boldsymbol{R}_\zeta^K\|_{0,\zeta},$$

thus using Theorem 1.2, (1.47) and the regularity of the second level meshes, we get

$$h_\zeta^{1/2}\|\boldsymbol{R}_\zeta^K\|_{0,\zeta}\preceq\sum_{\tau\in\omega_\zeta}\Big[(1+h_\tau)|\boldsymbol{u}-\boldsymbol{u}_{H,h}|_{1,\tau}+(1+h_\tau)\|\boldsymbol{u}-\boldsymbol{u}_{H,h}\|_{0,\tau}+\|p-p_{H,h}\|_{0,\tau}\Big]$$
$$\preceq\sum_{\tau\in\omega_\zeta}\Big[|\boldsymbol{u}-\boldsymbol{u}_{H,h}|_{1,\tau}+\|\boldsymbol{u}-\boldsymbol{u}_{H,h}\|_{0,\tau}+\|p-p_{H,h}\|_{0,\tau}\Big].$$

Netx, let $\zeta\in\mathcal{E}_b^K$. Using Theorem 1.2 and the regularity of the partition $\mathcal{T}_h^K$, we arrive at

$$\|\boldsymbol{b}_\zeta^K\|_{1,\tau}\preceq\sqrt{h_\tau+h_\tau^{-1}}\|\boldsymbol{R}_\zeta^K\|_{0,\zeta}\preceq h_\zeta^{-1/2}\|\boldsymbol{R}_\zeta^K\|_{0,\zeta}.$$

Now consider

$$a_K(\boldsymbol{u},\boldsymbol{v})+b_K(\boldsymbol{v},p)=\sum_{\tau\in\mathcal{T}_h^K}\Big(a_\tau(\boldsymbol{u},\boldsymbol{v})+b_\tau(\boldsymbol{v},p)\Big),$$

where $a_\tau(\cdot,\cdot)=a_K(\cdot,\cdot)\Big|_\tau$ and $b_\tau(\cdot,\cdot)=b_K(\cdot,\cdot)\Big|_\tau$. Using again Lemma 1.2, Theorem 1.2, (1.47), (1.15) and the regularity of the meshes of the second level, it holds

$$(\boldsymbol{R}_\zeta^K,\boldsymbol{b}_\zeta^K)_\zeta=\boldsymbol{R}_h(\boldsymbol{b}_\zeta^K)-\sum_{\tau\in\omega_\zeta}(\boldsymbol{R}_\tau^K,\boldsymbol{b}_\zeta^K)_\tau$$
$$=a_K(\boldsymbol{u}-\boldsymbol{u}_{H,h},\boldsymbol{b}_\zeta^K)+b_K(\boldsymbol{b}_\zeta^K,p-p_{H,h})+\langle\boldsymbol{\lambda}-\boldsymbol{\lambda}_H,\boldsymbol{b}_\zeta^K\rangle_{\partial K}-\sum_{\tau\in\omega_\zeta}(\boldsymbol{R}_\tau^K,\boldsymbol{b}_\zeta^K)_\tau$$
$$=\sum_{\tau\in\omega_\zeta}\Big(a_\tau(\boldsymbol{u}-\boldsymbol{u}_{H,h},\boldsymbol{b}_\zeta^K)+b_\tau(\boldsymbol{b}_\zeta^K,p-p_{H,h})-(\boldsymbol{R}_\tau^K,\boldsymbol{b}_\zeta^K)_\tau\Big)+\langle\boldsymbol{\lambda}-\boldsymbol{\lambda}_H,\boldsymbol{b}_\zeta^K\rangle_{\partial K}$$
$$\preceq\sum_{\tau\in\omega_\zeta}\Big(|\boldsymbol{u}-\boldsymbol{u}_{H,h}|_{1,\tau}+\|\boldsymbol{u}-\boldsymbol{u}_{H,h}\|_{0,\tau}+\|p-p_{H,h}\|_{0,\tau}\Big)h_\zeta^{-1/2}\|\boldsymbol{R}_\zeta^K\|_{0,\zeta}$$
$$+\|\boldsymbol{\lambda}-\boldsymbol{\lambda}_H\|_{-\frac{1}{2},\partial K}\|\boldsymbol{b}_\zeta^K\|_{\frac{1}{2},\partial K}$$
$$\preceq\sum_{\tau\in\omega_\zeta}\Big(|\boldsymbol{u}-\boldsymbol{u}_{H,h}|_{1,\tau}+\|\boldsymbol{u}-\boldsymbol{u}_{H,h}\|_{0,\tau}+\|p-p_{H,h}\|_{0,\tau}\Big)h_\zeta^{-1/2}\|\boldsymbol{R}_\zeta^K\|_{0,\zeta}$$
$$+\|\boldsymbol{\lambda}-\boldsymbol{\lambda}_H\|_{-\frac{1}{2},\partial K}h_\zeta^{-1/2}\|\boldsymbol{R}_\zeta^K\|_{0,\zeta},$$

thus we get (1.48). □

To present the main result we need to define the following discrete norm for the velocity

$$\|\boldsymbol{v}\|_{\mathbf{V},\omega_F} := \left\{ \sum_{K\in\omega_F} \left[H_K^{-2}\|\boldsymbol{v}\|_{0,K}^2 + |\boldsymbol{v}|_{1,K}^2 \right] \right\}^{1/2},$$

for all $F \in \mathcal{E}_H$.

We are now in position to establish the results that show the efficiency and reliatibity of the error estimator η.

Theorem 1.7 (Main Result)**.** *Let $(\boldsymbol{u},p) \in \mathbf{V}\times Q$ the continuous solution of MHM method and $(\boldsymbol{u}_{H,h},p_{h,h}) \in \mathbf{V}_h \times Q_h$ the discrete solution of two-level MHM method, given in (1.21) and (1.32), and with $\boldsymbol{\lambda}$ and $\boldsymbol{\lambda}_H$ solutions of (1.20) and (1.24) respectively. Then*

$$\|(\boldsymbol{u}-\boldsymbol{u}_{H,h},p-p_{H,h})\|_{\mathbf{V}\times Q} \preceq \eta.$$

Moreover, given $F \in \mathcal{E}_H$, we have

$$\eta_{1,F} \preceq \|\boldsymbol{u}-\boldsymbol{u}_{H,h}\|_{\mathbf{V},\omega_F},$$

and

$$\eta_{2,K} \preceq \|(\boldsymbol{u}-\boldsymbol{u}_{H,h},p-p_{H,h})\|_{\mathbf{V}(K)\times Q(K)} + \|\boldsymbol{\lambda}-\boldsymbol{\lambda}_H\|_{-\frac{1}{2},\partial K}, \tag{1.49}$$

for all $K \in \mathcal{T}_H$.

Proof. Let us $(\boldsymbol{u}_H,p_h)$ be the solution of the one-level MHM method given in (1.31). Applying Lemma 1.3, (1.46) and the triangular inequality, we get

$$\|(\boldsymbol{u}-\boldsymbol{u}_{H,h},p-p_{H,h})\|_{\mathbf{V}\times Q} \le \|(\boldsymbol{u}-\boldsymbol{u}_H,p-p_H)\|_{\mathbf{V}\times Q} + \|(\boldsymbol{u}_H-\boldsymbol{u}_{H,h},p_H-p_{H,h})\|_{\mathbf{V}\times Q} \preceq \eta.$$

On the other hand, since $\boldsymbol{R}_F \in L^2(F)^d$, then

$$\|\boldsymbol{R}_F\|_{0,F}^2 = \frac{1}{2}(\boldsymbol{R}_F, [\![\boldsymbol{u}-\boldsymbol{u}_{H,h}]\!])_F \le \frac{1}{2}\|\boldsymbol{R}_F\|_{0,F}\| [\![\boldsymbol{u}-\boldsymbol{u}_{H,h}]\!] \|_{0,F},$$

and by Lemma 2.6, we arrive to

$$\|\boldsymbol{R}_F\|_{0,F} \preceq H_F^{1/2} \sum_{K\in\omega_F} \left(H_K^{-2}\|\boldsymbol{u}-\boldsymbol{u}_{H,h}\|_{0,K}^2 + |\boldsymbol{u}-\boldsymbol{u}_{H,h}|_{1,K}^2 \right)^{1/2} \preceq H_F^{1/2}\|\boldsymbol{u}-\boldsymbol{u}_{H,h}\|_{\mathbf{V},\omega_F}.$$

Finally, using the definition (1.33) of $\eta_{2,K}$ and Theorem 1.6, we arrive at

$$\begin{aligned}
\eta_{2,K} &\preceq \sum_{\tau\in\mathcal{T}_h^K} \left[h_\tau \|\boldsymbol{R}_\tau^K\|_{0,\tau} + \|\nabla\cdot\boldsymbol{u}_{H,h}\|_{0,\tau} \right] + \sum_{\zeta\in\mathcal{E}_h^K} h_\zeta^{1/2}\|\boldsymbol{R}_\zeta^K\|_{0,\zeta} \\
&\preceq \left[\|\boldsymbol{u}-\boldsymbol{u}_{H,h}\|_{0,K} + |\boldsymbol{u}-\boldsymbol{u}_{H,h}|_{1,K} + \|p-p_{H,h}\|_{0,K} \right] + \|\boldsymbol{\lambda}-\boldsymbol{\lambda}_H\|_{-\frac{1}{2},\partial K} \\
&\preceq \|(\boldsymbol{u}-\boldsymbol{u}_{H,h},p-p_{H,h})\|_{\mathbf{V}(K)\times Q(K)} + \|\boldsymbol{\lambda}-\boldsymbol{\lambda}_H\|_{-\frac{1}{2},\partial K},
\end{aligned}$$

which finishes the proof. □

Remark 1.7. *If we assume that $\boldsymbol{\lambda} \in L^2(\partial\mathcal{T}_H)$, then it is easy to prove that we can modify (1.49) as follows*

$$\eta_{2,K} \preceq \|(\boldsymbol{u}-\boldsymbol{u}_{H,h},p-p_{H,h})\|_{\mathbf{V}(K)\times Q(K)} + h_K^{1/2}\|\boldsymbol{\lambda}-\boldsymbol{\lambda}_H\|_{0,\partial K},$$

and then the right-hand side is fully computable if the exact solution is available.

1.5 Numerical validation

This section presents numerical validations, using three different examples, to demonstrate the reliability and efficiency of our a posteriori error estimator. We validate an adaptive refinement algorithm procedure based on refining faces, which keeps the topology of the first–level mesh untouched.

For all $F \in \mathcal{E}_H$, we define

$$\eta_F := \left\{ \sum_{\tilde{F} \in \mathcal{T}_{\tilde{H}}(F)} \eta_{1,\tilde{F}}^2 \right\}^{1/2} + \sum_{K \in \omega_F} \eta_{2,K}, \quad \text{with} \quad \eta_{1,\tilde{F}} := \frac{\|\boldsymbol{R}_F\|_{0,\tilde{F}}}{H_F^{1/2}}. \tag{1.50}$$

Thus the adaptive algorithm that uses (1.50) is the following

Algorithm 1 Adaptivity by faces procedure

Require: $\theta \in (0,1)$ and a coarse first–level mesh $\mathcal{T}_H$.

1: Solve the discrete problems (1.24) and (1.28)–(1.29) on the current mesh.
2: For each $F \in \mathcal{E}_H$, compute the local error indicator η_F in (1.50).
3: Given $F \in \mathcal{E}_H$ such that $\eta_F \geq \theta \max_{F \in \mathcal{E}_H} \eta_F$, refine $\tilde{F} \in \mathcal{T}_{\tilde{H}}(F)$ such that $\eta_{1,\tilde{F}} = \max_{\mathcal{T}_{\tilde{H}}(F)} \eta_{1,\tilde{F}}$, and if $\eta_{1,F} < \sum_{K \in \omega_F} \eta_{2,K}$ also refine the second–level meshes $\mathcal{T}_h^K$ for $K \in \omega_F$.
4: If the stop criterion is not satisfied, repeat the algorithm.

Using the procedure given in the Algorithm 1, the first-level mesh does not change, and only the local problem associated with elements "touched" by the estimator needs to be revisited. Thereby, only a few extra entries must be computed and assembled into the global system in each adaption step. This algorithm is particularly attractive for use in real three–dimensional problems since it dramatically decreases the computational cost involved in the adaptive procedure and avoids three-dimensional global re–meshing.

1.5.1 A smooth solution

The domain is $\Omega := (0,1) \times (0,1)$, $\nu := 1, \gamma := 1$, $\boldsymbol{\alpha} := \left(\frac{1}{\sqrt{2}}, \frac{1}{\sqrt{2}}\right)$, $\boldsymbol{f}$ and the boundary conditions are chosen such that the exact solution is given by

$$\begin{aligned} u_1(x,y) &:= -256x^2(x-1)^2y(y-1)(2y-1), \\ u_2(x,y) &:= -u_1(y,x), \\ p(x,y) &:= (x-y)^6 - \frac{1}{28}. \end{aligned}$$

Using a uniform refinement in the first level mesh, with one element at the second level mesh, and polynomial degrees, on the faces, $\boldsymbol{\Lambda}_l$, $l = 0, 1, 2$, Table 1.1 shows the convergence of the a posteriori error estimators η_1, η_2 and the effectivity index, E defined by

$$E := \frac{\eta}{\|(\boldsymbol{u} - \boldsymbol{u}_{H,h}, p - p_{H,h})\|_{\mathbf{V} \times Q}},$$

where η is given in (2.39). Observe that the effectivity index stays close to 1 in all scenarios.

l	H	$\|(\boldsymbol{u}-\boldsymbol{u}_{H,h}, p-p_{H,h})\|_{\mathbf{V}\times Q}$	η_1	η_2	E
2	0.25	0.8472405×10^{-1}	0.6778663×10^{-2}	0.9707391×10^{-1}	1.225775
	0.125	0.9915863×10^{-2}	0.9197585×10^{-3}	0.1084051×10^{-1}	1.186005
	0.0625	0.1208512×10^{-2}	0.1213830×10^{-3}	0.1300599×10^{-2}	$1.176639E$
	0.03125	0.1497330×10^{-3}	0.1572163×10^{-4}	0.1604838×10^{-3}	1.176798
	0.015625	0.1865182×10^{-4}	0.2006059×10^{-5}	0.1997001×10^{-4}	1.178227
1	0.25	0.3228006	0.8209395×10^{-1}	0.3214077	1.250003
	0.125	0.7916980×10^{-1}	0.2200528×10^{-1}	0.8110115×10^{-1}	1.302346
	0.0625	0.1960050×10^{-1}	0.5795234×10^{-2}	0.1957939×10^{-2}	1.294591
	0.03125	0.4904711×10^{-2}	0.1499087×10^{-2}	0.4759787×10^{-2}	1.276094
	0.015625	0.1228986×10^{-2}	0.3820426×10^{-3}	0.1169730×10^{-2}	1.262644
0	0.25	0.2585779×10	0.1103852×10	0.1311145×10	0.9339536
	0.125	0.1314891×10	0.6038400	0.6121682×10	0.9247977
	0.0625	0.6590541	0.3207728	0.3056109	0.9504282
	0.03125	0.3296247	0.1652682	0.1529013	0.9652478
	0.015625	0.1648197	0.8381923×10^{-1}	0.7646742×10^{-1}	0.9724971

Table 1.1: Exact error, a posteriori error estimators and effectivity index for $\boldsymbol{u}_{H,h}\in\mathbb{P}_3^2$, $p_{H,h}\in\mathbb{P}_3$ and $\boldsymbol{\lambda}_{H,h}\in\boldsymbol{\Lambda}_l$, $l=0,1,2$.

Figures 1.2, 1.3 and 1.4 validate the convergence orders for the MHM method. The expected orders $\mathcal{O}(H^{l+1})$, $l=0,1,2$, in the $\|\cdot\|_{\mathbf{V}\times Q}$ norm, for the error estimator η are also observed.

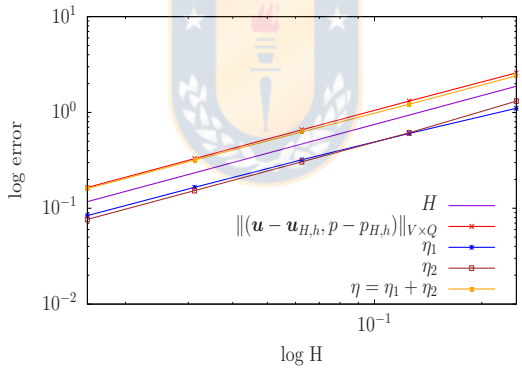

Figure 1.2: Estimated and exact error curves for $\boldsymbol{u}_{H,h}\in\mathbb{P}_3^2$, $p_{H,h}\in\mathbb{P}_3$ and $\boldsymbol{\lambda}_{H,h}\in\boldsymbol{\Lambda}_0$.

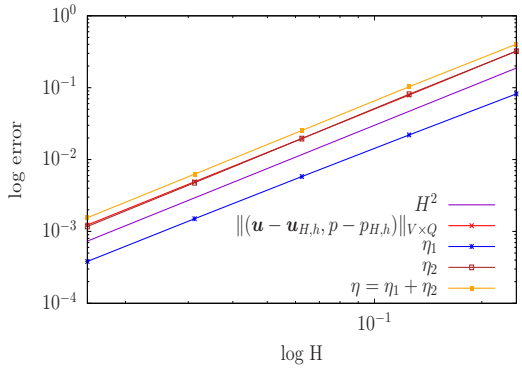

Figure 1.3: Estimated and exact error curves for $\boldsymbol{u}_{H,h} \in \mathbb{P}_3^2$, $p_{H,h} \in \mathbb{P}_3$ and $\boldsymbol{\lambda}_{H,h} \in \boldsymbol{\Lambda}_1$.

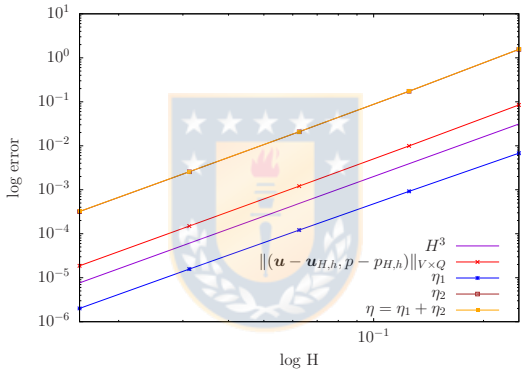

Figure 1.4: Estimated and exact error curves for $\boldsymbol{u}_{H,h} \in \mathbb{P}_3^2$, $p_{H,h} \in \mathbb{P}_3$ and $\boldsymbol{\lambda}_{H,h} \in \boldsymbol{\Lambda}_2$.

1.5.2 Boundary layer solution

We consider the domain $\Omega := (0,1)\times(0,1)$, $\nu := 10^{-2}$, $\gamma = 1$, $\boldsymbol{\alpha} := \left(\frac{1}{\sqrt{2}}, \frac{1}{\sqrt{2}}\right)$, $\boldsymbol{f}$ and the boundary conditions are chosen such that the exact solution is given by:

$$u_1(x,y) := y - \frac{1-e^{y/\nu}}{1-e^{1/\nu}}, \quad u_2(x,y) := x - \frac{1-e^{x/\nu}}{1-e^{1/\nu}}, \quad p(x,y) := (x-y)^8 - \frac{1}{45}.$$

The solutions u_1 and u_2 exhibit boundary layers at $y=1$ and $x=1$, respectively. A structured mesh of 64 elements in the first level is used. In all the calculations $\boldsymbol{u}_{H,h} \in \mathbb{P}_3^2$, $p_{H,h} \in \mathbb{P}_3$ and $\boldsymbol{\lambda}_{H,h} \in \boldsymbol{\Lambda}_1$. Figure 1.5 shows the adaptivity procedure by faces (Algorithm 1) and isovalues of vertical component of velocity. The red dots in the mesh of the first level represent faces where more basis functions have been added to improve the approximation of $\boldsymbol{\Lambda}_1$. In the second level a structured mesh, that coincides with $\mathcal{T}_{\tilde{H}}(F)$, $F \in \partial K$, $K \in \mathcal{T}_H$, is used.

The adaptive algorithm associated to the multiscale estimator induces an anisotropic adaptation on faces due to the sharp boundary layers. Also observe that the solution is improved without changing the topology of the coarse first level mesh.

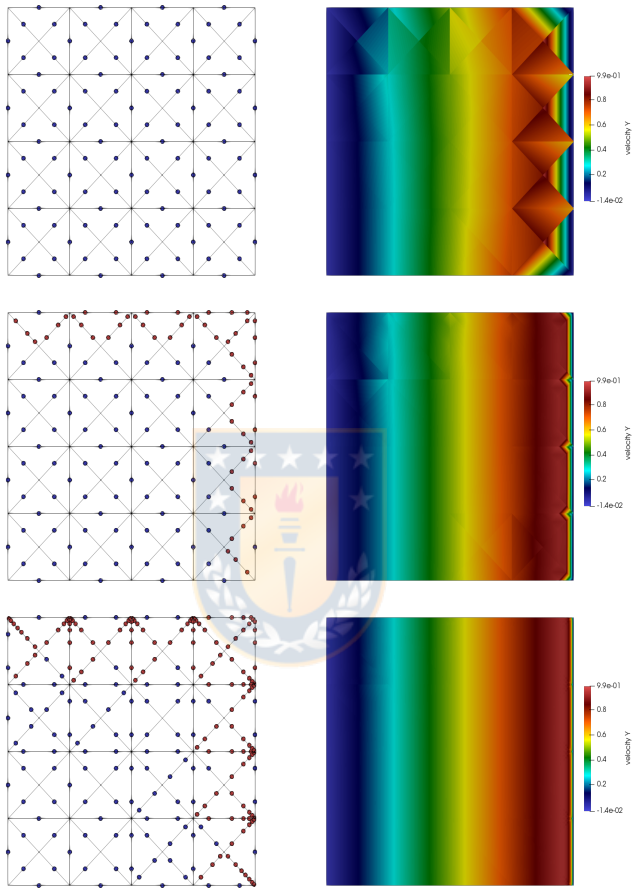

Figure 1.5: Adaptivity procedure by faces (left) and isovalues of vertical component (right). Here $\boldsymbol{u}_{H,h} \in \mathbb{P}_3^2$, $p_{H,h} \in \mathbb{P}_3$ and $\boldsymbol{\lambda}_{H,h} \in \boldsymbol{\Lambda}_1$.

1.5.3 Solution with an inner layer

Let $\Omega := (0,1)^2$, $\nu := 10^{-3}$, $\gamma := 0$ and $\boldsymbol{\alpha} := (1,0)$. We consider $\phi(x,y) := x^2(1-x)^2y^2(1-y)^2\,(1-\tanh(75-150x))$, $\boldsymbol{f}$ and the boundary conditions are chosen such that the exact

solution is

$$\boldsymbol{u} := \boldsymbol{curl}\,\phi = \left(\frac{\partial\phi}{\partial y}, -\frac{\partial\phi}{\partial x}\right), \qquad p := (x-y)^6 - \frac{1}{28}.$$

This solution presents an inner layer around $x = 1/2$. For this case, we choose a first level mesh which is not aligned to advection. In Figure 1.6 we present the adaptive procedure by faces for this test case. The red dots near the inner layer indicate the faces where basis functions were added to the subspace $\boldsymbol{\Lambda}_1$. In the second level a structured mesh, that coincides with $\mathcal{T}_{\tilde{H}}(F)$, $F \in \partial K$, $K \in \mathcal{T}_H$, is used.

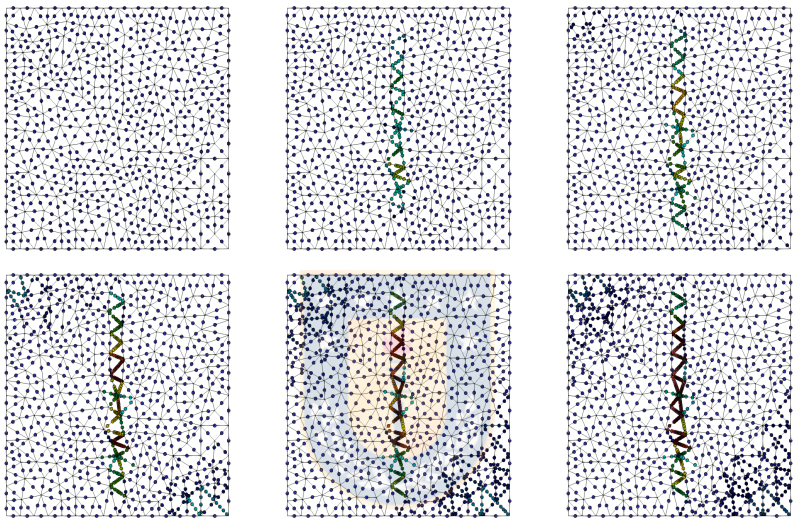

Figure 1.6: Adaptivity procedure by faces at iterations 0, 5, 10, 20, 30 and 50 (from top–right to bottom–left).

Figure 1.7 shows the isolines of the absolute value of the velocity at iterations 0, 5, 10, 20, 30 and 50 of the adaptive procedure. Here we set $\boldsymbol{u}_{H,h} \in \mathbb{P}_3^2$, $p_{H,h} \in \mathbb{P}_3$ and $\boldsymbol{\lambda}_{H,h} \in \boldsymbol{\Lambda}_1$. Observe the great improvements in the solution by just adding a few extra dof at the right location induced by the multiscale estimator

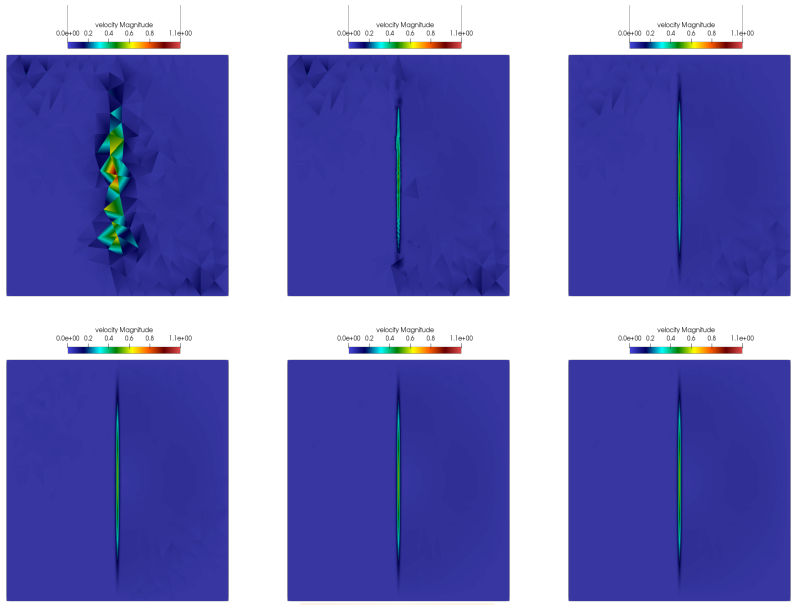

Figure 1.7: Isolines of the absolute value of the velocity field at iterations 0, 5, 10, 20, 30 and 50. Here $\boldsymbol{u}_{H,h} \in \mathbb{P}_3^2$, $p_{H,h} \in \mathbb{P}_3$ and $\boldsymbol{\lambda}_{H,h} \in \boldsymbol{\Lambda}_1$.

The improvements to the computed solution in the final adapted mesh can be seen in Figure 1.8, where we show the profile of the components of the velocity near the inner layer in horizontal cuts. We notice that the adapted scheme captures the inner layer correctly by comparing it with the exact solution.

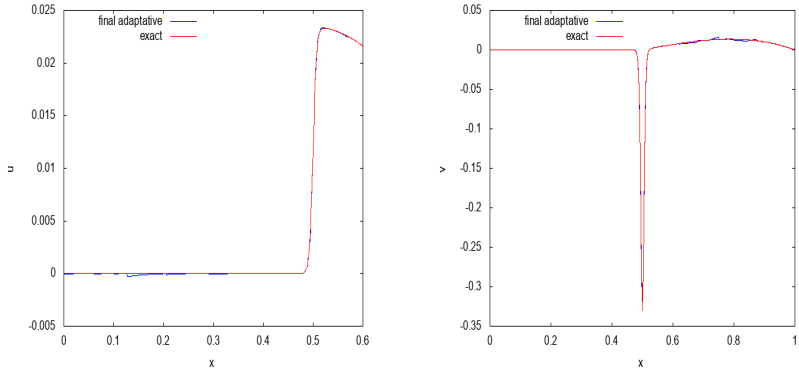

Figure 1.8: Tangential velocity profiles at $y = 0.25$ (left) and normal velocity profiles at $y = 0.5$ in iteration final of the adaptive process. Here $\boldsymbol{u}_{H,h} \in \mathbb{P}_3^2$ and $\boldsymbol{\lambda}_{H,h} \in \boldsymbol{\Lambda}_1$.

CHAPTER 2

An adaptive stabilized finite element method for the Darcy's equations with pressure dependent viscosities

The content of this chapter corresponds to the article R. Araya, C. Carcamo, A. Poza. "An adaptive stabilized finite element method for the Darcy's equations with pressure dependent viscosities". submitted to Comput. Method. Appl. Mech. Engrg.

2.1 Introduction

In many important applications, as for example, in oil reservoir, contaminant transport, mesoscale blood flows, filter design and water resource problems, it is necessary to study the flow of fluids in a porous medium. The first model to study this phenomenon corresponds to the Darcy model (see [66]) when it is considered that the viscosity of the flow is a constant function and where the pressure is independent of viscosity. Later on, it was shown experimentally that in a wide variety of industrial applications, for certain kind flow, as in the case of organic liquid, the viscosity can depend on the pressure (see [51]). This situation is presented, for example, when the viscosity depends exponentially on the pressure (see [51]), turning the Darcy problem into a nonlinear problem (for details on the derivation, see[134]).

For the classical Darcy equation, there are a large number of numerical schemes that approximate the velocity and pressure of the fluid, starting with mixed methods that consider the stable subspace of $H(\mathrm{div};\Omega)$, as the Raviart-Thomas elements [135] Brezzi-Douglas-Marini family [44]. For a non complete list of these stable schemes, see [150, 41, 46, 30, 118, 124], and the references therein.
On the other hand, in fluid dynamics simulations the use of equal-order interpolation subspaces for the pressure and the velocity is a desirable property, but, unfortunately this choice does not lead to stable finite element methods in the sense of Babuska-Brezzi-Ladyzenskaya (see [90], and the references therein). In order to overcome this problem, several stabilized finite-element methods have been proposed in the last decades. A common class of this method, adding residual terms to the Galerkin formulation, are SUPG/PSPG or SDFEM methods (see, for instance [148, 83, 123, 125]). A small variation of these schemes is the called Residual Local Projection (RELP) stabilized methods which reintroduced the residues through interpolation operators (fluctuation operators) on finite dimensional spaces through the solution of local problems (see, for example [27] for the Stokes equations, for the Darcy equations [80] and [11] for the Navier–Stokes equations). When the extra terms are not

residual-based, then we have, for example, the Orthogonal Subscales method (see [63]), the CIP methods (see [53]), or the Local Projection Stabilization (LPS) method (see [34]). The LPS methods can also be seen as a simplification of the RELP method. This method considers symmetric term-by-term fluctuation terms generating a simpler method, but lacking the consistency of the method (see, for instance [29] for the Oseen equations and [18] for the Navier–Stokes equations). Another list of stabilized schemes for the linear Darcy equation are [122, 94, 26, 54, 64, 65]. A different strategy to consider this problem consists of multilevel approximation as the Multiscale Hybrid–Mixed (MHM) method (for details, see [97, 70]).

Concerning the nonlinear Darcy equation when, for instance, the viscosity depends on the pressure, the list of numerical schemes is not long. In [22], an approximation of the nonlinear equation in a circular well domain using a spectral element discretization was propose and analyzed. In [8] this strategy was extended to consider an a posteriori error estimator to improve the performance of a simplified model where the dependence of pressure does not vary too much. In [35], the authors use an Euler's implicit scheme to extend the spectral element discretization to the non-stationary case. A study of the convergence of a stable finite element discretization can be found in [89] for the nonlinear problem when the dependence of the viscosity on the pressure is a bounded function. A mixed finite element method with, a Lagrange multiplier, was introduced and analyzed in [86] for stable subspaces. The authors also introduced an a posteriori error estimator to improve the quality of theirs results. Extending the ideas of [122], a stabilized finite element method was proposed in [125] when the dependence of viscosity on the pressure can occur in several different ways. Recently, a scalable numerical formulation based on variational inequalities was presented in [120] and the convergence of this two last scheme was done in numerical form.

The purpose of this chapter is to present and analyze a stabilized finite element method for the nonlinear Darcy equations when the viscosity can depend exponentially on the pressure, for example when this dependency satisfies the Barus law [31]. As in [86], we use a change of variable that allows us to transform the nonlinear equation into a linear problem and then, using the ideas of [122], we define a new stabilized finite element method. This new scheme is free of mesh dependent stabilization parameters and allow the use of the classical $\mathbb{P}_k^d \times \mathbb{P}_k$ elements for the velocity and pressure. For the stability of the method, we use some tools presented in [86], as the Banach fixed point Theorem and a generalized Lax–Milgram Theorem. In the convergence analysis we use strategies coming from the analysis of other classical stabilized finite element method (for details, see [84, 28]). Thus, our contribution is the numerical analysis of the discrete scheme, and the definition an analysis of a residual-based a posteriori error estimator.

This chapter is organized as follows. In Section 2.2 we introduce the nonlinear Darcy equation together with the variational formulation of the linear problem that is obtained from a change of variable. This section end with some preliminary results that will be needed later. Section 2.3 is devoted to prove the existence and uniqueness of solution to the variational formulation. In addition, we describe the proposed stabilized finite element approximation and include the well-posedness of this scheme. This section also includes a priori error estimates for the elements $\mathbb{P}_k^d \times \mathbb{P}_k$. In Section 2.4, we present and analyze an a posteriori error estimator related to the new stabilized scheme. We also present the equivalence between the error estimator and the approximate error in natural norms. In

Section 2.5 we present the adaptive procedure joint with numerical results that confirm the a priori error results and the performance of the a posteriori error estimator. Finally, in 2.5.3 we prove a technical result that will be essential for our adaptive scheme.

2.2 Model problem and preliminary results

Let Ω be a bounded domain in $\mathbb{R}^d$, $d=2,3$ with polygonal boundary $\partial\Omega$ divided in Γ_D and Γ_N, with $\Gamma_D \cap \Gamma_N = \emptyset$ and $\Gamma_D \neq \emptyset$. We focus in to seek the velocity and pressure solution $(\tilde{\boldsymbol{u}}, \tilde{p})$ to the nonlinear Darcy equations, with mixed boundary condition, given by:

$$\begin{cases} \alpha(\tilde{p})\,\tilde{\boldsymbol{u}} + \nabla \tilde{p} &= \boldsymbol{f} \quad \text{in } \Omega, \\ \nabla \cdot \tilde{\boldsymbol{u}} &= 0 \quad \text{in } \Omega, \\ \tilde{p} &= \tilde{\varphi} \quad \text{on } \Gamma_D, \\ \tilde{\boldsymbol{u}} \cdot \boldsymbol{n} &= 0 \quad \text{on } \Gamma_N, \end{cases} \tag{2.1}$$

where $\alpha(\tilde{p})$ is the drag function, $\tilde{\varphi} \in H^{1/2}(\Gamma_D)$ is the prescribed pressure in Γ_D, $\boldsymbol{f} \in L^2(\Omega)^d$ is a given source and $\boldsymbol{n}$ is the unit outward normal vector to $\partial\Omega$.

Remark 2.1. *When $\Gamma_N = \partial\Omega$ it is necessary, for the uniqueness of the solution, to impose the condition $\int_\Omega \tilde{p} = 0$. In this chapter, we consider $|\Gamma_D| > 0$, which is more complex to analyze.*

In the standard Darcy equation, the drag coefficient α is equal to the ratio of the viscosity μ of the fluid and the permeability κ of the porous media, i.e.

$$\alpha = \frac{\mu}{\kappa}. \tag{2.2}$$

In this chapter, we follow Barus [31], who proposed the exponential dependence of viscosity on pressure which is given by the function

$$\mu(s) = \mu_0 e^{\gamma s}, \quad \forall s \in \mathbb{R}, \tag{2.3}$$

where μ_0 is a positive constant and γ is called the Barus coefficient, which can be obtained experimentally (see [51]). Thereby, from (2.2) and (2.3) we get

$$\alpha(s) = \alpha_0 e^{\gamma s}, \quad \forall s \in \mathbb{R}, \tag{2.4}$$

where $\alpha_0 := \dfrac{\mu_0}{\kappa}$.

Now, thanks to the (2.4) and in view of analysis, we will rewrite the problem (2.1) in a more convenient form. To this end, the first equality of (2.1) is reduced to

$$\tilde{\boldsymbol{u}} = \frac{1}{\alpha(\tilde{p})}(\boldsymbol{f} - \nabla \tilde{p}) = \frac{1}{\alpha_0} e^{-\gamma \tilde{p}} \boldsymbol{f} + \frac{1}{\alpha_0 \gamma} \nabla (e^{-\gamma \tilde{p}}).$$

If we define $\boldsymbol{u} := \tilde{\boldsymbol{u}}$, and $p := e^{-\gamma \tilde{p}} - 1$, and using (2.1), we can formulate the following Darcy equation

$$\begin{cases} \boldsymbol{u} &= \dfrac{1}{\alpha_0}(p+1)\boldsymbol{f} + \dfrac{1}{\varepsilon}\nabla p \quad \text{in } \Omega, \\ \nabla \cdot \boldsymbol{u} &= 0 \quad \text{in } \Omega, \\ p &= \varphi \quad \text{on } \Gamma_D, \\ \boldsymbol{u} \cdot \boldsymbol{n} &= 0 \quad \text{on } \Gamma_N, \end{cases} \tag{2.5}$$

where $\varepsilon := \alpha_0 \gamma > 0$ and $\varphi := e^{-\gamma \tilde{\varphi}} - 1$. This transformation was introduced in [86], where the authors present a similar mixed variational formulation for (2.5), with different Hilbert spaces and using a Lagrange multiplier to weakly impose some boundary conditions.

In the sequel we will use the following Hilbert spaces,

$$\boldsymbol{H} := \{\boldsymbol{v} \in H(\mathrm{div};\Omega) : \boldsymbol{v}\cdot\boldsymbol{n} = 0 \text{ on } \Gamma_N\},$$
$$\tilde{Q} := L^2(\Omega),$$

and the norms

$$\|\boldsymbol{v}\|_{\boldsymbol{H}} = \|\boldsymbol{v}\|_{\mathrm{div};\Omega} \qquad \text{and} \qquad \|q\|_{\tilde{Q}} = \|q\|_{0,\Omega},$$

for all $\boldsymbol{v} \in \boldsymbol{H}$ and $q \in \tilde{Q}$.

The variational formulation of problem (2.5) can be written as: *Find* $(\boldsymbol{u}, p) \in \boldsymbol{H} \times \tilde{Q}$ *such that*

$$a(\boldsymbol{u},\boldsymbol{v}) + b(\boldsymbol{v},p) = \langle \boldsymbol{v}\cdot\boldsymbol{n}, \varphi\rangle_{\Gamma_D} + \gamma\,(p\boldsymbol{f},\boldsymbol{v}) + \gamma\,(\boldsymbol{f},\boldsymbol{v}) \qquad \forall \boldsymbol{v} \in \boldsymbol{H}, \tag{2.6}$$
$$b(\boldsymbol{u},q) = 0 \qquad \forall q \in \tilde{Q}, \tag{2.7}$$

where $a : \boldsymbol{H}\times\boldsymbol{H} \longrightarrow \mathbb{R}$ and $b : \boldsymbol{H}\times\tilde{Q} \longrightarrow \mathbb{R}$ are the bilinear forms defined by

$$a(\boldsymbol{u},\boldsymbol{v}) := \varepsilon\,(\boldsymbol{u},\boldsymbol{v}) \qquad \forall (\boldsymbol{u},\boldsymbol{v}) \in \boldsymbol{H}\times\boldsymbol{H}, \tag{2.8}$$
$$b(\boldsymbol{v},q) := (q, \nabla\cdot\boldsymbol{v}) \qquad \forall (\boldsymbol{v},q) \in \boldsymbol{H}\times\tilde{Q}. \tag{2.9}$$

Here $(\cdot,\cdot)$ stands for the $L^2(\Omega)$-inner product, where we use the same notation for vector, or tensor, valued functions, and $\langle\cdot,\cdot\rangle_{\Gamma_D}$ is the duality pairing between $H^{-1/2}(\Gamma_D)$ and $H^{1/2}(\Gamma_D)$.

Also we consider the norm, on $H^{-1/2}(\Gamma_D)$, given by

$$\|\mu\|_{-1/2,\Gamma_D} := \inf_{\substack{\boldsymbol{\sigma}\in H(\mathrm{div};\Omega)\\ \boldsymbol{\sigma}\cdot\boldsymbol{n}=\mu \text{ on } \Gamma_D}} \|\boldsymbol{\sigma}\|_{\boldsymbol{H}}, \tag{2.10}$$

for all $\mu \in H^{-1/2}(\Gamma_D)$.

We equip the space $\boldsymbol{H}\times\tilde{Q}$ with the product norm

$$\|(\boldsymbol{w},r)\|_{\boldsymbol{H}\times\tilde{Q}} = \|\boldsymbol{w}\|_{\boldsymbol{H}} + \|r\|_{0,\Omega}.$$

Throughout this paper C and C_i, $i > 0$ will denote positive constants independent of the mesh size h, but who may depend on the parameter ε.

The next result states some inequalities which will be used in the sequel.

Lemma 2.1. *Let* $a(\cdot,\cdot)$ *and* $b(\cdot,\cdot)$ *be the bilinear forms given by* (2.8) *and* (2.9)*, respectively. Then, there exists a positive constant* β_b*, such that*

$$|a(\boldsymbol{u},\boldsymbol{v})| \leq \varepsilon\|\boldsymbol{u}\|_{\boldsymbol{H}}\|\boldsymbol{v}\|_{\boldsymbol{H}} \qquad \forall\, \boldsymbol{u},\boldsymbol{v} \in \boldsymbol{H}, \tag{2.11}$$
$$|b(\boldsymbol{v},q)| \leq \|q\|_{\tilde{Q}}\|\boldsymbol{v}\|_{\boldsymbol{H}} \qquad \forall\, \boldsymbol{v} \in \boldsymbol{H}, \forall q \in \tilde{Q}, \tag{2.12}$$
$$\sup_{\boldsymbol{v}\in\boldsymbol{H}} \frac{b(\boldsymbol{v},q)}{\|\boldsymbol{v}\|_{\boldsymbol{H}}} \geq \beta_b\,\|q\|_{\tilde{Q}} \qquad \forall q \in \tilde{Q}. \tag{2.13}$$

Proof. The proof of (2.11) and (2.12) follows from the norm definitions. For (2.13) see [42, (7.1.13)]. □

The next result guarantees the solvability of problem (2.6)-(2.7).

Theorem 2.1. *Assume that* $\boldsymbol{f} \in L^\infty(\Omega)^d$ *and*

$$\left(\frac{1}{\varepsilon} + \frac{2}{\beta_b}\right)\gamma\|\boldsymbol{f}\|_{\infty,\Omega} < 1. \tag{2.14}$$

Then, problem (2.6)-(2.7) *has a unique solution* $(\boldsymbol{u},p) \in \boldsymbol{H}\times\tilde{Q}$ *and there exist a positive constant* C*, independent of* ε *and* γ*, such that*

$$\|(\boldsymbol{u},p)\|_{\boldsymbol{H}\times\tilde{Q}} \leq C\left(\frac{1}{\varepsilon} + \frac{2}{\beta_b}\right)\|\boldsymbol{f}\|_{\infty,\Omega}. \tag{2.15}$$

Proof. The proof is an adaptation of [86, Theorem 3.1]. □

In the rest of this chapter, we find the pressure solution $p \in Q := H^1(\Omega)$, and over $\boldsymbol{H}\times Q$ we will define the following norm

$$|||(\boldsymbol{w},r)||| := \varepsilon^{1/2}\|\boldsymbol{w}\|_{\boldsymbol{H}} + \|r\|_{1,\Omega},$$

for all $(\boldsymbol{w},r) \in \boldsymbol{H}\times Q$.

2.3 The stabilized finite element method

From now on, we denote by $\{\mathcal{T}_h\}_{h>0}$ a regular family of triangulations of $\bar{\Omega}$ composed by simplexes. For a $\mathcal{T}_h$ we will denote by T the elements of the triangulation, and by $\mathcal{E}_h$ the set of all edges (faces) of $\mathcal{T}_h$, with the splitting $\mathcal{E}_h = \mathcal{E}_\Omega \cup \mathcal{E}_D \cup \mathcal{E}_N$, where $\mathcal{E}_\Omega$ stands for the edges (faces) lying in the interior of Ω, $\mathcal{E}_D$ and $\mathcal{E}_N$ stands for the edges (faces) on the boundaries Γ_D and Γ_N, respectively. As usual h_T means the diameter of T, $h = \max_{T\in\mathcal{T}_h} h_T$, and $h_F := |F|$ for $F \in \mathcal{E}_h$.

We introduce two finite element subspaces of $\boldsymbol{H}$ and Q, given by

$$\begin{aligned}\boldsymbol{H}_h &:= \{\boldsymbol{v} \in C(\overline{\Omega})^d \,:\, \boldsymbol{v}|_T \in \mathbb{P}_k(T)^d, \quad \forall T \in \mathcal{T}_h\} \cap \boldsymbol{H},\\ Q_h &:= \{q \in C(\overline{\Omega}) \,:\, q|_T \in \mathbb{P}_k(T), \quad \forall T \in \mathcal{T}_h\},\end{aligned}$$

with $k \geq 1$, where $\mathbb{P}_k$ stands for the space of polynomials of total degree less or equal to k.

Next, we consider the following discrete stabilized scheme: *Find* $(\boldsymbol{u}_h,p_h) \in \boldsymbol{H}_h \times Q_h$ such that

$$B_{\mathrm{stab}}((\boldsymbol{u}_h,p_h),(\boldsymbol{v}_h,q_h)) = \langle \boldsymbol{v}_h\cdot\boldsymbol{n},\varphi\rangle_{\Gamma_D} + \gamma((p_h+1)\boldsymbol{f},\boldsymbol{v}_h) - \frac{1}{2}\big(\varepsilon^{-1}\gamma(p_h+1)\boldsymbol{f},\varepsilon\boldsymbol{v}_h + \nabla q_h\big), \tag{2.16}$$

for all $(\boldsymbol{v}_h,q_h) \in \boldsymbol{H}_h \times Q_h$, where

$$\begin{aligned}B_{\mathrm{stab}}((\boldsymbol{w}_h,r_h),(\boldsymbol{v}_h,q_h)) &:= a(\boldsymbol{w}_h,\boldsymbol{v}_h) + b(\boldsymbol{v}_h,r_h) - b(\boldsymbol{w}_h,q_h)\\ &\quad -\frac{1}{2}\big(\varepsilon^{-1}(\varepsilon\boldsymbol{w}_h - \nabla r_h),\varepsilon\boldsymbol{v}_h + \nabla q_h\big) + \varepsilon(\nabla\cdot\boldsymbol{w}_h,\nabla\cdot\boldsymbol{v}_h).\end{aligned} \tag{2.17}$$

Remark 2.2. *This scheme, as well as the proposed in [125], is based on the stabilized finite element method, for the linear Darcy equation, presented in [122], with the difference that in our scheme we add an* $\varepsilon(\nabla\cdot\boldsymbol{u}_h,\nabla\cdot\boldsymbol{v}_h)$ *term which improves the quality of the numerical results.*

As it is well known, the bilinear form $b(\cdot,\cdot)$ does not satisfies an inf–sup condition, using the subspaces $\boldsymbol{H}_h$ and Q_h, but it satisfies the following weak inf–sup condition.

Lemma 2.2. *There exist positive constants* β_w *and* λ*, independent of* ε *and* h*, such that*

$$\sup_{\boldsymbol{v}_h\in\boldsymbol{H}_h}\frac{b(\boldsymbol{v}_h,p_h)}{\|\boldsymbol{v}_h\|_{\boldsymbol{H}}}\geq\beta_w\,\|p_h\|_{0,\Omega}-\lambda\,|p_h|_{1,\Omega}\qquad\forall p_h\in Q_h. \tag{2.18}$$

Proof. The proof of this result uses similar arguments to those used in [84, Lemma 3.3]. Let $p_h\in Q_h$, then there exist $\bar{p}_h\in\mathbb{R}$ and $p_h^*\in L_0^2(\Omega)$, such that $p_h=\bar{p}_h+p_h^*$. Additionally, there exists $\boldsymbol{w}\in H_0^1(\Omega)^d$ (see [90]) such that

$$(\nabla\cdot\boldsymbol{w},p_h)=(\nabla\cdot\boldsymbol{w},p_h^*)\geq C_1\|p_h^*\|_{0,\Omega}\|\boldsymbol{w}\|_{1,\Omega}. \tag{2.19}$$

Furthermore, let $\mathcal{C}_h\boldsymbol{w}\in\boldsymbol{H}_h\cap H_0^1(\Omega)^d$ the Clément interpolate of $\boldsymbol{w}$ (see [60]). This interpolation operator satisfies

$$\left\{\sum_{K\in\mathcal{T}_h}h_K^{-2}\|\boldsymbol{w}-\mathcal{C}_h\boldsymbol{w}\|_{0,K}^2\right\}^{1/2}\leq C_2\|\boldsymbol{w}\|_{1,\Omega}, \tag{2.20}$$

and

$$\|\mathcal{C}_h\boldsymbol{w}\|_{1,\Omega}\leq C_3\|\boldsymbol{w}\|_{1,\Omega}. \tag{2.21}$$

Using (2.19) and integration by parts, we get that

$$\begin{aligned}(\nabla\cdot\mathcal{C}_h\boldsymbol{w},p_h)&=(\nabla\cdot\mathcal{C}_h\boldsymbol{w},p_h^*)\\&=(\nabla\cdot(\mathcal{C}_h\boldsymbol{w}-\boldsymbol{w}),p_h^*)+(\nabla\cdot\boldsymbol{w},p_h^*)\\&\geq\sum_{K\in\mathcal{T}_h}(\mathcal{C}_h\boldsymbol{w}-\boldsymbol{w},\nabla p_h^*)_K+C_1\|p_h^*\|_{0,\Omega}\|\boldsymbol{w}\|_{1,\Omega}.\end{aligned}$$

Using Cauchy-Schwarz inequality and (2.20), we obtain

$$\begin{aligned}(\nabla\cdot\mathcal{C}_h\boldsymbol{w},p_h)&\geq-\left(\sum_{K\in\mathcal{T}_h}h_K^{-2}\|\mathcal{C}_h\boldsymbol{w}-\boldsymbol{w}\|_{0,K}^2\right)^{1/2}\left(\sum_{K\in\mathcal{T}_h}h_K^2\|\nabla p_h^*\|_{0,K}^2\right)^{1/2}+C_1\|p_h^*\|_{0,\Omega}\|\boldsymbol{w}\|_{1,\Omega}\\&\geq\left\{-C_2\left(\sum_{K\in\mathcal{T}_h}h_K^2\|\nabla p_h^*\|_{0,K}^2\right)^{1/2}+C_1\|p_h^*\|_{0,\Omega}\right\}\|\boldsymbol{w}\|_{1,\Omega},\end{aligned}$$

and, in consequence

$$\frac{(\nabla\cdot\mathcal{C}_h\boldsymbol{w},p_h)}{\|\boldsymbol{w}\|_{1,\Omega}}\geq C_1\|p_h^*\|_{0,\Omega}-C_2\left(\sum_{K\in\mathcal{T}_h}h_K^2\|\nabla p_h^*\|_{0,K}^2\right)^{1/2}. \tag{2.22}$$

We can assume (see [84]) that, for a reasonable mesh, there exist $\boldsymbol{z}_h \in \boldsymbol{H}_h$, $\boldsymbol{z}_h \neq \boldsymbol{0}$, such that

$$\frac{(\nabla \cdot \boldsymbol{z}_h, \bar{p}_h)}{\|\boldsymbol{z}_h\|_{1,\Omega}} \geq C_4 \|\bar{p}_h\|_{0,\Omega}. \tag{2.23}$$

Let $\tilde{\boldsymbol{v}}_h := \|\boldsymbol{w}\|_{1,\Omega}^{-1} \mathcal{C}_h \boldsymbol{w} + \delta \|\boldsymbol{z}_h\|_{1,\Omega}^{-1} \boldsymbol{z}_h$, with $\delta > 0$. It is clear that $\tilde{\boldsymbol{v}}_h \in \boldsymbol{H}_h$ and using (2.22), (2.23), we get

$$\begin{aligned}
(\nabla \cdot \tilde{\boldsymbol{v}}_h, p_h) &= \frac{(\nabla \cdot \mathcal{C}_h \boldsymbol{w}, p_h)}{\|\boldsymbol{w}\|_{1,\Omega}} + \delta \frac{(\nabla \cdot \boldsymbol{z}_h, \bar{p}_h)}{\|\boldsymbol{z}_h\|_{1,\Omega}} + \delta \frac{(\nabla \cdot \boldsymbol{z}_h, p_h^*)}{\|\boldsymbol{z}_h\|_{1,\Omega}} \\
&\geq C_1 \|p_h^*\|_{0,\Omega} - C_2 \left(\sum_{K \in \mathcal{T}_h} h_K^2 \|\nabla p_h^*\|_{0,K}^2 \right)^{1/2} + \delta C_4 \|\bar{p}_h\|_{0,\Omega} - \delta C_5 \|p_h^*\|_{0,\Omega} \\
&\geq C_6 \|p_h\|_{0,\Omega} - C_7 \left(\sum_{K \in \mathcal{T}_h} h_K^2 \|\nabla p_h^*\|_{0,K}^2 \right)^{1/2},
\end{aligned}$$

assuming that $\delta < C_1/C_5$. On the other hand, note that the definition of $\tilde{\boldsymbol{v}}_h$ and (2.21) shows $\|\tilde{\boldsymbol{v}}_h\|_{\boldsymbol{H}} \leq C \|\tilde{\boldsymbol{v}}_h\|_{1,\Omega} \leq C C_3 + C\delta$, and hence, we have that

$$\sup_{\boldsymbol{v}_h \in \boldsymbol{H}_h} \frac{(\nabla \cdot \boldsymbol{v}_h, p_h)}{\|\boldsymbol{v}_h\|_{\boldsymbol{H}}} \geq C_8 \|p_h\|_{0,\Omega} - C_9 \left(\sum_{K \in \mathcal{T}_h} h_K^2 \|\nabla p_h\|_{0,K}^2 \right)^{1/2},$$

which conclude the proof. □

The following result will be fundamental to prove the well–posedness of the stabilized finite element scheme. The proof is based on the same arguments used in [28, Lemma 4.1].

Lemma 2.3. *Let $B_{\mathrm{stab}}(\cdot,\cdot)$ be the bilinear form defined in (2.17). Then there is a positive constant β_s, independent of h and ε, such that*

$$\sup_{(\boldsymbol{v}_h, q_h) \in \boldsymbol{H}_h \times Q_h} \frac{B_{\mathrm{stab}}((\boldsymbol{u}_h, p_h), (\boldsymbol{v}_h, q_h))}{|||(\boldsymbol{v}_h, q_h)|||} \geq \beta_s \, |||(\boldsymbol{u}_h, p_h)|||, \tag{2.24}$$

for all $(\boldsymbol{u}_h, p_h) \in \boldsymbol{H}_h \times Q_h$.

Proof. Let $(\boldsymbol{u}_h, p_h) \in \boldsymbol{H}_h \times Q_h$ and let $\boldsymbol{w}_h \in \boldsymbol{H}_h$ be a function for which the supremum in Lemma 2.2 is attained, and such that $\|\boldsymbol{w}_h\|_{\boldsymbol{H}} = \|p_h\|_{0,\Omega}$. If we consider $\tilde{\boldsymbol{w}}_h = -\boldsymbol{w}_h$, we have

$$\frac{-(p_h, \nabla \cdot \tilde{\boldsymbol{w}}_h)}{\|\tilde{\boldsymbol{w}}_h\|_{\boldsymbol{H}}} = \frac{(p_h, \nabla \cdot \boldsymbol{w}_h)}{\|\boldsymbol{w}_h\|_{\boldsymbol{H}}} \geq \beta_w \|p_h\|_{0,\Omega} - \lambda |p_h|_{1,\Omega},$$

and therefore,

$$-(p_h, \nabla \cdot \tilde{\boldsymbol{w}}_h) \geq \beta_w \|p_h\|_{0,\Omega}^2 - \lambda |p_h|_{1,\Omega} \|\tilde{\boldsymbol{w}}_h\|_{\boldsymbol{H}}. \tag{2.25}$$

Then, for $(\boldsymbol{v}_h, q_h) := (\boldsymbol{u}_h - \delta \tilde{\boldsymbol{w}}_h, p_h)$, with $\delta > 0$, we get that

$$\begin{aligned}
B_{\mathrm{stab}}((\boldsymbol{u}_h, p_h), (\boldsymbol{v}_h, q_h)) &= B_{\mathrm{stab}}((\boldsymbol{u}_h, p_h), (\boldsymbol{u}_h, p_h)) - \delta \, B_{\mathrm{stab}}((\boldsymbol{u}_h, p_h), (\tilde{\boldsymbol{w}}_h, 0)) \\
&= B_{\mathrm{stab}}((\boldsymbol{u}_h, p_h), (\boldsymbol{u}_h, p_h)) - \delta \left[B_{\mathrm{stab}}((\boldsymbol{u}_h, 0), (\tilde{\boldsymbol{w}}_h, 0)) + B_{\mathrm{stab}}((\boldsymbol{0}, p_h), (\tilde{\boldsymbol{w}}_h, 0)) \right]
\end{aligned}$$

$$
\begin{aligned}
=&\frac{1}{2}\varepsilon\|\boldsymbol{u}_h\|_{0,\Omega}^2+\varepsilon\|\nabla\cdot\boldsymbol{u}_h\|_{0,\Omega}^2+\frac{1}{2}\varepsilon^{-1}|p_h|_{1,\Omega}^2\\
&-\delta\left[\frac{1}{2}\varepsilon(\boldsymbol{u}_h,\tilde{\boldsymbol{w}}_h)+\varepsilon(\nabla\cdot\boldsymbol{u}_h,\nabla\cdot\tilde{\boldsymbol{w}}_h)+(p_h,\nabla\cdot\tilde{\boldsymbol{w}}_h)+\frac{1}{2}(\nabla p_h,\tilde{\boldsymbol{w}}_h)\right]\\
=&\frac{1}{2}\varepsilon\|\boldsymbol{u}_h\|_{0,\Omega}^2+\varepsilon\|\nabla\cdot\boldsymbol{u}_h\|_{0,\Omega}^2+\frac{1}{2}\varepsilon^{-1}|p_h|_{1,\Omega}^2\\
&-\frac{\delta}{2}\varepsilon(\boldsymbol{u}_h,\tilde{\boldsymbol{w}}_h)-\delta\varepsilon(\nabla\cdot\boldsymbol{u}_h,\nabla\cdot\tilde{\boldsymbol{w}}_h)-\delta(p_h,\nabla\cdot\tilde{\boldsymbol{w}}_h)-\frac{\delta}{2}(\nabla p_h,\tilde{\boldsymbol{w}}_h)\\
\geq&\frac{1}{2}\varepsilon\|\boldsymbol{u}_h\|_{0,\Omega}^2+\varepsilon\|\nabla\cdot\boldsymbol{u}_h\|_{0,\Omega}^2+\frac{1}{2}\varepsilon^{-1}|p_h|_{1,\Omega}^2+\delta\beta_w\|p_h\|_{0,\Omega}^2\\
&-\delta\lambda|p_h|_{1,\Omega}\|\tilde{\boldsymbol{w}}_h\|_{\boldsymbol{H}}-\frac{\delta}{2}\varepsilon(\boldsymbol{u}_h,\tilde{\boldsymbol{w}}_h)-\delta\varepsilon(\nabla\cdot\boldsymbol{u}_h,\nabla\cdot\tilde{\boldsymbol{w}}_h)-\frac{\delta}{2}(\nabla p_h,\tilde{\boldsymbol{w}}_h)\\
\geq&\frac{1}{2}\varepsilon\|\boldsymbol{u}_h\|_{0,\Omega}^2+\varepsilon\|\nabla\cdot\boldsymbol{u}_h\|_{0,\Omega}^2+\frac{1}{2}\varepsilon^{-1}|p_h|_{1,\Omega}^2+\delta\beta_w\|p_h\|_{0,\Omega}^2\\
&-\frac{\delta}{2}\varepsilon\|\boldsymbol{u}_h\|_{0,\Omega}\|\tilde{\boldsymbol{w}}_h\|_{0,\Omega}-\delta\varepsilon\|\nabla\cdot\boldsymbol{u}_h\|_{0,\Omega}\|\nabla\cdot\tilde{\boldsymbol{w}}_h\|_{0,\Omega}\\
&-\frac{\delta}{2}|p_h|_{1,\Omega}\|\tilde{\boldsymbol{w}}_h\|_{0,\Omega}-\delta\lambda|p_h|_{1,\Omega}\|\tilde{\boldsymbol{w}}_h\|_{\boldsymbol{H}}.
\end{aligned}
$$

Now, using Young's inequality $2ab\leq\frac{a^2}{\gamma}+\gamma b^2$, for all $a,b,\gamma>0$, and the fact that $\|\tilde{\boldsymbol{w}}_h\|_{\boldsymbol{H}}=\|p_h\|_{0,\Omega}$, we get

$$
\begin{aligned}
B_{\mathrm{stab}}((\boldsymbol{u}_h,p_h),(\boldsymbol{v}_h,q_h))\geq&\frac{1}{2}\varepsilon\|\boldsymbol{u}_h\|_{0,\Omega}^2+\varepsilon\|\nabla\cdot\boldsymbol{u}_h\|_{0,\Omega}^2+\frac{1}{2}\varepsilon^{-1}|p_h|_{1,\Omega}^2+\delta\beta_w\|p_h\|_{0,\Omega}^2\\
&-\frac{\delta\varepsilon}{4\gamma_1}\|\boldsymbol{u}_h\|_{0,\Omega}^2-\frac{\delta\varepsilon\gamma_1}{4}\|\tilde{\boldsymbol{w}}_h\|_{0,\Omega}^2\\
&-\frac{\delta\varepsilon}{2\gamma_2}\|\nabla\cdot\boldsymbol{u}_h\|_{0,\Omega}^2-\frac{\delta\varepsilon\gamma_2}{2}\|\nabla\cdot\tilde{\boldsymbol{w}}_h\|_{0,\Omega}^2\\
&-\frac{\delta}{4\gamma_3}|p_h|_{1,\Omega}^2-\frac{\delta\gamma_3}{4}\|\tilde{\boldsymbol{w}}_h\|_{0,\Omega}^2\\
&-\frac{\delta\lambda}{2\gamma_4}|p_h|_{1,\Omega}^2-\frac{\delta\lambda\gamma_4}{2}\|\tilde{\boldsymbol{w}}_h\|_{\boldsymbol{H}}^2\\
\geq&\frac{1}{2}\varepsilon\left(1-\frac{\delta}{2\gamma_1}\right)\|\boldsymbol{u}_h\|_{0,\Omega}^2+\varepsilon\left(1-\frac{\delta}{2\gamma_2}\right)\|\nabla\cdot\boldsymbol{u}_h\|_{0,\Omega}^2\\
&+\frac{1}{2}\left(\varepsilon^{-1}-\frac{\delta}{2\gamma_3}-\frac{\delta\lambda}{2\gamma_4}\right)|p_h|_{1,\Omega}^2\\
&+\delta\left(\beta_w-\frac{\delta\varepsilon\gamma_1}{4}-\frac{\delta\varepsilon\gamma_2}{2}-\frac{\delta\gamma_3}{4}-\frac{\delta\lambda\gamma_4}{2}\right)\|p_h\|_{0,\Omega}^2\\
\geq&\frac{1}{2}\varepsilon\left(1-\frac{\delta}{2\gamma_1}\right)\|\boldsymbol{u}_h\|_{0,\Omega}^2+\varepsilon\left(1-\frac{\delta}{2\gamma_2}\right)\|\nabla\cdot\boldsymbol{u}_h\|_{0,\Omega}^2\\
&+\frac{1}{2}\left(\varepsilon^{-1}-\frac{\delta}{2\gamma_3}-\frac{\delta\lambda}{2\gamma_4}\right)|p_h|_{1,\Omega}^2+\delta C_{10}\|p_h\|_{0,\Omega}^2,
\end{aligned}
$$

with $C_{10}>0$, if $\gamma_1,\gamma_2,\gamma_3$ and γ_4 are chosen small enough.

Now, if we choose $0<\delta<\min\left\{2\gamma_1, 2\gamma_2, \dfrac{2\gamma_3\gamma_4\varepsilon^{-1}}{\gamma_4+\gamma_3\lambda}, \varepsilon^{-1/2}\right\}$, we have

$$B_{\mathrm{stab}}((\boldsymbol{u}_h,p_h),(\boldsymbol{v}_h,q_h)) \geq C\,|||(\boldsymbol{u}_h,p_h)|||^2. \tag{2.26}$$

On the other hand, using the definition of $\boldsymbol{v}_h, q_h, \delta$ and the triangle inequality, we have

$$|||(\boldsymbol{v}_h,q_h)||| \leq \sqrt{\varepsilon}\,\|\boldsymbol{u}_h\|_{\boldsymbol{H}} + \delta\sqrt{\varepsilon}\,\|p_h\|_{0,\Omega} + \|p_h\|_{1,\Omega} \leq C\,|||(\boldsymbol{u}_h,p_h)|||,$$

thus, using (2.26), we complete the proof. □

Remark 2.3. *This result is also valid for the continuous spaces $\boldsymbol{H}$ and Q and it will be used in the analysis of the a posteriori error estimator proposed in Section 2.4 (for details, see Lemma 2.7). On the other hand, if we use stable subspaces of $\boldsymbol{H}$ and Q, as for example, Raviart-Thomas elements of degree k, for the velocity, and piecewise polynomial elements of order k, for the pressure, or the Brezzi-Douglas-Marini spaces of order k, for the velocity, and piecewise polynomial elements of order $k-1$, for the pressure, Lemma 2.3 is also true (for details on stable subspaces, see [42]). In both cases the proof is similar to that proposed for Lemma 2.7 and therefore (3.28) can be seen as an augmented finite element method when stable subspaces of $\boldsymbol{H}$ and Q are used.*

Concerning the well-posedness of the stabilized discrete problem (3.28), we have the following result.

Theorem 2.2. *Let $\beta_s>0$ as in (2.24) and $\beta_c>0$ as in (2.1). If*

$$\gamma\,\|\boldsymbol{f}\|_{\infty,\Omega} \leq \frac{\min\{\beta_s,\beta_c\}\,\varepsilon^{1/2}}{3+\varepsilon^{-1/2}}, \tag{2.27}$$

then the discrete stabilized problem (3.28) has a unique solution $(\boldsymbol{u}_h,p_h)\in \boldsymbol{H}_h\times Q_h$.

Proof. To prove the result, we write the solution of the problem (3.28), as the solution of a fixed point problem. Thereby, given $r\in L^2(\Omega)$, we define the linear functionals

$$\boldsymbol{F}_r^s : \boldsymbol{H}_h\times Q_h \longrightarrow \mathbb{R} \quad \text{and} \quad \boldsymbol{F}^s : \boldsymbol{H}_h\times Q_h \longrightarrow \mathbb{R},$$

by

$$\boldsymbol{F}_r^s(\boldsymbol{v}_h,q_h) := \gamma(r\,\boldsymbol{f},\boldsymbol{v}_h) - \frac{1}{2}\big(\varepsilon^{-1}\gamma\, r\,\boldsymbol{f}, \varepsilon\,\boldsymbol{v}_h+\nabla q_h\big),$$
$$\boldsymbol{F}^s(\boldsymbol{v}_h,q_h) := \langle \boldsymbol{v}_h\cdot\boldsymbol{n},\varphi\rangle_{\Gamma_D} + \gamma(\boldsymbol{f},\boldsymbol{v}_h) - \frac{1}{2}\big(\varepsilon^{-1}\gamma\,\boldsymbol{f}, \varepsilon\,\boldsymbol{v}_h+\nabla q_h\big).$$

Now, we can write equation (3.28) as

$$B_{\mathrm{stab}}((\boldsymbol{u}_h,p_h),(\boldsymbol{v}_h,q_h)) = \boldsymbol{F}_{p_h}^s(\boldsymbol{v}_h,q_h) + \boldsymbol{F}^s(\boldsymbol{v}_h,q_h) \qquad \forall\,(\boldsymbol{v}_h,q_h)\in \boldsymbol{H}_h\times Q_h.$$

If we assume that $\boldsymbol{f}\in L^\infty(\Omega)^d$, the functional $\boldsymbol{F}_r^s$ satisfy

$$|\boldsymbol{F}_r^s(\boldsymbol{v}_h,q_h)| \leq \gamma\|r\|_{0,\Omega}\|\boldsymbol{f}\|_{\infty,\Omega}\|\boldsymbol{v}_h\|_{0,\Omega} + \frac{1}{2}\varepsilon^{-1}\gamma\|r\|_{0,\Omega}\|\boldsymbol{f}\|_{\infty,\Omega}\big\{\varepsilon\|\boldsymbol{v}_h\|_{0,\Omega}+\|\nabla q_h\|_{0,\Omega}\big\}$$

$$\leq \gamma\varepsilon^{-1/2}\|r\|_{0,\Omega}\|\boldsymbol{f}\|_{\infty,\Omega}|||(\boldsymbol{v}_h,q_h)||| + \frac{1}{2}\varepsilon^{-1}\gamma\|r\|_{0,\Omega}\|\boldsymbol{f}\|_{\infty,\Omega}\left\{\varepsilon^{1/2}+1\right\}|||(\boldsymbol{v}_h,q_h)|||$$

$$\leq \frac{\varepsilon^{-1/2}}{2}\left\{3+\varepsilon^{-1/2}\right\}\gamma\|r\|_{0,\Omega}\|\boldsymbol{f}\|_{\infty,\Omega}|||(\boldsymbol{v}_h,q_h)|||. \tag{2.28}$$

Moreover, let $T_h : \boldsymbol{H}_h \times Q_h \longrightarrow \boldsymbol{H}_h \times Q_h$ the operator defined, for a given $(\boldsymbol{w}_h, r_h) \in \boldsymbol{H}_h \times Q_h$, by

$$T_h(\boldsymbol{w}_h, r_h) = (\bar{\boldsymbol{u}}_h, \bar{p}_h),$$

where $(\bar{\boldsymbol{u}}_h, \bar{p}_h) \in \boldsymbol{H}_h \times Q_h$ is the unique solution of the linear problem

$$B_{\text{stab}}((\bar{\boldsymbol{u}}_h,\bar{p}_h),(\boldsymbol{v}_h,q_h)) = \boldsymbol{F}^s_{r_h}(\boldsymbol{v}_h,q_h) + \boldsymbol{F}^s(\boldsymbol{v}_h,q_h) \qquad \forall\,(\boldsymbol{v}_h,q_h) \in \boldsymbol{H}_h \times Q_h.$$

In this way, the discrete problem (3.28) can be written as follows: *Find* $(\boldsymbol{u}_h, p_h) \in \boldsymbol{H}_h \times Q_h$ *such that*

$$T_h(\boldsymbol{u}_h, p_h) = (\boldsymbol{u}_h, p_h).$$

Now, we can observe that

$$T_h(\boldsymbol{w}_h, r_h) = (\boldsymbol{u}_h^0, p_h^0) + S_h(\boldsymbol{w}_h, r_h) \qquad \forall (\boldsymbol{w}_h, r_h) \in \boldsymbol{H}_h \times Q_h,$$

where $(\boldsymbol{u}_h^0, p_h^0) \in \boldsymbol{H}_h \times Q_h$ is the unique solution of the auxiliar problem

$$B_{\text{stab}}((\boldsymbol{u}_h^0,p_h^0),(\boldsymbol{v}_h,q_h)) = \boldsymbol{F}^s(\boldsymbol{v}_h,q_h), \quad \forall\,(\boldsymbol{v}_h,q_h) \in \boldsymbol{H}_h \times Q_h, \tag{2.29}$$

and $S_h : \boldsymbol{H}_h \times Q_h \longrightarrow \boldsymbol{H}_h \times Q_h$ is the linear operator defined by

$$S_h(\boldsymbol{w}_h, r_h) = (\tilde{\boldsymbol{u}}_h, \tilde{p}_h) \in \boldsymbol{H}_h \times Q_h,$$

where $(\tilde{\boldsymbol{u}}_h, \tilde{p}_h) \in \boldsymbol{H}_h \times Q_h$ satisfies the problem

$$B_{\text{stab}}((\tilde{\boldsymbol{u}}_h,\tilde{p}_h),(\boldsymbol{v}_h,q_h)) = \boldsymbol{F}^s_{r_h}(\boldsymbol{v}_h,q_h), \quad \forall\,(\boldsymbol{v}_h,q_h) \in \boldsymbol{H}_h \times Q_h. \tag{2.30}$$

Furthermore, using the continuous dependence result and inequality (2.28), we have that

$$|||S_h(\boldsymbol{w}_h, r_h)||| = |||(\tilde{\boldsymbol{u}}_h, \tilde{p}_h)||| \leq \frac{\varepsilon^{-1/2}}{2\beta_s}\left\{3+\varepsilon^{-1/2}\right\}\gamma\|r_h\|_{0,\Omega}\|\boldsymbol{f}\|_{\infty,\Omega}. \tag{2.31}$$

Let $(\boldsymbol{w}_h^1, r_h^1), (\boldsymbol{w}_h^2, r_h^2) \in \boldsymbol{H}_h \times Q_h$. Then, from (2.31) we have

$$\begin{aligned}
|||T_h(\boldsymbol{w}_h^1, r_h^1) - T_h(\boldsymbol{w}_h^2, r_h^2)||| &= |||S_h(\boldsymbol{w}_h^1, r_h^1) - S_h(\boldsymbol{w}_h^2, r_h^2)||| \\
&= |||S_h(\boldsymbol{w}_h^1 - \boldsymbol{w}_h^2, r_h^1 - r_h^2)||| \\
&\leq \frac{\varepsilon^{-1/2}}{2\beta_s}\left\{3+\varepsilon^{-1/2}\right\}\gamma\|r_h^1 - r_h^2\|_{0,\Omega}\|\boldsymbol{f}\|_{\infty,\Omega} \\
&\leq \frac{\varepsilon^{-1/2}}{2\beta_s}\left\{3+\varepsilon^{-1/2}\right\}\gamma\|\boldsymbol{f}\|_{\infty,\Omega}|||(\boldsymbol{w}_h^1 - \boldsymbol{w}_h^2, r_h^1 - r_h^2)|||.
\end{aligned}$$

Thus, using condition (2.27), we have that

$$|||T_h(\boldsymbol{w}_h^1, r_h^1) - T_h(\boldsymbol{w}_h^2, r_h^2)||| \leq \frac{1}{2}|||(\boldsymbol{w}_h^1 - \boldsymbol{w}_h^2, r_h^1 - r_h^2)|||.$$

The result follows using the Banach fixed point theorem. □

We consider the Lagrange interpolants $\boldsymbol{I}_h : H^{k+1}(\Omega)^d \longrightarrow \boldsymbol{H}_h$ and $\mathcal{J}_h : H^{k+1}(\Omega) \longrightarrow Q_h$ such that (see [75] for details):

$$|\boldsymbol{u} - \boldsymbol{I}_h\boldsymbol{u}|_{l,\Omega} \leq Ch^{s-l}|\boldsymbol{u}|_{s,\Omega}, \tag{2.32}$$

$$|p - \mathcal{J}_h p|_{l,\Omega} \leq Ch^{s-l}|p|_{s,\Omega}, \tag{2.33}$$

for all $\boldsymbol{u} \in H^s(\Omega)^d$ and all $p \in H^s(\Omega)$ with $l = 0,1$ and $1 \leq s \leq k+1$.

Lemma 2.4. *Let $(\boldsymbol{u},p)$ and $(\boldsymbol{u}_h,p_h)$ be the solutions of (2.5) and (3.28), respectively. If $(\boldsymbol{u},p) \in H^{k+1}(\Omega)^d \cap \boldsymbol{H} \times H^{k+1}(\Omega)$, then it holds*

$$|B_{\text{stab}}((\boldsymbol{u}-\boldsymbol{u}_h,p-p_h),(\boldsymbol{v}_h,q_h))| \leq \frac{\varepsilon^{-1/2}}{2}(3+\varepsilon^{-1/2})\gamma\|\boldsymbol{f}\|_{\infty,\Omega}\|p-p_h\|_{0,\Omega}|||(\boldsymbol{v}_h,q_h)|||, \tag{2.34}$$

for all $(\boldsymbol{v}_h,q_h) \in \boldsymbol{H}_h \times Q_h$.

Proof. Using the regularity of the solution $(\boldsymbol{u},p)$ of (2.5), we can prove that $\varepsilon\boldsymbol{u} - \gamma(p+1)\boldsymbol{f} - \nabla p = \boldsymbol{0}$, $\nabla\cdot\boldsymbol{u} = 0$ and $p = \varphi$ on Γ_D. Now, using integration by parts and the definition of $B_{\text{stab}}(\cdot,\cdot)$, we have

$$\begin{aligned}
B_{\text{stab}}((\boldsymbol{u}-\boldsymbol{u}_h,p-p_h),(\boldsymbol{v}_h,q_h)) &= B_{\text{stab}}((\boldsymbol{u},p),(\boldsymbol{v}_h,q_h)) - B_{\text{stab}}((\boldsymbol{u}_h,p_h),(\boldsymbol{v}_h,q_h)) \\
&= \varepsilon(\boldsymbol{u},\boldsymbol{v}_h) + (p,\nabla\cdot\boldsymbol{v}_h) - (q_h,\nabla\cdot\boldsymbol{u}) \\
&\quad - \frac{1}{2}\big(\varepsilon^{-1}(\varepsilon\boldsymbol{u}-\nabla p),\varepsilon\boldsymbol{v}_h+\nabla q_h\big) + \varepsilon(\nabla\cdot\boldsymbol{u},\nabla\cdot\boldsymbol{v}_h) \\
&\quad - \langle\boldsymbol{v}_h\cdot\boldsymbol{n},\varphi\rangle_{\Gamma_D} - \gamma((p_h+1)\boldsymbol{f},\boldsymbol{v}_h) + \frac{1}{2}\big(\varepsilon^{-1}\gamma(p_h+1)\boldsymbol{f},\varepsilon\boldsymbol{v}_h+\nabla q_h\big) \\
&= (\varepsilon\boldsymbol{u} - \gamma(p_h+1)\boldsymbol{f} - \nabla p,\boldsymbol{v}_h) \\
&\quad - \frac{1}{2}\big(\varepsilon^{-1}\big[\varepsilon\boldsymbol{u}-\nabla p-\gamma(p_h+1)\boldsymbol{f}\big],\varepsilon\boldsymbol{v}_h+\nabla q_h\big) \\
&= \big(\gamma(p-p_h)\boldsymbol{f},\boldsymbol{v}_h\big) - \frac{1}{2}\big(\varepsilon^{-1}\gamma(p-p_h)\boldsymbol{f},\varepsilon\boldsymbol{v}_h+\nabla q_h\big) \\
&= \frac{1}{2}\big(\gamma(p-p_h)\boldsymbol{f},\boldsymbol{v}_h\big) - \frac{1}{2}\big(\varepsilon^{-1}\gamma(p-p_h)\boldsymbol{f},\nabla q_h\big) \\
&\leq \frac{1}{2}\Big\{\gamma\|p-p_h\|_{0,\Omega}\|\boldsymbol{f}\|_{\infty,\Omega}\varepsilon^{-1/2} + \gamma\|p-p_h\|_{0,\Omega}\|\boldsymbol{f}\|_{\infty,\Omega}\varepsilon^{-1}\Big\}\cdot \\
&\qquad |||(\boldsymbol{v}_h,q_h)||| \\
&= \frac{\varepsilon^{-1/2}}{2}(1+\varepsilon^{-1/2})\gamma\|\boldsymbol{f}\|_{\infty,\Omega}\|p-p_h\|_{0,\Omega}|||(\boldsymbol{v}_h,q_h)||| \\
&\leq \frac{\varepsilon^{-1/2}}{2}(3+\varepsilon^{-1/2})\gamma\|\boldsymbol{f}\|_{\infty,\Omega}\|p-p_h\|_{0,\Omega}|||(\boldsymbol{v}_h,q_h)|||,
\end{aligned}$$

and the result follows. □

Theorem 2.3 (Main Result)**.** *Let $(\boldsymbol{u},p) \in H^{k+1}(\Omega)^d \cap \boldsymbol{H} \times H^{k+1}(\Omega)$, be the solution of (2.5) and $(\boldsymbol{u}_h,p_h) \in \boldsymbol{H}_h \times Q_h$ solution of (3.28). If we assume (2.27), then it holds*

$$|||(\boldsymbol{u}-\boldsymbol{u}_h,p-p_h)||| \leq C\,h^k\left\{(\varepsilon^{1/2}+1)\,\|\boldsymbol{u}\|_{k+1,\Omega} + (\varepsilon^{-1/2}+\varepsilon^{-1}+1)\,\|p\|_{k+1,\Omega}\right\},$$

with $C > 0$ independent of h and ε.

Proof. Let

$$(\eta^{\boldsymbol{u}},\eta^{p}):=(\boldsymbol{u}-\boldsymbol{I}_h\boldsymbol{u},p-\mathcal{J}_h p)\quad\text{and}\quad(e_h^{\boldsymbol{u}},e_h^{p}):=(\boldsymbol{u}_h-\boldsymbol{I}_h\boldsymbol{u},p_h-\mathcal{J}_h p).$$

Using the definition of $\mathcal{B}$ given in (2.17), and Cauchy–Schwarz inequality, we have

$$\begin{aligned}
&B_{\mathrm{stab}}((\eta^{\boldsymbol{u}},\eta^{p}),(\boldsymbol{v}_h,q_h))\\
&=\varepsilon(\eta^{\boldsymbol{u}},\boldsymbol{v}_h)+(\eta^{p},\nabla\cdot\boldsymbol{v}_h)-(q_h,\nabla\cdot\eta^{\boldsymbol{u}})-\frac{1}{2}\left(\varepsilon^{-1}(\varepsilon\eta^{\boldsymbol{u}}-\nabla\eta^{p}),\varepsilon\boldsymbol{v}_h+\nabla q_h\right)+\varepsilon\left(\nabla\cdot\eta^{\boldsymbol{u}},\nabla\cdot\boldsymbol{v}_h\right)\\
&\leq\Big\{\varepsilon^{1/2}\|\eta^{\boldsymbol{u}}\|_{0,\Omega}+\varepsilon^{-1/2}\|\eta^{p}\|_{0,\Omega}+\|\nabla\cdot\eta^{\boldsymbol{u}}\|_{0,\Omega}+\frac{1}{2}\left(\varepsilon^{1/2}+1\right)\big[\|\eta^{\boldsymbol{u}}\|_{0,\Omega}\\
&\quad+\varepsilon^{-1}\left|\eta^{p}\right|_{1,\Omega}\big]+\varepsilon^{1/2}\|\nabla\cdot\eta^{\boldsymbol{u}}\|_{0,\Omega}\Big\}\,|||(\boldsymbol{v}_h,q_h)|||\qquad(2.35)\\
&\leq\Big\{\frac{1}{2}\left(3\varepsilon^{1/2}+1\right)\|\eta^{\boldsymbol{u}}\|_{0,\Omega}+(\varepsilon^{1/2}+1)\|\nabla\cdot\eta^{\boldsymbol{u}}\|_{0,\Omega}+\varepsilon^{-1/2}\|\eta^{p}\|_{0,\Omega}\qquad(2.36)\\
&\quad+\frac{1}{2}\varepsilon^{-1}(\varepsilon^{1/2}+1)\left|\eta^{p}\right|_{1,\Omega}\Big\}\,|||(\boldsymbol{v}_h,q_h)|||.\qquad(2.37)
\end{aligned}$$

Using lemmas 2.3 and 2.4, and inequality (2.35), we get that

$$\begin{aligned}
B_{\mathrm{stab}}((e_h^{\boldsymbol{u}},e_h^{p}),(\boldsymbol{v}_h,q_h))&=B_{\mathrm{stab}}((\eta^{\boldsymbol{u}},\eta^{p}),(\boldsymbol{v}_h,q_h))-B_{\mathrm{stab}}((\boldsymbol{u}-\boldsymbol{u}_h,p-p_h),(\boldsymbol{v}_h,q_h))\\
&\leq\Big[\frac{1}{2}\left(3\varepsilon^{1/2}+1\right)\|\eta^{\boldsymbol{u}}\|_{0,\Omega}+(\varepsilon^{1/2}+1)\|\nabla\cdot\eta^{\boldsymbol{u}}\|_{0,\Omega}\\
&\quad+\varepsilon^{-1/2}\|\eta^{p}\|_{0,\Omega}+\frac{1}{2}\varepsilon^{-1}(\varepsilon^{1/2}+1)\left|\eta^{p}\right|_{1,\Omega}\Big]\,|||(\boldsymbol{v}_h,q_h)|||\\
&\quad+\frac{\varepsilon^{-1/2}}{2}(3+\varepsilon^{-1/2})\gamma\|\boldsymbol{f}\|_{\infty,\Omega}\|p-p_h\|_{0,\Omega}\,|||(\boldsymbol{v}_h,q_h)|||.
\end{aligned}$$

Now, using Lemma 2.3 and (2.27), we have

$$\begin{aligned}
&\beta_s\,|||(e_h^{\boldsymbol{u}},e_h^{p})|||\\
&\leq\frac{1}{2}\left(3\varepsilon^{1/2}+1\right)\|\eta^{\boldsymbol{u}}\|_{0,\Omega}+(\varepsilon^{1/2}+1)\|\nabla\cdot\eta^{\boldsymbol{u}}\|_{0,\Omega}+\varepsilon^{-1/2}\|\eta^{p}\|_{0,\Omega}+\\
&\quad\frac{1}{2}\varepsilon^{-1}(\varepsilon^{1/2}+1)\left|\eta^{p}\right|_{1,\Omega}+\frac{\varepsilon^{-1/2}}{2}(3+\varepsilon^{-1/2})\gamma\|\boldsymbol{f}\|_{\infty,\Omega}\|p-p_h\|_{0,\Omega}\\
&\leq\frac{1}{2}\left(3\varepsilon^{1/2}+1\right)\|\eta^{\boldsymbol{u}}\|_{0,\Omega}+(\varepsilon^{1/2}+1)\|\nabla\cdot\eta^{\boldsymbol{u}}\|_{0,\Omega}+\varepsilon^{-1/2}\|\eta^{p}\|_{0,\Omega}+\\
&\quad\frac{1}{2}\varepsilon^{-1}(\varepsilon^{1/2}+1)\left|\eta^{p}\right|_{1,\Omega}+\frac{\varepsilon^{-1/2}}{2}(3+\varepsilon^{-1/2})\gamma\|\boldsymbol{f}\|_{\infty,\Omega}|||(\boldsymbol{u}-\boldsymbol{u}_h,p-p_h)|||\\
&\leq\frac{1}{2}\left(3\varepsilon^{1/2}+1\right)\|\eta^{\boldsymbol{u}}\|_{0,\Omega}+(\varepsilon^{1/2}+1)\|\nabla\cdot\eta^{\boldsymbol{u}}\|_{0,\Omega}+\varepsilon^{-1/2}\|\eta^{p}\|_{0,\Omega}+\\
&\quad\frac{1}{2}\varepsilon^{-1}(\varepsilon^{1/2}+1)\left|\eta^{p}\right|_{1,\Omega}+\frac{\beta_s}{2}\,|||(\boldsymbol{u}-\boldsymbol{u}_h,p-p_h)|||.\qquad(2.38)
\end{aligned}$$

Furthermore, using the triangle inequality and (2.38), we obtain

$$|||(\boldsymbol{u}-\boldsymbol{u}_h,p-p_h)|||\leq|||(\eta^{\boldsymbol{u}},\eta^{p})|||+\frac{1}{2}\,|||(\boldsymbol{u}-\boldsymbol{u}_h,p-p_h)|||$$

$$+C\left\{(\varepsilon^{1/2}+1)\,\|\eta^{\boldsymbol{u}}\|_{\boldsymbol{H}}+\varepsilon^{-1/2}\|\eta^{p}\|_{0,\Omega}+\varepsilon^{-1}(\varepsilon^{1/2}+1)\,|\eta^{p}|_{1,\Omega}\right\},$$

thus

$$|||(\boldsymbol{u}-\boldsymbol{u}_h,p-p_h)|||\leq C\left\{|||(\eta^{\boldsymbol{u}},\eta^{p})|||+(\varepsilon^{1/2}+1)\,\|\eta^{\boldsymbol{u}}\|_{\boldsymbol{H}}+\varepsilon^{-1/2}\|\eta^{p}\|_{0,\Omega}+\varepsilon^{-1}\ (\varepsilon^{1/2}+1)\,|\eta^{p}|_{1,\Omega}\right\}.$$

Finally, using the properties of $\boldsymbol{I}_h$ and $\mathcal{J}_h$, we have

$$|||(\eta^{\boldsymbol{u}},\eta^{p})|||\leq C\,h^{k}\left\{\varepsilon^{1/2}\,\|\boldsymbol{u}\|_{k+1,\Omega}+\|p\|_{k+1,\Omega}\right\},$$

and the result follows. □

2.4 A posteriori error analysis

In this section, we present a residual a posteriori error estimator for the stabilized finite element method (3.28). Let $\Gamma_{D,h}$ be the partition of Γ_D inherited from the triangulation $\mathcal{T}_h$, and define the mesh size $h_D:=\max\{|F|:F\in\Gamma_{D,h}\}$. For simplicity, we assume that

- $\boldsymbol{f}$ is a piecewise polynomial in Ω; i.e $\boldsymbol{f}\Big|_K\in\mathbb{P}_l(K)^d,\forall K\in\mathcal{T}_h,l\geq 0$.
- φ is a continuous piecewise polynomial in $\Gamma_{D,h}$; i.e $\varphi\in C^0(\Gamma_{D,h}),\varphi\Big|_F\in\mathbb{P}_l(F),\forall F\in\Gamma_{D,h},l\geq 0$.

For each $K\in\mathcal{T}_h$ and each $F\in\mathcal{E}_D$, we define the residuals

$$\mathcal{R}_K:=\Big(\gamma\,(p_h+1)\boldsymbol{f}-\varepsilon\,\boldsymbol{u}_h+\nabla p_h\Big)\Big|_K,$$
$$\mathcal{R}_F:=(\varphi-p_h)\Big|_F.$$

Thus, our residual–based error estimator is given by

$$\eta:=\left\{\sum_{K\in\mathcal{T}_H}\eta_K^2\right\}^{1/2},\tag{2.39}$$

where, for each $K\in\mathcal{T}_h$, we have that

$$\eta_K^2:=\|\mathcal{R}_K\|_{0,K}^2+\varepsilon^2\,\|\nabla\cdot\boldsymbol{u}_h\|_{0,K}^2+\sum_{F\subset\mathcal{E}(K)\cap\mathcal{E}_D}h_F^{-1}\,\|\mathcal{R}_F\|_{0,F}^2.\tag{2.40}$$

Lemma 2.5. *Let $(\boldsymbol{u},p)\in\boldsymbol{H}\times Q$ and $(\boldsymbol{u}_h,p_h)\in\boldsymbol{H}_h\times Q_h$, be the solutions of (2.5) and (3.28), respectively. Then, for all $(\boldsymbol{v},q)\in\boldsymbol{H}\times Q$, we have*

$$B_{\mathrm{stab}}((\boldsymbol{u}-\boldsymbol{u}_h,p-p_h),(\boldsymbol{v},q))$$

$$= \langle \boldsymbol{v}\cdot\boldsymbol{n}, \varphi - p_h\rangle_{\Gamma_D} + \frac{1}{2}\left(\varepsilon^{-1/2}\gamma(p-p_h)\boldsymbol{f}, \varepsilon^{1/2}\boldsymbol{v} - \varepsilon^{-1/2}\nabla q\right)$$
$$+ \frac{1}{2}\sum_{K\in\mathcal{T}_h}\left(\varepsilon^{-1/2}(\mathcal{R}_K), \varepsilon^{1/2}\boldsymbol{v} - \varepsilon^{-1/2}\nabla q\right)_K + (q, \nabla\cdot\boldsymbol{u}_h) - \varepsilon(\nabla\cdot\boldsymbol{u}_h, \nabla\cdot\boldsymbol{v}).$$

Proof. Using (2.6), (2.7), (3.28) and integration by parts, we get that

$$\begin{aligned}
&B_{\mathrm{stab}}((\boldsymbol{u}-\boldsymbol{u}_h, p-p_h), (\boldsymbol{v}, q))\\
=&B_{\mathrm{stab}}((\boldsymbol{u}, p), (\boldsymbol{v}, q)) - B_{\mathrm{stab}}((\boldsymbol{u}_h, p_h), (\boldsymbol{v}, q))\\
=&\langle \boldsymbol{v}\cdot\boldsymbol{n}, \varphi\rangle_{\Gamma_D} + \gamma((p+1)\boldsymbol{f}, \boldsymbol{v}) - \frac{1}{2}\left(\varepsilon^{-1}(\gamma(p+1)\boldsymbol{f}), \varepsilon\boldsymbol{v} + \nabla q\right)\\
&- \varepsilon(\boldsymbol{u}_h, \boldsymbol{v}) - (p_h, \nabla\cdot\boldsymbol{v}) + (q, \nabla\cdot\boldsymbol{u}_h) + \frac{1}{2}\left(\varepsilon^{-1}(\varepsilon\boldsymbol{u}_h - \nabla p_h), \varepsilon\boldsymbol{v} + \nabla q\right) - \varepsilon(\nabla\cdot\boldsymbol{u}_h, \nabla\cdot\boldsymbol{v})\\
=&\langle \boldsymbol{v}\cdot\boldsymbol{n}, \varphi\rangle_{\Gamma_D} + \gamma((p+1)\boldsymbol{f}, \boldsymbol{v}) + \varepsilon(\nabla\cdot\boldsymbol{u}, \nabla\cdot\boldsymbol{v}) - \varepsilon(\boldsymbol{u}_h, \boldsymbol{v}) - (p_h, \nabla\cdot\boldsymbol{v}) + (q, \nabla\cdot\boldsymbol{u}_h)\\
&+ \frac{1}{2}\left(\varepsilon^{-1}(\varepsilon\boldsymbol{u}_h - \nabla p_h - \gamma(p+1)\boldsymbol{f}), \varepsilon\boldsymbol{v} + \nabla q\right) - \varepsilon(\nabla\cdot\boldsymbol{u}_h, \nabla\cdot\boldsymbol{v})\\
=&\langle \boldsymbol{v}\cdot\boldsymbol{n}, \varphi - p_h\rangle_{\Gamma_D} + (\gamma(p+1)\boldsymbol{f} - \varepsilon\boldsymbol{u}_h + \nabla p_h, \boldsymbol{v}) + \varepsilon(\nabla\cdot\boldsymbol{u}, \nabla\cdot\boldsymbol{v}) + (q, \nabla\cdot\boldsymbol{u}_h)\\
&+ \frac{1}{2}\left(\varepsilon^{-1}(\varepsilon\boldsymbol{u}_h - \nabla p_h - \gamma(p+1)\boldsymbol{f}), \varepsilon\boldsymbol{v} + \nabla q\right) - \varepsilon(\nabla\cdot\boldsymbol{u}_h, \nabla\cdot\boldsymbol{v})\\
=&\langle \boldsymbol{v}\cdot\boldsymbol{n}, \varphi - p_h\rangle_{\Gamma_D} + (\gamma(p-p_h)\boldsymbol{f}, \boldsymbol{v}) + (\gamma(p_h+1)\boldsymbol{f} - \varepsilon\boldsymbol{u}_h + \nabla p_h, \boldsymbol{v}) + \varepsilon(\nabla\cdot\boldsymbol{u}, \nabla\cdot\boldsymbol{v}) + (q, \nabla\cdot\boldsymbol{u}_h)\\
&- \frac{1}{2}\left(\varepsilon^{-1}(\gamma(p-p_h)\boldsymbol{f}), \varepsilon\boldsymbol{v} + \nabla q\right) + \frac{1}{2}\left(\varepsilon^{-1}(\varepsilon\boldsymbol{u}_h - \nabla p_h - \gamma(p_h+1)\boldsymbol{f}), \varepsilon\boldsymbol{v} + \nabla q\right) - \varepsilon(\nabla\cdot\boldsymbol{u}_h, \nabla\cdot\boldsymbol{v})\\
=&\langle \boldsymbol{v}\cdot\boldsymbol{n}, \varphi - p_h\rangle_{\Gamma_D} + (\gamma(p-p_h)\boldsymbol{f}, \boldsymbol{v}) + \sum_{K\in\mathcal{T}_h}(\mathcal{R}_K, \boldsymbol{v})_K + \varepsilon(\nabla\cdot\boldsymbol{u}, \nabla\cdot\boldsymbol{v}) + (q, \nabla\cdot\boldsymbol{u}_h)\\
&- \frac{1}{2}\left(\varepsilon^{-1}(\gamma(p-p_h)\boldsymbol{f}), \varepsilon\boldsymbol{v} + \nabla q\right) - \frac{1}{2}\sum_{K\in\mathcal{T}_h}\left(\varepsilon^{-1}(\mathcal{R}_K), \varepsilon\boldsymbol{v} + \nabla q\right)_K - \varepsilon(\nabla\cdot\boldsymbol{u}_h, \nabla\cdot\boldsymbol{v})\\
=&\langle \boldsymbol{v}\cdot\boldsymbol{n}, \varphi - p_h\rangle_{\Gamma_D} + \frac{1}{2}(\varepsilon^{-1/2}\gamma(p-p_h)\boldsymbol{f}, \varepsilon^{1/2}\boldsymbol{v} - \varepsilon^{-1/2}\nabla q)\\
&+ \frac{1}{2}\sum_{K\in\mathcal{T}_h}\left(\varepsilon^{-1/2}(\mathcal{R}_K), \varepsilon^{1/2}\boldsymbol{v} - \varepsilon^{-1/2}\nabla q\right)_K + (q, \nabla\cdot\boldsymbol{u}_h) - \varepsilon(\nabla\cdot\boldsymbol{u}_h, \nabla\cdot\boldsymbol{v}),
\end{aligned}$$

and the result follows. □

To introduce the main result of this section, we need to define the following mesh–dependent norm for the pressure

$$\|p\|_{\omega_F} := \left\{\sum_{K\in\omega_F}\left[h_K^{-2}\|p\|_{0,K}^2 + |p|_{1,K}^2\right]\right\}^{1/2},$$

for all $p\in Q$, and for all $F\in\mathcal{E}_h$, where ω_F is the set of elements K of $\mathcal{T}_h$ such that $F\in\partial K$.

Lemma 2.6. *There exists $C>0$, independent of h, such that*

$$\|\psi\|_{0,\partial K}^2 \le C\left\{h_K^{-1}\|\psi\|_{0,K}^2 + h_K|\psi|_{1,K}^2\right\},$$

for all $K\in\mathcal{T}_h$ and all $\psi\in H^1(K)$.

Proof. See [4, Theorem 3.10] or [43, (10.3.8)]. □

We are ready to prove the efficiency and reliability of the error estimator (2.39).

Theorem 2.4. *Let $(\boldsymbol{u},p)\in \boldsymbol{H}\times Q$ and $(\boldsymbol{u}_h,p_h)\in \boldsymbol{H}_h\times Q_h$, be the solutions of (2.5) and (3.28), respectively, and suppose valid (2.27). Then, the following holds*

$$|||(\boldsymbol{u}-\boldsymbol{u}_h,p-p_h)||| \leq C\,\varepsilon^{-1/2}\max\left\{1,\varepsilon^{-1/2}\right\}\eta,$$

where $C>0$ is independent of ε,γ and h, and

$$\eta_K \leq C\left\{\varepsilon^2\,\|\boldsymbol{u}-\boldsymbol{u}_h\|^2_{\mathrm{div},K}+\beta_K^2\,\|p-p_h\|^2_{1,K}+\sum_{F\subset\mathcal{E}(K)\cap\mathcal{E}_D}\|p-p_h\|^2_{\omega_F}\right\},$$

for all $K\in\mathcal{T}_h$, where $\beta_K:=\max\left\{\gamma\,\|\boldsymbol{f}\|_{\infty,\Omega},1\right\}$.

Proof. From [58, 133] we have the following inverse estimate $\|\varphi-p_h\|_{1/2,\Gamma_D}\leq Ch_D^{-1/2}\|\varphi-p_h\|_{0,\Gamma_D}$, thus using Cauchy-Schwarz inequality, the definition of norm $\|\cdot\|_{-1/2,\Gamma_D}$ given in (2.10) and Lemma 2.5, we get

$$\begin{aligned}
&B_{\mathrm{stab}}((\boldsymbol{u}-\boldsymbol{u}_h,p-p_h),(\boldsymbol{v},q))\\
\leq& C\,\|\boldsymbol{v}\cdot\boldsymbol{n}\|_{-1/2,\Gamma_D}\|\varphi-p_h\|_{1/2,\Gamma_D}+\frac{1}{2}\,\varepsilon^{-1/2}\|p-p_h\|_{0,\Omega}\,\gamma\|\boldsymbol{f}\|_{\infty,\Omega}\,\|\varepsilon^{1/2}\boldsymbol{v}-\varepsilon^{-1/2}\nabla q\|_{0,\Omega}+\\
&\frac{1}{2}\sum_{K\in\mathcal{T}_h}\varepsilon^{-1/2}\|\mathcal{R}_K\|_{0,K}\|\varepsilon^{1/2}\boldsymbol{v}-\varepsilon^{-1/2}\nabla q\|_{0,K}+\|q\|_{0,\Omega}\|\nabla\cdot\boldsymbol{u}_h\|_{0,\Omega}+\varepsilon\,\|\nabla\cdot\boldsymbol{u}_h\|_{0,\Omega}\|\nabla\cdot\boldsymbol{v}\|_{0,\Omega}\\
\leq& C\,h_D^{-1/2}\|\boldsymbol{v}\|_{\boldsymbol{H}}\|\varphi-p_h\|_{0,\Gamma_D}+\frac{1}{2}\,\varepsilon^{-1/2}\|p-p_h\|_{0,\Omega}\,\gamma\|\boldsymbol{f}\|_{\infty,\Omega}\,\|\varepsilon^{1/2}\boldsymbol{v}-\varepsilon^{-1/2}\nabla q\|_{0,\Omega}+\\
&\frac{1}{2}\sum_{K\in\mathcal{T}_h}\varepsilon^{-1/2}\|\mathcal{R}_K\|_{0,K}\|\varepsilon^{1/2}\boldsymbol{v}-\varepsilon^{-1/2}\nabla q\|_{0,K}+\|q\|_{0,\Omega}\|\nabla\cdot\boldsymbol{u}_h\|_{0,\Omega}+\varepsilon\,\|\nabla\cdot\boldsymbol{u}_h\|_{0,\Omega}\|\nabla\cdot\boldsymbol{v}\|_{0,\Omega}\\
\leq& C\,\|\boldsymbol{v}\|_{\boldsymbol{H}}\left\{\sum_{F\subset\mathcal{E}_D}h_F^{-1}\,\|\varphi-p_h\|^2_{0,F}\right\}^{1/2}+\frac{1}{2}\,\varepsilon^{-1/2}\|p-p_h\|_{0,\Omega}\,\gamma\|\boldsymbol{f}\|_{\infty,\Omega}\left\{\varepsilon^{1/2}\,\|\boldsymbol{v}\|_{0,\Omega}+\varepsilon^{-1/2}\,|q|_{1,\Omega}\right\}+\\
&C\left\{\sum_{K\in\mathcal{T}_h}\left[\varepsilon^{-1}\,\|\mathcal{R}_K\|^2_{0,K}+\varepsilon\,\|\nabla\cdot\boldsymbol{u}_h\|^2_{0,K}\right]\right\}^{1/2}\cdot\\
&\left\{\sum_{K\in\mathcal{T}_h}\left[\varepsilon\|\boldsymbol{v}\|^2_{0,K}+\varepsilon\,\|\nabla\cdot\boldsymbol{v}\|^2_{0,K}+\varepsilon^{-1}\,\|q\|^2_{0,K}+\varepsilon^{-1}\,|q|^2_{1,K}\right]\right\}^{1/2} \qquad (2.41)\\
\leq&\frac{1}{2}\,\varepsilon^{-1/2}\|p-p_h\|_{0,\Omega}\,\gamma\|\boldsymbol{f}\|_{\infty,\Omega}\left\{\varepsilon^{1/2}\,\|\boldsymbol{v}\|_{0,\Omega}+\varepsilon^{-1/2}\,|q|_{1,\Omega}\right\}+\\
&C\left\{\sum_{K\in\mathcal{T}_h}\left[\varepsilon^{-1}\,\|\mathcal{R}_K\|^2_{0,K}+\varepsilon\,\|\nabla\cdot\boldsymbol{u}_h\|^2_{0,K}+\sum_{F\subset\mathcal{E}(K)\cap\mathcal{E}_D}\varepsilon^{-1}h_F^{-1}\,\|\mathcal{R}_F\|^2_{0,F}\right]\right\}^{1/2}\cdot\\
&\left\{\varepsilon\|\boldsymbol{v}\|^2_{\boldsymbol{H}}+\varepsilon^{-1}\,\|q\|^2_{1,\Omega}\right\}^{1/2} \qquad (2.42)
\end{aligned}$$

$$\leq \varepsilon^{-1/2}\max\left\{1,\varepsilon^{-1/2}\right\}\left\{\frac{1}{2}\|p-p_h\|_{0,\Omega}\gamma\|\boldsymbol{f}\|_{\infty,\Omega}+C\eta\right\}|||(\boldsymbol{v},q)|||. \tag{2.43}$$

Additionally, from Lemma 2.7, (2.27) and (2.43), we arrive at

$$\begin{aligned}
&\beta_c\,|||(\boldsymbol{u}-\boldsymbol{u}_h,p-p_h)||| \\
\leq\ & \sup_{(\boldsymbol{v},q)\in\boldsymbol{H}\times Q}\frac{\mathcal{B}((\boldsymbol{u}-\boldsymbol{u}_h,p-p_h),(\boldsymbol{v},q))}{|||(\boldsymbol{v},q)|||} \\
\leq\ & \varepsilon^{-1/2}\max\left\{1,\varepsilon^{-1/2}\right\}\frac{1}{2}\|p-p_h\|_{0,\Omega}\gamma\|\boldsymbol{f}\|_{\infty,\Omega}+C\varepsilon^{-1/2}\max\left\{1,\varepsilon^{-1/2}\right\}\eta \\
\leq\ & \frac{3+\varepsilon^{-1/2}}{2}\varepsilon^{-1/2}\|p-p_h\|_{1,\Omega}\gamma\|\boldsymbol{f}\|_{\infty,\Omega}+C\varepsilon^{-1/2}\max\left\{1,\varepsilon^{-1/2}\right\}\eta \\
\leq\ & \frac{\beta_c}{2}\|p-p_h\|_{1,\Omega}+C\varepsilon^{-1/2}\max\left\{1,\varepsilon^{-1/2}\right\}\eta,
\end{aligned} \tag{2.44}$$

and therefore,

$$|||(\boldsymbol{u}-\boldsymbol{u}_h,p-p_h)||| \leq C\varepsilon^{-1/2}\max\left\{1,\varepsilon^{-1/2}\right\}\eta.$$

On the other hand, using the definition of $\mathcal{R}_K$ and (2.5), we deduce that

$$\begin{aligned}
\|\mathcal{R}_K\|_{0,K} &= \|\gamma p_h\boldsymbol{f}+\gamma\boldsymbol{f}-\varepsilon\boldsymbol{u}_h+\nabla p_h\|_{0,K} \\
&= \|\gamma p_h\boldsymbol{f}+\varepsilon u-\gamma p\boldsymbol{f}-\nabla p-\varepsilon\boldsymbol{u}_h+\nabla p_h\|_{0,K} \\
&= \|\gamma(p_h-p)\boldsymbol{f}+\varepsilon(\boldsymbol{u}-\boldsymbol{u}_h)+\nabla(p_h-p)\|_{0,K} \\
&\leq \|p-p_h\|_{0,K}\gamma\|\boldsymbol{f}\|_{\infty,K}+\varepsilon\|\boldsymbol{u}-\boldsymbol{u}_h\|_{0,K}+|p-p_h|_{1,K}.
\end{aligned} \tag{2.45}$$

In addition, as $\nabla\cdot\boldsymbol{u}=0$ in Ω, we have

$$\|\nabla\cdot\boldsymbol{u}_h\|_{0,K} = \|\nabla\cdot(\boldsymbol{u}-\boldsymbol{u}_h)\|_{0,K}. \tag{2.46}$$

Similarly, as $p=\varphi$ on Γ_D, using the triangle inequality, Lemma 2.6 and the mesh regularity, we have that

$$h_F^{-1}\|\mathcal{R}_F\|_{0,F}^2 = h_F^{-1}\|p-p_h\|_{0,F}^2 \leq C\sum_{K\in\omega_F}\left[h_K^{-2}\|p-p_h\|_{0,K}^2+|p-p_h|_{1,K}^2\right]. \tag{2.47}$$

Finally, using the definition of η_K and (2.45)–(2.47), we get the result.

□

2.5 Numerical results

In this section we present some numerical tests that illustrate the performance of our adapted stabilized finite element method given in (3.28). In particular, we confirm the results presented in Theorem 3.1 and the quality of the a posteriori error estimator (2.39) for the Darcy equation (2.5).

The stabilized finite element scheme was implemented using the open source finite element library FEniCS [116].

Recall that we use the notation $\mathbb{P}_k^d \times \mathbb{P}_k$ to mean that the velocity and the pressure are approximated using piecewise continuous polynomials of total degree at most k.

We will use the following notation for the error in velocity and pressure, respectively

$$e_{\boldsymbol{u}} := \|\boldsymbol{u} - \boldsymbol{u}_h\|_{\boldsymbol{H}}, \qquad \text{and} \qquad e_p := \|p - p_h\|_{1,\Omega},$$

while the convergence rates are denoted by

$$r_m(x) = \frac{\log(e_x^i / e_x^{i-1})}{\log(h^i / h^{i-1})}, \quad \text{with } x \in \{\boldsymbol{u}, p\},$$

where m is the polynomial degree, h^i, h^{i-1}, and, e_x^i, e_x^{i-1} represent two consecutive mesh sizes and two consecutive errors, respectively.

Finally, we define the effectivity index E as follows

$$E := \frac{\eta}{|||(\boldsymbol{u} - \boldsymbol{u}_h, p - p_h)|||}.$$

Our adaptive algorithm is given by

Algorithm 2 Adaptivity procedure

Require: $\theta \in (0,1)$ and a coarse mesh $\mathcal{T}_h$.

1: Solve the stabilized discrete scheme (3.28) on the current mesh.
2: For each $K \in \mathcal{T}_h$, compute the local error indicator η_K given by (2.40).
3: Given $K \in \mathcal{T}_h$ such that $\eta_K \geq \theta \max_{K' \in \mathcal{T}_h} \eta_{K'}$, mark K and generate a new mesh $\mathcal{T}_h$ refining the marked elements.
4: If the stop criterion is not satisfied, go to step 1.

2.5.1 Analytic solution

In this example, we will test the approximation capability of the stabilized method in a non-convex domain with a nearly singular solution close to the origin of coordinates. We will also show that our error estimator adapts the meshes where it is expected and has a good effectivity index.

In this case our domain is $\Omega := \left\{(x,y) \in \mathbb{R}^2 : x^2 + y^2 \leq 1\right\} \setminus (0,1)^2$, with $\Gamma_N := (0,1) \times \{0\} \cup \{0\} \times (0,1)$ and $\Gamma_D := \partial\Omega \setminus \Gamma_N$. The data $\boldsymbol{f}$ and φ are such that the exact solution is given by

$$\boldsymbol{u}(x,y) := [(x-c)^2 + (y-c)^2]^{-1/2}(c-y, x-c), \quad p(x,y) := \frac{1 - x^2 - y^2}{(x-c)^2 + (y-c)^2},$$

where $c = 0.025$. For the drag function (2.4), we take $\alpha_0 = 1.0$, while $\gamma = 1, 10^{-2}, 10^{-4}$.

Note that in this case $\boldsymbol{f}(x,y) = [h(x,y)]^{-1}\big(f_1(x,y), f_2(x,y)\big)$, where

$$f_1(x,y) = \frac{c-y}{\sqrt{(x-c)^2 + (y-c)^2}} + \frac{2x}{\varepsilon((x-c)^2 + (y-c)^2)} + \frac{(1-x^2-y^2)(2x-2c)}{\varepsilon((x-c)^2 + (y-c)^2)^2}$$

$$f_2(x,y) = \frac{x-c}{\sqrt{(x-c)^2 + (y-c)^2}} + \frac{2y}{\varepsilon((x-c)^2 + (y-c)^2)} + \frac{(1-x^2-y^2)(2y-2c)}{\varepsilon((x-c)^2 + (y-c)^2)^2}$$

$$h(x,y) = \frac{\left[1 - x^2 - y^2 + (c-x)^2 + (c-y)^2\right]}{\left[(c-x)^2 + (c-y)^2\right]}.$$

In this experiment, we consider a post-processed pressure $\tilde{p}_h := \dfrac{1}{\gamma}\log(p_h + 1)$ used to approximate the exact pressure $\tilde{p}$ of the original problem (2.1).

In Tables 2.1 – 2.6 we show the approximation error using $\mathbb{P}_1^2 \times \mathbb{P}_1$ and $\mathbb{P}_2^2 \times \mathbb{P}_2$. We note that the errors on the velocity and pressure have the order predicted by Theorem 3.1. On the other hand, the error estimator η, given by (2.39), has a quite good quality reflected on the fact that effectivity indexes are close to the unity. Note that there is a small degradation of the effectivity index when ε goes to 0.

h	$\|p-p_h\|_{1,\Omega}$	$r_1(p)$	$\|\boldsymbol{u}-\boldsymbol{u}_h\|_{\boldsymbol{H}}$	$r_1(u)$	$\|\|\|(\boldsymbol{u}-\boldsymbol{u}_h, p-p_h)\|\|\|$	η	E
0.079946	2056.657064	-	54.729693	-	2111.386757	1888.309544	0.894346
0.039990	1318.996805	0.641253	28.518113	0.941022	1347.514919	1315.964898	0.976587
0.019998	868.049234	0.603722	13.842753	1.042973	881.891987	854.508058	0.968949
0.010000	463.443573	0.905514	5.588739	1.308725	469.032312	460.407948	0.981612
0.005000	235.075873	0.979267	1.851054	1.594176	236.926927	234.680437	0.990518
0.002500	115.909138	1.020132	0.579464	1.675556	116.488602	115.857322	0.994581

Table 2.1: $\mathbb{P}_1^2 \times \mathbb{P}_1$ stabilized scheme with a quasi-uniform refinement and $\varepsilon = 1$.

h	$\|p-p_h\|_{1,\Omega}$	$r_1(p)$	$\|\boldsymbol{u}-\boldsymbol{u}_h\|_{\boldsymbol{H}}$	$r_1(u)$	$\|\|\|(\boldsymbol{u}-\boldsymbol{u}_h, p-p_h)\|\|\|$	η	E
0.079946	2055.714421	-	5464.968894	-	2602.211310	1884.365482	0.724140
0.039990	1319.171243	0.640401	2851.557217	0.939039	1604.326965	1316.475766	0.820578
0.020000	868.110785	0.603812	1381.329850	1.045919	1006.243770	854.723621	0.849420
0.010000	463.470837	0.905531	558.754010	1.305961	519.346238	460.505925	0.886703
0.005000	235.078411	0.979337	185.072224	1.594125	253.585634	234.689286	0.925483
0.002500	115.909236	1.020147	57.943499	1.675370	121.703586	115.857687	0.951966

Table 2.2: $\mathbb{P}_1^2 \times \mathbb{P}_1$ stabilized scheme with a quasi-uniform refinement and $\varepsilon = 10^{-2}$.

h	$\|p-p_h\|_{1,\Omega}$	$r_1(p)$	$\|\boldsymbol{u}-\boldsymbol{u}_h\|_{\boldsymbol{H}}$	$r_1(u)$	$\|\|\|(\boldsymbol{u}-\boldsymbol{u}_h, p-p_h)\|\|\|$	η	E
0.079946	2055.705163	-	546489.178588	-	7520.596949	1884.326586	0.250555
0.039990	1319.173081	0.640392	285155.519779	0.939019	4170.728279	1316.481140	0.315648
0.019998	868.112101	0.603811	138413.649790	1.045919	2252.248599	854.727871	0.379500
0.010000	463.471114	0.905533	55875.284002	1.308893	1022.223954	460.506911	0.450495
0.005000	235.078437	0.979337	18507.189808	1.594124	420.150335	234.689375	0.558584
0.002500	115.909237	1.020147	5794.347388	1.675368	173.852711	115.857691	0.666413

Table 2.3: $\mathbb{P}_1^2 \times \mathbb{P}_1$ stabilized scheme with a quasi-uniform refinement and $\varepsilon = 10^{-4}$.

h	$\|p-p_h\|_{1,\Omega}$	$r_2(p)$	$\|\boldsymbol{u}-\boldsymbol{u}_h\|_{\boldsymbol{H}}$	$r_2(u)$	$\|\|\|(\boldsymbol{u}-\boldsymbol{u}_h, p-p_h)\|\|\|$	η	E
0.0799	1107.895742	-	60.328929	-	1167.701879	967.730613	0.828748
0.0399	470.076480	1.237528	18.287520	1.761370	488.364000	457.382915	0.936561
0.0199	169.449270	1.4726600	3.462993	2.410449	172.912263	170.783398	0.987688
0.0099	51.791285	1.710069	0.686595	2.335218	52.477880	51.906513	0.989112
0.0049	13.031846	1.990669	0.080419	3.094040	13.112265	13.041533	0.994606
0.0024	3.230428	2.012244	0.009300	3.112197	3.239729	3.230962	0.997294

Table 2.4: $\mathbb{P}_2^2 \times \mathbb{P}_2$ stabilized scheme with a quasi-uniform refinement and $\varepsilon = 1$.

h	$\|p-p_h\|_{1,\Omega}$	$r_2(p)$	$\|\boldsymbol{u}-\boldsymbol{u}_h\|_{\boldsymbol{H}}$	$r_2(u)$	$\|\|\|(\boldsymbol{u}-\boldsymbol{u}_h, p-p_h)\|\|\|$	η	E
0.079946	1107.408226	-	6033.736118	-	1710.781838	967.887247	0.565757
0.039990	470.062955	1.237020	1828.499303	1.723048	652.912885	457.301064	0.700401
0.019998	169.448973	1.472322	346.295943	2.401102	204.078568	170.782099	0.836845
0.010000	51.791298	1.710316	68.659412	2.334812	58.657239	51.906578	0.884913
0.005000	13.031845	1.990668	8.041910	3.093847	13.836036	13.041530	0.942577
0.002500	3.230428	2.012244	0.930030	3.112189	3.323431	3.230962	0.972176

Table 2.5: $\mathbb{P}_2^2 \times \mathbb{P}_2$ stabilized scheme with a quasi-uniform refinement and $\varepsilon = 10^{-2}$.

h	$\|p-p_h\|_{1,\Omega}$	$r_2(p)$	$\|\boldsymbol{u}-\boldsymbol{u}_h\|_{\boldsymbol{H}}$	$r_2(u)$	$\|\|\|(\boldsymbol{u}-\boldsymbol{u}_h, p-p_h)\|\|\|$	η	E
0.079946	1107.408586	-	603374.475161	-	7141.153338	967.888845	0.135537
0.039990	470.062821	1.237021	182849.680322	1.723453	2298.559625	457.300247	0.198951
0.019998	169.448970	1.472321	34629.590957	2.401101	515.744880	170.782086	0.331137
0.010000	51.791298	1.710316	6865.941117	2.334813	120.450710	51.906579	0.430936
0.005000	13.031845	1.990668	804.191016	3.093847	21.073755	13.041530	0.618852
0.002500	3.230428	2.012244	93.003039	3.112188	4.160459	3.230962	0.776588

Table 2.6: $\mathbb{P}_2^2 \times \mathbb{P}_2$ stabilized scheme with a quasi-uniform refinement and $\varepsilon = 10^{-4}$.

In Figure 2.1 we show some of the adapted meshes obtained with Algorithm 2. Note that most of the refinement is close to the origin due to the fact that the exact solution has a singularity at the point (c,c) with $c = 0.025$, which is close to $(0,0)$. Finally, in Figure 2.2 we compare the approximated solution, obtained by our proposed scheme, and the exact solution. Note that the approximated solution has a good agreement with the exact one.

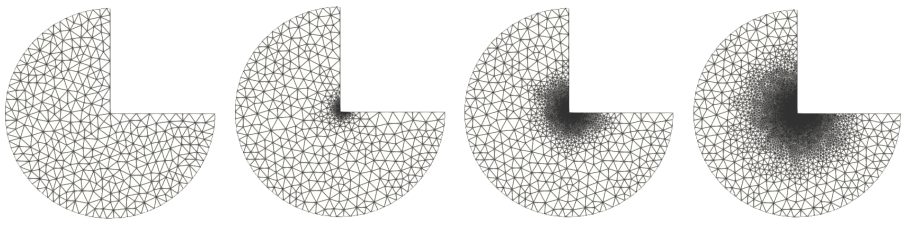

$\mathcal{T}_{h,0}$ $\mathcal{T}_{h,8}$ $\mathcal{T}_{h,16}$ $\mathcal{T}_{h,20}$

Figure 2.1: Suite of adaptive meshes in the iteration 0, 8, 16 and 20.

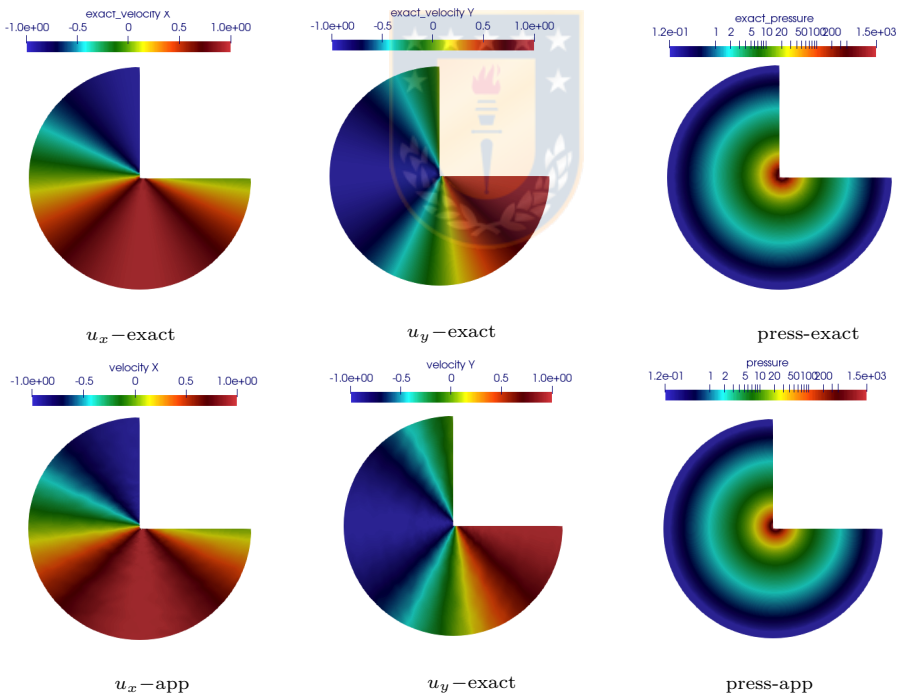

u_x-exact u_y-exact press-exact

u_x-app u_y-exact press-app

Figure 2.2: Components of the exact solution (top) compared with the approximated solution (bottom) obtained using $\mathbb{P}_1^2 \times \mathbb{P}_1$ on the final adapted mesh of 178,596 elements.

2.5.2 A reservoir simulation

For our second problem, we have taken a reservoir problem from [125]. Here $\Omega := (0,2) \times (0,1)$, $\alpha_0 = 1$ and $\gamma = 0.005$. On Γ_D^1 we prescribe $p = p_{atm} = 1.0$ and on $\Gamma_D^2, p = p_{enh} = 5$. On the rest of the boundary we impose $\boldsymbol{v} \cdot \boldsymbol{n} = 0$.

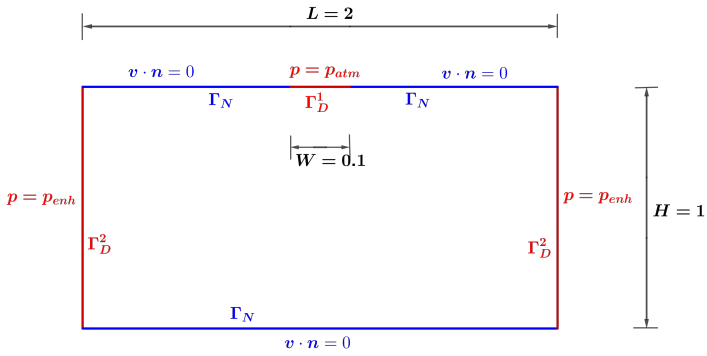

Figure 2.3: Sketch of Ω with Dirichlet boundary conditions for the pressure in Γ_D^1 and Γ_D^2, and normal trace zero for the velocity in Γ_N.

As in the previous example, we show in Figure 2.4 some of the adapted meshes obtained with Algorithm 2. Note that most of the refinement is close to the Γ_D^1, which is consistent with the physics of the problem. Finally, in Figures 2.5 and 2.6, we compare the approximated solution, obtained by our stabilized scheme, and the reference solution. Note that the approximated solution has a good agreement with the referent one.

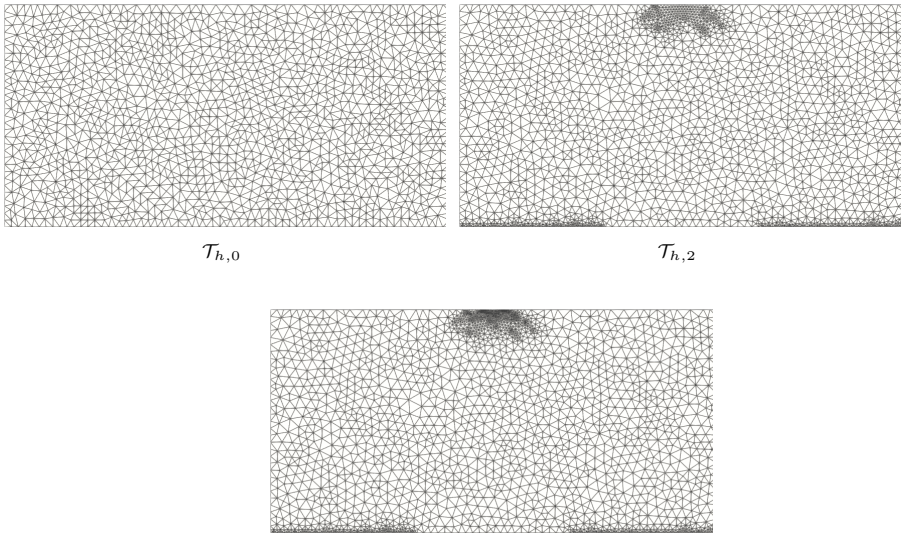

$\mathcal{T}_{h,0}$ $\mathcal{T}_{h,2}$

$\mathcal{T}_{h,9}$

Figure 2.4: Suite of adaptive meshes in the iteration 0, 2 and 9.

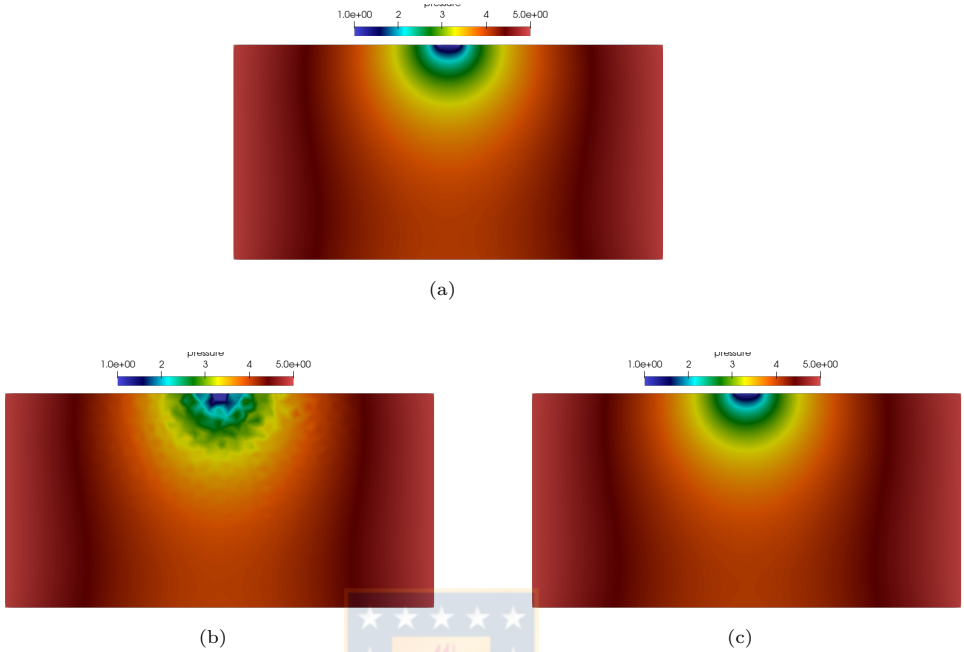

Figure 2.5: Isolines of the pressure: (a) Reference solution on a fine uniform mesh with 773,034; (b) Pressure computed using $\mathbb{P}_1^2 \times \mathbb{P}_1$ finite element spaces with 1,286 elements on the initial mesh; (c) Pressure computed using $\mathbb{P}_1^2 \times \mathbb{P}_1$ finite element spaces with 6,994 elements on the adapted mesh.

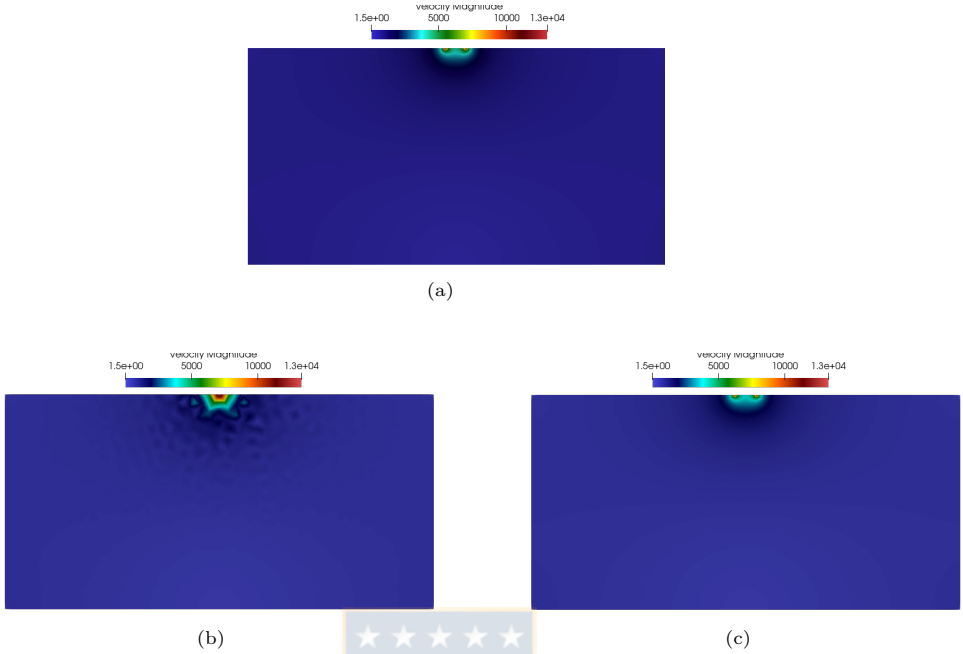

Figure 2.6: Isolines of the velocity: (a) Reference solution on a fine uniform mesh with 773,034; (b) Velocity computed using $\mathbb{P}_1^2 \times \mathbb{P}_1$ finite element spaces with 1,286 elements on the initial mesh; (c) Velocity computed using $\mathbb{P}_1^2 \times \mathbb{P}_1$ finite element spaces with 6,994 elements on the adapted mesh.

2.5.3 A 3D simulation

Let $\Omega := (0,1)^3$, and let $\boldsymbol{f}$ such that the exact solution is given by

$$\boldsymbol{u}(x,y,z) := \frac{1}{2}(-y^2, z^2, x^2) \qquad \text{and} \qquad p(x,y,z) := 2 + xyz.$$

We assume that $\Gamma_D := \{0\}\times]0,1[\times]0,1[\cup]0,1[\times\{0\}\times]0,1[\cup]0,1[\times]0,1[\times\{0\}$ with $\varphi := 2$, and $\Gamma_N := \partial\Omega \backslash \Gamma_D$. We choose $\alpha_0 = 1.0$ and $\gamma = 0.25$, i.e. $\varepsilon = 0.25$.

Note that in this case we have $\boldsymbol{f}(x,y,z) := [h(x,y,z)]^{-1}\big(f_1(x,y,z), f_2(x,y,z), f_3(x,y,z)\big)$, where

$$\begin{aligned} f_1(x,y,z) &= -\frac{1}{2}y^2 + \frac{1}{\varepsilon}yz \\ f_2(x,y,z) &= \frac{1}{2}z^2 + \frac{1}{\varepsilon}xz \\ f_3(x,y,z) &= \frac{1}{2}x^2 + \frac{1}{\varepsilon}xy \\ h(x,y,z) &= 3 + xyz. \end{aligned}$$

In Table 2.7 we present the approximation errors and our a posteriori error estimator η. As in the two-dimensional case, we can see that the errors on the velocity $\|\boldsymbol{u}-\boldsymbol{u}_h\|_{\boldsymbol{H}}$ and pressure $\|p-p_h\|_{0,\Omega}$ show a perfect agreement with those predicted by the theory. Moreover, the effectivity index for the residual a posteriori error estimator η is close to one.

h	$\|p-p_h\|_{1,\Omega}$	$r_1(p)$	$\|\boldsymbol{u}-\boldsymbol{u}_h\|_{\boldsymbol{H}}$	$r_1(u)$	$\|\|\|(\boldsymbol{u}-\boldsymbol{u}_h, p-p_h)\|\|\|$	η	E
0.8660	0.2649	-	0.2323	-	0.3523	0.2797	0.7938
0.4330	0.1552	0.7709	0.0786	1.5625	0.1740	0.1626	0.9344
0.2165	0.0823	0.9156	0.0230	1.7708	0.0854	0.0861	1.0080
0.1082	0.0419	0.9721	0.0063	1.8497	0.0424	0.0439	1.0359
0.0541	0.0211	0.9913	0.0017	1.8859	0.0211	0.0221	1.0448
0.0270	0.0105	0.9974	0.0004	1.9047	0.0105	0.01107	1.0470

Table 2.7: $\mathbb{P}_1^3 \times \mathbb{P}_1$ stabilized scheme with a quasi-uniform refinement and $\varepsilon = 0.25$.

Finally, we present the approximated solutions obtained with the stabilized scheme in a highly uniform refined mesh in Figure 2.7. Here we used $\mathbb{P}_1^3 \times \mathbb{P}_1$ elements and we observe that the overall results are in accordance with the expected ones.

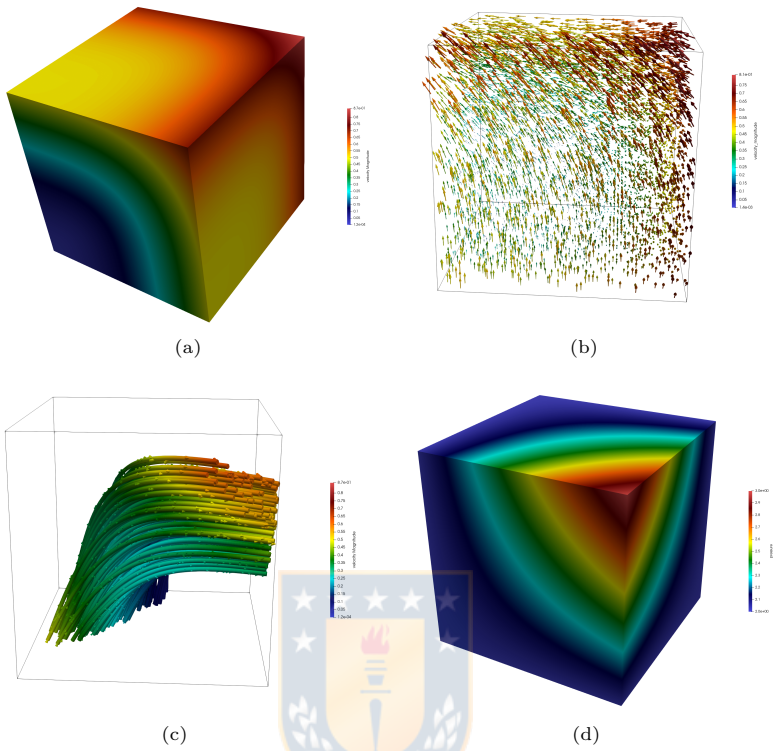

Figure 2.7: Approximated solution. (a) Velocity magnitude; (b) velocity vectors; (c) velocity streamlines; (d) isovalues of the pressure. We use $\mathbb{P}_1^3 \times \mathbb{P}_1$ elements on a uniform mesh of 1,572,864 elements.

Appendix

Lemma 2.7. *There exists a positive constant β_c, independent of ε, such that*

$$\sup_{(\boldsymbol{v},q)\in \boldsymbol{H}\times Q} \frac{B_{\mathrm{stab}}((\boldsymbol{u},p),(\boldsymbol{v},q))}{|||(\boldsymbol{v},q)|||} \geq \beta_c \, |||(\boldsymbol{v},q)|||, \tag{2.1}$$

for all $(\boldsymbol{u},p) \in \boldsymbol{H}\times Q$.

Proof. Given $p \in L^2(\Omega)$, from [42], there exists $\boldsymbol{w} \in \boldsymbol{H}$ such that $\nabla\cdot\boldsymbol{w} = -p$ and $\|\boldsymbol{w}\|_{\boldsymbol{H}} \leq C\|p\|_{0,\Omega}$. Then, for $(\boldsymbol{v},q) := (\boldsymbol{u}-\delta\boldsymbol{w},p)$, with $\delta > 0$, we have

$$\begin{aligned} B_{\mathrm{stab}}((\boldsymbol{u},p),(\boldsymbol{v},q)) &= B_{\mathrm{stab}}((\boldsymbol{u},p),(\boldsymbol{u},p)) - \delta\, B_{\mathrm{stab}}((\boldsymbol{u},p),(\boldsymbol{w},0)) \\ &= B_{\mathrm{stab}}((\boldsymbol{u},p),(\boldsymbol{u},p)) - \delta\left[B_{\mathrm{stab}}((\boldsymbol{u},0),(\boldsymbol{w},0)) + B_{\mathrm{stab}}((\boldsymbol{0},p),(\boldsymbol{w},0))\right] \\ &= \frac{1}{2}\varepsilon\,\|\boldsymbol{u}\|_{0,\Omega}^2 + \varepsilon\,\|\nabla\cdot\boldsymbol{u}\|_{0,\Omega}^2 + \frac{1}{2}\varepsilon^{-1}\,|p|_{1,\Omega}^2 \end{aligned}$$

$$
\begin{aligned}
&-\delta\left[\frac{1}{2}\varepsilon\left(\boldsymbol{u},\boldsymbol{w}\right)+\varepsilon\left(\nabla\cdot\boldsymbol{u},\nabla\cdot\boldsymbol{w}\right)+\left(p,\nabla\cdot\boldsymbol{w}\right)+\frac{1}{2}\left(\nabla p,\boldsymbol{w}\right)\right]\\
&=\frac{1}{2}\varepsilon\left\|\boldsymbol{u}\right\|_{0,\Omega}^{2}+\varepsilon\left\|\nabla\cdot\boldsymbol{u}\right\|_{0,\Omega}^{2}+\frac{1}{2}\varepsilon^{-1}\left|p\right|_{1,\Omega}^{2}\\
&-\frac{\delta}{2}\varepsilon\left(\boldsymbol{u},\boldsymbol{w}\right)-\delta\varepsilon\left(\nabla\cdot\boldsymbol{u},\nabla\cdot\boldsymbol{w}\right)-\delta\left(p,\nabla\cdot\boldsymbol{w}\right)-\frac{\delta}{2}\left(\nabla p,\boldsymbol{w}\right)\\
&=\frac{1}{2}\varepsilon\left\|\boldsymbol{u}\right\|_{0,\Omega}^{2}+\varepsilon\left\|\nabla\cdot\boldsymbol{u}\right\|_{0,\Omega}^{2}+\frac{1}{2}\varepsilon^{-1}\left|p\right|_{1,\Omega}^{2}+\delta\left\|p\right\|_{0,\Omega}^{2}\\
&-\frac{\delta}{2}\varepsilon\left(\boldsymbol{u},\boldsymbol{w}\right)-\delta\varepsilon\left(\nabla\cdot\boldsymbol{u},\nabla\cdot\boldsymbol{w}\right)-\frac{\delta}{2}\left(\nabla p,\boldsymbol{w}\right)\\
&\geq\frac{1}{2}\varepsilon\left\|\boldsymbol{u}\right\|_{0,\Omega}^{2}+\varepsilon\left\|\nabla\cdot\boldsymbol{u}\right\|_{0,\Omega}^{2}+\frac{1}{2}\varepsilon^{-1}\left|p\right|_{1,\Omega}^{2}+\delta\left\|p\right\|_{0,\Omega}^{2}\\
&-\frac{\delta}{2}\varepsilon\left\|\boldsymbol{u}\right\|_{0,\Omega}\left\|\boldsymbol{w}\right\|_{0,\Omega}-\delta\varepsilon\left\|\nabla\cdot\boldsymbol{u}\right\|_{0,\Omega}\left\|\nabla\cdot\boldsymbol{w}\right\|_{0,\Omega}-\frac{\delta}{2}|p|_{1,\Omega}\left\|\boldsymbol{w}\right\|_{0,\Omega}.
\end{aligned}
$$

The result follows using similar arguments as in the proof of the Lemma 2.3. □

CHAPTER 3

Error analysis of pressure reconstruction from discrete velocities

The content of this chapter corresponds to the article R. Araya, C. Bertoglio, C. Carcamo. "Error analysis of pressure reconstruction from discrete velocities". submitted to Inverse Problems.

3.1 Introduction

The pressure difference is an important criteria for the severity diagnosis of blood flow obstruction. The gold standard in clinical practice is invasive catheterization.

Given that there are recommendations to avoid its use [151], to compute the pressure difference from measured flow fields is strongly preferred.

Time-resolved 3D velocity encoded magnetic resonance imaging, or *4D flow MRI*, offers measuring the complete 3D velocity field within a region of interest [121, 142]. The measured velocities can then be inserted in the linear momentum balance of the incompressible Navier-Stokes equations (NSE) and the velocity terms laid in the right-hand-side while the pressure holds as an unknown, i.e.,for a given measurement of the velocity $\boldsymbol{u}$, the pressure gradient ∇p is found by solving:

$$\nabla p = -\boldsymbol{f}_{\boldsymbol{u}} \text{ in } \Omega \tag{3.1}$$

with $\Omega \subset \mathbb{R}^d$ and $\boldsymbol{f}_{\boldsymbol{u}} := (\boldsymbol{u}\cdot\nabla)\boldsymbol{u} - \nu\Delta\boldsymbol{u}$., where the proper function spaces will be defined for each of the methods throughout the article.

In practice, those measurements are obtained at limited spatial resolution –given by the voxel size in the image – and therefore the velocity entering to the right-hand-side corresponds to an interpolated version of the exact velocity. Therefore, there is not a unique numerical approach to compute the reconstructed pressures. A review and preliminary numerical comparison of methods can be found in [37]. Among those methods, only a few can compute pressure fields and not just averaged pressure differences between two locations.

The first one is the so-called Pressure Poisson Estimator (PPE) [73, 141] and it consists of applying the divergence to the NSE obtaining a pressure Poisson equation, similarly as it is used in projection methods [93]. However, the original PPE method cannot include the viscous contribution to the pressure gradient at the level of accuracy of the measured data. Therefore, recently in [130] the PPE method was modified by adding a boundary term with the viscous contribution.

Another more modern method corresponds to the Stokes Estimator (STE) was reported in [146]. The STE consists in adding to the NSE the Laplacian of an artificial incompress-

ible velocity field with null trace leading to a linear Stokes problem for both pressure and artificial velocity fields. Such artificial velocity is supposed to be zero for perfect velocity measurements. The STE has shown more accurate results than the PPE in numerically simulated data [146, 37] and in real phantom and patient data [126]. However, the STE method is considerably more expensive computationally than the PPE.

To the best of the authors' knowledge, neither a mathematical convergence analysis of both PPE and STE methods or a comparison among discretization schemes for each of the methods has been reported.

Therefore, the purpose of this chapter is to propose a strategy for performing a priori error analysis and applied it to the PPE and STE methods. The strategy is based on the splitting of the solution in two components and adding their contributions to the overall error. Moreover, for both methods we studied different discretization strategies in order to verify the theoretical analysis and give insights on the cost-effectiveness of each approach.

The remainder of this chapter is organized as follows. In Section 3.2 we present and analyze the PPE method in the standard and modified variants using Continuos Galerkin approaches. Section 3.3 introduces the STE and analyzes the classical Taylor-Hood and a tailored PSPG discretization. Then, in Section 3.4 we show numerical results using three known analytical solutions for the NSE, confirming the a priori error analysis.

3.2 The Poisson Pressure Estimator

3.2.1 The continuous problem

The Poisson Pressure Estimator (PPE) consists in obtaining the pressure from the classical Navier-Stokes equation by mean a Poisson equation. That is, by applying the divergence operator on Equation (3.1) one gets

$$\begin{cases} -\Delta q & = \nabla \cdot \boldsymbol{f_u}, & \text{in } \Omega \\ -\frac{\partial q}{\partial \boldsymbol{n}} & = \boldsymbol{f_u} \cdot \boldsymbol{n}, & \text{on } \partial\Omega \\ \int_\Omega q \, dx & = 0, \end{cases} \tag{3.2}$$

with $\boldsymbol{n}$ the outward normal vector of $\partial\Omega$. We will make use of the function spaces $\boldsymbol{H} := [H^1(\Omega)]^d, \mathbf{V} := [H_0^1(\Omega)]^d$ and

$$\boldsymbol{H}_j := \begin{cases} \left\{ \boldsymbol{v} \in \boldsymbol{H} : \Delta \boldsymbol{v} \in [L^2(\Omega)]^d \right\} & \text{if } j = 1 \\ \left\{ \boldsymbol{v} \in \boldsymbol{H} : \nabla \times (\nabla \times \boldsymbol{u}) \in [L^2(\Omega)]^d \right\} & \text{if } j = 2 \end{cases}$$

$$Q_j := \begin{cases} \left\{ r \in H^1(\Omega) : \int_\Omega r dx = 0 \right\} & \text{if } j = 1 \\ \left\{ r \in H^1(\Omega) : \boldsymbol{n} \cdot \operatorname{curl} r \in L^2(\partial\Omega) \text{and} \int_\Omega r \, dx = 0 \right\} & \text{if } j = 2 \end{cases}$$

Assuming $\boldsymbol{u} \in \boldsymbol{H}_j$, the weak formulation of the (3.2) is given by: Find $q \in Q_1$ such that

$$\mathcal{A}(q, r) = F_{\boldsymbol{u}}^j(r), \quad \forall \, r \in Q_j, \tag{3.3}$$

where $\mathcal{A}(q, r) = (\nabla q, \nabla r)_\Omega$ and

$$F_{\boldsymbol{u}}^j(r) = -((\boldsymbol{u} \cdot \nabla)\boldsymbol{u}, \nabla r)_\Omega + \delta_{1j}(\nu \Delta \boldsymbol{u}, \nabla r)_\Omega + \delta_{2j} \langle \boldsymbol{n} \times \nabla r, \nu \nabla \times \boldsymbol{u} \rangle_{\partial\Omega}, \tag{3.4}$$

where δ_{ij} is the Kronecker delta. We refer to Standard-PPE if $j=1$ and Modified-PPE if $j=2$ [130].

The uniqueness of the solution of Problem (3.3) follows from the Lax-Milgram lemma for $j=1$ and Generalized Lax-Milgram lemma for $j=2$ [75]. Indeed, the coercivity of the left-side is straightforward. The continuity of $F^j_{\boldsymbol{u}}$ is obtained thanks to the identity

$$-(\nabla r, \nu\nabla\times(\nabla\times\boldsymbol{u}))_\Omega = \langle \boldsymbol{n}\times\nabla r, \nu\nabla\times\boldsymbol{u}\rangle_{\partial\Omega}, \tag{3.5}$$

and then

$$|F^j_{\boldsymbol{u}}(r)| \le (\|(\boldsymbol{u}\cdot\nabla)\boldsymbol{u}\|_{0,\Omega} + \delta_{1j}\nu\|\Delta\boldsymbol{u}\|_{0,\Omega} + \delta_{2j}\nu\|\nabla\times(\nabla\times\boldsymbol{u})\|_{0,\Omega})|r|_{1,\Omega}$$

3.2.2 Continuous Galerkin discretizations

The finite element spaces for the pressure approximation and velocity interpolation are:

$$\begin{aligned} Q_{jh} &:= \left\{ q_h \in Q_j : q_h|_K \in \mathbb{P}_k(K) \quad \forall K \in \mathcal{T}_h \right\}, \\ \boldsymbol{H}_{jh} &:= \left\{ v_h \in \boldsymbol{H}_j : v_h|_K \in \mathbb{P}_1(K) \quad \forall K \in \mathcal{T}_h \right\}. \end{aligned}$$

We will also consider the interpolation operator $\mathcal{J}_h : Q_j \cap H^{k+1}(\Omega) \to Q_{jh}$ and $\mathcal{L}_h : \boldsymbol{H}_j \cap [H^2(\Omega)]^d \to H_{jh}$ such that:

$$\begin{aligned} |q-\mathcal{J}_h q|_{m,\Omega} &\le a_k h^{k+1-m}|q|_{k+1,\Omega}, \qquad \forall\, q \in H^{k+1}(\Omega),\ 0\le m\le k+1. \\ |\boldsymbol{v}-\mathcal{L}_h\boldsymbol{v}|_{m,\Omega} &\le a_k h^{2-m}|\boldsymbol{v}|_{2,\Omega}, \qquad \forall\, \boldsymbol{v} \in H^2(\Omega),\ 0\le m\le 2. \end{aligned} \tag{3.6}$$

Thus, the Galerkin scheme associated with the continuous variational formulation (3.3) reads as follows: Find $q_h \in Q_{jh}$ such that

$$\mathcal{A}(q_h, r_h) := F^j_{\boldsymbol{u}_h}(r_h) \quad \forall\, r_h \in Q_{jh}, \tag{3.7}$$

with

$$F^j_{\boldsymbol{u}_h}(r_h) = -((\mathcal{L}_h\boldsymbol{u}\cdot\nabla)\mathcal{L}_h\boldsymbol{u}, \nabla r_h)_\Omega + \delta_{2j}\langle \boldsymbol{n}\times\nabla r_h, \nu\nabla\times\mathcal{L}_h\boldsymbol{u}\rangle_{\partial\Omega}, \tag{3.8}$$

According to discrete Lax-Milgram Theorem, Problem (3.7) has a unique solution $q_h \in Q_{jh}$.

Remark 3.1. *Note that from the definitions (3.4) and (3.8) we can assure that the problem (3.7) is not a Galerkin scheme of the continuous problem (3.3).*

The strategy to prove convergence is to use the known Strang's lemma for conformal and non-consistent cases.

Lemma 3.1. *Let us assume that $\boldsymbol{u} \in H^2(\Omega)$. Then,*

$$\|(\boldsymbol{u}\cdot\nabla)\boldsymbol{u} - (\mathcal{L}_h\boldsymbol{u}\cdot\nabla)\mathcal{L}_h\boldsymbol{u}\|_{0,\Omega} \le \tilde{C}(a_1 + a_2 C_I)h|\boldsymbol{u}|_{2,\Omega}\|\boldsymbol{u}\|_{2,\Omega}. \tag{3.9}$$

with a_1, a_2 the error interpolation constants, $\tilde{C}$ is an injection constant and C_I an inverse inequality constant.

Proof. Using properties of interpolation given by (3.6) and Young inequality we obtain

$$\begin{aligned}\|(\boldsymbol{u}\cdot\nabla)\boldsymbol{u}-(\mathcal{L}_h\boldsymbol{u}\cdot\nabla)\mathcal{L}_h\boldsymbol{u}\|_{0,\Omega} \leq& \|(\boldsymbol{u}\cdot\nabla)(\boldsymbol{u}-\mathcal{L}_h\boldsymbol{u})\|_{0,\Omega}+\|((\boldsymbol{u}-\mathcal{L}_h\boldsymbol{u})\cdot\nabla)\mathcal{L}_h\boldsymbol{u}\|_{0,\Omega}\\ \leq& |\boldsymbol{u}-\mathcal{L}_h\boldsymbol{u}|_{1,\Omega}\|\boldsymbol{u}\|_{\infty,\Omega}+\|\nabla\mathcal{L}_h\boldsymbol{u}\|_{\infty,\Omega}\|\boldsymbol{u}-\mathcal{L}_h\boldsymbol{u}\|_{0,\Omega}\\ \leq& a_1 h|\boldsymbol{u}|_{2,\Omega}\tilde{C}\|\boldsymbol{u}\|_{2,\Omega}+C_I h^{-1}\|\mathcal{L}_h\boldsymbol{u}\|_{\infty,\Omega}a_2h^2|\boldsymbol{u}|_{2,\Omega}\\ \leq& \tilde{C}a_1 h|\boldsymbol{u}|_{2,\Omega}\|\boldsymbol{u}\|_{2,\Omega}+a_2C_I h\|\boldsymbol{u}\|_{\infty,\Omega}|\boldsymbol{u}|_{2,\Omega}\\ \leq& \tilde{C}a_1 h|\boldsymbol{u}|_{2,\Omega}\|\boldsymbol{u}\|_{2,\Omega}+a_2\tilde{C}C_I h\|\boldsymbol{u}\|_{2,\Omega}|\boldsymbol{u}|_{2,\Omega}\\ =& \tilde{C}(a_1+a_2C_I)h|\boldsymbol{u}|_{2,\Omega}\|\boldsymbol{u}\|_{2,\Omega} \end{aligned} \tag{3.10}$$

□

Lemma 3.2. *Assume that* $\boldsymbol{u}\in\boldsymbol{H}_j\cap H^2(\Omega)^d$ *if* $j=1$ *and* $\boldsymbol{u}\in\boldsymbol{H}_j$ *with* $\boldsymbol{u}\big|_{\partial\Omega}\in[H^2(\partial\Omega)]^d$ *if* $j=2$. *Then,*

$$\sup_{\substack{r_h\in Q_{jh}\\ r_h\neq 0}}\frac{|F^j_{\boldsymbol{u}}(r_h)-F^k_{\boldsymbol{u}_h}(r_h)|}{|r_h|_{1,\Omega}}\leq C_1 h|\boldsymbol{u}|_{2,\Omega}\|\boldsymbol{u}\|_{2,\Omega}+\delta_{1,j}\|\Delta\boldsymbol{u}\|_{0,\Omega}+\delta_{2,j}C_2\nu h^{1/2}|\boldsymbol{u}|_{2,\partial\Omega}$$

Proof.

$$\begin{aligned}\sup_{\substack{r_h\in Q_{jh}\\ r_h\neq 0}}\frac{|F^j_{\boldsymbol{u}}(r_h)-F^k_{\boldsymbol{u}_h}(r_h)|}{|r_h|_{1,\Omega}} \leq& \|(\boldsymbol{u}\cdot\nabla)\boldsymbol{u}-(\mathcal{I}_h\boldsymbol{u}\cdot\nabla)\mathcal{I}_h\boldsymbol{u}\|_{0,\Omega}+\delta_{1,j}\|\Delta\boldsymbol{u}\|_{0,\Omega}\\ &+\delta_{2,j}\sup_{\substack{r_h\in Q_{jh}\\ r_h\neq 0}}\frac{|\langle\boldsymbol{n}\times\nabla r_h,\nu\nabla\times(u-\mathcal{I}_h\boldsymbol{u})\rangle_{\partial\Omega}|}{|r_h|_{1,\Omega}}.\end{aligned}$$

For the first term in above inequality we use Lemma 3.1 and for the third term we have

$$\frac{\displaystyle\sum_{F\in\mathcal{E}_h\cap\partial\Omega}|\langle\boldsymbol{n}\times\nabla r_h,\nu\nabla\times(u-\mathcal{I}_h\boldsymbol{u})\rangle_F|}{|r_h|_{1,\Omega}}\leq\frac{\displaystyle\sum_{F\in\mathcal{E}_h\cap\partial\Omega}\nu\|\nabla r_h\|_{0,F}\|\nabla\times(u-\mathcal{I}_h\boldsymbol{u})\|_{0,F}}{|r_h|_{1,\Omega}} \tag{3.11}$$

Now, thanks to [68, Lemma 1.46], we have

$$\|\nabla r_h\|_{0,F}=\leq C_{tr}h_K^{-1/2}|r_h|_{1,K}, \tag{3.12}$$

where $C_{tr}=\left(\dfrac{(k+1)(k+2)}{2}\right)^{1/2}$ (see [154, Theorem 3]). Besides, from [143, Lemma 10.8] we get

$$\|\nabla\times(\boldsymbol{u}-\mathcal{I}_h\boldsymbol{u})\|_{0,F}\leq|\boldsymbol{u}-\mathcal{I}_h\boldsymbol{u}|_{1,F}\leq a_{2,I}\,h_K\,|\boldsymbol{u}|_{2,F}. \tag{3.13}$$

and then, from (3.11), (3.12) and (3.13) we arrive to

$$\frac{\displaystyle\sum_{F\in\mathcal{E}_h\cap\partial\Omega}|\langle\boldsymbol{n}\times\nabla r_h,\nu\nabla\times(u-\mathcal{I}_h\boldsymbol{u})\rangle_F|}{|r_h|_{1,\Omega}}\leq C_{tr}\,a_{2,I}\,\nu\,h^{1/2}|\boldsymbol{u}|_{2,\partial\Omega},$$

being $C_2=C_{tr}\,a_{2,I}$, which allows us arrive to the desired result, where $C_1=\tilde{C}(a_1+a_2C_I)$.

□

Finally, the next theorem holds.

Theorem 3.1 (Main Result I). *Let $q \in Q_j \cap H^{k+1}(\Omega)$ and $q_h \in Q_{jh}$ solutions of (3.3) and (3.7), respectively. In addition, we assume that $\boldsymbol{u} \in \boldsymbol{H}_j \cap [H^2(\Omega)]^d$ and $\boldsymbol{u} \in \boldsymbol{H}_j$ with $\boldsymbol{u}\big|_{\partial\Omega} \in [H^2(\partial\Omega)]^d$, for $j = 1$ and $j = 2$ respectively. Then,*

$$|q - q_h|_{1,\Omega} \leq a_k h^k |q|_{k+1,\Omega} + C_1 h |\boldsymbol{u}|_{2,\Omega} \|\boldsymbol{u}\|_{2,\Omega} + \delta_{1,j} \|\Delta \boldsymbol{u}\|_{0,\Omega} + \delta_{2,j} C_2 \nu h^{1/2} |\boldsymbol{u}|_{2,\partial\Omega}$$

with $k \geq 1$.

Proof. Thanks to the Strang's Lemma (see [75, Lemma 2.27]) we have that

$$|q - q_h|_{1,\Omega} \leq \sup_{\substack{r_h \in Q_{jh} \\ r_h \neq 0}} \frac{|F^j_{\boldsymbol{u}}(r_h) - F^j_{\boldsymbol{u}_h}(r_h)|}{|r_h|_{1,\Omega}} + 2 \inf_{r_h \in Q_{jh}} |q - r_h|_{1,\Omega}$$

The bound for the first term in the right-hand side follows directly from Lemma 3.2. For the second term, we will consider the interpolation operator, and then

$$\inf_{r_h \in Q_{jh}} |q - r_h|_{1,\Omega} \leq |q - \mathcal{J}_h q|_{1,\Omega} \leq a_k h^k |q|_{k+1,\Omega}$$

□

Corollary 3.1. *Let the hypothesis of Theorem 3.1 hold with Ω is convex polygonal domain. Then,*

$$\begin{aligned} \|q - q_h\|_{0,\Omega} \leq & C_r\, a_k h^{k+1} |q|_{k+1,\Omega} + C_1\, C_p h |\boldsymbol{u}|_{2,\Omega} \|\boldsymbol{u}\|_{2,\Omega} + \delta_{1,j}\, C_p \|\Delta \boldsymbol{u}\|_{0,\Omega} \\ & + \delta_{2,j}\, C_2\, C_p\, \nu h^{1/2} |\boldsymbol{u}|_{2,\partial\Omega} \end{aligned}$$

with C_r the regularity constant and $k \geq 1$.

Proof. The proof starts taking $\tilde{q}_h \in Q_{jh}$ such that satisfy Equation (3.3). It follows from the triangle inequality that

$$\|q - q_h\|_{0,\Omega} \leq \|q - \tilde{q}_h\|_{0,\Omega} + \|\tilde{q}_h - q_h\|_{0,\Omega} \tag{3.14}$$

The bound estimation for $\|q - \tilde{q}_h\|_{0,\Omega}$ is obtained solving the problem

$$-\Delta r = q - \tilde{q}_h,$$

with the Dirichlet conditon zero and applying the known Aubin-Nitsche Lemma [75, Lemma 2.31] and interpolation properties leading to

$$\|q - \tilde{q}_h\|_{0,\Omega} \leq C_r h |q - \tilde{q}_h|_{1,\Omega} \leq C_r a_k h^{k+1} |q|_{k+1,\Omega}. \tag{3.15}$$

For the second term of the right-hand side in (3.14) we proceed as follows:

$$|\tilde{q}_h - q_h|_{1,\Omega} \leq \sup_{\substack{r_h \in Q_{jh} \\ r_h \neq 0}} \frac{A(\tilde{q}_h - q_h, r_h)}{|r_h|_{1,\Omega}} \leq \sup_{\substack{r_h \in Q_{jh} \\ r_h \neq 0}} \frac{F^j_{\boldsymbol{u}}(r_h) - F^j_{\boldsymbol{u}_h}(r_h)}{|r_h|_{1,\Omega}}.$$

From Lemma 3.2 and Poincaré inequality, we get

$$\| \tilde{q}_h - q_h\|_{0,\Omega} \leq C_p|\tilde{q}_h - q_h|_{1,\Omega} \leq C_1\, C_p h|\boldsymbol{u}|_{2,\Omega}\|\boldsymbol{u}\|_{2,\Omega} + \delta_{1,j}\, C_p\|\Delta\boldsymbol{u}\|_{0,\Omega} \tag{3.16}$$

$$+ \delta_{2,j}\, C_2\, C_p\, \nu h^{1/2}|\boldsymbol{u}|_{2,\partial\Omega}. \tag{3.17}$$

Hence, the result is a direct consequence of the estimates (3.15) and (3.16).

□

3.3 The Stokes Estimator

3.3.1 The continuous problem

The STE consists then in adding the Laplacian of an incompressible auxiliary velocity $\boldsymbol{w} \in \mathbf{V}$ and to the left-hand side of (3.1):

$$\begin{aligned} -\Delta\boldsymbol{w} + \nabla q &= -\boldsymbol{f}_{\boldsymbol{u}} \quad \text{in } \Omega \\ \nabla\cdot\boldsymbol{w} &= 0 \quad \text{in } \Omega. \end{aligned} \tag{3.18}$$

Let us define the space $P = L^2_0(\Omega)$. Hence, we can define the weak problem of (3.18) as: *Find* $(\boldsymbol{w}, q) \in \mathbf{V}\times P$ *such that*

$$\mathcal{B}((\boldsymbol{w},q),(\boldsymbol{v},r)) = \mathcal{G}_{\boldsymbol{u}}(\boldsymbol{v},r) \quad \forall(\boldsymbol{v},r)\in\mathbf{V}\times P, \tag{3.19}$$

where

$$\begin{aligned} \mathcal{B}((\boldsymbol{w},q),(\boldsymbol{v},r)) &:= (\nabla\boldsymbol{w},\nabla\boldsymbol{v})_\Omega - (q,\nabla\cdot\boldsymbol{v})_\Omega + (r,\nabla\cdot\boldsymbol{w})_\Omega \\ \mathcal{G}_{\boldsymbol{u}}(\boldsymbol{v},r) &:= -((\boldsymbol{u}\cdot\nabla)\boldsymbol{u},\boldsymbol{v})_\Omega - \nu(\nabla\boldsymbol{u},\nabla\boldsymbol{v})_\Omega. \end{aligned} \tag{3.20}$$

For the analysis, we will use the following norm

$$\|(\boldsymbol{v},r)\|_{\mathbf{V}\times P} := |\boldsymbol{v}|_{1,\Omega} + \|r\|_{0,\Omega},$$

and if F is an linear functional operator we use the norm

$$\|F\|_{(\mathbf{V}\times P)'} := \sup_{\substack{(\boldsymbol{v},r)\in\mathbf{V}\times P \\ (\boldsymbol{v},r)\neq\boldsymbol{0}}} \frac{|F(\boldsymbol{v},r)|}{\|(\boldsymbol{v},r)\|_{\mathbf{V}\times P}} \tag{3.21}$$

Note that the problem (3.19) is well posed thanks to the $\mathbf{V}-$ellipticity of the bilinear form $(\nabla\boldsymbol{w},\nabla\boldsymbol{v})_\Omega$, and $(q,\nabla\cdot\boldsymbol{w})_\Omega$ satisfy an inf-sup condition (cf. [75, Prop. 2.36]).

Lemma 3.3. *There exists a positive constant* $C_{\mathcal{B}}$ *such that*

$$\|\mathcal{B}\| \leq C_{\mathcal{B}}.$$

Proof. Using triangular inequality, Cauchy-Schwarz inequality, together to the inequalities $1 \leq \sqrt{d}$ and $\sqrt{a^2+b^2} \leq a+b$, with $a, b \geq 0$, we get

$$|\mathcal{B}((\boldsymbol{w},q),(\boldsymbol{v},r))| \leq |\boldsymbol{w}|_{1,\Omega}|\boldsymbol{v}|_{1,\Omega} + \sqrt{d}\|q\|_{0,\Omega}|\boldsymbol{v}|_{1,\Omega} + \sqrt{d}\|r\|_{0,\Omega}|\boldsymbol{w}|_{1,\Omega}$$

$$
\begin{aligned}
&\leq \sqrt{d}|\boldsymbol{w}|_{1,\Omega}|\boldsymbol{v}|_{1,\Omega} + \sqrt{d}\|q\|_{0,\Omega}|\boldsymbol{v}|_{1,\Omega} + \sqrt{d}\|r\|_{0,\Omega}|\boldsymbol{w}|_{1,\Omega} \\
&\leq \sqrt{d}(|\boldsymbol{w}|_{1,\Omega}^2 + |\boldsymbol{w}|_{1,\Omega}^2 + \|q\|_{0,\Omega})^{1/2}(|\boldsymbol{v}|_{1,\Omega}^2 + |\boldsymbol{v}|_{1,\Omega}^2 + \|r\|_{0,\Omega})^{1/2} \\
&\leq C_{\mathcal{B}}(|\boldsymbol{w}|_{1,\Omega}^2 + \|q\|_{0,\Omega}^2)^{1/2}(|\boldsymbol{v}|_{1,\Omega}^2 + \|r\|_{0,\Omega}^2)^{1/2} \\
&\leq C_{\mathcal{B}}\|(\boldsymbol{w},q)\|_{\mathbf{V}\times P}\|(\boldsymbol{v},r)\|_{\mathbf{V}\times P},
\end{aligned}
$$

and the result is obtained directly, with $C_{\mathcal{B}} = 2\sqrt{d}$. □

3.3.2 Discrete spaces

Let us denote by $\{\mathcal{T}_h\}$ a regular family partition of Ω composed of triangular elements K of diameter h_K. We will denote by h the mesh size, where $h = \max\{h_K : K \in \mathcal{T}_h\}$.

Now, for each h let $\mathbf{W}_h$ and P_h be finite-dimensional spaces such that:

$$
\begin{aligned}
\mathbf{W}_h &:= \left\{\boldsymbol{v}_h \in [H^1(\Omega)]^d : \boldsymbol{v}_h|_K \in [\mathbb{P}_l(K)]^d \quad \forall K \in \mathcal{T}_h\right\}, \\
P_h &:= \{q_h \in P : q_h|_K \in \mathbb{P}_k(K) \quad \forall K \in \mathcal{T}_h\}, \\
\boldsymbol{H}_h &:= \left\{\boldsymbol{w}_h \in \boldsymbol{H} : \boldsymbol{w}_h|_K \in [\mathbb{P}_1(K)]^d \quad \forall K \in \mathcal{T}_h\right\}.
\end{aligned}
$$

For our error analysis we will need to make use of some known results.

Theorem 3.2. *For all $\boldsymbol{w} \in [\mathbb{P}_l(K)]^d$ there holds,*

$$
\|\nabla \boldsymbol{w}\|_{0,K} \leq \sqrt{\kappa_l}\frac{|\partial K|}{|K|}\|\boldsymbol{w}\|_{0,K}. \tag{3.22}
$$

For $d = 2$, it holds $\kappa_1 = 6$ and $\kappa_2 = \dfrac{45}{2}$.

Proof. See [129, Theorem 2] □

Corollary 3.2. *For $d = 2$ and $l = 1$ there holds*

$$
\|\nabla \boldsymbol{w}\|_{0,K} \leq C_I h_K^{-1}\|\boldsymbol{w}\|_{0,K}, \tag{3.23}
$$

where $C_I = \dfrac{6\sqrt{\kappa_1}}{\sin^2(\theta)}$, being θ the minimun angle of the element K.

Proof. The proof is a direct consequence of the minimum angle condition and Theorem 3.2. □

3.3.3 Taylor-Hood discretization

For the discrete STE we set $\mathbf{V}_h = \mathbf{W}_h \cap \mathbf{V}$ where inf-sup stable pairs of finite elements requires the use of different spaces for velocity and pressure and for this reason we take Taylor-Hood, where $l = k+1$. Otherwise, it is not possible to use conforming spaces of lowest order for the discrete velocity. Furthermore, we will consider the property of interpolation operator $\mathcal{I}_h : \mathbf{V} \cap [H^{k+1}(\Omega)]^d \to \mathbf{V}_h$:

$$
|\boldsymbol{w} - \mathcal{I}_h\boldsymbol{w}|_{m,\Omega} \leq a_k h^{k+1-m}|\boldsymbol{w}|_{k+1,\Omega}, \qquad \forall \boldsymbol{w} \in [H^{k+1}(\Omega)]^d,\ 0 \leq m \leq k+1, \tag{3.24}
$$

Thereby, the discrete version of the problem (3.19) reads as follows: *Find* $(\boldsymbol{w}_h, q_h) \in \mathbf{V}_h \times P_h$ *such that*

$$\mathcal{B}((\boldsymbol{w}_h, q_h), (\boldsymbol{v}_h, r_h)) = \mathcal{G}_{\boldsymbol{u}_h}(\boldsymbol{v}_h, r_h) \quad \forall (\boldsymbol{v}_h, r_h) \in \mathbf{V}_h \times P_h, \tag{3.25}$$

where the bilinear form $\mathcal{B}$ is like in the continuous case, and

$$\mathcal{G}_{\boldsymbol{u}_h}(\boldsymbol{v}_h, r_h) := -((\mathcal{L}_h \boldsymbol{u} \cdot \nabla)\mathcal{L}_h \boldsymbol{u}, \boldsymbol{v}_h)_\Omega - \nu(\nabla \mathcal{L}_h \boldsymbol{u}, \nabla \boldsymbol{v}_h)_\Omega, \tag{3.26}$$

with $\mathcal{L}_h : [H^2(\Omega)]^d \longrightarrow \boldsymbol{H}_h$ a Lagrange interpolant.

Lemma 3.4. *There exists a constant* β_1*, independent of* h*, such that*

$$\sup_{\substack{(\boldsymbol{v}_h, r_h) \in \mathbf{V}_h \times P_h \\ (\boldsymbol{v}_h, r_h) \neq \mathbf{0}}} \frac{\mathcal{B}((\boldsymbol{w}_h, q_h), (\boldsymbol{v}_h, r_h))}{\|(\boldsymbol{v}_h, r_h)\|_{\mathbf{V} \times P}} \geq \beta_1 \|(\boldsymbol{w}_h, q_h)\|_{\mathbf{V} \times P}, \qquad \forall\, (\boldsymbol{w}_h, q_h) \in \mathbf{V}_h \times P_h.$$

Proof. See equation [90, (1.39)] and [90, Corollary 4.1] □

For the next result, we consider the pair $(\tilde{\boldsymbol{w}}_h, \tilde{q}_h) \in \mathbf{V}_h \times P_h$, such that

$$\mathcal{B}((\tilde{\boldsymbol{w}}_h, \tilde{q}_h), (\boldsymbol{v}_h, r_h)) = \mathcal{G}_{\boldsymbol{u}}(\boldsymbol{v}_h, r_h) \quad \forall (\boldsymbol{v}_h, r_h) \in \mathbf{V}_h \times P_h, \tag{3.27}$$

where $\mathcal{G}_{\boldsymbol{u}}(\boldsymbol{v}_h, r_h) = -((\boldsymbol{u} \cdot \nabla)\boldsymbol{u}, \boldsymbol{v}_h)_{0,\Omega} - \nu(\nabla \boldsymbol{u}, \nabla \boldsymbol{v}_h)_\Omega$ with the continuous velocity $\boldsymbol{u}$. Let us recall the following convergence result.

Lemma 3.5. *Let* $(\boldsymbol{w}, q)$ *and* $(\tilde{\boldsymbol{w}}_h, \tilde{q}_h)$ *solutions of* (3.19) *and* (3.27) *respectively. Assume that* $(\boldsymbol{w}, q) \in [H_0^1(\Omega) \cap H^{k+1}(\Omega)]^d \times [L_0^2(\Omega) \cap H^k(\Omega)]$*, with* $k \geq 1$*. Then, there exists* $C > 0$ *independent of* h *such that*

$$\|(\boldsymbol{w} - \tilde{\boldsymbol{w}}_h, q - \tilde{q}_h)\|_{\mathbf{V} \times P} \leq C_1 C_2 h^k \big(|\boldsymbol{w}|_{k+1,\Omega} + |q|_{k,\Omega}\big),$$

with $C_2 = 1 + \dfrac{C_{\mathcal{B}}}{\beta_1}$ *and* β_1 *being the constant given in Lemma 3.4.*

Proof. See [75, Lemma 2.44] □

In order to show the convergence of q_h (Main Result I, see later Theorem 3.3), we set the following Lemma.

Lemma 3.6. *Let* $(\boldsymbol{w}_h, q_h), (\tilde{\boldsymbol{w}}_h, \tilde{q}_h) \in \mathbf{V}_h \times P_h$*, solutions of* (3.25) *and* (3.27) *respectively, and* β_1 *the constant given in Lemma 3.4. Then,*

$$\|(\tilde{\boldsymbol{w}}_h - \boldsymbol{w}_h, \tilde{q}_h - q_h)\|_{\mathbf{V} \times P} \leq \beta_1^{-1} \|\mathcal{G}_{\boldsymbol{u}} - \mathcal{G}_{\boldsymbol{u}_h}\|_{(\mathbf{V} \times P)'}$$

with $(\mathcal{G}_{\boldsymbol{u}} - \mathcal{G}_{\boldsymbol{u}_h})(\boldsymbol{v}_h, r_h) := -((\boldsymbol{u} \cdot \nabla)\boldsymbol{u} - (\mathcal{L}_h \boldsymbol{u} \cdot \nabla)\mathcal{L}_h \boldsymbol{u}, \boldsymbol{v}_h)_\Omega - \nu(\nabla \boldsymbol{u} - \nabla \mathcal{L}_h \boldsymbol{u}, \nabla \boldsymbol{v}_h)_\Omega$.

Proof. By Lemma 3.4 together with the Cauchy - Schwarz inequality, we arrive to the inequality

$$\beta_1 \|(\tilde{\boldsymbol{w}}_h - \boldsymbol{w}_h, \tilde{q}_h - q_h)\|_{\mathbf{V} \times P} \leq \sup_{\substack{(\boldsymbol{v}_h, r_h) \in \mathbf{V}_h \times P_h \\ (\boldsymbol{v}_h, r_h) \neq \mathbf{0}}} \frac{\mathcal{B}((\tilde{\boldsymbol{w}}_h - \boldsymbol{w}_h, \tilde{q}_h - q_h), (\boldsymbol{v}_h, r_h))}{\|(\boldsymbol{v}_h, r_h)\|_{\mathbf{V} \times P}}$$

$$
\begin{aligned}
&= \sup_{\substack{(\boldsymbol{v}_h,r_h)\in \mathbf{V}_h\times P_h \\ (\boldsymbol{v}_h,r_h)\neq \mathbf{0}}} \frac{\mathcal{G}_{\boldsymbol{u}}(\boldsymbol{v}_h,r_h)-\mathcal{G}_{\boldsymbol{u}_h}(\boldsymbol{v}_h,r_h)}{\|(\boldsymbol{v}_h,r_h)\|_{\mathbf{V}\times P}} \\
&= \sup_{\substack{(\boldsymbol{v}_h,r_h)\in \mathbf{V}_h\times P_h \\ (\boldsymbol{v}_h,r_h)\neq \mathbf{0}}} \frac{(\mathcal{G}_{\boldsymbol{u}}-\mathcal{G}_{\boldsymbol{u}_h})(\boldsymbol{v}_h,r_h)}{\|(\boldsymbol{v}_h,r_h)\|_{\mathbf{V}\times P}} \\
&\leq \|\mathcal{G}_{\boldsymbol{u}}-\mathcal{G}_{\boldsymbol{u}_h}\|_{(\mathbf{V}\times P)'}.
\end{aligned}
$$

□

Lemma 3.7. *Let $\mathcal{G}_{\boldsymbol{u}}$ and $\mathcal{G}_{\boldsymbol{u}_h}$ be as in (3.20) and (3.26) respectively and denote by $(\mathbf{V}\times P)'$ the dual space of the product space $\mathbf{V}\times P$. In addition, we assume that $\boldsymbol{u}\in[H^2(\Omega)]^d$. Then*

$$
\|\mathcal{G}_{\boldsymbol{u}}-\mathcal{G}_{\boldsymbol{u}_h}\|_{(\mathbf{V}\times P)'} \leq h|\boldsymbol{u}|_{2,\Omega}\left[C_p\tilde{C}(a_1+a_2\,C_I)\|\boldsymbol{u}\|_{2,\Omega}+\nu\,a_1\right].
$$

Proof.

$$
\begin{aligned}
\|\mathcal{G}_{\boldsymbol{u}}(\boldsymbol{v}_h,r_h)-\mathcal{G}_{\boldsymbol{u}_h}(\boldsymbol{v}_h,r_h)\|_{0,\Omega} \leq \|(\boldsymbol{u}\cdot\nabla)\boldsymbol{u}-(\mathcal{L}_h\boldsymbol{u}\cdot\nabla)\mathcal{L}_h\boldsymbol{u})\|_{0,\Omega}\|\boldsymbol{v}_h\|_{0,\Omega} \\
+\nu\|\nabla\boldsymbol{u}-\nabla\mathcal{L}_h\boldsymbol{u}\|_{0,\Omega}\|\nabla\boldsymbol{v}_h\|_{0,\Omega}.
\end{aligned}
$$

For the first term of the right-hand side, we use Lemma 3.1.

For the second term of the right-hand-side, we have from the interpolation bounds:

$$
\|\nabla(\boldsymbol{u}-\mathcal{L}_h\boldsymbol{u})\|_{0,\Omega} \leq a_1 h|\boldsymbol{u}|_{2,\Omega}.
$$

Finally, using the above inequalities and Poincaré inequality we get

$$
\begin{aligned}
\|(\mathcal{G}_{\boldsymbol{u}}-\mathcal{G}_{\boldsymbol{u}_h})(\boldsymbol{v}_h,r_h)\|_{0,\Omega} &\leq h|\boldsymbol{u}|_{2,\Omega}\left[C_p\tilde{C}\,(a_1+a_2\,C_I)\|\boldsymbol{u}\|_{2,\Omega}+\nu\,a_1\right]|\boldsymbol{v}_h|_{1,\Omega} \\
&\leq h|\boldsymbol{u}|_{2,\Omega}\left[C_p\tilde{C}\,(a_1+a_2\,C_I)\|\boldsymbol{u}\|_{2,\Omega}+\nu\,a_1\right]\|(\boldsymbol{v}_h,r_h)\|_{\mathbf{V}\times P},
\end{aligned}
$$

where C_p is the Poincaré constant. Thereby, we arrive straight to the result of the lemma.

□

Finally, we can derive the first main convergence result.

Theorem 3.3 (Main Result II)**.** *Assume that $(\boldsymbol{w},q)\in[H_0^1(\Omega)\cap H^{k+1}(\Omega)]^d\times[L_0^2(\Omega)\cap H^k(\Omega)]$ and $\boldsymbol{u}\in[H^2(\Omega)]^d$. Then,*

$$
\begin{aligned}
|\boldsymbol{w}-\boldsymbol{w}_h|_{1,\Omega}+\|q-q_h\|_{0,\Omega} \leq C_1C_2h^k\big(|\boldsymbol{w}|_{k+1,\Omega}+|q|_{k,\Omega}\big) \\
+\beta_1^{-1}h|\boldsymbol{u}|_{2,\Omega}\left(\rho C_p\tilde{C}\,(a_1+a_2\,C_I)\|\boldsymbol{u}\|_{2,\Omega}+\mu\,a_1\right).
\end{aligned}
$$

Proof. The proof follows from Lemmas 3.5 3.6 and 3.7 . □

3.3.4 Stabilized PSPG discretization

Let us consider again the Stokes problem given as in (3.18) and its respective variational formulation (3.19). We will now analyze the PSPG Stabilization [107] with the end of comparing the error of convergence between the pressure obtained with both schemes.

We want to use spaces of finite element of order k for the velocity and the pressure, i.e., $k = l$, by means of the following stabilized formulation.

$$\mathcal{B}^s((\boldsymbol{w}_h, q_h)(\boldsymbol{v}_h, r_h)) = \mathcal{G}^s_{\boldsymbol{u}_h}(\boldsymbol{v}_h, r_h) \tag{3.28}$$

where

$$\mathcal{B}^s((\boldsymbol{w}_h, q_h)(\boldsymbol{v}_h, r_h)) := \mathcal{B}((\boldsymbol{w}_h, q_h)(\boldsymbol{v}_h, r_h)) + \sum_{K\in\mathcal{T}_H} \delta\, h_K^2 (\nabla q_h, \nabla r_h)_K$$

$$\mathcal{G}^s_{\boldsymbol{u}_h}(\boldsymbol{v}_h, r_h) := \mathcal{G}_{\boldsymbol{u}_h}(\boldsymbol{v}_h, r_h) + \sum_{K\in\mathcal{T}_H} \delta\, h_K^2 (-\boldsymbol{f}_{\boldsymbol{u}_h}, \nabla r_h)_K$$

with $\mathcal{B}((\cdot,\cdot),(\cdot,\cdot))$ and $\mathcal{G}_{\boldsymbol{u}_h}(\cdot,\cdot)$ defined as in (3.26), and

$$\boldsymbol{f}_{\boldsymbol{u}_h} := (\mathcal{L}_h \boldsymbol{u} \cdot \nabla)\mathcal{L}_h \boldsymbol{u}. \tag{3.29}$$

Remark 3.2. *Note that the term $\Delta \boldsymbol{w}_h$ is not included in the stabilization. This is possible to do while keeping strong consistency since $\boldsymbol{w} = \boldsymbol{0}$. Our choice allows also to avoid conditional well-posedness of the discrete solution as in standard PSPG stabilized formulations.*

Let us define the mesh-dependent norm on the product space $\mathbf{V} \times P$

$$\|(\boldsymbol{v}, r)\|_h^2 := \mathcal{B}^s((\boldsymbol{v}, r), (\boldsymbol{v}, r)) = \|\nabla \boldsymbol{v}\|_{0,\Omega}^2 + \sum_{K\in\mathcal{T}_H} \delta h_K^2 \|\nabla r\|_{0,K}^2. \tag{3.30}$$

Remark 3.3. *It is possible to prove that $\|(\boldsymbol{v}_h, r_h)\|_h \preceq \|(\boldsymbol{v}_h, r_h)\|_{\mathbf{V}\times P}$ for all $(\boldsymbol{v}_h, r_h) \in \mathbf{V}_h \times P_h$. Indeed, applying the inequality (3.23) and the previous assumptions we get*

$$\|(\boldsymbol{v}_h, r_h)\|_h^2 := \|\nabla \boldsymbol{v}_h\|_{0,\Omega}^2 + \sum_{K\in\mathcal{T}_H} \delta h_K^2 \|\nabla r_h\|_{0,K}^2 \le \|\nabla \boldsymbol{v}_h\|_{0,\Omega}^2 + \delta C_I^2 \|r_h\|_{0,\Omega}^2$$
$$\le \max\left\{1, \delta C_I^2\right\} (\|\nabla \boldsymbol{v}_h\|_{0,\Omega}^2 + \|r_h\|_{0,\Omega}^2),$$

and then,

$$\|(\boldsymbol{v}_h, r_h)\|_h \le C_{eq} \|(\boldsymbol{v}_h, r_h)\|_{\mathbf{V}\times P}, \tag{3.31}$$

where

$$C_{eq} = \left[\max\left\{1, \delta C_I^2\right\}\right]^{1/2}$$

Lemma 3.8.

$$\|\mathcal{B}^s\| \le C_{\mathcal{B}^s} = \max\left\{C_{\mathcal{B}}, \sqrt{\delta} C_{eq} C_I\right\} \tag{3.32}$$

Proof. Using the inequalities (3.23) and (3.31), Theorem 3.3 and Cauchy-Schwarz inequality we obtain that

$$\begin{aligned}
|\mathcal{B}^s((\boldsymbol{w}_h,q_h),(\boldsymbol{v}_h,r_h))| &\leq \|\mathcal{B}\|\|(\boldsymbol{w}_h,q_h)\|_{\mathbf{V}\times P}\|(\boldsymbol{v}_h,r_h)\|_{\mathbf{V}\times P} + \sum_{K\in\mathcal{T}_H}\delta h_K^2\|\nabla q_h\|_{0,K}\|\nabla r_h\|_{0,K}\\
&\leq C_{\mathcal{B}}\|(\boldsymbol{w}_h,q_h)\|_{\mathbf{V}\times P}\|(\boldsymbol{v}_h,r_h)\|_{\mathbf{V}\times P}\\
&+\left(\sum_{K\in\mathcal{T}_H}\delta h_K^2\|\nabla q_h\|_{0,K}^2\right)^{1/2}\left(\sum_{K\in\mathcal{T}_H}\delta h_K^2\|\nabla r_h\|_{0,K}^2\right)^{1/2}\\
&\leq C_{\mathcal{B}}\|(\boldsymbol{w}_h,q_h)\|_{\mathbf{V}\times P}\|(\boldsymbol{v}_h,r_h)\|_{\mathbf{V}\times P} + \left(\sum_{K\in\mathcal{T}_H}\delta C_I^2\|q_h\|_{0,K}^2\right)^{1/2}\|(\boldsymbol{v}_h,r_h)\|_h\\
&\leq C_{\mathcal{B}^s}\|(\boldsymbol{w}_h,q_h)\|_{\mathbf{V}\times P}\|(\boldsymbol{v}_h,r_h)\|_{\mathbf{V}\times P},
\end{aligned}$$

and then the result follows.

□

In the next lemmas we will consider the pair $(\tilde{\boldsymbol{w}}_h,\tilde{q}_h)\in\mathbf{V}_h\times P_h$ which are solution of the equation

$$\mathcal{B}^s((\boldsymbol{w}_h,q_h)(\boldsymbol{v}_h,r_h)) = \mathcal{G}^s_{\boldsymbol{u}}(\boldsymbol{v}_h,r_h),\qquad \forall\,(\boldsymbol{v}_h,r_h)\in\mathbf{V}_h\times P_h \tag{3.33}$$

where

$$\mathcal{G}^s_{\boldsymbol{u}}(\boldsymbol{v}_h,r_h) := \mathcal{G}_{\boldsymbol{u}}(\boldsymbol{v}_h,r_h) + \sum_{K\in\mathcal{T}_H}\delta\, h_K^2(\boldsymbol{f}_{\boldsymbol{u}},\nabla r_h)_K.$$

We highlight that the solvability of the problem (3.33) has been guaranteed in [107].

Lemma 3.9. *Let $(\boldsymbol{w},q)$ and $(\tilde{\boldsymbol{w}}_h,\tilde{q}_h)$ solutions of (3.19) and (3.33) respectively. Assume that $(\boldsymbol{w},q)\in[H_0^1(\Omega)\cap H^{k+1}(\Omega)]^d\times[L_0^2(\Omega)\cap H^k(\Omega)]$. Then, there is $C>0$ independent of h such that*

$$|\boldsymbol{w}-\tilde{\boldsymbol{w}}_h|_{1,\Omega} + \|q-\tilde{q}_h\|_{0,\Omega} \leq C_1\,C_3\,h^k\left(|\boldsymbol{w}|_{k+1,\Omega}+|q|_{k,\Omega}\right)$$

with $C_3 = 1+\|\mathcal{B}^s\|$.

Proof. We note that $(\boldsymbol{w},q)$ and $(\tilde{\boldsymbol{w}}_h,\tilde{q}_h)$ satisfy the orthogonality property

$$\mathcal{B}^s((\boldsymbol{w}-\tilde{\boldsymbol{w}}_h,q-\tilde{q}_h),(\boldsymbol{v}_h,r_h)) = 0\qquad \forall(\boldsymbol{v}_h,r_h)\in\mathbf{V}_h\times P_h.$$

Indeed, thanks to the consistency of bilinear form $\mathcal{B}$ we get

$$\begin{aligned}
\mathcal{B}^s((\boldsymbol{w}-\tilde{\boldsymbol{w}}_h,q-\tilde{q}_h),(\boldsymbol{v}_h,r_h)) &= \mathcal{B}((\boldsymbol{w}-\tilde{\boldsymbol{w}}_h,q-\tilde{q}_h),(\boldsymbol{v}_h,r_h)) + \sum_{K\in\mathcal{T}_H}\delta h_K^2(\nabla q,\nabla r_h)_K\\
&-\sum_{K\in\mathcal{T}_H}\delta h_K^2(\nabla\tilde{q}_h,\nabla r_h)_K\\
&=\sum_{K\in\mathcal{T}_H}\delta h_K^2(\boldsymbol{f}_{\boldsymbol{u}},\nabla r_h)_K - \sum_{K\in\mathcal{T}_H}\delta h_K^2(\boldsymbol{f}_{\boldsymbol{u}},\nabla r_h)_K\\
&=0.
\end{aligned}$$

By the triangle inequality we can get,

$$\begin{aligned}\|(\boldsymbol{w}-\tilde{\boldsymbol{w}}_h, q-\tilde{q}_h)\|_{\mathbf{V}\times P} &= |\boldsymbol{w}-\mathcal{I}_h\boldsymbol{w}+\mathcal{I}_h\boldsymbol{w}-\boldsymbol{w}_h|_{1,\Omega}+\|q-\mathcal{J}_h q+\mathcal{J}_h q-q_h\|_{0,\Omega}\\ &\leq \|(\boldsymbol{w}-\mathcal{I}_h\boldsymbol{w}, q-\mathcal{J}_h q)\|_{\mathbf{V}\times P}+\|(\tilde{\boldsymbol{w}}_h-\mathcal{I}_h\boldsymbol{w}, \tilde{q}_h-\mathcal{J}_h q)\|_{\mathbf{V}\times P}. \quad (3.34)\end{aligned}$$

For the second term of the right-hand side, we must consider the result earned in [107] from where we get

$$\begin{aligned}\|(\tilde{\boldsymbol{w}}_h-\mathcal{I}_h\boldsymbol{w}, \tilde{q}_h-\mathcal{J}_h q)\|_{\mathbf{V}\times P} &\leq \sup_{\substack{(\boldsymbol{v}_h,r_h)\in\mathbf{V}_h\times P_h\\(\boldsymbol{v}_h,r_h)\neq\mathbf{0}}} \frac{\mathcal{B}^s((\tilde{\boldsymbol{w}}_h-\mathcal{I}_h\boldsymbol{w}, \tilde{q}_h-\mathcal{J}_h q),(\boldsymbol{v}_h,r_h))}{\|(\boldsymbol{v}_h,r_h)\|_h}\\ &= \sup_{\substack{(\boldsymbol{v}_h,r_h)\in\mathbf{V}_h\times P_h\\(\boldsymbol{v}_h,r_h)\neq\mathbf{0}}} \frac{\mathcal{B}^s((\boldsymbol{w}-\mathcal{I}_h\boldsymbol{w}, q-\mathcal{J}_h q),(\boldsymbol{v}_h,r_h))}{\|(\boldsymbol{v}_h,r_h)\|_h}\\ &\leq \|\mathcal{B}^s\|\|(\boldsymbol{w}-\mathcal{I}_h\boldsymbol{w}, q-\mathcal{J}_h q)\|_{\mathbf{V}\times P},\end{aligned}$$

and so, from this inequality and (3.34) we obtain

$$\|(\boldsymbol{w}-\tilde{\boldsymbol{w}}_h, q-\tilde{q}_h)\|_{\mathbf{V}\times P} \leq \big(1+\|\mathcal{B}^s\|\big)\|(\boldsymbol{w}-\mathcal{I}_h\boldsymbol{w}, q-\mathcal{J}_h q)\|_{\mathbf{V}\times P}$$

and thereby we arrive to

$$|\boldsymbol{w}-\tilde{\boldsymbol{w}}_h|_{1,\Omega}+\|q-\tilde{q}_h\|_{0,\Omega} \leq C_1C_3h^k\big(|\boldsymbol{w}|_{k+1,\Omega}+|q|_{k,\Omega}\big),$$

. □

Lemma 3.10. *Let $(\tilde{\boldsymbol{w}}_h,\tilde{q}_h)$ and $(\boldsymbol{w}_h,q_h)$ be solutions of (3.33) and (3.28), respectively. Additionally, we assume that $\boldsymbol{u}\in[H^2(\Omega)]^d$. Then, the following bound is satisfied:*

$$\|(\tilde{\boldsymbol{w}}_h-\boldsymbol{w}_h,\tilde{q}_h-q_h)\|_h \leq \|\mathcal{G}_{\boldsymbol{u}}-\mathcal{G}_{\boldsymbol{u}_h}\|_{(\mathbf{V}\times P)'}+\sqrt{\delta}h^2T(a_1,a_2,\boldsymbol{u},h)|\boldsymbol{u}|_{2,\Omega}+\sqrt{\delta}\nu h\|\Delta\boldsymbol{u}\|_{0,\Omega},$$

Proof. Let $\boldsymbol{e}_h^{\boldsymbol{w}}:=\tilde{\boldsymbol{w}}_h-\boldsymbol{w}_h$ and $e_h^q:=\tilde{q}_h-q_h$. Then, thanks to the stability of $\mathcal{B}^s$ given in (3.30) we have

$$\begin{aligned}&\|(\boldsymbol{e}_h^{\boldsymbol{w}},e_h^q)\|_h\\ &= \frac{\mathcal{B}^s((\boldsymbol{e}_h^{\boldsymbol{w}},e_h^q)(\boldsymbol{e}_h^{\boldsymbol{w}},e_h^q))}{\|(\boldsymbol{e}_h^{\boldsymbol{w}},e_h^q)\|_h}\\ &\leq \sup_{\substack{(\boldsymbol{v}_h,r_h)\in\mathbf{V}_h\times P_h\\(\boldsymbol{v}_h,r_h)\neq\mathbf{0}}} \frac{\mathcal{B}^s((\boldsymbol{e}_h^{\boldsymbol{w}},e_h^q)(\boldsymbol{v}_h,q_h))}{\|(\boldsymbol{v}_h,q_h)\|_h}\\ &= \sup_{\substack{(\boldsymbol{v}_h,r_h)\in\mathbf{V}_h\times P_h\\(\boldsymbol{v}_h,r_h)\neq\mathbf{0}}} \frac{\mathcal{G}_{\boldsymbol{u}}^s(\boldsymbol{v}_h,r_h)-\mathcal{G}_{\boldsymbol{u}_h}^s(\boldsymbol{v}_h,r_h)}{\|(\boldsymbol{v}_h,q_h)\|_h}\\ &= \sup_{\substack{(\boldsymbol{v}_h,r_h)\in\mathbf{V}_h\times P_h\\(\boldsymbol{v}_h,r_h)\neq\mathbf{0}}} \frac{\mathcal{G}_{\boldsymbol{u}}(\boldsymbol{v}_h,r_h)-\mathcal{G}_{\boldsymbol{u}_h}(\boldsymbol{v}_h,r_h)-\displaystyle\sum_{K\in\mathcal{T}_H}\delta h_K^2(\boldsymbol{f}_{\boldsymbol{u}}-\boldsymbol{f}_{\boldsymbol{u}_h},\nabla r_h)_K}{\|(\boldsymbol{v}_h,q_h)\|_h}\end{aligned}$$

We take the term within sum, making use of the Cauchy-Schwarz inequality and proceeding similarly as in (3.10), we obtain

$$
\begin{aligned}
&-\sum_{K\in\mathcal{T}_H}\delta h_K^2(\boldsymbol{f}_{\boldsymbol{u}}-\boldsymbol{f}_{\boldsymbol{u}_h},\nabla r_h)_K\\
&=\sum_{K\in\mathcal{T}_H}\delta h_K^2((\boldsymbol{u}\cdot\nabla)\boldsymbol{u}-(\mathcal{L}_h\boldsymbol{u}\cdot\nabla)\mathcal{L}_h\boldsymbol{u},\nabla r_h)_K\\
&-\nu\sum_{K\in\mathcal{T}_H}\delta h_K^2(\Delta\boldsymbol{u},\nabla r_h)_K\\
&\leq\sum_{K\in\mathcal{T}_H}\delta h_K^2\|(\boldsymbol{u}\cdot\nabla)\boldsymbol{u}-(\mathcal{L}_h\boldsymbol{u}\cdot\nabla)\mathcal{L}_h\boldsymbol{u}\|_{0,\Omega}\|\nabla r_h\|_{0,K}\\
&+\nu\sum_{K\in\mathcal{T}_H}\delta h_K^2\|\Delta\boldsymbol{u}\|_{0,K}\|\nabla r_h\|_{0,K}\\
&\leq\left(\sum_{K\in\mathcal{T}_H}\delta h_K^2\|(\boldsymbol{u}\cdot\nabla)\boldsymbol{u}-(\mathcal{L}_h\boldsymbol{u}\cdot\nabla)\mathcal{L}_h\boldsymbol{u}\|_{0,K}^2\right)^{1/2}\left(\sum_{K\in\mathcal{T}_H}\delta h_K^2\|\nabla r_h\|_{0,K}^2\right)^{1/2}\\
&+\nu\left(\sum_{K\in\mathcal{T}_H}\delta h_K^2\|\Delta\boldsymbol{u}\|_{0,K}^2\right)^{1/2}\left(\sum_{K\in\mathcal{T}_H}\delta h_K^2\|\nabla r_h\|_{0,K}^2\right)^{1/2}\\
&\leq\sqrt{\delta}h^2\tilde{C}(a_1+a_2C_I)|\boldsymbol{u}|_{2,\Omega}\|\boldsymbol{u}\|_{2,\Omega}\|(\boldsymbol{v}_h,r_h)\|_h\\
&+\nu\sqrt{\delta}\left(\sum_{K\in\mathcal{T}_H}h_K^2\|\Delta\boldsymbol{u}\|_{0,K}^2\right)^{1/2}\|(\boldsymbol{v}_h,r_h)\|_h\\
&\leq\sqrt{\delta}h^2\tilde{C}(a_1+a_2C_I)|\boldsymbol{u}|_{2,\Omega}\|\boldsymbol{u}\|_{2,\Omega}\|(\boldsymbol{v}_h,r_h)\|_h\\
&+\nu\sqrt{\delta}h\|\Delta\boldsymbol{u}\|_{0,\Omega}\|(\boldsymbol{v}_h,r_h)\|_h.
\end{aligned}
$$

□

As a main result of this section, by employing the approximation properties and a priori estimates, we obtain the next result.

Theorem 3.4 (Main Result III)**.** *Assume that the hypothesis of Theorem 3.3 hold. Then,*

$$
\begin{aligned}
|\boldsymbol{w}-\boldsymbol{w}_h|_{1,\Omega}+\|q-q_h\|_{0,\Omega}\leq C_1C_3h^k\left(|\boldsymbol{w}|_{k+1,\Omega}+|q|_{k,\Omega}\right)+\nu\sqrt{\delta}h\|\Delta\boldsymbol{u}\|_{0,\Omega}\\
+h|\boldsymbol{u}|_{2,\Omega}\left[C_p\tilde{C}\,(a_1+a_2\,C_I)\|\boldsymbol{u}\|_{2,\Omega}+\nu\,a_1+\sqrt{\delta}hC_p\tilde{C}\,(a_1+a_2\,C_I)\|\boldsymbol{u}\|_{2,\Omega}\right].
\end{aligned}
$$

Proof. The proof follows from combining the results of Lemmas 3.7, 3.9 and 3.10. □

3.4 Numerical Results

In this section we present some numerical examples to illustrate the theoretical results previously described. The legends in the plots follow the notation:

- $e_1(q)$: Pressure error in L^2-norm with $\mathbb{P}_1$
- $e_2(q)$: Pressure error in L^2-norm with $\mathbb{P}_2$,

with

$$e_i(q) := \frac{\|q - q_h\|_{0,\Omega}}{\|q\|_{0,\Omega}}.$$

Let us clarify that the next examples are with a exact solucion owing to our goal is to check mainly the convergence, because previosly have been validated the methods in real problems (see [126]).

Example 3.1. *For the first example, we consider the exact solution of the two dimensional Kovasznay flow*

$$\boldsymbol{u}(x,y) = \begin{pmatrix} 1 - e^{\lambda x}\cos(2\pi y) \\ \frac{\lambda}{2\pi} e^{\lambda x}\sin(2\pi y) \end{pmatrix}, \quad p(x,y) = \frac{1}{2}e^{\lambda x} - (e^{3\lambda} - e^{-\lambda}),$$

where $\Omega = \left(-\frac{1}{2}, \frac{3}{2}\right) \times \left(0, 2\right)$ *and the parameter* λ *is given by* $\lambda = \frac{1}{2\nu} - \sqrt{\frac{1}{4\nu^2} + 4\pi^2}$. *For this ilustration we have taken the Reynold number as in [137] which is given by* $Re = \frac{1}{\nu}$.

The convergence results are shown in figure 3.1 and the isovalues in figures 3.2, 3.3, 3.4 and 3.5.

Example 3.2. *Next we turn to the testing the scheme, where the computational domain is the rectangle* $\Omega = [0,1]^2$ *and we consider the exact solution of the Navier-Stokes equation given by*

$$u(x,y) = (\frac{\nu}{4}e^x \sin(\nu y), \frac{1}{4}e^x \cos(\nu y)) \quad \text{and} \quad p(x,y) = -\frac{\nu}{2}e^{2x} + \frac{\nu}{4}(e^2 - 1) \tag{3.35}$$

The convergence results are shown in figure 3.6 and the isovalues in figures 3.7, 3.8, 3.9 and 3.10.

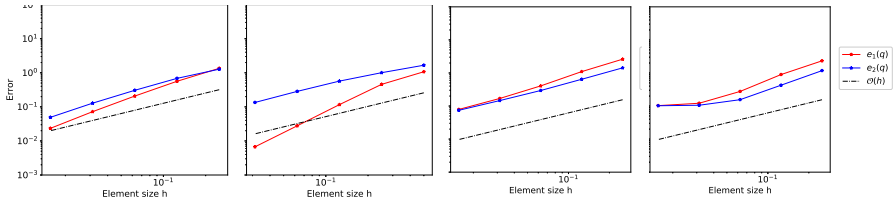

$\nu = 1$ - STE(TH) $\nu = 1$ - STE(STA) $\nu = 1$ - PPE(mod) $\nu = 1$ - PPE (stand)

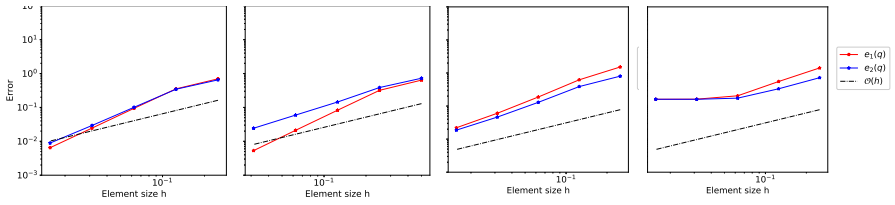

$\nu = 0.1$ - STE(TH) $\nu = 0.1$ - STE(STA) $\nu = 0.1$ - PPE(mod) $\nu = 0.1$ - PPE (stand)

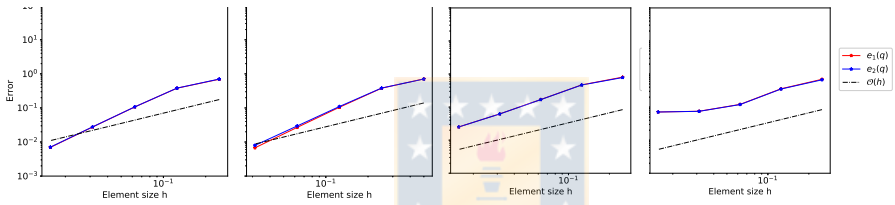

$\nu = 0.01$ - STE(TH) $\nu = 0.01$ - STE(STA) $\nu = 0.01$ - PPE(mod) $\nu = 0.01$ - PPE (stand)

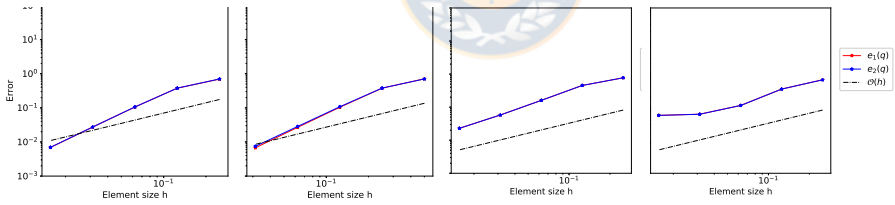

$\nu = 0.001$ - STE(TH) $\nu = 0.001$-STE(STA) $\nu = 0.001$-PPE(mod) $\nu = 0.001$-PPE (stand)

Figure 3.1: Pressure error curves and bounds for viscosities values $1, 10^{-1}, 10^{-2}$ and 10^{-3} of Example 1 (Kovaznay flow). The figures for the modified PPE do not present the error bound as explained in the beginning of Section 3.4.

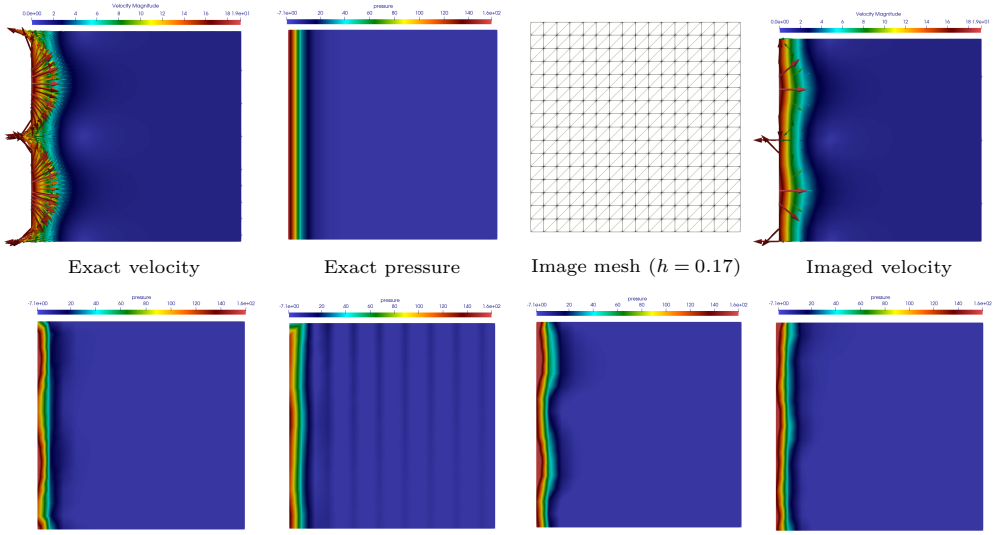

Figure 3.2: $\mathbb{P}_1$-interpolated reference velocity and pressure fields (top) and reconstructed pressure fields with order $k = 1$ (bottom) for $\nu = 1$ in Example 3.1 (Kovaznay flow).

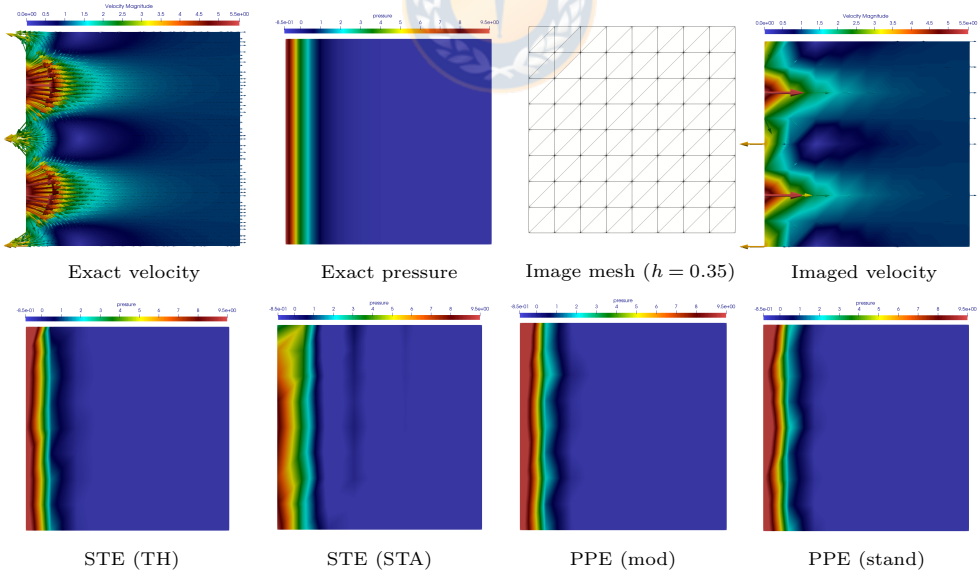

Figure 3.3: $\mathbb{P}_1$-interpolated reference velocity and pressure fields (top) and reconstructed pressure fields with order $k = 1$ (bottom) for $\nu = 0.1$ in Example 3.1 (Kovaznay flow).

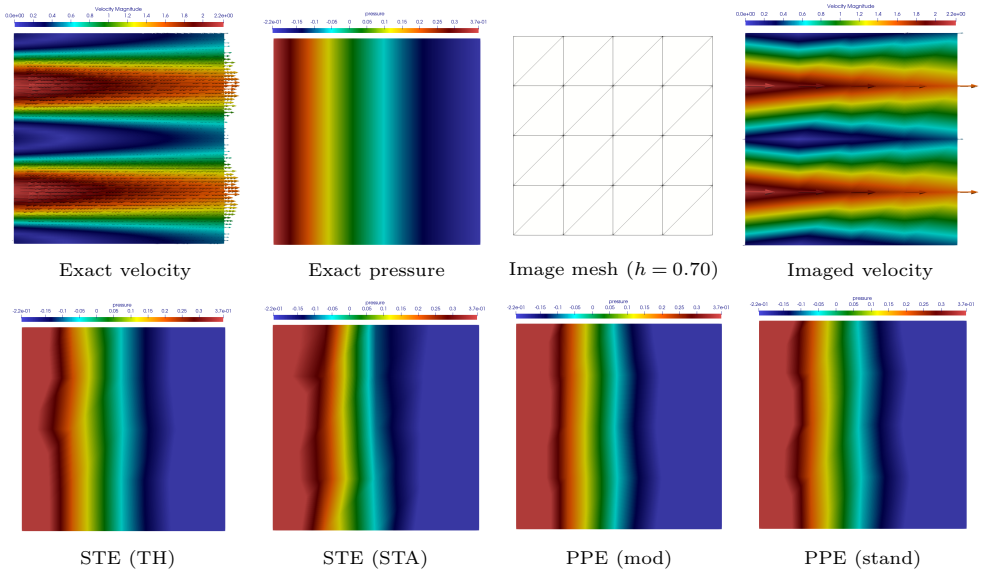

Figure 3.4: $\mathbb{P}_1$-interpolated reference velocity and pressure fields (top) and reconstructed pressure fields with order $k = 1$ (bottom) for $\nu = 0.01$ in Example 3.1 (Kovaznay flow).

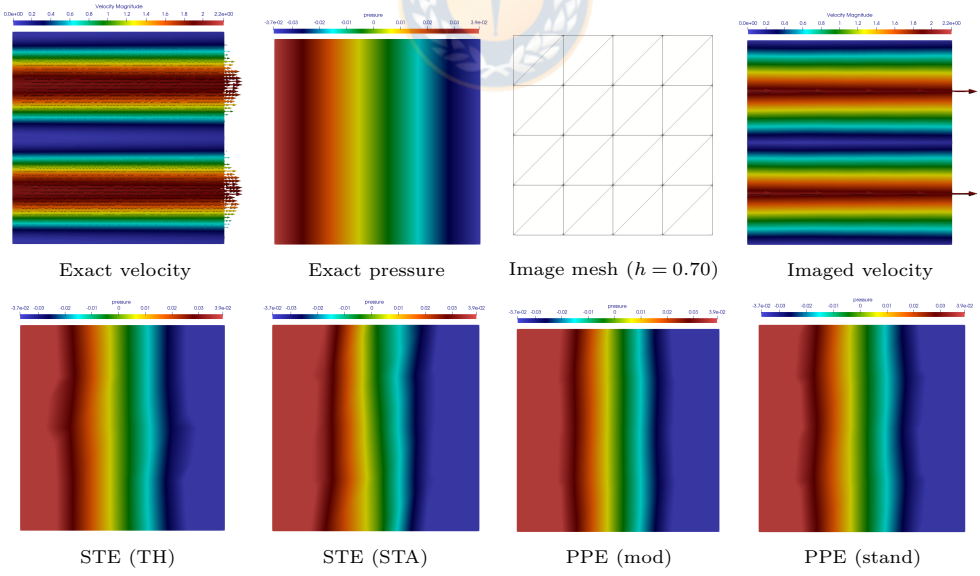

Figure 3.5: $\mathbb{P}_1$-interpolated reference velocity and pressure fields (top) and reconstructed pressure fields with order $k = 1$ (bottom) for $\nu = 0.001$ in Example 3.1 (Kovaznay flow).

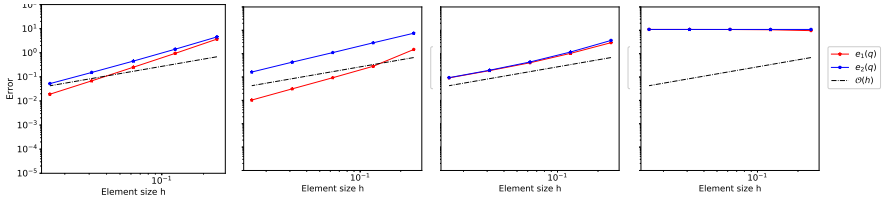

$\nu = 2\pi$ - STE (TH) $\nu = 2\pi$ - STE (STA) $\nu = 2\pi$ - PPE (mod) $\nu = 2\pi$ - PPE (stand)

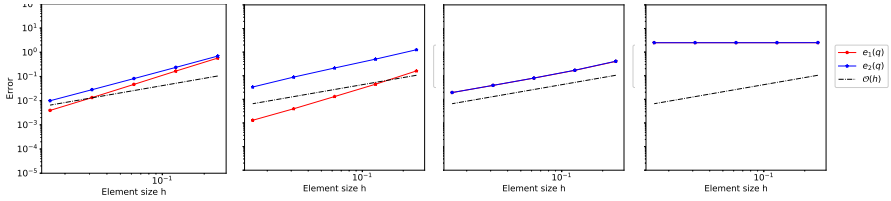

$\nu = \pi$ - STE (TH) $\nu = \pi$ - STE (STA) $\nu = \pi$ - PPE (mod) $\nu = \pi$ - PPE (stand)

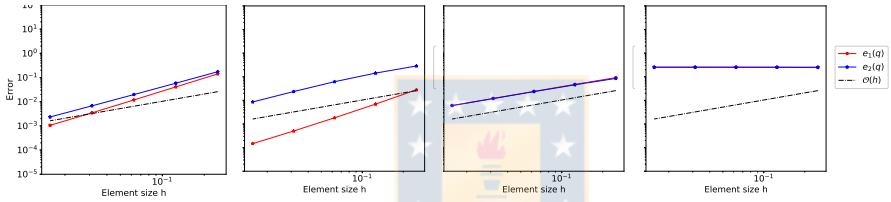

$\nu = \frac{\pi}{2}$ - STE (TH) $\nu = \frac{\pi}{2}$ - STE (STA) $\nu = \frac{\pi}{2}$ - PPE (mod) $\nu = \frac{\pi}{2}$ - PPE (stand)

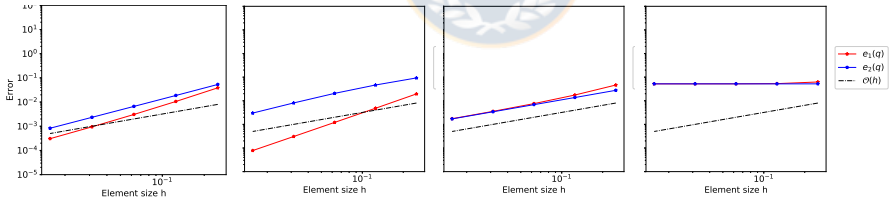

$\nu = \frac{\pi}{4}$ - STE (TH) $\nu = \frac{\pi}{4}$ - STE (STA) $\nu = \frac{\pi}{4}$ - PPE (mod) $\nu = \frac{\pi}{4}$ - PPE (stand)

Figure 3.6: Pressure error curves and bounds for viscosities values $\pi/4, \pi/2, \pi$ and 2π of Example 3.2. The figures for the modified PPE do not present the error bound as explained in the beginning of Section 3.4.

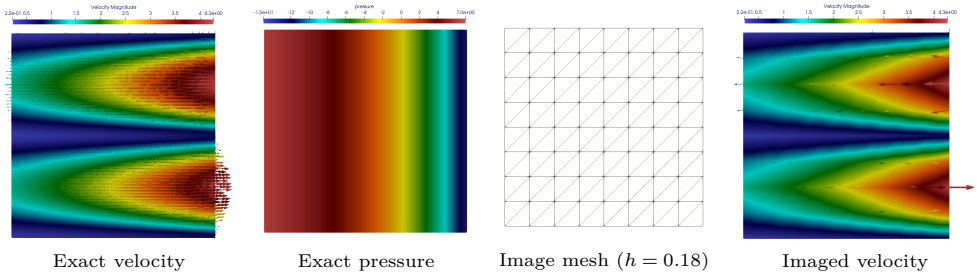

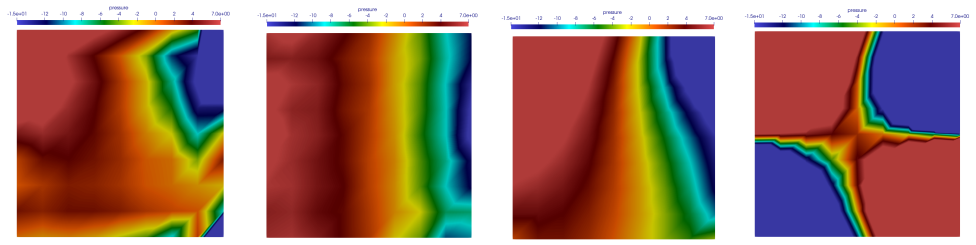

Figure 3.7: $\mathbb{P}_1$-interpolated reference velocity and pressure fields (top) and reconstructed pressure fields with order $k = 1$ (bottom) for $\nu = 2\pi$ in Example 3.2.

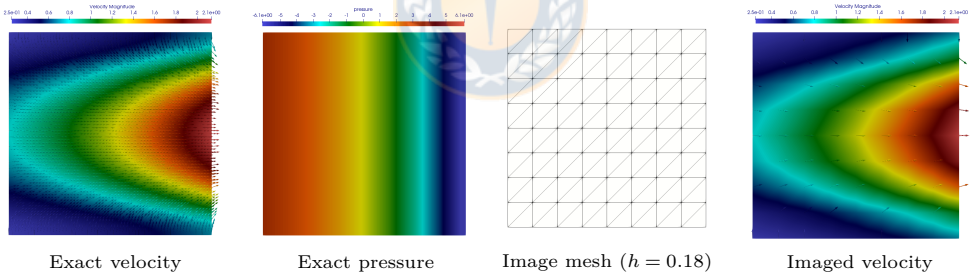

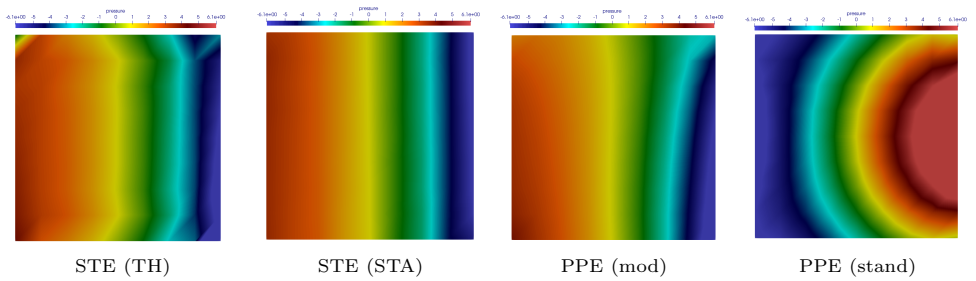

Figure 3.8: $\mathbb{P}_1$-interpolated reference velocity and pressure fields (top) and reconstructed pressure fields with order $k = 1$ (bottom) for $\nu = \pi$ in Example 3.2.

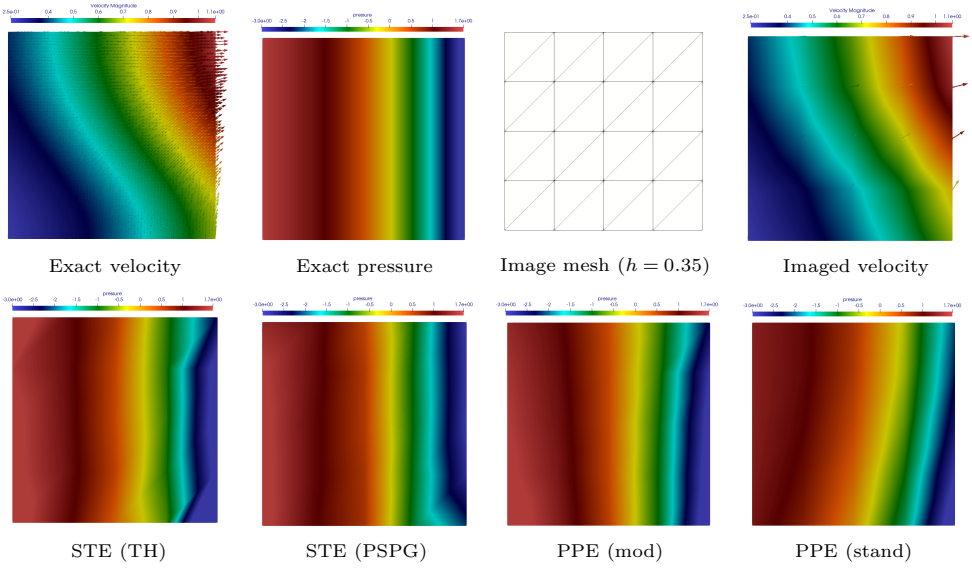

Figure 3.9: $\mathbb{P}_1$-interpolated reference velocity and pressure fields (top) and reconstructed pressure fields with order $k = 1$ (bottom) for $\nu = \pi/2$ in Example 3.2.

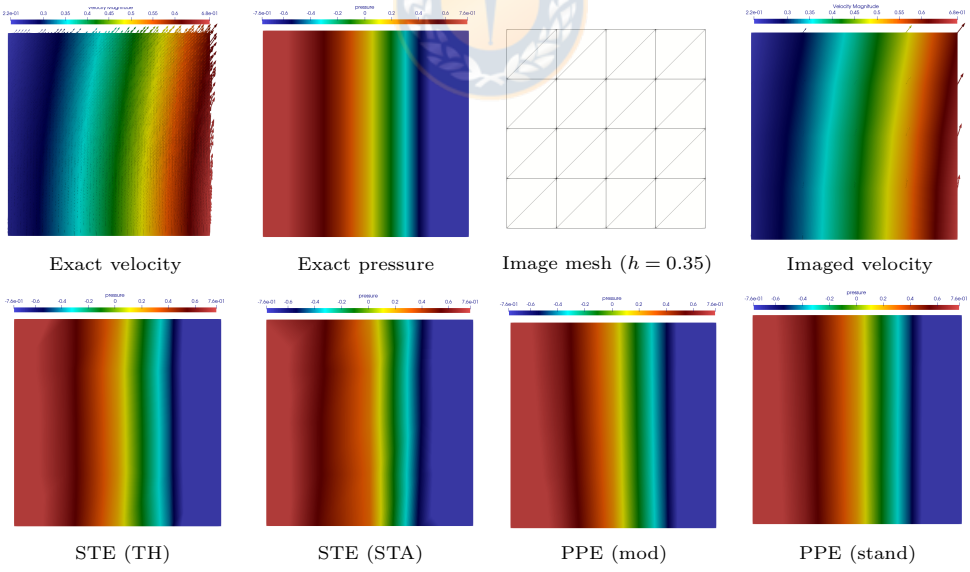

Figure 3.10: $\mathbb{P}_1$-interpolated reference velocity and pressure fields (top) and reconstructed pressure fields with order $k = 1$ (bottom) for $\nu = \pi/4$ in Example 3.2.

Conclusion

Summary

In this thesis, we have proposed and analysed PDE-based fluid models such as Navier-Stokes, Oseen and nonlinear Darcy. We have proved their solvability using the classical Ladyzhenskaya–Babuška–Brezzi, proposed and used stabilized schemes and obtained approximated solutions by using adaptive strategies, with a strong emphasis on stabilized finite element methods.

In Chapter 1 we proposed an extension of the MHM method to the Oseen equations based on previous works for the Stokes model [16] and the advection-diffusion equation [98]. Owing to the structure of the MHM, we also introduced and analyzed a new residual a posteriori error estimator for which we showed that local efficiency and reliability concerning natural norms. The estimator is multi-level and therefore it can consider different scales, and handle the solutions of singularly perturbed problems as the ones in the Oseen equations under advective or reactive regimes. From a theoretical viewpoint, the dependence of constants (in the equivalence estimates) regarding the physical parameters as well as the degree of polynomial interpolation on faces deserves further investigation. The numerical verifications performed in this chapter pointed to the robustness of the estimator in terms of those dependencies, but the precise proof remains an open problem. The natural extension of the proposed methodology to the nonlinear Navier-Stokes equations is currently under investigation.

In Chapter 2, we have introduced a new stabilized formulation for a Darcy equation with exponentially pressure-dependent porosity in two or three dimensions. We included well–posed results as a priori error estimated under standard assumptions. This new formulation allows us to use equal-order of interpolation spaces for both velocity and pressure.
Besides, we introduced and studied an a posteriori error estimator of the residual type. In particular, we prove the equivalence between our error estimator and the approximation error.
We also included some numerical examples to show the theoretical results for both a priori and a posteriori error bounds.

Chapter 3 was focused on the error analysis of methods for approximation of the pressure from discrete velocity fields, STE and PPE. The STE is analyzed using the classical Taylor-Hood finite element spaces and pressure-stabilizing Petrov-Galerkin (PSPG). The PPE is analyzed using a continuous Galerkin method, where two versions of the PPE have been considered, the classical approach without a viscous term and a new approach with a boundary viscous term as proposed in [130].
Due to the piecewise linear nature of the measured velocities, the error bounds indicate

terms of different convergence orders. However, for the numerical examples with polynomial order 1 and 2 for the pressure mainly convergence order 1 is observed. Therefore, in contrast to a classical problem solved by finite elements with analytical right-hand-side, here we can see that it is not worth increasing the polynomial order.
A remarkable result is that in each example the relative error decreases as the Reynolds number increases possibly due to the reduction of the viscous contribution which appear to be more difficult to retrieve for all methods.
The numerical results show that the methods of choice are the STE-PSPG and the Modified-PPE leading to the best error-cost relations. However, it remains to be clarified if the modification of the PPE achieves comparable accuracies using measured MRI data in real arteries, where the viscous contribution appears to be negligible and the data has larger errors in the boundaries due to imaging artifacts.

Perspectives

The solutions of nonlinear equations are open problems in many fluid applications. Equations such as Darcy, Forchheimer, Stokes, among others, have a nonlinear version to be solved. Additionally, there exist applications where the fluid is moving in two or more phases, allowing it to be studied by coupled models. For such reasons, we are interested in extending the theory developed in chapter 2, but now studied while the fluid is not acting in a porous medium.

About the methods to recover the pressure, we have observed the occurrence of other viewpoints to approach the problems, thus providing new alternative forms to reconstruct the pressure with more efficiency and with less cost. Taking advantage of the analysis of the modified-PPE, we are interested in recycling the method for the design of other methods, such as stabilized schemes, where we will to able to use STE-PPE under the same problem. On the other hand, we are interested in studying the case when the auxiliary velocity satisfies the boundary condition $\boldsymbol{w} \cdot \boldsymbol{n} = 0$, because apparently, with that condition the mathematical problem is closer to the real observed cases.

Finally, we know little about efficient methods to solve problems where there is fluid-structure interaction and the fluid is moving in a porous medium. Taking into consideration the advantages of the splitting or projection methods, we have considered addressing the problems modeling fluid motion in arteries, where the fluid flows through porosities.

Bibliography

[1] A. Abdulle and A. Nonnenmacher. "A posteriori error estimates in quantities of interest for the finite element heterogeneous multiscale method". In: *Numer. Methods Partial Differential Equations* 29.5 (2013), pp. 1629–1656. DOI: 10.1002/num.21769.

[2] D.J. Acheson. *Elementary Fluid Dynamics*. Oxford Applied Mathematics and Computing Science Series. Clarendon Press, 1990. DOI: /10.1002/aic.690390431.

[3] G. Acosta, R. Durán, and M. Muschietti. "Solutions of the divergence operator on John domains". In: *Adv. Math.* 206.2 (2006), pp. 373–401. DOI: 10.1023/A:1025806612592.

[4] S. Agmon. *Lectures on elliptic boundary value problems*. AMS Chelsea Publishing, Providence, RI, 2010. DOI: 10.1090/chel/369.

[5] A. Agouzal and J. M. Thomas. "Une méthode déléments finis hybrides en décomposition de domaines". In: *RAIRO-Math Model Num.* 29.6 (1995), pp. 749–765.

[6] N. Ahmed, T. Chacón, V. John, and S. Rubino. "A review of variational multiscale methods for the simulation of turbulent incompressible flows". In: *Arch. Comput. Methods Eng.* 24.1 (2017), pp. 115–164. DOI: 10.1007/s11831-015-9161-0.

[7] E. Ahusborde, M. Azaiez, F. Ben Belgacem, and C. Bernardi. "Automatic simplification of Darcy's equations with pressure dependent permeability". In: *ESAIM Math. Model. Numer. Anal.* 47.6 (2013), pp. 1797–1820. DOI: 10.1051/m2an/2013089.

[8] E. Ahusborde, M. Azaıez, F. Ben Belgacem, and C. Bernardi. "Automatic simplification of Darcy's equations with pressure dependent permeability". In: *ESAIM Math. Model. Numer. Anal.* 47.6 (2013), pp. 1797–1820. DOI: 10.1051/m2an/2013089.

[9] M. Ainsworth and J. T. Oden. *A posteriori error estimation in finite element analysis*. Pure and Applied Mathematics (New York). Wiley-Interscience [John Wiley & Sons], New York, 2000. DOI: 10.1002/9781118032824.

[10] M. Ainsworth and J.T. Oden. *A posteriori error estimation in finite element analysis*. Vol. 37. Pure and Applied Mathematics. New York: John Willey & Sons, 2011. DOI: 10.1002/9781118032824.

[11] R. Araya, G. R. Barrenechea, A. H. Poza, and F. Valentin. "Convergence analysis of a residual local projection finite element method for the Navier-Stokes equations". In: *SIAM J. Numer. Anal.* 50.2 (2012), pp. 669–699. DOI: 10.1137/110829283.

[12] R. Araya, G. R. Barrenechea, and F. Valentin. "A stabilized finite-element method for the Stokes problem including element and edge residuals". In: *IMA J. Numer. Anal.* 27.1 (2007), pp. 172–197. DOI: 10.1137/120888223.

[13] R. Araya, C. Bertoglio, C. Cárcamo, A. H. Poza, and F. Valentin. "Multiscale Hybrid-Mixed Method for the Oseen equation". In preparation. 2020.

[14] R. Araya, C. Carcamo, A. Poza, and F. Valentin. "An adaptive multiscale hybrid-mixed method for the Oseen equations". In: *Adv. Comput. Math.* 47.15 (2021). DOI: 10.1007/s10444-020-09833-8.

[15] R. Araya, C. Harder, D. Paredes, and F. Valentin. "Multiscale Hybrid-Mixed Method". In: *SIAM J. Numer. Anal.* 51.6 (2013), pp. 3505–3531. DOI: 10.1137/120888223.

[16] R. Araya, C. Harder, A. H. Poza, and F. Valentin. "Multiscale hybrid-mixed method for the Stokes and Brinkman Equations - The Method". In: *Comput. Methods Appl. Mech. Engrg.* 324.1 (2017), pp. 172–197. DOI: 10.1016/j.cma.2017.05.027.

[17] R. Araya, A. Poza, and F. Valentin. "An adaptive residual local projection finite element method for the Navier–Stokes equations". In: *Adv. Comput. Math* 40.5 (Dec. 2014), pp. 1093–1119. DOI: 10.1007/s10444-014-9343-6.

[18] R. Araya, A.H. Poza, and F. Valentin. "A low-order local projection method for the incompressible Navier-Stokes equations in two- and three-dimensions". In: *IMA J. Numer. Anal.* 36.1 (2016), pp. 267–295. DOI: 10.1093/imanum/drv004.

[19] R. Araya, R. Rebolledo, and F. Valentin. "On a multiscale a posteriori error estimator for the Stokes and Brinkman equations". In: *IMA J. Numer. Anal.* (2019). DOI: 10.1093/imanum/drz053.

[20] T. Arbogast, G. Pencheva, M. F. Wheeler, and I. Yotov. "A multiscale mortar mixed finite element method". In: *Multiscale Model. Simul.* 6.1 (2007), pp. 319–346. DOI: 10.1137/060662587.

[21] D. N. Arnold and F. Brezzi. "Mixed and nonconforming finite element methods: Implementation, postprocessing and error estimates". In: *RAIRO-Math Model Num.* 19.1 (1985), pp. 7–32. DOI: 10.1051/m2an/1985190100071.

[22] M. Azaiez, F. Ben Belgacem, and N. Bernardi C.and Chorfi. "Spectral discretization of Darcy's equations with pressure dependent porosity". In: *Appl. Math. Comput.* 217.5 (2010), pp. 1838–1856. DOI: 10.1016/j.amc.2010.06.014.

[23] I. Babuska and E. Osborn. "Generalized finite element methods: Their performance and their relation to mixed methods". In: *SIAM J. Num. Anal.* 20.3 (1983), pp. 510–536.

[24] J. Baiges and R. Codina. "Variational multiscale error estimators for solid mechanics adaptive simulations: an orthogonal subgrid scale approach". In: *Comput. Methods Appl. Mech. Engrg.* 325 (2017), pp. 37–55. DOI: 10.1016/j.cma.2017.07.008.

[25] G. Barrenechea, M. Fernández, and C. Vidal. *A stabilized finite element method for the Oseen equation with dominating reaction.* Research Report RR-5213. INRIA, 2004, p. 21. URL: https://hal.inria.fr/inria-00070780.

[26] G. R. Barrenechea, L. P. Franca, and F. Valentin. "A Petrov-Galerkin enriched method: a mass conservative finite element method for the Darcy equation". In: *Comput. Methods Appl. Mech. Engrg.* 196.21-24 (2007), pp. 2449–2464. DOI: 10.1016/j.cma.2007.01.004.

[27] G. R. Barrenechea and F. Valentin. "A residual local projection method for the Oseen equation". In: *Comput. Methods Appl. Mech. Engrg.* 199.29-32 (2010), pp. 1906–1921. DOI: 10.1016/j.cma.2010.01.014.

[28] G.R. Barrenechea and F. Valentin. "An unusual stabilized finite element method for a generalized Stokes problem". In: *Numer. Math.* 92.4 (2002), pp. 653–677. DOI: 10.1007/s002110100371.

[29] G.R. Barrenechea and F. Valentin. "Beyond pressure stabilization: a low-order local projection method for the Oseen equation". In: *Internat. J. Numer. Methods Engrg.* 86.7 (2011), pp. 801–815. DOI: 10.1002/nme.3075.

[30] T. Barrios, J. Cascón, and M. González. "A posteriori error analysis of an augmented mixed finite element method for Darcy flow". In: *Comput. Methods Appl. Mech. Engrg.* 283 (2015), pp. 909–922. DOI: 10.1016/j.cma.2014.10.035.

[31] C. Barus. "Isothermal, Isopiestics and Isometric Relative to Viscosity". In: *Am. J. Sci.* 45.266 (1893), pp. 87–96. DOI: 10.2475/ajs.s3-45.266.87.

[32] H. Baumgartner, P. Bonhoeffer, N. De Groot, F. De Haan, J. Deanfield, N. Galie, M. Gatzoulis, C. Gohlke-Baerwolf, H. Kaemmerer, P. Kilner, F Meijboom, B. Mulder, E. Oechslin, J. Oliver, A. Serraf, A. Szatmari, E. Thaulow, P. Vouhe, and E. Walma. "ESC Guidelines for the Management of Grown-up Congenital Heart Disease (New Version 2010) The Task Force on the Management of Grown-up Congenital Heart Disease of the European Society of Cardiology (ESC)". In: *Eur. Heart J.* 31.23 (2010), pp. 2915–2957. DOI: 10.1093/eurheartj/ehq249.

[33] M. Bebendorf. "A note on the poincaré inequality for convex domains". In: *Z. Anal. Anwendungen* 22.4 (2003), pp. 751–756. DOI: 10.4171/ZAA/1170.

[34] R. Becker and M. Braack. "A finite element pressure gradient stabilization for the Stokes equations based on local projections". In: *Calcolo* 38.4 (2001), pp. 173–199. DOI: 10.1007/s10092-001-8180-4.

[35] C. Bernardi, S. Maarouf, and D. Yakoubi. "Spectral discretization of an unsteady flow through a porous solid". In: *Calcolo* 53.4 (2016), pp. 659–690. DOI: 10.1007/s10092-015-0168-6.

[36] L. C. Berselli, T. Iliescu, and W. J. Layton. *Mathematics of large eddy simulation of turbulent flows*. Scientific Computation. Springer-Verlag, Berlin, 2006. DOI: 10.1007/b137408.

[37] C. Bertoglio, R. Nuñez, F. Galarce, D. Nordsletten, and A. Osses. "Relative pressure estimation from velocity measurements in blood flows: State-of-the-art and new approaches". In: *Int. J. Numer. Meth. Biomed. Engng.* 34.2 (2018). DOI: 10.1002/cnm.2925.

[38] C. Bertóglio, R. Núñez, F. Galarce, D. Nordsletten, and A. Osses. "Relative pressure estimation from velocity measurements in blood flows: State-of-art and new approaches". In: *Int. J. Numer. Meth. Biomed. Engng.* 34 (2017). DOI: 10.1002/cnm.2925.

[39] C. Bi, C. Wang, and Y. Lin. "Two-grid finite element method and its a posteriori error estimates for a nonmonotone quasilinear elliptic problem under minimal regularity of data". In: *Comput. Math. Appl.* 76.1 (2018), pp. 98–112. DOI: 10.1016/j.camwa.2018.04.006.

[40] J. Blasco and R. Codina. "A finite element formulation for the Stokes problem allowing equal velocity-pressure interpolation". In: *Comput. Methods Appl. Mech. Engrg.* 143.3–4 (1997), pp. 373–391. DOI: 10.1016/S0045-7825(96)01154-1.

[41] P. Bochev and C. Dohrmann. "A computational study of stabilized, low-order C^0 finite element approximations of Darcy equations". In: *Comput. Mech.* 38.4-5 (2006), pp. 310–333. DOI: 10.1007/s00466-006-0036-y.

[42] D. Boffi, F. Brezzi, and M. Fortin. *Mixed Finite Element Methods and Applications*. Vol. 44. Springer Series in Computational Mathematics. Springer Berlin Heidelberg, Jan. 2013. DOI: 10.1007/978-3-642-36519-5.

[43] S. C. Brenner and L. R. Scott. *The mathematical theory of finite element methods*. Third. Vol. 15. Texts in Applied Mathematics. Springer, New York, 2008. DOI: 10.1007/978-0-387-75934-0.

[44] F. Brezzi, J. Douglas, and L. Marini. "Two families of mixed finite elements for second order elliptic problems". In: *Numer. Math.* 47.2 (1985), pp. 217–235. DOI: 10.1007/BF01389710.

[45] F. Brezzi and M. Fortin. *Mixed and hybrid finite element methods*. Springer Series in Computational Mathematics. Berlin, New-York: Springer-Verlag, 1991. DOI: 10.1007/978-1-4612-3172-1.

[46] F. Brezzi, M. Fortin, and L. D. Marini. "Error analysis of piecewise constant pressure approximations of Darcy's law". In: *Comput. Methods Appl. Mech. Engrg.* 195.13-16 (2006), pp. 1547–1559. ISSN: 0045-7825. DOI: 10.1016/j.cma.2005.05.027.

[47] F. Brezzi and D. Marini. "Error estimates for the three-field formulation with bubble stabilization". In: *Math. Comp.* 70.235 (2000), pp. 911–934. DOI: 10.1090/S0025-5718-00-01250-3.

[48] F. Brezzi and L. D. Marini. "A three-field domain decomposition method". In: *Domain Decomposition in Science and Engineering*. Ed. by A. Quarteroni and et al. Providence: American Mathematical Society, 1994, pp. 27–34.

[49] F. Brezzi and J. Pitkaranta. *On the stabilization of finite element approximations of the Stokes problem*. Vol. 10. Hackbusch W. (eds) Efficient Solutions of Elliptic Systems. Notes on Numerical Fluid Mechanics. Springer, New York, 1984. DOI: 10.1007/978-3-663-14169-3_2.

[50] F. Brezzi and A. Russo. "Stabilization Techniques for the Finite Element Method". In: *Applied and Industrial Mathematics, Venice—2*. Springer, Dordrecht, 2000, pp. 47–58.

[51] P. W. Bridgman. "The Physics of High Pressure". In: *Nature* 131 (1933), p. 259. DOI: 10.1038/131259a0.

[52] A. Brooks and T.J.R. Hugues. "Streamline upwind/Petrov-Galerkin formulations for convection dominated flows with particular emphasis on the incompressible Navier-Stokes equations". In: *Comput. Methods Appl. Mech. Engrg.* 32.1–3 (1982), pp. 199–259. DOI: 10.1016/0045-7825(82)90071-8.

[53] E. Burman, M. A. Fernández, and P. Hansbo. "Continuous interior penalty finite element method for Oseen's equations". In: *SIAM J. Numer. Anal.* 44.3 (2006), pp. 1248–1274. DOI: 10.1137/040617686.

[54] E. Burman and P. Hansbo. "A unified stabilized method for Stokes' and Darcy's equations". In: *J. Comput. Appl. Math.* 198.1 (2007), pp. 35–51. DOI: 10.1016/j.cam.2005.11.022.

[55] E. Burman and P. Hansbo. "Edge stabilization for the generalized Stokes problem: a continuous interior penalty method". In: *Comput. Methods Appl. Mech. Engrg.* 195.19-22 (2006), pp. 2393–2410. DOI: 10.1016/j.cma.2005.05.009.

[56] A. Cesmelioglu, B. Cockburn, N. C. Nguyen, and J. Peraire. "Analysis of HDG methods for Oseen equations". In: *J. Sci. Comput.* 55.2 (2013), pp. 392–431. DOI: 10.1007/s10915-012-9639-y.

[57] L. Chamoin and F. Legoll. "*A posteriori* error estimation and adaptive strategy for the control of MsFEM computations". In: *Comput. Methods Appl. Mech. Engrg.* 336 (2018), pp. 1–38. DOI: 10.1016/j.cma.2018.02.016.

[58] J. Cheung, M. Perego, P. Bochev, and M. Gunzburger. "Optimally accurate higher-order finite element methods for polytopial approximations of domains with smooth boundaries". In: *Math. Comp.* 88.319 (2019), pp. 2187–2219. DOI: 10.1090/mcom/3415.

[59] A. Chorin and J. Marsden. *A Mathematical Introduction to Fluid Mechanics*. Vol. 4. Series in Applied Mathematics. Springer-Verlag New York, 1993, pp. XII+172. DOI: 10.1007/978-1-4612-0883-9.

[60] Ph. Clément. "Approximation by finite element functions using local regularization". In: *R.A.I.R.O. Anal. Numer.* 9.R-2 (1975), pp. 77–84. DOI: 10.1051/m2an/197509R200771.

[61] B. Cockburn and J. Gopalakrishnan. "A characterization of hybridized mixed methods for second order elliptic problems". In: *SIAM J. Numer. Anal.,* 42.1 (2004), pp. 283–301. DOI: 10.1137/S0036142902417893.

[62] B. Cockburn, J. Gopalakrishnan, and R. Lazarov. "Unified hybridization of discontinuous Galerkin, mixed, and continuous Galerkin methods for second order elliptic problems". In: *SIAM J. Numer. Anal.* 47.2 (2009), pp. 1319–1365. DOI: 10.1137/070706616.

[63] R. Codina. "Analysis of a stabilized finite element approximation of the Oseen equations using orthogonal subscales". In: *Appl. Numer. Math.* 58.3 (2008), pp. 264–283. DOI: 10.1016/j.apnum.2006.11.011.

[64] M. R. Correa and A. F. D. Loula. "Unconditionally stable mixed finite element methods for Darcy flow". In: *Comput. Methods Appl. Mech. Engrg.* 197.17-18 (2008), pp. 1525–1540. DOI: 10.1016/j.cma.2007.11.025.

[65] M. R. Correa, J. C. Rodriguez, A. M. Farias, D. de Siqueira, and P. Devloo. "Hierarchical high order finite element spaces in $H(\mathrm{div},\Omega)\times H^1(\Omega)$ for a stabilized mixed formulation of Darcy problem". In: *Comput. Math. Appl.* 80.5 (2020), pp. 1117–1141. DOI: 10.1016/j.camwa.2020.06.003.

[66] H. Darcy. *Les Fontaines Publiques de la Ville de Dijon*. Paris: Victor Dalmont, 1856.

[67] D. Di Pietro and J. Droniou. *The Hybrid High-Order Method for Polytopal Meshes*. Vol. 159. Applied Mathematical Sciences. New York: Springer-Verlag, 2004. DOI: 10.1007/978-1-4757-4355-5.

[68] D. Di Pietro and A. Ern. *Mathematical Aspects of Discontinuous Galerkin Methods*. Springer-Verlag Berlin Heidelberg, 2012. DOI: 10.1007/978-3-642-22980-0.

[69] J Douglas and J. Wang. "An absolutely stabilized finite element method for the Stokes problem". In: *Math. Comp.* 52.186 (1989), pp. 495–508. DOI: 10.1137/S0036142903416547.

[70] O. Durán, P. R. B. Devloo, S. M. Gomes, and F. Valentin. "A multiscale hybrid method for Darcy's problems using mixed finite element local solvers". In: *Comput. Methods Appl. Mech. Engrg.* 354 (2019), pp. 213–244. ISSN: 0045-7825. DOI: 10.1016/j.cma.2019.05.013.

[71] R. Durán. "An elementary proof of the continuity from $L^2_0(\Omega)$ to $H^1_0(\Omega)$ of Bogovskii's right inverse of the divergence". In: *Rev. Un. Mat. Argentina* 53.2 (2012), pp. 59–78.

[72] W. E, B. Engquist, X. Li, W. Ren, and E. Vanden-Eijnden. "Heterogeneous multiscale methods: a review". In: *Commun. Comput. Phys.* 2.3 (2007), pp. 367–450.

[73] T. Ebbers, L. Wigström, A. Bolger, J. Engvall, and M Karlsson. "Estimation of relative cardiovascular pressure using time-resolved three-dimensional phase contrast MRI." In: *Magn. Reson. Med* 45 (2001), pp. 872–879. DOI: 10.1002/mrm.1116.

[74] Y. Efendiev, J. Galvis, and T. Y. Hou. "Generalized multiscale finite element methods (GMsFEM)". In: *J. Comput. Phys.* 251 (2013), pp. 116–135. DOI: 10.1016/j.jcp.2013.04.045.

[75] A. Ern and J.-L. Guermond. *Theory and practice of finite elements*. Vol. 159. Applied Mathematical Sciences. Springer-Verlag, New York, 2004. DOI: 10.1007/978-1-4757-4355-5.

[76] V. Ervin, W. Layton, and J. Maubach. "A posteriori error estimators for a two-level finite element method for the Navier-Stokes equations". In: *Numer. Meth. Part. D.E.* 12.3 (1996), pp. 333–346. DOI: 10.1002/(SICI)1098-2426(199605)12:3<333::AID-NUM4>3.0.CO;2-P.

[77] C. Farhat, I. Harari, and L. P. Franca. "The discontinuous enrichment method". In: *Comput. Methods Appl. Mech. Engrg.* 190.48 (2001). DOI: 10.1016/S0045-7825(01)00232-8.

[78] H. Fernando, C Harder, D. Paredes, and F. Valentin. "Numerical multiscale methods for a reaction-dominated model". In: *Comput. Methods Appl. Mech. Engrg.* 201-204 (2012), pp. 228–244. DOI: 10.1016/j.cma.2011.09.007.

[79] P. Forchheimer. "Wasserbewegung durch Boden. Z." In: *Ver. Deutsh. Ing.* 45 (1901), pp. 1782–1788.

[80] L. P. Franca, C. Harder, and F. Valentin. "On a residual local projection method for the Darcy equation". In: *C. R. Math. Acad. Sci. Paris* 347.17-18 (2009), pp. 1105–1110. DOI: 10.1016/j.crma.2009.06.016.

[81] L. P. Franca and A. L. Madureira. "Element diameter free stability parameters for stabilized methods applied to fluids". In: *Comput. Methods Appl. Mech. Engrg.* 105.3 (1993), pp. 395–403. DOI: 10.1016/0045-7825(93)90065-6.

[82] L. P. Franca, A. L. Madureira, and F. Valentin. "Towards multiscale functions: enriching finite element spaces with local but not bubble-like functions". In: *Comput. Methods Appl. Mech. Engrg.* 194.27-29 (2005), pp. 3006–3021. DOI: 10.1016/j.cma.2004.07.029.

[83] L.P. Franca, S.L. Frey, and T.J. R. Hughes. "Stabilized finite element methods. I. Application to the advective-diffusive model". In: *Comput. Methods Appl. Mech. Engrg.* 95.2 (1992), pp. 253–276. DOI: 10.1016/0045-7825(92)90143-8.

[84] L.P. Franca and R. Stenberg. "Error analysis of Galerkin least squares methods for the elasticity equations". In: *SIAM J. Numer. Anal.* 28.6 (1991), pp. 1680–1697. DOI: 10.1137/0728084.

[85] G. Gatica, R. Oyarzua, and J. Sayas. "Analysis of fully-mixed finite element methods for the Stokes-Darcy coupled problem". In: *Math. Comp.* 80.276 (2011), pp. 1911–1948. DOI: 10.2307/23075260.

[86] G. Gatica, R. Ruiz-Baier, and G. Tierra. "A mixed finite element method for Darcy's equations with pressure dependent porosity". In: *Math. Comp.* 85 (2016), pp. 1–33. DOI: 10.1090/mcom/2980.

[87] G.N. Gatica. *A Simple Introduction to the Mixed Finite Element Method:Theory and Applications*. Springer Briefs in Mathematics, Springer, 2014. DOI: 10.1007/978-3-319-03695-3.

[88] G.N. Gatica. *Introducción al Anális Funcional. Teoría y Aplicaciones*. Editorial Reverté, 2014.

[89] V. Girault, F. Murat, and A. Salgado. "Finite element discretization of Darcy's equations with pressure dependent porosity". In: *M2AN Math. Model. Numer. Anal.* 44.6 (2010), pp. 1155–1191. DOI: 10.1051/m2an/2010019.

[90] V. Girault and P.A. Raviart. *Finite element methods for Navier–Stokes equations: Theory and algorithms*. Springer Series in Computational Mathematics. Springer-Verlag Berlin Heidelberg, 1986. DOI: 10.1007/978-3-642-61623-5.

[91] V. Girault and M. F. Wheeler. "Numerical discretization of a Darcy-Forchheimer model". In: *Numer. Math.* 110.2 (2008), pp. 161–198. DOI: 10.1007/s00211-008-0157-7.

[92] P. Gresho and R. Sani. "On pressure boundary conditions for the incompressible Navier–Stokes equations." In: *Int. J. Numer. Meth. Fluids* 23 (1987), pp. 1111–1145. DOI: 10.1002/fld.1650071008.

[93] J.L. Guermond, P. Minev, and J. Shen. "An overview of projection methods for incompressible flows." In: *Comput. Methods Appl. Mech. Engrg.* 195 (2006), pp. 6011–6045. DOI: 10.1016/j.cma.2005.10.010.

[94] P. Hansbo, M. Larson, and A. Massing. "A stabilized cut finite element method for the Darcy problem on surfaces". In: *Comput. Methods Appl. Mech. Engrg.* 326 (2017), pp. 298–318. ISSN: 0045-7825. DOI: 10.1016/j.cma.2017.08.007.

[95] I. Harari and T.J.R. Hughes. "What are C and h?: Inequalities for the analysis and design of finite element methods". In: *Comput Methods. Appl. Mech. Engrg.* 97 (1992), pp. 157–192. DOI: 10.1016/0045-7825(92)90162-D.

[96] C. Harder, A. L. Madureira, and F. Valentin. "A hybrid-mixed method for elasticity". In: *ESAIM Math. Model. Numer. Anal.* 50.2 (2016), pp. 311–336. DOI: 10.1051/m2an/2015046.

[97] C. Harder, D. Paredes, and F. Valentin. "A family of multiscale hybrid-mixed finite element methods for the Darcy equation with rough coefficients". In: *J. Comput. Phys.* 245 (2013), pp. 107–130. DOI: 10.1016/j.jcp.2013.03.019.

[98] C. Harder, D. Paredes, and F. Valentin. "On a Multiscale Hybrid-Mixed Method for Advective-Reactive Dominated Problems with Heterogenous Coefficients". In: *SIAM Multiscale Model. and Simul.* 13.2 (2015), pp. 491–518. DOI: 10.1137/130938499.

[99] C. Harder and F. Valentin. *Foundations of the MHM method, in Building Bridges: Connections and Challenges in Modern Approaches to Numerical Partial Differential Equations*. Lecture Notes in Computational Science and Engineering, 2016. DOI: 10.1007/978-3-319-41640-3.

[100] P. Henning, A. Målqvist, and D. Peterseim. "A localized orthogonal decomposition method for semi-linear elliptic problems". In: *ESAIM Math. Model. Numer. Anal.* 48.5 (2014), pp. 1331–1349. DOI: 10.1051/m2an/2013141.

[101] P. Henning and M. Ohlberger. "A-posteriori error estimate for a heterogeneous multiscale approximation of advection-diffusion problems with large expected drift". In: *Discrete Contin. Dyn. Syst. Ser. S* 9.5 (2016), pp. 1393–1420. DOI: 10.3934/dcdss.2016056.

[102] T. Y. Hou and X.-H. Wu. "A multiscale finite element method for elliptic problems in composite materials and porous media". In: *J. Comput. Phys.* 134.1 (1997), pp. 169–189. DOI: 10.1006/jcph.1997.5682.

[103] T. Y. Hou, X.-H. Wu, and Z. Cai. "Convergence of a multiscale finite element method for elliptic problems with rapidly oscillating coefficients". In: *Math. Comp.* 68.227 (1999), pp. 913–943. DOI: 10.1090/S0025-5718-99-01077-7.

[104] T.J.R. Hughes. "A simple scheme for developing 'upwind' finite elements". In: *Int. J. Numer. Meth. Eng* 12 (1978), pp. 1359–1365. DOI: 10.1002/nme.1620120904.

[105] T.J.R. Hughes. "Multiscale phenomena: Green's functions, the Dirichlet-to-Neumann formulation, subgrid scale models, bubbles and the origins of stabilized methods". In: *Comput. Methods Appl. Mech. Engrg.* 127 (1995), pp. 387–401. DOI: 10.1016/0045-7825(95)00844-9.

[106] T.J.R. Hughes. "The Finite Element Method: Linear Static and Dynamic Finite Element Analysis". In: *Comput.-Aided Civ. Inf.* (1989). DOI: 10.1111/j.1467-8667.1989.tb00025.x.

[107] T.J.R Hugues, L. Franca, and M. Balestra. "A new finite element Formulation for computational fluis dynamics: V. Circumventing the Babuska-Brezzi condition: A stable Petrov-Galerkin formulation of the Stokes problem accommodating equal-order interpolations". In: *Comput Methods. Appl. Mech. Engrg.* 59 (1986), pp. 85–99. DOI: 10.1016/0045-7825(86)90025-3.

[108] T.J.R. Hugues and L. Franca. "A new finite element formulation for computational fluid dynamics. VII. The Stokes problem with various well-posed boundary conditions: symmetric formulations that converge for all velocity/pressure spaces". In: *Comput Methods. Appl. Mech. Engrg.* 65 (1987), pp. 85–96. DOI: 10.1016/0045-7825(87)90184-8.

[109] D. Irisarri and G. Hauke. "A posteriori pointwise error computation for 2-D transport equations based on the variational multiscale method". In: *Comput. Methods Appl. Mech. Engrg.* 311 (2016), pp. 648–670. DOI: 10.1016/j.cma.2016.09.001.

[110] V. John. *Finite Element Methods for Incompressible Flow Problems*. Vol. 51. Springer Series in Computational Mathematics. Switzerland: Springer International Publishing, 2016. DOI: 10.1007/978-3-319-45750-5.

[111] V. John. *Large eddy simulation of turbulent incompressible flows*. Vol. 34. Lecture Notes in Computational Science and Engineering. Springer-Verlag, Berlin, 2004. DOI: 10.1007/978-3-642-18682-0.

[112] V. John. "Residual a posteriori error estimates for two-level finite element methods for the Navier-Stokes equations". In: *Appl. Numer. Math.* 37.4 (2001), pp. 503–518. DOI: 10.1016/S0168-9274(00)00058-1.

[113] F. Kikuchi and X. Liu. "Estimation of interpolation error constants for the P0 and P1 triangular finite elements". In: *Comput Methods. Appl. Mech. Engrg.* 196 (Aug. 2007), pp. 3750–3758. DOI: 10.1016/j.cma.2006.10.029.

[114] H. P. Langtangen and A. Logg. *Solving PDEs in Python*. Springer, 2017. ISBN: 978-3-319-52461-0. DOI: 10.1007/978-3-319-52462-7.

[115] R.S. Laugesen and B.A. Siudeja. "Minimizing Neumann fundamental tones of triangles: An optimal Poincaré inequality". In: *J. Differ. Equ.* 249 (2010), pp. 118–135. DOI: 10.1016/j.jde.2010.02.020.

[116] A. Logg, G.Wells, and K.A. Mardal, eds. *Automated solution of differential equations by the finite element method. The FEniCS book*. Vol. 84. Lecture Notes in Computational Science and Engineering. Springer-Verlag Berlin Heidelberg, 2012. DOI: 10.1007/978-3-642-23099-8.

[117] H. López, B. Molina, and J. Salas. "Comparison between different numerical discretizations for a Darcy-Forchheimer model". In: *Electron. Trans. Numer. Anal.* 34 (2009), pp. 187–203. URL: http://eudml.org/doc/224769.

[118] Z. Lotfian and M. V. Sivaselvan. "Mixed finite element formulation for dynamics of porous media". In: *Internat. J. Numer. Methods Engrg.* 115.2 (2018), pp. 141–171. DOI: 10.1002/nme.5799.

[119] A. Madureira. *Numerical Analysis of Multiscale Problems*. Springer-Verlag Berlin Heidelberg, 2012. ISBN: 978-3-642-43124-1. DOI: 110.1007/978-3-642-22061-6.

[120] N. Mapakshi, J. Chang, and K. Nakshatrala. "A scalable variational inequality approach for flow through porous media models with pressure-dependent viscosity". In: *J. Comput. Phys.* 359 (2018), pp. 137–163. DOI: 10.1016/j.jcp.2018.01.022.

[121] M. Markl, A. Frydrychowicz, S. Kozerke, M. Hope, and O. Wieben. "4D flow MRI". In: *J. Magn. Reson. Imaging* 36.5 (2012), pp. 1015–1036. DOI: 10.1002/jmri.23632..

[122] A. Masud and T. J. R. Hughes. "A stabilized mixed finite element method for Darcy flow". In: *Comput. Methods Appl. Mech. Engrg.* 191.39–40 (2002), pp. 4341–4370. DOI: 10.1016/S0045-7825(02)00371-7.

[123] A. Masud and J. Kwack. "A stabilized mixed finite element method for the first-order form of advection–diffusion equation". In: *Int. J. Numer. Methods Fluids* 57.9 (2008), pp. 1321–1348. DOI: 10.1002/fld.1842.

[124] F. Morales. "A conforming primal-dual mixed formulation for the 2D multiscale porous media flow problem". In: *Comput. Appl. Math.* 38.2 (2019). DOI: 10.1007/s40314-019-0808-6.

[125] K. B. Nakshatrala and K.R. Rajagopal. "A numerical study of fluids with pressure-dependent viscosity flowing through a rigid porous medium". In: *Int. J. Numer. Methods Fluids* 67.3 (2011), pp. 342–368. DOI: 10.1002/fld.2358.

[126] D. Nolte, J. Urbina, J. Sotelo, L. Sok, C. Montalba, I. Valverde, A. Osses, S. Uribe, and C. Bertoglio. *Validation of 4D-flow-based pressure difference estimators*. Apr. 2019. URL: https://hal.archives-ouvertes.fr/hal-02113750.

[127] M. Ohlberger. "A posteriori error estimates for the heterogeneous multiscale finite element method for elliptic homogenization problems". In: *Multiscale Model. Simul.* 4.1 (2005), pp. 88–114. DOI: 10.1137/040605229.

[128] H Omran, H. Schmidt, M. Hackenbroch, S. Illien, P. Berhardt, G. Von Der Recke, S. Fimmers R. Flacke, G. Layer, C. Pohl, B. Luderitz, H. Schild, and T. Sommer. "Silent and Apparent Cerebral Embolism after Retrograde Catheterisation of the Aortic Valve in Valvular Stenosis: A Prospective, Randomised Study". In: *The Lancet* 361.9365 (2003), pp. 1241–1246. DOI: 10.1016/S0140-6736(03)12978-9.

[129] S. Ozisik, B. Riviere, and T. Warburton. *On the Constants in the Inverse Inequalities in L^2*. Tech. rep. 2010. DOI: https://hdl.handle.net/1911/102161.

[130] D. Pacheco and O. Steinbach. "A continuous finite element framework for the pressure Poisson equation allowing non-Newtonian and compressible flow behavior". In: *Int. J. Numer. Meth. Fluids* (2020), pp. 1–11. DOI: 10.1002/fld.4936.

[131] D. Paredes, F. Valentin, and H. M. Versieux. "On the robustness of multiscale hybrid-mixed methods". In: *Math. Comp.* 86.304 (2017), pp. 525–548. DOI: 10.1090/mcom/3108.

[132] G. V. Pencheva, M. Vohralık, M. F. Wheeler, and T. Wildey. "Robust a posteriori error control and adaptivity for multiscale, multinumerics, and mortar coupling". In: *SIAM J. Numer. Anal.* 51.1 (2013), pp. 526–554. DOI: 10.1137/110839047.

[133] S. Prössdorf and B. Silbermann. *Numerical analysis for integral and related operator equations*. Vol. 52. Operator Theory: Advances and Applications. Birkhäuser Verlag, Basel, 1991, p. 542.

[134] K. R. Rajagopal. "On a hierarchy of approximate models for flows of incompressible fluids through porous solids". In: *Math. Models Methods Appl. Sci.* 17.2 (2007), pp. 215–252. DOI: 10.1142/S0218202507001899.

[135] P.-A. Raviart and J. M. Thomas. "Primal hybrid finite element methods for 2nd order elliptic equations". In: *Math. Comp.* 31.138 (1977), pp. 391–413. DOI: 10.2307/2006423.

[136] C. Ren and Y. Ma. "Residual a posteriori error estimate of a new two-level method for steady Navier-Stokes equations". In: *J. Syst. Sci. Complex.* 19.4 (2006), pp. 478–490. DOI: 10.1007/s11424-006-0478-5.

[137] S. Rhebergen and G.N. Wells. "A Hybridizable Discontinuous Galerkin Method for the Navier–Stokes Equations with Pointwise Divergence-Free Velocity Field". In: *J Sci Comput* 76 (2018), pp. 1484–1501. DOI: 10.1007/s10915-018-0671-4.

[138] R.R. Rosales, B. Seibold, D. Shirokoff, and D. Zhou. *High-order Methods for a Pressure Poisson Equation Reformulation of the Navier-Stokes Equations with Electric Boundary Conditions*. Tech. rep. 2020. DOI: arXiv:2002.09801.

[139] P. Sagaut. *Large eddy simulation for incompressible flows*. Second. Scientific Computation. Springer-Verlag, Berlin, 2002. DOI: 10.1007/978-3-662-04695-1.

[140] Chen Shaochun and Jikun Zhao. "Estimations of Constants in Inverse Inequalities for Finite Element Functions". In: *J. Comput. Math.* 31 (Sept. 2013). DOI: 10.4208/jcm.1307-m4063.

[141] N. Smith and et al. "A finite-element approach to the direct computation of relative cardiovascular pressure from time-resolved MR velocity data". In: *Med. Image Anal.* 16 (2012), pp. 1029–1037. DOI: 10.1016/j.media.2012.04.003.

[142] G. Soulat, P. McCarthy, and M. Markl. "4D Flow with MRI". In: *Annu. Rev. Biomed. Eng.* 22 (2020). DOI: 10.1146/annurev-bioeng-100219-110055.

[143] O. Steinbach. *Numerical Approximation Methods for Elliptic Boundary Value Problems: Finite and Boundary Elements*. Springer, New York, 2008. DOI: 10.1007/978-0-387-68805-3.

[144] R. Stenberg. "Error analysis of some finite element methods for the Stokes problem". In: *Math. Comp.* 54.190 (1990), pp. 495–508. DOI: 10.2307/2008498.

[145] G. Stoyan. "Towards discrete Velte decompositions and narrow bounds for the inf-sup constants". In: *Comp. Math. Appl.* 38 (1999), pp. 243–261. DOI: 10.1016/S0898-1221(99)00254-0.

[146] H. Svihlová, J. Hron, J. Málek, K.R. Rajagopoal, and K. Rajagopoal. "Determination of pressure data from velocity data with a view toward its application in cardiovascular mechanics. Part 1. Theoretical considerations". In: *Int. J. of Eng. Sci.* 105 (2016), pp. 108–127. DOI: 10.1016/j.ijengsci.2015.11.002.

[147] S. Tavener and T. Wildey. "Adjoint based a posteriori analysis of multiscale mortar discretizations with multinumerics". In: *SIAM J. Sci. Comput.* 35.6 (2013), A2621–A2642. DOI: 10.1137/12089973X.

[148] L. Tobiska and R. Verfürth. "Analysis of a streamline diffusion finite element method for the Stokes and Navier-Stokes equations". In: *SIAM J. Numer. Anal.* 33.1 (1996), pp. 107–127. ISSN: 0036-1429. DOI: 10.1137/0733007.

[149] A. Toselli and O. Widlund. *Domain Decomposition Methods-Algorithms and Theory*. Springer, Berlin 2005. Vol. 34. Springer Series in Computational Mathematics. DOI: 10.1007/b137868.

[150] J. M. Urquiza, D. N'Dri, A. Garon, and M. C. Delfour. "A numerical study of primal mixed finite element approximations of Darcy equations". In: *Comm. Numer. Methods Engrg.* 22.8 (2006), pp. 901–915. DOI: 10.1002/cnm.859.

[151] A. Vahanian and et al. "Guidelines on the management of valvular heart disease (version2012)". In: *Europ. Heart Jour.* 19.33 (2012), pp. 2451–2496. DOI: 10.1093/eurheartj/ehs109.

[152] R Verfüth. *A Posteriori Error Estimation Techniques for the Finite Element Methods*. 2013. DOI: 10.1093/acprof:oso/9780199679423.001.0001.

[153] R. Vitiello and et al. "Complications Associated with Pediatric Cardiac Catheterization". In: *J. Am. Coll. Cardiol.* 32.5 (1998), pp. 1433–1440. DOI: 10.1016/S0735-1097(98)00396-9.

[154] T. Warburton and Jan S. Hesthaven. "On the constants in hp-finite element trace inverse inequalities". In: *Comput. Methods Appl. Mech. Engrg. 1* 192.25 (2003), pp. 2765–2773. DOI: 10.1016/S0045-7825(03)00294-9.

[155] R. M. Wyman and et al. "Current Complications of Diagnostic and Thera-peutic Cardiac Catheterization". In: *J. Am. Coll. Cardiol.* 12.6 (1988), pp. 1400–1406. DOI: 10.1016/s0735-1097(88)80002-0.

[156] J. Xu. "Two-grid discretization techniques for linear and nonlinear PDEs". In: *SIAM J. Numer. Anal.* 33.5 (1996), pp. 1759–1777. DOI: 10.1137/S0036142992232949.

[157] J. Zhang and H. Rui. "A stabilized Crouzeix-Raviart element method for coupling Stokes and Darcy-Forchheimer flows". In: *Numer. Methods Partial Differential Equations* 33.4 (2017), pp. 1070–1094. DOI: 10.1002/num.22129.

[158] Y.-Z. Zhang, Y.-R. Hou, and H.-B. Wei. "Residual a posteriori error estimate of two level finite element method for natural convection problem". In: *Chin. J. Eng.* 32.1 (2015), pp. 116–130. DOI: 10.3969/j.issn.1005-3085.2015.01.012.